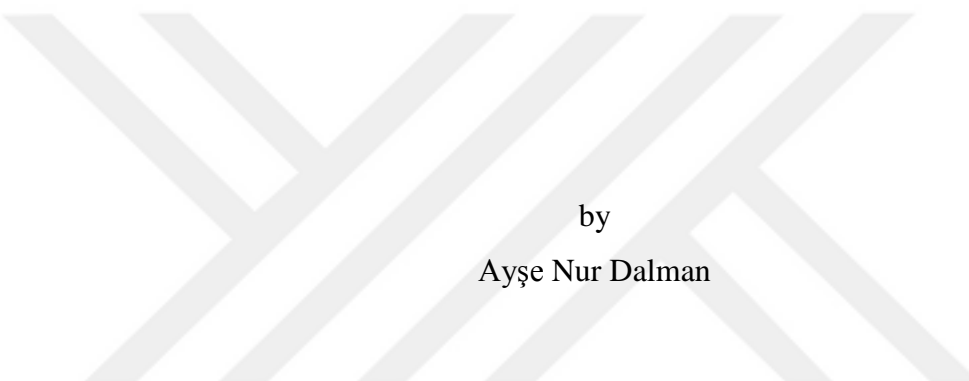


A WET-STOCK MANAGEMENT AND LEAK DETECTION SYSTEM FOR FUEL
TANKS



by

Ayşe Nur Dalman

Submitted to Graduate School of Natural and Applied Sciences
in Partial Fulfillment of the Requirements
for the Degree of Master of Science in
Chemical Engineering

Yeditepe University
2017

A WET-STOCK MANAGEMENT AND LEAK DETECTION SYSTEM FOR FUEL
TANKS

APPROVED BY:

Assist. Prof. Dr. Murat Oluş Özbek
(Thesis Supervisor)

Assoc. Prof. Dr. Kurtul Küçükada

Assist. Prof. Dr. Cem Levent Altan

DATE OF APPROVAL: / / 2017

ACKNOWLEDGEMENTS

I would like to express my special appreciation and thanks to my advisor Assist. Prof. Dr. Murat Oluş Özbeğ for his valuable suggestions, guidance and understanding throughout my study.

I would like to thank to my dear managers, especially Assist. Prof. Dr. Halit Tuğrul Genç, TORA Board Member Ertüm Tüfekçi and TORA Board Member Özgün Mutlu for their support and understanding during my study.

I would like to thank to my dear friends and moral supporters, especially to Akay Delihasan and Gökhan Çelik for their help and understanding during my study.

Last but not least, I wish to express my deepest thanks to my mother, my brother and my sisters for their great support, encouragement, and patience throughout my all education.

ABSTRACT

A WET-STOCK MANAGEMENT AND LEAK DETECTION SYSTEM FOR FUEL TANKS

One of the critical problems in wet-stock management is inaccurate (poor) tank calibration that masks the leakages. This study aims to prevent the masking effect and improve the leak detection for petroleum storage tanks. The common tank types used are simple cylindrical and cylindrical with dished heads. Through obtaining mathematical models for both tank types that convert the measured liquid height to accurate volume and taking into account the tank deformations this goal is achieved. The accounted deformations in tank parameters are radius, length, dished head depth, probe offset and tilt (axial and radial). The analysis of the real time data showed that the deformations can be categorized into two as uniform and non-uniform, both of which require different approaches. The simulations using the actual data gathered from different fuel service stations showed that the approach developed in this study is valid. Within the five sets of data collected from different tanks, the first tank is used only for its parameters to simulate the effects. The second one is classified as non-problematic that does not require any corrections and the uncorrected model data fits perfectly. Analysis of the third and fourth tanks showed uniform deformations, the deformation included tank models successfully predicted the real fuel volumes. The last tank was non-uniformly deformed. Although the parameterized models did not perform well for this case, inclusion of an error (or correction) function produced accurate results. The results showed that the variance in the uniformly deformed tanks reduced from -200 L – +20 L range to -20 L – +40 L range for and -300 L – +100 L range to -50 L – +20 L range for, which brings 81.3% and 81.1% improvement. In the non-uniform deformation case, by using only the parameterized models the variance changes from -800 L to +800 L range. However, inclusion of the error function reduces the variance to -15 L – +15 L range and brings a 97.7% improvement.

ÖZET

AKARYAKIT TANKLARI İÇİN STOK YÖNETİMİ VE SİZİNTİ TESPİT SİSTEMİ

Akaryakıt stok yönetiminde karşılaşılan en kritik problemlerden biri hatalı tank kalibrasyonudur ve hatalı tank kalibrasyonu sizıntıları maskelemektedir. Bu çalışmada amaçlanan, bu maskeleme etkisini ortadan kaldırmak ve petrol depolama tankları için sizıntı tespitini iyileştirmektir. Akaryakıt depolamada çoğunlukla bombeli ve bombesiz silindir tanklar kullanılmaktadır. Her iki tank türü içinde ölçülen sıvı seviyesini doğru hacim değerine dönüştüren matematiksel modeller oluşturularak ve tank deformasyonları göz önünde bulundurularak bu amaca ulaşılmıştır. Göz önünde bulundurulan tank parametreleri şunlardır: yarıçap, uzunluk, bombe derinliği, ölçüm noktası, aksiyel eğim ve radyal eğim. Gerçek zamanlı verilerin analizleri, tank deformasyonlarının düzenli ve dağınık olarak sınıflandırılabilceğini göstermiştir ve her sınıf farklı yaklaşımlar gerektirmektedir. Farklı akaryakıt servis istasyonlarından toplanan gerçek verilerin kullanıldığı simülasyon, geliştirilen yaklaşımın geçerli olduğunu göstermektedir. Farklı tanklara ait beş veri setinden ilki parametrelerin tanktaki sıvinin hacmine etkisini göstermek için kullanılmıştır. İkincisi hiç düzeltme gerektirmeyen problemsiz tank kalibrasyon cetveli olarak sınıflandırılmıştır. Üçüncü ve dördüncü tankların analizi, bu tanklarda üniform bozulma olduğunu göstermiştir ve deformé dahil olan tank modelleri gerçek yakıt hacimlerini başarıyla tahmin etmiştir. Son tankın dağınık biçimde deformé olduğu ispatlanmıştır. Bu durum için parametrelerle oluşturulmuş modeller iyi çalışmamış olmasına rağmen, hata (düzeltme) fonksiyonunun dahil edilmesi doğru (kesin) sonuçları üretmiştir. Sonuçlar, üniform deformé olmuş tanklardaki varyansın $-200L - +20L$ aralığından $-20L - +40L$ aralığına ve $-300L - +100L$ aralığından $-50L - +20L$ aralığına düşüğünü göstermiştir, böylece %81.3 ve %81.1 iyileştirme gerçekleştirilmiştir. Dağınık deformé olan tankın sadece parametrelerle oluşturulmuş modellerce verdiği varyans $-800L$ ila $+800 L$ arasında değişmektedir. Hata fonksiyonunun dahil edilmesiyle varyans trendi $-15L$ ila $+15L$ aralığına düşürülmüştür ve böylece %97.7 iyileştirme gerçekleştirilmiştir.

TABLE OF CONTENTS

ACKNOWLEDGEMENTS.....	iii
ABSTRACT.....	iv
ÖZET	v
LIST OF FIGURES	viii
LIST OF TABLES.....	xii
LIST OF SYMBOLS/ABBREVIATIONS	xiii
1. INTRODUCTION	1
1.1. UNDERGROUND STORAGE TANK (UST) SYSTEM	2
1.2. UNDERGROUND STORAGE TANK PIPING SYSTEMS	5
1.3. LEAK DETECTION IN FUEL SERVICE STATIONS	5
1.4. LEAK DETECTION FOR PETROLEUM USTs.....	6
1.4.1. Statistical Inventory Reconciliation (SIR)	8
1.4.2. Secondary Containment with Interstitial Monitoring	9
1.4.3. Automatic Tank Gauging (ATG) Systems	9
1.4.4. Vapor Monitoring (Including Tracer Compound Analysis)	10
1.4.5. Groundwater Monitoring	11
1.5. WET-STOCK MANAGEMENT (WSM) AT FUEL SERVICE STATIONS	11
1.6. TANK CALIBRATION.....	15
1.7. POOR TANK CALIBRATION	19
2. LITERATURE SURVEY	23
3. METHODOLOGY	26
3.1 SIMPLE CYLINDER TANK (SCT) MODEL	27
3.1.1 Radial (Horizontal) Tilt	28
3.1.2 Axial (Vertical) Tilt	30
3.2 CYLINDER TANK WITH DISHED HEAD (CTDH) MODEL	38
3.2.1 Radial (Horizontal) Tilt	42
3.2.2 Axial (Vertical) Tilt	42
3.3 VARIANCE	56
3.4 VARIANCE MINIMIZATION/REDUCTION	58

3.4.1	Uniform Adjustment	59
3.4.2	Non-uniform Adjustment.....	59
4.	RESULTS AND DISCUSSIONS	66
4.1.	SIMPLE CYLINDER TANK (SCT)	67
4.1.1.	Effect of Parameters on SCT Calibration Chart	68
4.2.	CYLINDER TANK WITH DISHED HEAD (CTDH).....	71
4.2.1.	Effect of Parameters on CTDH Calibration Chart.....	72
4.3.	VARIANCE MINIMIZATION/REDUCTION	73
4.3.1.	Non-problematic Tank	74
4.3.2.	Uniform Variance Adjustment.....	75
4.3.3.	Non-uniform Variance Adjustment	85
5.	CONCLUSIONS	89
6.	FUTURE WORK.....	90
APPENDIX A	95
APPENDIX B	102
APPENDIX C	122
APPENDIX D	123
APPENDIX E	140
APPENDIX F	166

LIST OF FIGURES

Figure 1.1. A typical fuel service station	1
Figure 1.2. Double wall steel petroleum UST	3
Figure 1.3. Typical steel and fiberglass USTs	3
Figure 1.4. Installation of underground petroleum storage tank.....	5
Figure 1.5. Leak detection methods for petroleum UST systems.....	7
Figure 1.6. Secondary containment with interstitial monitoring	9
Figure 1.7. Automatic tank gauging (ATG) systems, vapor monitoring and groundwater monitoring	10
Figure 1.8. TLS console and TLS magnetostrictive probe	16
Figure 1.9. Fuel level measurement.....	16
Figure 1.10. Comparison of LV graphs of cylindrical and rectangular tanks	17
Figure 1.11. Volumetric calibration technique	18
Figure 1.12. The 3D calibration scan and tank wireframe.....	19
Figure 1.13. Masking loss and actual fuel loss percentages	20
Figure 3.1. The side and the front view of SCT	27
Figure 3.2. Effect of radial tilt on the measured fuel level	29

Figure 3.3. Nonmeasurable (V_0) volume of SCT with positive axial tilt.....	30
Figure 3.4. High level fuel volume with positive axial tilt	32
Figure 3.5. Low level fuel volume with positive axial tilt.....	33
Figure 3.6. Nonmeasurable (V_0) volume of SCT with negative axial tilt	34
Figure 3.7. Critical fuel level determination for SCT with negative axial tilt	35
Figure 3.8. High level fuel volume with negative axial tilt	36
Figure 3.9. Low level fuel volume with negative axial tilt.....	37
Figure 3.10. The side view of a cylindrical tank with dished head (CTDH).....	39
Figure 3.11. The front view of a CTDH and the top view of a CTDH.....	40
Figure 3.12. The top view of one dished head volume.....	40
Figure 3.13. Two half-elliptical dished head volume determination	41
Figure 3.14. Two dished head volume determination	42
Figure 3.15. Nonmeasurable (V_0) volume of CTDH with positive axial tilt.....	43
Figure 3.16. Critical fuel level determination for CTDH with positive axial tilt	45
Figure 3.17. Fuel volume for positive axial tilt & wetted one dished head.....	46
Figure 3.18. Fuel volume for positive axial tilt & wetted two dished head.....	48

Figure 3.19. Nonmeasurable (V0) volume of CTDH with negative axial tilt	50
Figure 3.20. Critical fuel level determination for CTDH with negative axial tilt	52
Figure 3.21. Fuel volume for negative axial tilt & wetted both dished head.....	53
Figure 3.22. Fuel volume for negative axial tilt & wetted one dished head.....	55
Figure 4.1. Radius and length effects on the volume of SCT and liquid inside	69
Figure 4.2. Horizontal probe distance from the tank corner (M) effect on SCT volume	70
Figure 4.3. Radial (beta) tilt effect on calculated volume in SCT	70
Figure 4.4. Axial (alpha) tilt effect on SCT volume	71
Figure 4.5. Axial tilt (α) effect and radial tilt (β) effect.....	72
Figure 4.6. Radius (R) and length (L) effect.....	73
Figure 4.7. Dished head depth (H) and horizontal probe distance (M) effect	74
Figure 4.8. Non-problematic current calibration chart of the tank in Site C	74
Figure 4.9. Variance vs. volume graph for the tank in Site C	75
Figure 4.10. Variance distribution of the tank current chart in Site D	75
Figure 4.11. Normalized variance distribution of the tank current chart in Site D	76
Figure 4.12. All normalized variance distributions of the tank in Site D	77
Figure 4.13. First data group variance distribution of the tank in Site D	78

Figure 4.14. Second data group variance distribution of the tank in Site D	79
Figure 4.15. Variance comparison of current chart and model with all data groups for the tank in Site D	80
Figure 4.16. A sample of tank cover (unit in mm)	81
Figure 4.17. Variance distribution of the tank current chart in Site E.....	83
Figure 4.18. First data group variance distribution of the tank in Site E.....	83
Figure 4.19. Second data group variance distribution of the tank in Site E	84
Figure 4.20. Variance comparison of current chart and model with all data groups for the tank in Site E.....	84
Figure 4.21. Variance distribution of the tank current chart in Site B.....	87
Figure 4.22. Variance distribution of the tank in Site B after non-uniform adjustment.....	87
Figure 4.23. Comparison of ideal, current chart and adjusted variances	88

LIST OF TABLES

Table 1.1. Effect of poor tank calibration on daily variances.....	21
Table 3.1. A sample incoming data sequence.....	61
Table 4.1. Acquired dimensions of selected tanks.....	68
Table 4.2. Dimension comparison of provided by manufacturer and obtained by theoretical model for the tank in Site D.....	82
Table 4.3. Dimension comparison of provided by manufacturer and obtained by theoretical model for the tank in Site E	86

LIST OF SYMBOLS/ABBREVIATIONS

E	Error term
gph	Gallon per hour
h	Liquid height
h_{critical}	Critical liquid height
H	Dished head depth
L	Length
M	Gauge point (or probe offset)
r	Minor radius of ellipse
R	Radius
V	Volume
Var*	Normalized variance
α	Axial tilt angle
α_{fuel}	Thermal expansion coefficient
β	Radial tilt angle
ρ	Density
ATG	Automatic tank gauging
CTDH	Cylindrical tank with dished head
DOF	Degree of freedom
EPA	Environmental protection agency
GRP	Glass reinforced plastic
LG	Loss/Gain
LPG	Liquefied petroleum gas
LPG	Lower explosive limit
LV	Level to volume
POS	Point of sales
PD	Probability of detection
PFA	Probability of false alarm

SCT	Simple cylindrical tank
SIR	Statistical inventory reconciliation
TLS	Tank level sensor
UST	Underground storage tank
UEL	Upper explosive level
Var	Variance
WSM	Wet-stock management



1. INTRODUCTION

Governments, states and federal agencies regulate the safe management of hazardous chemicals including flammable and combustible substances. A person or a business, which uses, handles, stores or generates hazardous chemicals must comply with these regulations.



Figure 1.1. A typical fuel service station [1]

Fuel service stations store commercial grades of petroleum (e.g. unleaded, ultimate unleaded, ethonal blends), diesel and liquefied petroleum gas (LPG), all of which are classified as hazardous chemicals. Thus, station owners and operators have several responsibilities for the safe management of hazardous chemicals. Some of these responsibilities obligate the safe operation of/on [2]:

- The supply of the liquid and gaseous fuel products
- The fuel storage (infrastructure, maintenance, repair)
- The dispensing systems (infrastructure, maintenance, repair)
- The retail store

- The land ownership
- The protection of the environment from the hazardous chemicals (unleaded, diesel, ethanol blends)

Fuel service stations, also referred as “site”, has the potential for releasing pollutants into the environment, which endanger air, soil and water. Possible causes for the release include [3]:

- Damaged wall of underground storage tank
- Leaks of underground pipe
- Leaking or broken dispenser
- Overfill when road tanker is filling underground storage tank
- Overfill when refueling
- Non fuel proof pavement of refueling area or forecourt
- Lack of drainage
- General damage to fuel equipment and facilities

When fuel service stations are considered from the point of storage and delivery of hazardous chemicals, one of the most significant points is leak detection. A primary source of underground water contamination is fuel leaks from an underground storage tank (UST) system. Several leak detection methods are available for UST systems such as secondary containment with interstitial monitoring, automatic tank gauging (ATG), vapor monitoring, and Statistical Inventory Reconciliation (SIR).

Wet-stock management (WSM) at a site provides some advantages including leak detection. WSM service includes Statistical Inventory Reconciliation (SIR) method, alarm management, investigations and operations and deals with the losses entirely. Further informations about the UST systems, wet-stock management and leak detection systems are given below.

1.1. UNDERGROUND STORAGE TANK (UST) SYSTEM

A storage tank which stores petroleum products may either be buried in or be placed above the ground. The UST can be constructed as single skinned or double skinned (Figure 1.2) from different materials such as mild steel, glass reinforced plastic (GRP), or other composite materials.

An UST system consists of a storage tank and underground piping connected to the tank that has at least 10% of its combined volume underground. USTs containing petroleum, petroleum derivatives and certain other hazardous substances must comply with the prospective regulations. Generally, the requirements for a petroleum USTs and that of other hazardous substance USTs are alike [4].



Figure 1.2. Double wall steel petroleum UST [5]

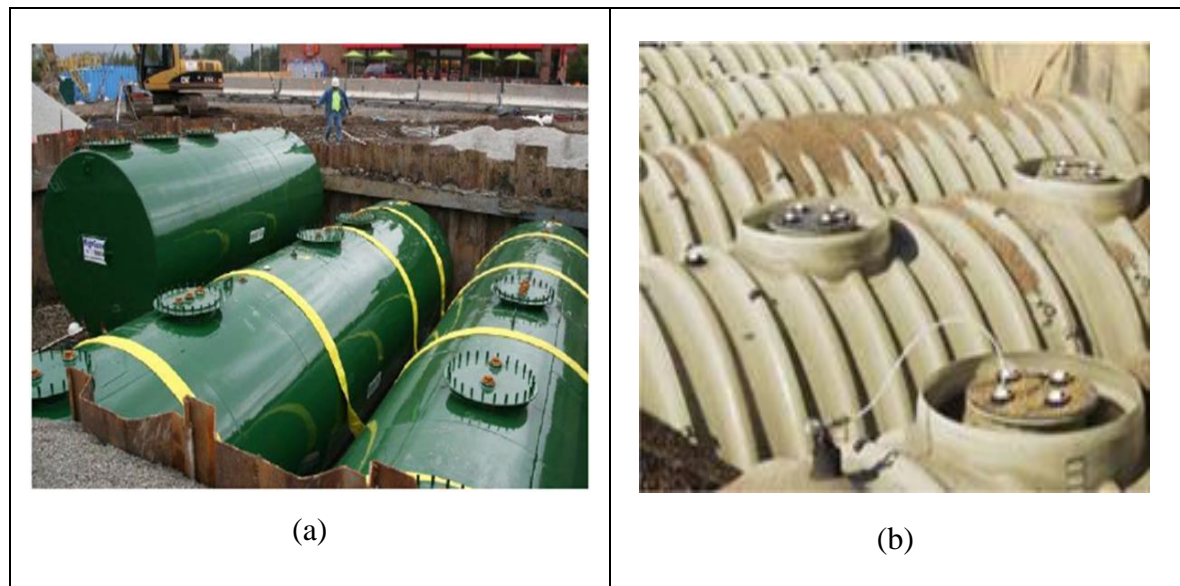


Figure 1.3. Typical (a) steel [4], and (b) fiberglass USTs [6]

USTs may be used commercially as in fuel service stations and convenience stores or non-commercially as in fleet service operators and local governments. The United States federal

regulations apply only to UST systems that store certain hazardous substances such as petroleum. In the US, about 680,000 USTs store petroleum or hazardous substances [7], which, in case of a release can harm the environment and human health. Following the start of the UST program in the US, the number of regulated UST systems significantly reduced when many of the substandard UST systems have been closed. Nearly all of the USTs regulated by the underground storage tank requirements contain petroleum. Environmental Protection Agency (EPA) estimates that less than 10,000 tanks hold hazardous substances covered by the UST regulations [7].

Double walled UST systems can be obtained placing one tank inside another. A single walled tank is the primary containment and a leak can easily escape into the environment whereas the second layer of the double walled UST encloses the leak. Double walled pipe systems can be obtained likewise. In the double walled UST systems, the confined space between first and second wall is called “interstitial”. In any case, a must have for a petroleum UST is a leak detection system, which points to the presence of any leak in that interstitial area through monitoring. Some requirements for the installation of petroleum UST systems are as follows [3].

- Petroleum USTs are buried in a tank pool in order to protect the environment any sudden releases/leaks. The tank pool is also called as “Tank Farm” (Figure 1.4). When the installation of petroleum USTs, steel tanks surrounded by concrete. The concrete is not intended to contain product lost from the tank, but might delay its release into the surrounding ground if it is not cracked or jointed.
- Double walled tanks should be installed on any new or redeveloped sites according to the new or updated UST regulation.
- Petroleum USTs should be installed with automatic tank gauging (ATG) systems to measure the level of product stored in the tank.
- Petroleum USTs should be installed with electronic or mechanical overfill protection devices.
- Where steel tanks are to be utilized, these should be protected using anti-corrosion paint in conjunction with effective leak detection and cathodic protection.
- Fugitive vapors due to breathing losses from USTs shall be released to the atmosphere through vents located at least 3 meters above the roof level.

- Fuel service station retailers are responsible for installation a suitable leak or spill detection system.

Before the regulation was enforced, UST systems were directly buried in the ground without any tank farm; however, an observation well was also dug out in order to detect any leak into the environment.



Figure 1.4. Installation of underground petroleum storage tank [8]

1.2. UNDERGROUND STORAGE TANK PIPING SYSTEMS

Petroleum USTs' piping systems must comply with the UST regulations, as well. The design of piping should be convenient for anticipated working pressures, temperatures and structural stresses and obey to related standard. The construction or installation material of piping should be compatible with petroleum products with which it will be in contact and should be resistant to heat that it may be exposed. When the corrosion of material is considered, it should be sufficiently resistant to guarantee acceptable life times [4]. Further regulations on the instalment and usage of the UST piping can be found in [3].

1.3. LEAK DETECTION IN FUEL SERVICE STATIONS

The leak detection in sites is crucial for environmental safety. Releases from USTs in the form of spill, overfill, leak through tank wall or piping can cause fires or explosions that threaten human safety. Releases from USTs can also seep into the soil and contaminate

groundwater with petroleum or other hazardous substances. The petroleum, which is not stored in controlled conditions or any releases from its containment threaten the environment, has risk to water supplies and is deleterious to aquatic life [9]. Petroleum is a highly volatile and highly flammable with a lower explosive limit (LEL) of 1.4% and an upper explosive limit (UEL) of 7.6% by volume [10]. Petroleum vapor can easily find a way to reach basements of constructions and public drains and it contacts with an ignition source with serious consequences. For example, in 2000, this kind of an explosion happened in Bayrampaşa/Istanbul. The reason of the explosion was the petroleum vapors leaking into the basement. The accident caused deaths of two people and injuries of three people [8].

The average cleanup cost for just one leaking UST was about \$50,000 in 2000 [11]. When releases have resulted in vapors in basements or underground utilities, or have contaminated potable wells, the cleanup costs quickly escalate into the hundreds of thousands of dollars. A long term ground water cleanup where potable water supplies have been affected can cost several million dollars over time. Properly installed and operated release detection equipment, however, would alert the operator to a discharge early on, allowing a quick response which would minimize both damage and costs [11].

Until the mid-1980's, most USTs were made of bare steel, which corrodes and causes leakage. Faulty installation or inadequate operation and maintenance procedures can also cause leakages. In fact, piping leaks are faced more frequently than tank leaks. Most of piping leaks occur at the joints, fittings and flanges, which experience stress during normal operations. On the other hand, improper tank filling practices cause even more release problems compared to leaky tanks or piping. Although, minor spillage during deliveries may not seem important, it may cause significant impact on the environment over time [11].

1.4. LEAK DETECTION FOR PETROLEUM USTs

“Leak detection” or “release detection” is a term used for any operation to determine if the UST system is leaking. Leak detection enables the owner/operator of the UST system to detect if the tanks and piping are leaking contaminants into the environment.

Actually, leak detection is obligatory to prevent or minimize the releases of regulated substances (petroleum, diesel, used oil, etc.) into the environment. It necessitates periodic

monitoring of the tank and its piping [12]. Most of existing leak detection methods require specialized equipment and techniques [13].

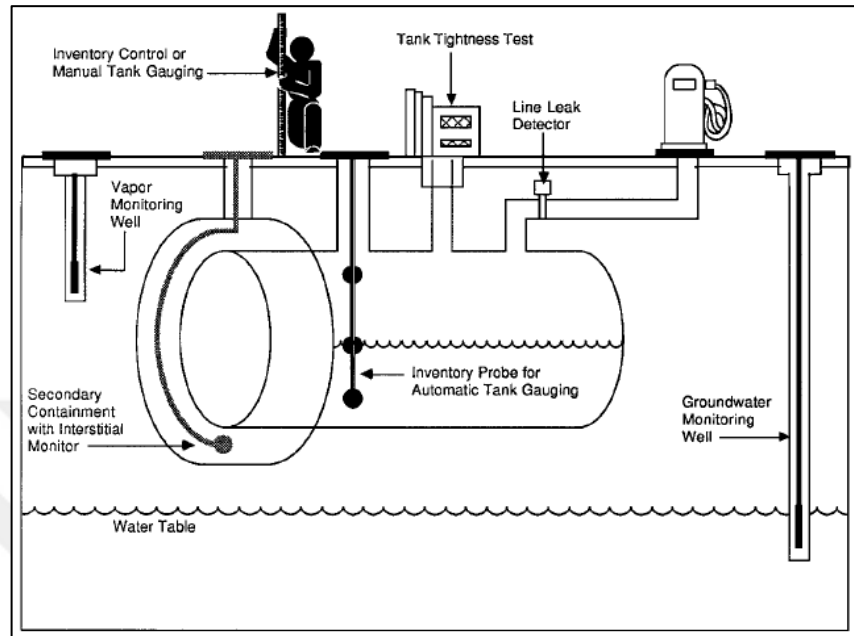


Figure 1.5. Leak detection methods for petroleum UST systems [14]

As of March 2005, almost 450,000 UST leaks had been confirmed in the USA [14]. At some cases without leak detection, leaks were discovered late, after contamination had spread, requiring difficult and costly cleanups. By contrast, effective leak detection enables quick response, thus, minimizing the extent of environmental damage and the threat to human health and safety. EPA has identified the following methods that might be used to meet the US federal leak detection requirements [14].

- Secondary containment with interstitial monitoring
- Automatic Tank Gauging systems (including continuous ATG systems)
- Vapor monitoring (including tracer compound analysis)
- Groundwater monitoring
- Statistical Inventory Reconciliation (SIR)
- Other methods meeting performance standards

The leak detection methods noted above are all monthly monitoring methods. Every UST along with its piping, should utilize at least of the given methods [14]. These methods are explained briefly in the following sections.

As of November 2017, in Turkey, it is observed that the necessary importance has not been given to leak detection for petroleum USTs. In 2006, as a first step, this issue has been deald in “TS 12820 Petrol filling stations – Safety requirements” that covers safety requirements for petrol filling stations. For this reason, there is not enough statistical data on leaky tanks in Turkey. Leak detection methods for petroleum tanks have been again discussed in the newest draft of this standard. A part of the related issue in the draft is that “Leak detection should be done for UST systems at the regular intervals in the fuel service stations and these systems should be rigged with audible or light or otherwise alarm systems. One of the leak detection systems for UST systems is Statistical Inventory Reconciliation (SIR) method based on data obtained from tank automation systems” [8].

1.4.1. Statistical Inventory Reconciliation (SIR)

Statistical inventory reconciliation (SIR) is similar to old-time inventory control, where the operator monitors tank volumes, deliveries, and sales using simple equipment. However, this kind of simple inventory control is comparatively imprecise and may result in large amounts of losses depending on the throughput.

By evaluating inventory data and utilizing statistical analysis, SIR can be more sensitive and accurate than ordinary inventory control. Small releases, which may would go unnoticed with simple inventory control, can be detected with SIR. This method depends on the actual data, thus two vendors' methods are not exactly alike due to the differences in the collected data and the provided results [15].

EPA regulatory performance standard of the leak detection for UST systems is that “Tank system must be tested for releases of 0.1 gallon per hour (9 L/day) with a probability of detection (PD) of 95% and a probability of false alarm (PFA) of 5%.” To be EPA certified to detect leaks in both tanks and plumbing lines, the leak detection system must be able to detect a leak of 0.1 gph (9L/day)” [16].

SIR method meets EPA performance standards, being able to detect releases of 0.1 gallon per hour (gph) with a PD of 95% and a PFA of 5%. Mostly, SIR vendors need a few months of good data in order to detect releases of this magnitude (9L/day) regardless of the tank size. Any SIR analysis has only three possible bottom-line responses which are ‘pass’,

'inconclusive', or 'fail'. If the estimated leak rate exceeds 9 L/day, which is also called the threshold leak rate, SIR analysis reports that the UST system is 'fail'. Otherwise, the UST system can be reported as 'pass', or 'inconclusive'. While a 'pass' denotes that there is any loss or leak in the UST system, an 'inconclusive' denotes that the collected data is not enough to analyze the UST system, which have no effective leak detection for that month [15].

1.4.2. Secondary Containment with Interstitial Monitoring

This method detects leaks in the space between the primary wall and a secondary barrier of the tank (Figure 1.6). The US federal UST regulation describes general performance requirements for interstitial monitoring with double-walled USTs, USTs fitted with internal liners, and USTs using secondary barriers [4].

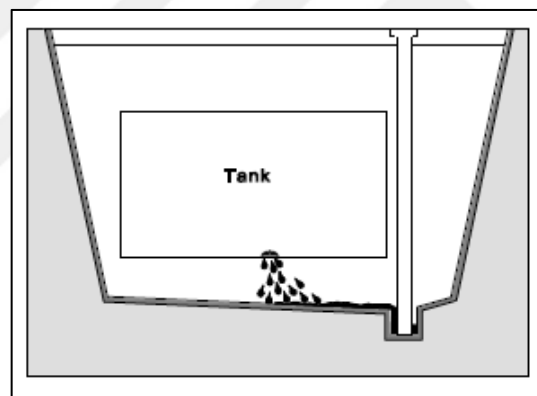


Figure 1.6. Secondary containment with interstitial monitoring [14]

1.4.3. Automatic Tank Gauging (ATG) Systems

As Figure 1.7 (a) shows, this method uses automated processes to monitor product level and perform inventory control. For example; TLS 350R is a multifunctional tank level sensor console, whose one of the functions is inventory control [4].

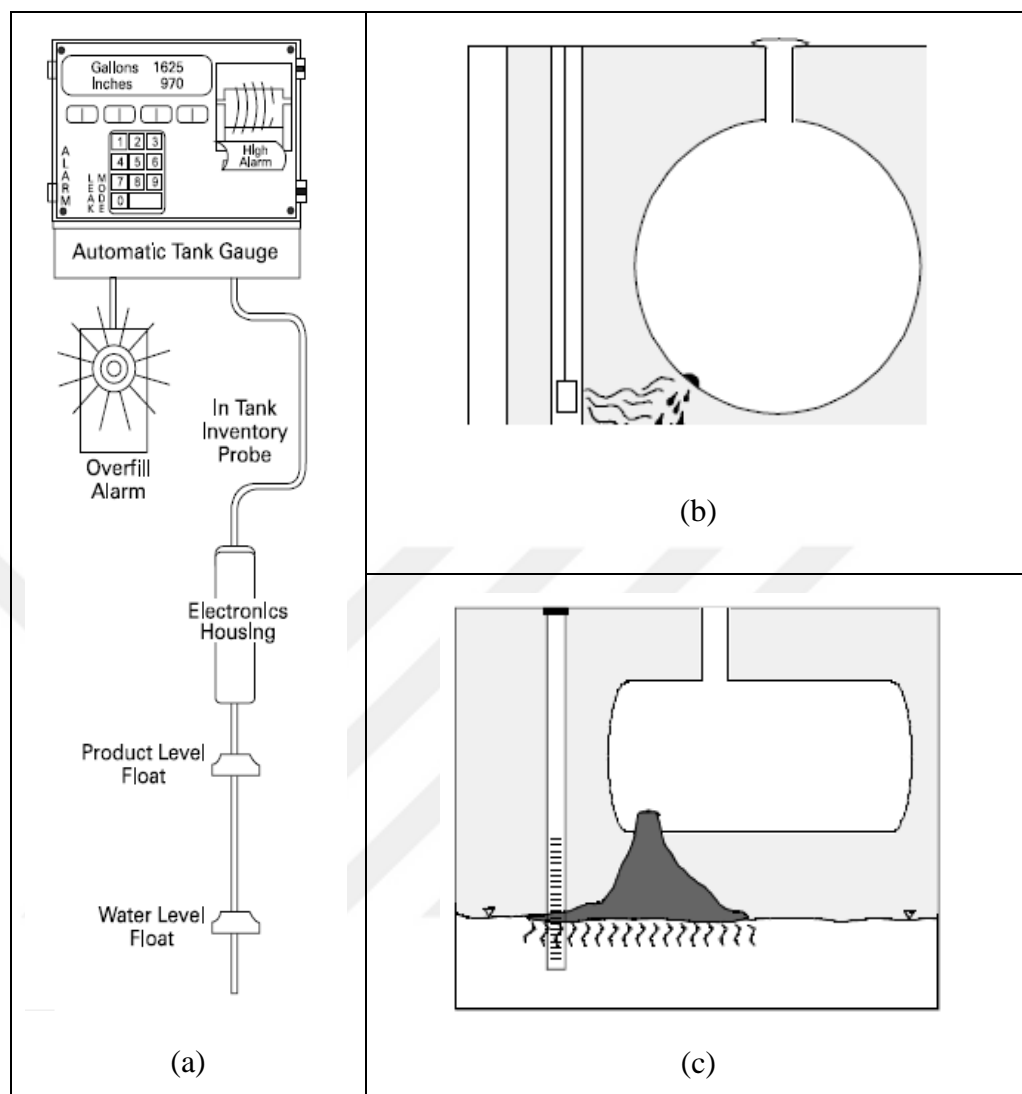


Figure 1.7. (a) Automatic Tank Gauging (ATG) systems [14] (b) Vapor monitoring [14] (c) Groundwater monitoring [14]

1.4.4. Vapor Monitoring (Including Tracer Compound Analysis)

This method samples for hydrocarbon vapors (sometimes called passive monitoring) or tracer compound vapors (sometimes called active monitoring) in the soil surrounding the UST (Figure 1.7 (b)). Released petroleum produces vapors that can be detected in the soil. The federal UST regulation describes several requirements for using vapor monitoring. For example, this method requires that the stored substance can migrate through a porous backfill material, so that it can be detected within 30 days. For this reason, a site assessment must be conducted prior to using the method to ensure site conditions meet the requirements [4].

1.4.5. Groundwater Monitoring

This method monitors the groundwater near an UST for the presence of released product in the water. Selected wells near the UST are checked frequently for petroleum (Figure 1.8 (c)). The UST regulation describes several requirements for using this method. Such as, this method is prohibited if the water table is more than 20 feet below the surface of the ground [4].

It is clear that leak detection control goes hand in hand with the inventory control of the liquid fuels. Because of the environmental hazards and the economic aspects, automated inventory control, or “Wet-Stock Management Services” also include leak detection systems.

1.5. WET-STOCK MANAGEMENT (WSM) AT FUEL SERVICE STATIONS

In technical terms, wet-stock is the liquid fuel contained in controlled storage conditions. Wet-stock management is a system based mainly on three headings: (i) leak detection, (ii) corrective-preventive-protective action, and (iii) cost saving. Most sites submit the periodic wet-stock data to a third party company in order to meet leak detection requirements. This company uses Statistical Inventory Reconciliation (SIR) method which detects unusual losses or gains. Even in the case of very low leak rate, leaks are detected much more quickly by SIR analysis preventing any further escape. Thanks to wet-stock management, all fuel service stations comply with the regulations [9].

First step is the wet-stock reconciliation. The inventory is calculated by subtracting the amount sold (i.e. output) from the amount of stock delivered into the underground storage tanks (i.e. input). Then, what is left in stock is measured. Any differences between what is expected to be in stock (i.e. theoretically calculated amount) and what is left in stock (i.e. measured amount) can be due to gains or losses [9]. West Yorkshire Fire & Rescue Service [17] defines stock or inventory control as follows: “Many fuel service station operators rely on a manual wet-stock reconciliation system to detect leaks from the storage tanks and pipework. The basic aim is that by finding how much fuel has come out of a tank through the dispensers (by checking the totalizer readings) and taking into account how much has been put into the tank. Thus, how much should be left in the tank can be calculated. Then,

how much fuel actually is in the tank is measured. If there has been a variance which could indicates loss or gain”.

The basic method for the wet-stock reconciliation, and/or inventory control is a proper material balance. Material balance is based on the law of conservation of mass, which states that mass is neither created nor destroyed. Material balance for a system that has certain boundaries is written as follows:

$$M_{in} + M_{gen} - M_{out} - M_{con} = M_{acc} \quad (1.1)$$

Any material, which enters leaves or accumulates in any system, can be accounted by Eq. 1.1. This equation can be applied to the total mass of the material or its' sub-systems such as molecular or atomic species involved in the process.

The accumulation term for steady-state continuous process equals to zero. Thus, the general mass balance equation can be simplified to:

$$M_{in} + M_{gen} = M_{out} + M_{con} \quad (1.2)$$

If the process is purely physical without a chemical or a nuclear reaction, the generation and consumption terms in Eq. 1.2 will become zero. The equation for steady-state physical process will further simplify to:

$$M_{in} = M_{out} \quad (1.3)$$

General material balance is applied to UST system which can be classified as a transient system, because they have an additional feature of continuous addition and/or removal components/streams. Accumulation term in the general material balance equation is not equal to zero for the transient systems. Besides, there is no chemical reaction in those UST systems. In addition, including time into equation through “rate of” expression (i.e. \dot{m}), the mass balance for transient systems with no chemical reaction will become:

$$\{\text{rate of accumulation}\} = \{\text{rate of input}\} - \{\text{rate of output}\} \quad (1.4)$$

If we introduce the below relationship between volume, density and mass.

$$M = \rho \times V \quad (1.5)$$

Eq. 1.4 can be expressed as:

$$\frac{d}{dt}(\rho V) = (\rho \dot{V})_{in} - (\rho \dot{V})_{out} \quad (1.6)$$

In Eq. 1.6, ρ , V and \dot{V} show the density, volume and volumetric flow rate, respectively. Assuming constant temperature, thus constant density gives:

$$\rho \frac{d}{dt}(V) = \dot{V}_{in} - \dot{V}_{out} \quad (1.7)$$

Assuming density is constant, it cancels out.

$$\frac{dV}{dt} = \dot{V}_{in} - \dot{V}_{out} \quad (1.8)$$

In order to utilize the Eq. 1.8, we need to identify following: while $t=0$, $V=V_0$ where V_0 is initial volume of tank contents. At time equal to zero ($t=0$), UST has an initial volume, $V_{initial}$. Depending on tank capacity, sales capacity and tank level, UST is refilled in a specific delivery period. Delivery volume recorded by an automatic tank gauging (ATG) is represented by $V_{delivery}$ and invoiced volume in the terminal (with respect to $T_{ref}=15^{\circ}\text{C}$) has been represented as $V_{invoiced}$. Dispensed volume from tank has been represented as V_{sales} . Final volume of tank content is V_{final} . Input and output streams of UST system are delivery volume and sales volume, respectively. Accumulation volume of that system is determined according to the equation.

$$\frac{dV}{dt} = \dot{V}_{delivery} - \dot{V}_{sales} \quad (1.9)$$

When analyzing the whole system, initially tank content is known as $V_{initial}$. The sum of the accumulated and initial volumes gives the book inventory. (What your recordkeeping indicates you should have). The final stick inventory is what ATG has measured.

Variance = Final Stick Inventory - Book Inventory

$$\text{Var} = V_{final} - (V_{initial} + V_{delivery} - V_{sales}) \quad (1.10)$$

Eq. 1.10 shows that “variance” is the difference between the calculated amount of fuel available in a tank at any given time, and the actual amount of fuel available in the tank. At this point, it should be noted that the calculated amount, which is obtained according to recorded deliveries and sales, is usually a true value unless a major mistake was done in book keeping. Thus, the main source of variance is the measurement errors. Depending on the error in the measurement, it can either be positive or negative (loss or gain). Variance is

collected under two main headings, which are “apparent variance” and “real variance”. Real variances are caused by physical fuel losses, which occur during incidents within a fuel service station. Thus, real variance is a loss of inventory which can have a significant impact that can result in fines or notice of violation. The primary sources of real variances are listed as follows:

- Delivery discrepancies
- Volume change due to temperature and Evaporation
- Pump calibration (Pump meter accuracy - Over dispense or Under dispense)
- Equipment problems
- Theft (Human intervention)
- Spillages
- Leaks

On the other hand, apparent variances are caused by measurement and accounting errors, and can lead to additional liabilities and tax implications for a business. The sources of apparent variances are adjusted losses caused by administration errors and poor tank calibration, those which can mask any actual fuel losses. Towing to their results, poor or inaccurate data are undesired cases in wet-stock management at fuel service stations [18].

Administration errors can be related to tanker deliveries, pump sales and tank level readings. Incorrect delivery quantity, inaccurate allocation of split pots, delivery assigned to the wrong tank, tank overfill-calculation of spillage/residual amount, wrong transfer/uplift quantities and allocating the delivery to the wrong day are relating reasons to tanker deliveries. Misreading of pump totalizers, miscalibration of sales from totalizer readings, POS (Point Of Sales) system problem and incorrect treatment of pump tests are relating reasons to pump sales. Inaccurate dipstick readings, short dipstick, poor probe calibration and poor tank calibration are related reasons to tank level readings. Furthermore, unrecorded end-of-day readings and those which are not in synch with pump totalizers readings (if process not automated) lead to apparent variance due to measurement and accounting errors relating to tank level readings [19].

1.6. TANK CALIBRATION

Error in volume conversions (i.e. converting measured liquid height to liquid volume) is a major cause for fuel variance and a major problem in WSM. For this reason, accurate measurement of tank level is one of the most important parameters for wet-stock management at fuel service stations. Dipsticks were once very common and are still used on some older fuel sites. There are several disadvantages of manual measurements which are inaccuracy, not appropriate with offset fills, not consonant with vapour recovery and limited access to tanks with traffic. Due to those disadvantages and necessity, electronic gauges were developed during the 1970s. One of the developer companies is Veeder-Root which introduced the TLS (Tank Level Sensor) (Figure 1.8 (a)) and Magnetostrictive probe (Figure 1.8 (b)) systems [20].

Poor probe calibration is the most significant cause of insufficient performance in electronic gauges, and, precise height to volume conversion is the essential basis for efficient reconciliation processes in wet-stock management at fuel service stations. The probe should register actual level of the fuel by comparing to an absolute measurement, detect the smallest fuel level change, and provide exactly the same reading every time the fuel level returns to exactly the same point. Magnetostrictive probes supply consistent source data for calibration algorithm to convert height to volume. It provides high quality height and temperature measurements [21].

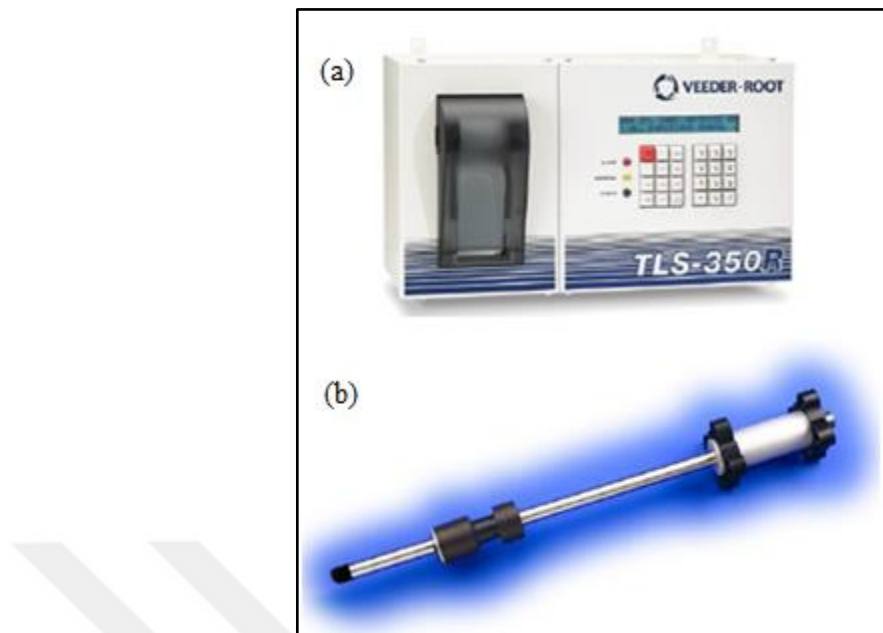


Figure 1.8. (a) TLS console (b) TLS magnetostrictive probe [21]

All methods of tank gauging measure the fuel level in the tank and the ullage, which is the space above the fuel level (Figure 1.9).

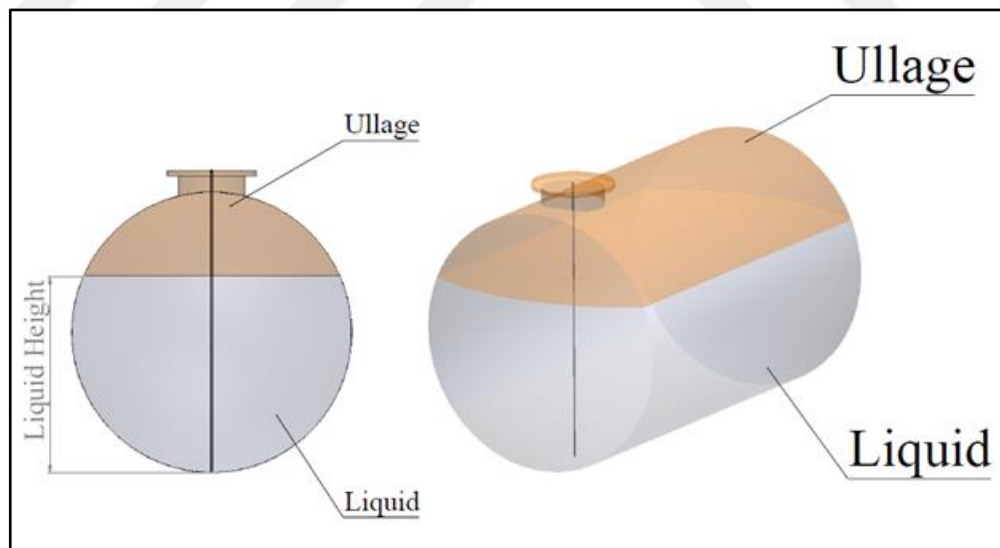


Figure 1.9. Fuel level measurement

The measured fuel level is then converted to volume according to tank calibration chart, which is installed into the TLS unit. The tank calibration chart in the TLS unit is a series of levels coupled with respective volumes. The chart prepared depends on the storage tank dimensions. Tank calibration charts for horizontal and vertical cylindrical tanks are given in

Figure 1.10 as an example. In this figure, it can be seen that while the chart of a vertical tank is a line with a constant slope, that of a horizontal tank slope is polynomial.

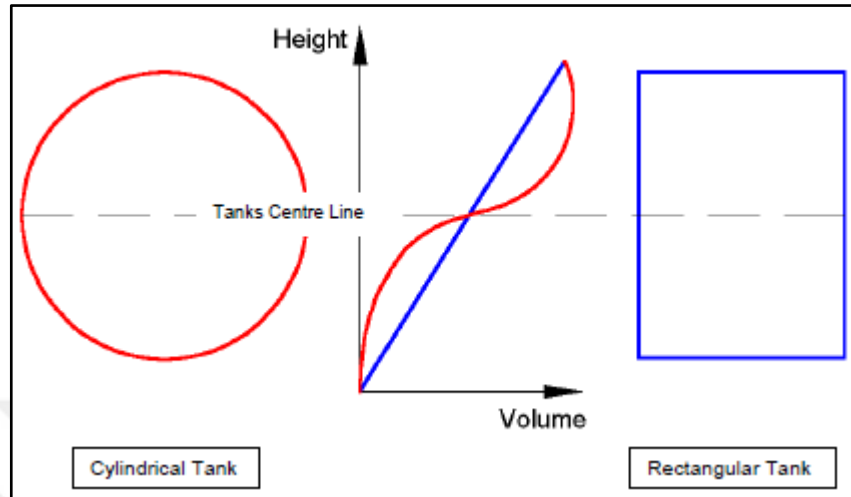


Figure 1.10. Comparison of LV graphs of cylindrical and rectangular tanks [20]

There are three essential parameters for tank calibration, which are diameter, total capacity and end shape (i.e. flat or capped). On a new site, sufficient parameters should be available to prepare an accurate tank calibration chart. Using these parameters, tank calibration chart is provided with the UST during installation. Not all that, the measurement of actual tank dimensions on an existing site (i.e. underground tank) is not possible [22].

There are several methods which are used to calibrate industrial storage tanks using their sizes, shapes and uses. The first method is called “Gravimetric Calibration”, which is more suitable for small capacity and movable tanks. In this method, the weight of empty tank is measured and then, the vessel is filled up with a liquid of known density. Then, the vessel is again weighed and the mass difference is obtained. Finally, the mass difference is converted to the product volume [23].

The second method is called “Geometric Calibration”, which is proper for large-capacity fixed tanks with known or measurable dimensions. Tank geometry equation is formed in order to determine product volume. Geometric calibration method is preferably used for tanks with regular shape such as, cylindrical or rectangular. The accuracy of tank dimensions, measurement uncertainties, and tank imperfections critically affects the preciseness of this method [23].

The third method is called “Volumetric Calibration”, which is suitable with underground tanks or large-capacity with irregular shapes or strong deformations. The method begins with filling a tank successively with volumetric standard or by a volumetric meter. Level and the corresponding volume are recorded and a LV (Level to Volume) chart is generated (Figure 1.11). When the volumetric and geometric calibration methods are compared, volumetric calibration often yields better precision. In contradistinction to the volumetric calibration, it is fast and does not require any liquid media that might cause production or tank problems [23].

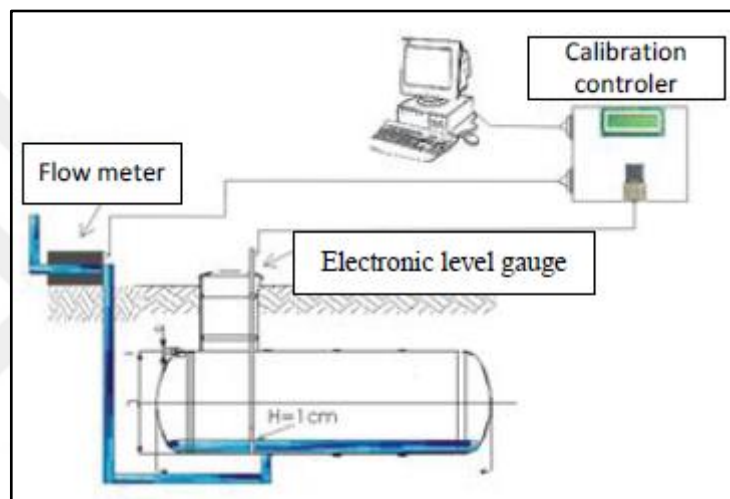


Figure 1.11. Volumetric calibration technique [24]

A newer calibration method is called “Laser Scanning Calibration”, which is an automated measuring system based on scanning method used for horizontal tank. Distance measurement by laser ranging technology and angular measurement by optic-encoding principle are applied to obtain coordinate values of points on tank inner shell (Figure 1.12 (a)) [25].

3D laser scanning which is a novel approach to the calibration of horizontal fuel tanks uses accurate laser and scans horizontal fuel tank from inside (Figure 1.12 (b)). Volume of the tank is determined and measurement uncertainty is estimated from scanned results using data processing algorithms. When the volumetric calibration and the 3D laser calibration are compared, it is obviously seen that volumetric calibration process involves a certain amount of water subject to the fuel tanks capacity and the fuel tanks must be cleaned again to avoid further incorrect tank usage after the process is completed. The 3D method has some advantages over volumetric calibration method. The advantage is time saving which the

calibration duration of the same tank with 30-40 m³ capacity takes 4 to 5 hours and 5 minutes for the 3D method and the volumetric method, respectively. In the 3D method, a full tank is scanned two or three times and the number of scans can be changed according to tank volume. Data processing lasts 5 minutes and total duration of calibration process is around 30-45 minutes [24].

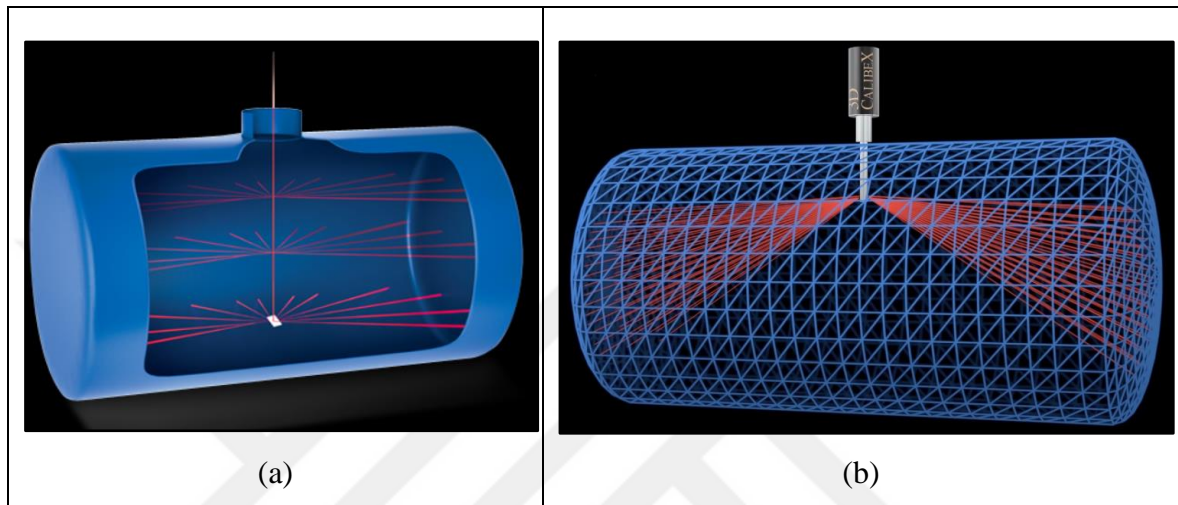


Figure 1.12. (a) The 3D calibration scan [26] (b) Tank wireframe [27]

Although initial tank calibration chart is provided by the tank manufacturer, problems may appear upon installing or throughout the time. The major problem faced stems during the conversion of the measured height to the fuel volume. As Figure 1.13, the most common reason for this problem is the wrong or poor calibration charts [18].

1.7. POOR TANK CALIBRATION

Tank calibration chart has a significant importance in calculating the inventory and ullage as well as accurate dipstick or probe measurements. Whilst tank charts themselves do not lead to a fuel loss, an incorrect tank calibration chart affects gathered inventory data and contributes to masking sources of real fuel loss. There are several reasons of inaccurate tank calibration chart. These are listed in the below [18]:

- The initial tank calibration chart which is provided by manufacturer could be inaccurate.
- Following the installation, tank could tilt in axial, in radial, or in both directions.

- Tank manufacturer specifications such as diameter, length and end shape could change with time (structural deformation) or reported inaccurately.
- Tank shape has been affected by additional support structures added around the tank (structural deformation).

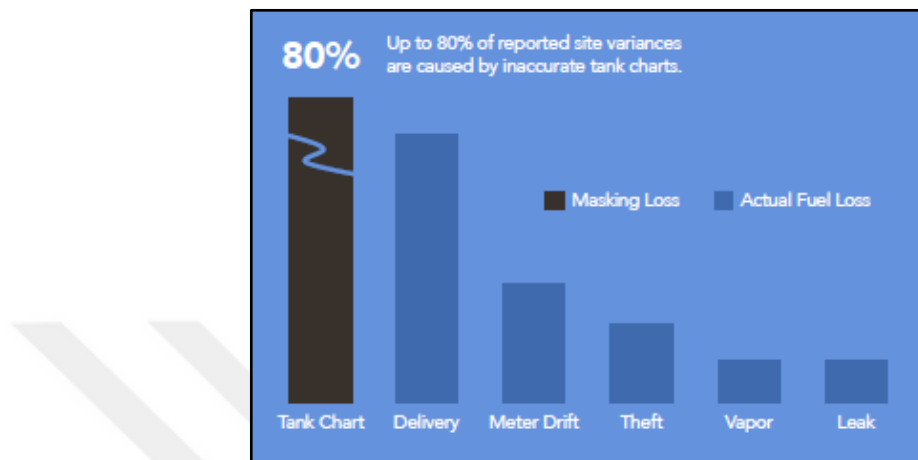


Figure 1.13. Masking loss and actual fuel loss percentages [18]

Veeder-Root [20] reports two conversion errors. A short conversion which is the first of these occurs when the tank system seems to be smaller than the corresponding tank calibration chart. The second of these is a long conversion error which appears to be larger than the corresponding tank calibration chart. The main obvious characteristic of short conversion error is large gains on delivery days offset by small losses on the majority of days following [28]. The same phenomenon is reported as “over calibrated” and “under calibrated” in [20]. A sample variance trend of a short conversion error can be seen in Table 1.1, in which “L/G” means “Loss/Gain” and it represents variance. In addition, “%L/G” column in the table is obtained by dividing sales by L/G (i.e. variance), and then multiplied by one hundred.

The specifications of the tank (diameter, length, and end shape) may be reported inaccurately or change throughout time (deformation). Moreover, after a period of time, USTs incline vertically or horizontally. That displacement leads to inaccurate tank calibration chart and corrupted total tank volume. Tank recalibration is a significant point under the aforementioned circumstances. There are a lot of calibration techniques such as gravimetric calibration, geometric calibration, volumetric calibration, and laser scanning calibration. On a site, sufficient tank dimension information should be available. However, on an existing one, tank dimensions have to be obtained from available data which are initial tank level and

initial tank temperature, final tank level and final tank temperature, sales during the period and delivery during the period.

Table 1.1. Effect of poor tank calibration on daily variances [20]

Day	Open	Delivery	Sales	Book	Close	L/G	%L/G
1	16556		3269	13287	12894	-393	-12.02%
2	12894	11000	2665	21229	21811	582	21.82%
3	21811		1777	20034	19841	-193	-10.85%
4	19841		1477	18364	18233	-131	-8.84%
5	18233		3432	14801	14519	-282	-8.21%
6	14519	11000	3702	21817	22289	472	12.75%
7	22289		3987	18302	17939	-363	-9.11%
<hr/>							
Total Sales			20309			-308	-1.52%

At this point, the causes for poor/inaccurate tank calibration can be grouped in two categories: (i) uniform deformations and (ii) non-uniform deformation. The aim of this study is to reduce or minimize the variance thus enable to detect the actual losses (i.e. leaks) in a UST system. For this purpose, several theoretical tank models are formed. Tank tilt, end shape and tank dimensions are taken as tank parameters by using geometric and trigonometric relations. The mathematical models are based on two tank types: (i) simple cylinder tank and (ii) simple cylinder with spherical dished head. The effect of positive and negative tank tilt on the measured fuel level is investigated by determining geometric relations. All considered tank parameters (R , L , H , M , α , β) were tested by using real time data for different site to obtain better or accurate height to volume data. As a result, the apparent variance appearing due to the wrong volume conversion is eliminated. Virtual variances are removed and the masking effects of poor tank calibration on real variances are eliminated.

This manuscript is organized as follows. A literature survey on previous studied on the related subjects is given in Section 2. Theoretical tank models and mathematical relations are given in Section 3. Section 4 includes the results of the modeling studies with

discussions. Conclusion is given in Section 5. Finally, the last section of this study is Section 6 : Future work.



2. LITERATURE SURVEY

Many researchers from universities and industrial companies have spent time on trying to find the effects of the tank geometry, fuel level gage position, and inclination of the tank on the differences between the ideal volume and the calibrated volume of the underground storage tanks.

In the work of V.V. Nosach [29], calibration characteristics of twenty types of inclined cylindrical storage tanks were examined by a geometric method and it was found that the inclination angle and the probe location are very influential factors when it is to calibrate an inclined storage tank. It was reported in the paper that the inclination angle would have little effect on the calibration characteristics if the probe was located in the middle of the tank and the inclination angles greater than 0.001 should have been taken into consideration if the probe was located above or below the middle of the tank.

Y. Zhipeng and C. Shengshuang [30] performed a set of experiments whose data is used to determine deflection parameters of lateral angular deflection and vertical deflection inclination angle with nonlinear least squares method and the help of deformation integral model. It is concluded in the article that vertical and horizontal deflection of the storage tank are deduced from the model and so that tank calibration table could be obtained exactly after tank deformation.

C. Li, Y. Yuan, L. Song, Y. Tan and G. Wang [22] developed a fuel volume and height relationship using an integral method for two tanks with different geometrical end caps and then tanks with longitudinal inclination and lateral deflection were studied to obtain a nonlinear optimization model by using cut-complement algorithm and Newton iterative method so that deflection parameters were calculated using computer software. It was noted that accurate calibration was unable to be obtained when the tank was almost full or had very little fuel in it.

Ma. Gorawski, M. Skrzewski, Mi. Gorawski, and A. Gorawska [31] reported in their articles that leakage, theft, or other errors might lead to variances in values of fuel stored in the tank, sold from the dispenser and delivered by the tanker so that a tank calibration method based on a neural networks algorithm was presented to improve the calculation.

In the work of V. Knyva and M. Knyva [24], a new tank calibration method based on 3D laser scans and advanced data processing was presented to meet the need for recalibration of horizontal fuel tanks due to deformations induced by the installations or any geological reasons. It was concluded by the authors that with this new technique calibration time could be reduced by 3 to 4 times, the measurement expanded the standard uncertainties as required by Lithuania's standard.

W. Xie, X. Wang, H. Cui and J. Chen [32] obtained an oil volume to vertical, horizontal tilt and displayed height of the fuel model, then according to the fuel data given in a day, an optimization model for a tilted fuel tank was constructed to get parameters for horizontal and vertical tilting for that specific case by using the nonlinear least squares method so that a new tank-volume meter was available which recovered the tilted oil tanks due to deformation of the ground work and construction.

J.Wang, Z. Liu, L. Tong, L. Guo, X. Bao, and L. Zhang [25] presented a volume measurement method based on laser scanning principle for horizontal tanks. An experimental system was designed and it was reported that relative errors for all tests were smaller than 0.4% for full range of liquid level that satisfies the horizontal tank calibration regulation.

Y. Li, A. Yang, and X. Wang [33] established a mathematical model which indicates the relation of fuel volume, fuel height and the position parameters such as vertical tilt angle and the horizontal deflection angle of a horizontal cylindrical tank with spherical ends. Deflection parameters could be determined by using actual test data with this mathematical model so that the calibrated volume information could be supplied. The authors indicated that the inclination angle had a great effect on the tank capacity indicator. They also reported that although the mathematical model neglected the influence of the temperature and pressure on the tank, these effects could be taken into account by correction methods and calculus formula.

Y.K. Sharma, A. Majhi, V.S. Kukreti, and M.O. Garg [34] indicated in their article about the breathing loss of gasoline that the main reason of fuel losses in retailing operation was the volatile nature of gasoline so that determination of the that loss became crucial because it had continued to exist all the time leading to somewhat environmental and financial burden on the country. In their study of gasoline losses, they have proposed an empirical model for

the calculation of the breathing loss of both underground and above ground storage tanks. A user-friendly model was established so that day to day estimation of the loss has been possible with easily accessible parameters such as the surface temperature of the tank, reid vapor pressure and number of days, minimum and maximum temperature variations and ullage of the tanks.

M. Gorawski, A. Gorawska, and K. Pasterak [13] revealed the TUBE algorithm in their manuscript about the early detection of fuel leaks from underground storage tanks. They indicated that specialized equipment have been needed for most of the leak detection techniques so that it would be very desirable to use software-based methods that have worked with data analysis because they would require no changes in the infrastructure of the petrol stations. Provided with an autonomous algorithm, the TUBE method is said to detect fuel leakage from underground storage tanks by using only stored, sold and delivered fuel data and identify any uncertainties and oscillations in data to approach more stable trends which was also compliant with the EPA SIR standard.

3. METHODOLOGY

In this section, theoretical tank models are established in order to obtain correct liquid height to liquid volume relations. By incorporating the possible tank deformations into volume equations, variance trend is improved and the masking effect of poor tank calibration chart is prevented.

Commonly used petroleum storage tank types are simple cylindrical and simple cylindrical with dished head. Therefore, these two type are explained in a detail by considering different parameters such as radius, length, dished head depth, probe offset and tilt (i.e. axial and radial or both). Mainly, using a specific tank (i.e. simple cylindrical tank), two essential factors are investigated. Firstly, simple cylinder tank with flat ends was examined and its volume equations were derived. Then, the effect of factors on its volume was determined. If dished head is available, the tank model is classified as ‘cylindrical tank with dished head’. The spherical dished head volume equation was investigated. The total volume of this tank type is obtained by summation of a simple cylindrical tank volume and two dished heads. Another factor is the tilt angle. A tank can be tilted axially (i.e. α), radially (i.e. β), or in both directions (i.e. α and β). Considering negative and positive tank tilt, various theoretical tank models were derived using these two basic tank models.

After the establishment of tank models, adjustment types are explained. These adjustments depend on the deformation type, which are uniform and non-uniform. According to the variance pattern, the adjustment type is chosen and the procedure is applied. This will be explained in Section 4: Results & Discussions.

Obtaining precise liquid height to liquid volume relations instead of already existing poor tank charts is the main focus of this study. One major assumption is that, the measured liquid height (h) should not include errors. The experience and the actual applications of the level probes validate this assumption.

The obtained models enable us to detect the nature of the deformation and thus required correction. Upon obtaining the corrected parameters, the variances were re-calculated by using the corrected volumes. However, in the case of non-uniform deformations, changing the tank parameters did not improve the local errors in the tank. For such a case, an error (or

corrector) function is derived. As it can be seen in Section 4: Results & Discussions, the methods applied reduces the apparent variance and enables the detection of the small leaks.

3.1 SIMPLE CYLINDER TANK (SCT) MODEL

Petroleum USTs are in the cylindrical form with various ends such as flat ends, spherical dished head and elliptical dished head. Here, we start with a simple cylinder tank (SCT) model. A cylinder body with no dished head is classified as SCT. The simplest case for obtaining height to volume relation is the horizontal SCT as shown in Figure 3.1.

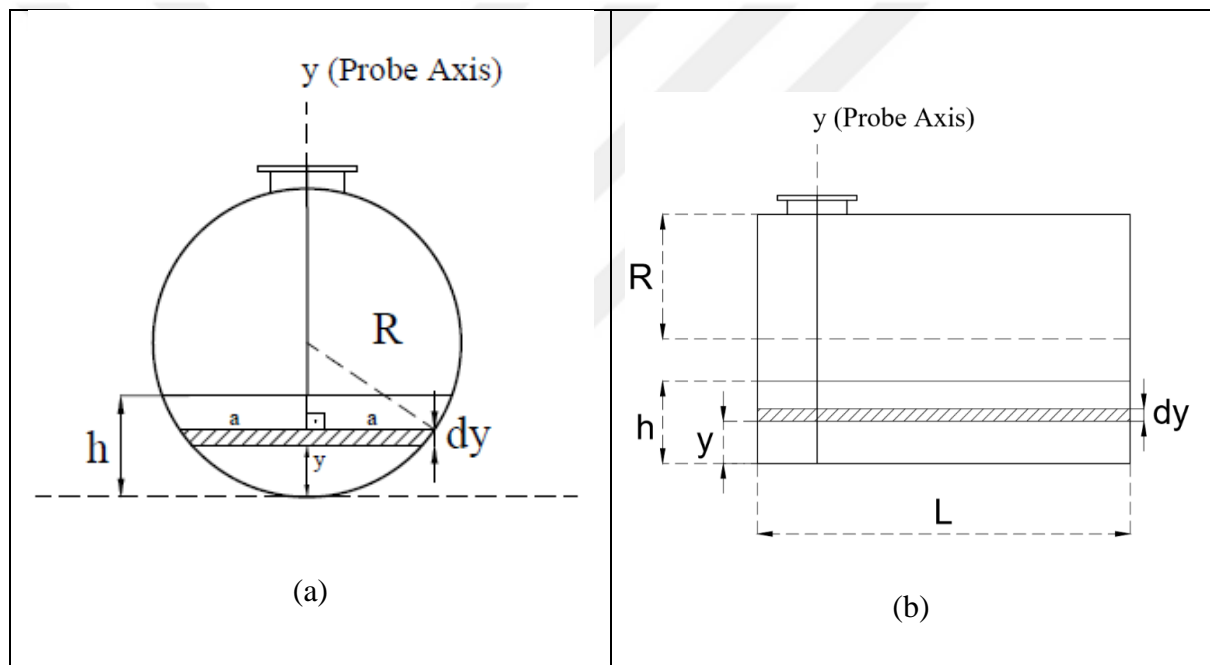


Figure 3.1. The side (a) and the front (b) view of SCT

As Figure 3.1 (a) shows, the required parameters to drive the height to volume (h -V) model of this tank are:

R: Tank radius

a: Half lenght of fuel surface

h : Instant fuel height

The volume of the liquid of height “ h ” in a SCT is determined by integrating the chosen slice along the tank height (h). Appendix A.1 gives the details of the derivations.

$$V_c = L \left[\sqrt{2Rh - h^2} (h - R) + R^2 \cos^{-1} \left(1 - \frac{h}{R} \right) \right] \quad (3.1)$$

By using Eq. 3.1, it is possible to calculate the volume of the liquid at level “h” in a horizontal simple cylinder tank.

3.1.1 Radial (Horizontal) Tilt

One of the major problems in accurate tank calibration is the tilting of the tanks. It is possible for an UST to tilt in axial, radial, or in both directions. As the first case here, we will consider the tilting of the tank along radial (or horizontal) plane. This kind of a tilt of β degrees (Figure 3.2) can be considered as one of the following cases:

- (i) Assuming the probe keeps its relative perpendicularity with respect to tank axes, the probe will tilt β degrees with the tank, or
- (ii) Assuming the tank does not tilt radially, the probe may tilt β degrees.

It can be seen that in both of the cases above, the contact angle and height of the probe and the liquid surface would be the same, which is actually an essential point. Another point is the tilt being symmetrical in either positive or negative directions. These simplifications help us to drive a single relation for the ‘corrected height (h)’ based on the ‘wrong measurement (h')’. The corrected height can be inserted directly into the height to volume (h - V) relations. Figure 3.2 shows that we have included this effect into our models by defining on horizontal tilt angle, (β).

As Figure 3.2 shows that the required parameters to drive the height to volume (h - V) model of this tank are:

R : Tank radius

h : True liquid height (Fuel level when tank position is parallel to the ground plane)

h' : Measured liquid height by probe

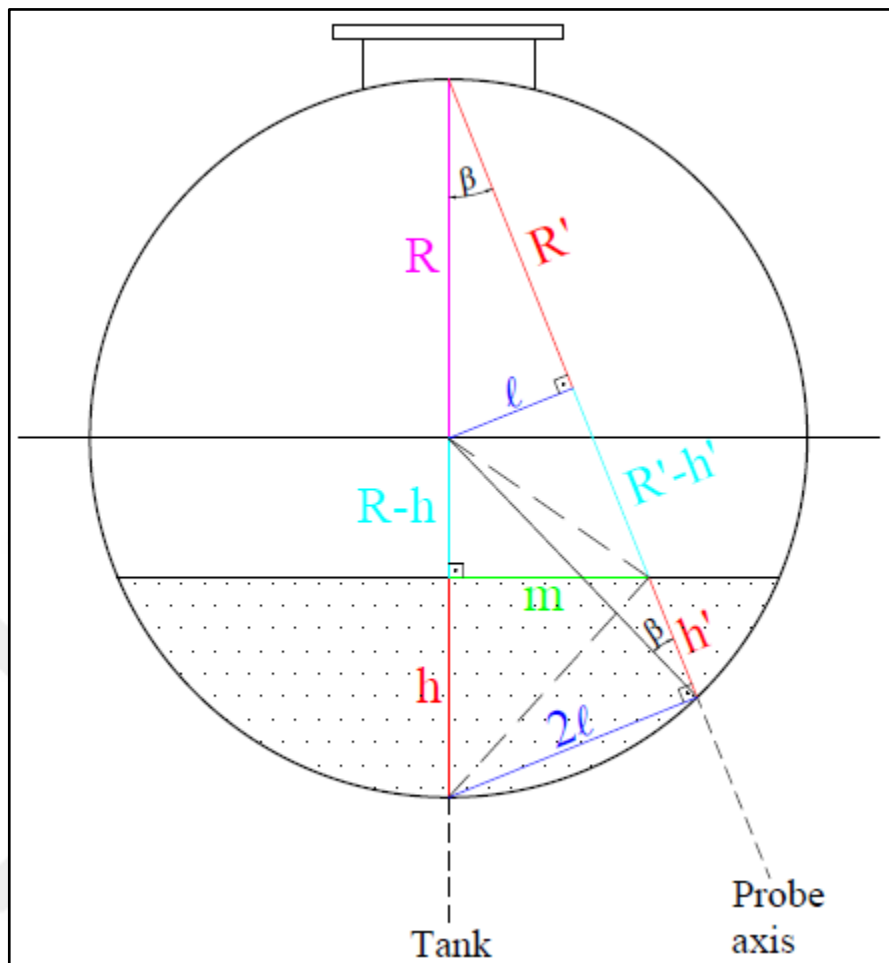


Figure 3.2. Effect of radial tilt on the measured fuel level

Using simple geometric rules, the relation between the measured fuel level and the true fuel level is determined as follows. The details of the derivation can be seen in Appendix A.2.

$$h' = (h - 2R \sin^2 \beta) \sec \beta$$

Or it can be expressed as follows:

$$h = h_{\text{corrected}} = \frac{h'}{\sec \beta} + 2R \sin^2 \beta \quad (3.2)$$

Upon measuring the wrong level (h') and correcting it, this corrected height (h) can be used in Eq. 3.1 for both the tank tilt and/or the probe tilt cases. Symmetrical tilt in $+\beta$ direction produces same results with tilt in $-\beta$ direction.

3.1.2 Axial (Vertical) Tilt

Following the radial tilt given above, we will continue with the derivations for a tilt in axial (vertically) direction. Unlike the radial tilt case, this time, tilts in $+\alpha$ and $-\alpha$ directions (Figures 3.3 and 3.6) produce different results because of the asymmetry introduced by the man-hole (i.e. probe) position. Another effect of this asymmetry is the position and the volume of the liquid that lies beneath the minimum probe (i.e. measurable) level. Thus, both cases will be treated separately.

Effect of Positive Axial Tilt ($\alpha > 0$):

Nonmeasurable volume of SCT with positive axial tilt is determined using the geometric relations and the below Figure 3.3.

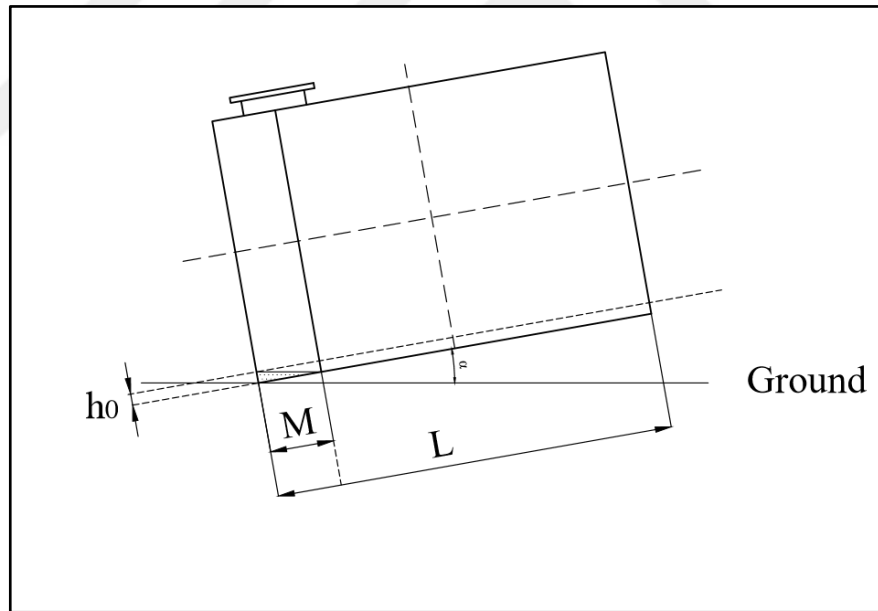


Figure 3.3. Nonmeasurable (V_0) volume of SCT with positive axial tilt

h_0 : The fuel level in the tank, mm

The slope of the fuel line is determined as follows.

$$\tan \alpha = \frac{h_0}{M}$$

$$h_0 = M \tan \alpha \quad (3.3)$$

Calculable h_0 is obtained by Eq. 3.3 and inserted into the Eq. 3.1. Thus, nonmeasurable fuel volume (V_0) is calculated as follows.

$$V(h_0) = L \left[\sqrt{2Rh_0 - h_0^2} (h_0 - R) + R^2 \cos^{-1} \left(1 - \frac{h_0}{R} \right) \right] \quad (3.4)$$

Where,

$$V_0 = \frac{V(h_0)}{2} \quad (3.5)$$

Critical Fuel Level (h_{critical}) for $\alpha > 0$:

Volume formula to be used in liquid volume determination varies depending on the liquid level and the critical liquid level (h_{critical}) is the determinant of which formula to use. h_{critical} is the liquid level at which the liquid begins to wet both of the tank sides. In a dished tank, it can also be considered as the level at which second cap begins to fill, as well.

$$h_{\text{critical}} = (L - M) \tan \alpha \quad (3.6)$$

If the fuel level is equal and less than the critical fuel level, the relation used is ‘low level simple cylinder volume’. Otherwise, ‘high level simple cylinder volume’ relation is used.

$h_{\text{critical}} < h_a$ High Level Simple Cylinder Volume

$h_{\text{critical}} \geq h_a$ Low Level Simple Cylinder Volume

High Level Fuel Volume for $\alpha > 0$:

For a tank with axial tilt, the measured fuel level is first compared with h_{critical} . If it is greater than h_{critical} , the tank is classified as ‘high level SCT’ and fuel volume is determined as follows.

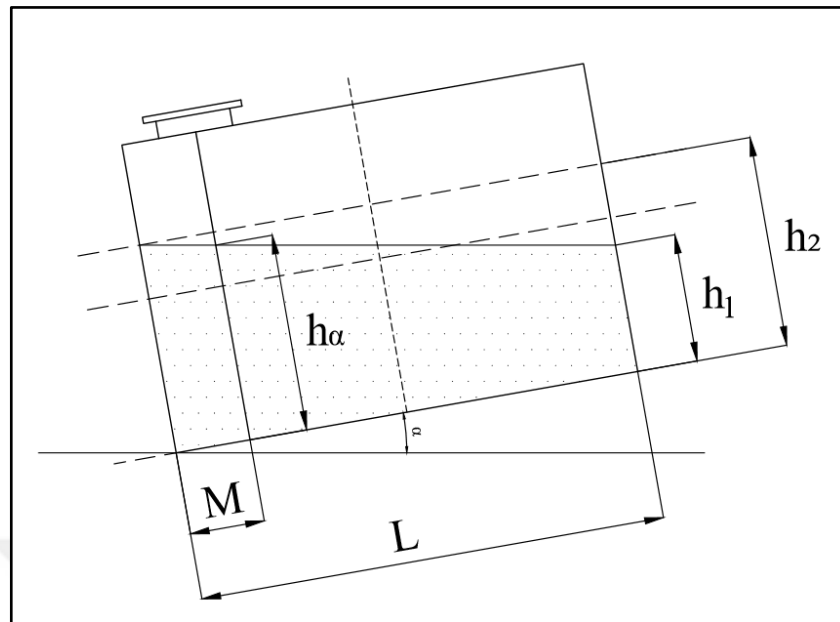


Figure 3.4. High level fuel volume with positive axial tilt

The variables used for this case are:

h_1 : The minimum distance of the fuel level to the tank bottom

h_2 : The maximum distance of the fuel level to the tank bottom

h_a : Fuel level measured by the probe (This is a known value.)

h_1 and h_2 are written in terms of measured fuel level (h_a) by using general slope equation and Figure 3.4. The details of the derivation can be seen in Appendix A.3. The results of the derivation are:

$$h_1 = h_a - (L - M) \tan \alpha \quad (3.7)$$

$$h_2 = h_a + M \tan \alpha \quad (3.8)$$

Then, the levels which are h_1 and h_2 (Eq. 3.7 and Eq. 3.8) are put into the Eq. 3.1 to obtain the liquid volume in the tank.

$$V_{\text{total}} = \frac{V(h_1) + V(h_2)}{2} \quad (3.9).$$

As Eq. 3.9 shows, it is possible to obtain the total volume of the liquid in a vertically tilted through the summation of two calculable volumes.

Low Level Fuel Volume for $\alpha>0$:

If the fuel level in a SCT drops below the critical value (h_{critical}), the tank is classified as ‘low level SCT’ and fuel volume can be obtained by calculating an equivalent height (h_3) as follows:

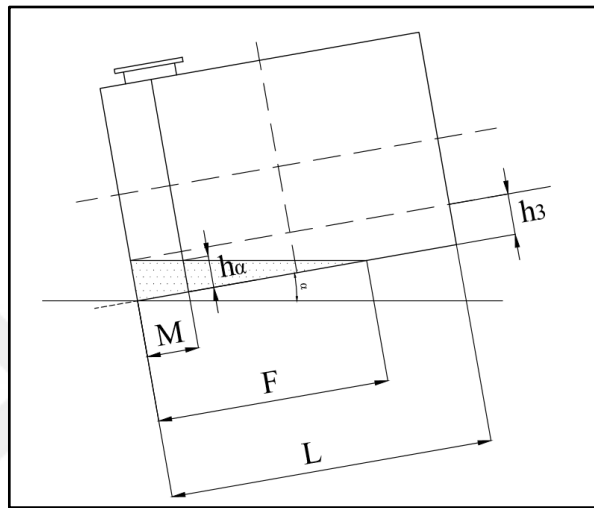


Figure 3.5. Low level fuel volume with positive axial tilt

h_3 : The maximum distance of the fuel level to the tank bottom

h_3 is written in terms of measured fuel level (h_a) using geometric relations and the details of the derivation can be seen in Appendix A.4.

$$h_3 = h_a + M \tan \alpha \quad (3.10)$$

The determined h_3 is put into the Eq. 3.1 by replacing “L” with “F”.

$$V = \frac{F \left[\sqrt{2Rh_3 - h_3^2} (h_3 - R) + R^2 \cos^{-1} \left(1 - \frac{h_3}{R} \right) \right]}{2} \quad (3.11)$$

Effect of Negative Axial Tilt ($\alpha<0$):

Nonmeasurable volume of SCT with negative axial tilt is determined using the geometric relations and the below Figure 3.6.

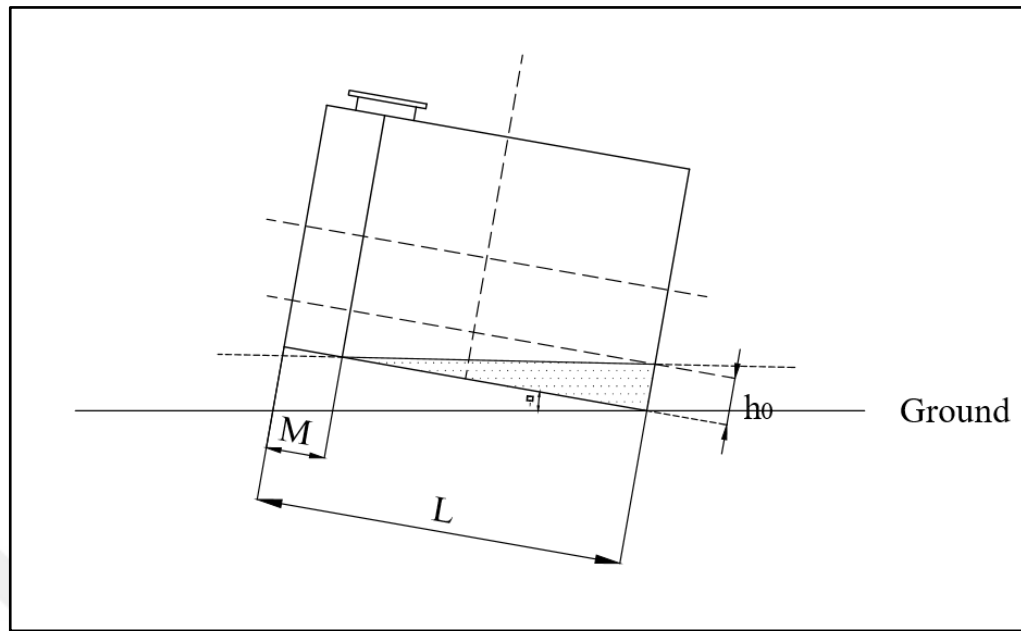


Figure 3.6. Nonmeasurable (V_0) volume of SCT with negative axial tilt

h_0 is the height of the fuel in the tank. The calculation of the slope of the fuel line is initially required to determine the nonmeasurable fuel volume, V_0 for the SCT with negative axial tilt.

$$\tan(-\alpha) = \frac{h_0}{L-M}$$

$$h_0 = (L-M) \tan(-\alpha) \quad (3.12)$$

h_0 place into the Eq. 3.1 by replacing “L” with “(L-M)”, and the fuel volume is determined.

$$V_0 = \frac{(L-M) \left[\sqrt{2Rh_0 - h_0^2} (h_0 - R) + R^2 \cos^{-1} \left(1 - \frac{h_0}{R} \right) \right]}{2} \quad (3.13)$$

Critical Fuel Level ($h_{critical}$) $\alpha < 0$:

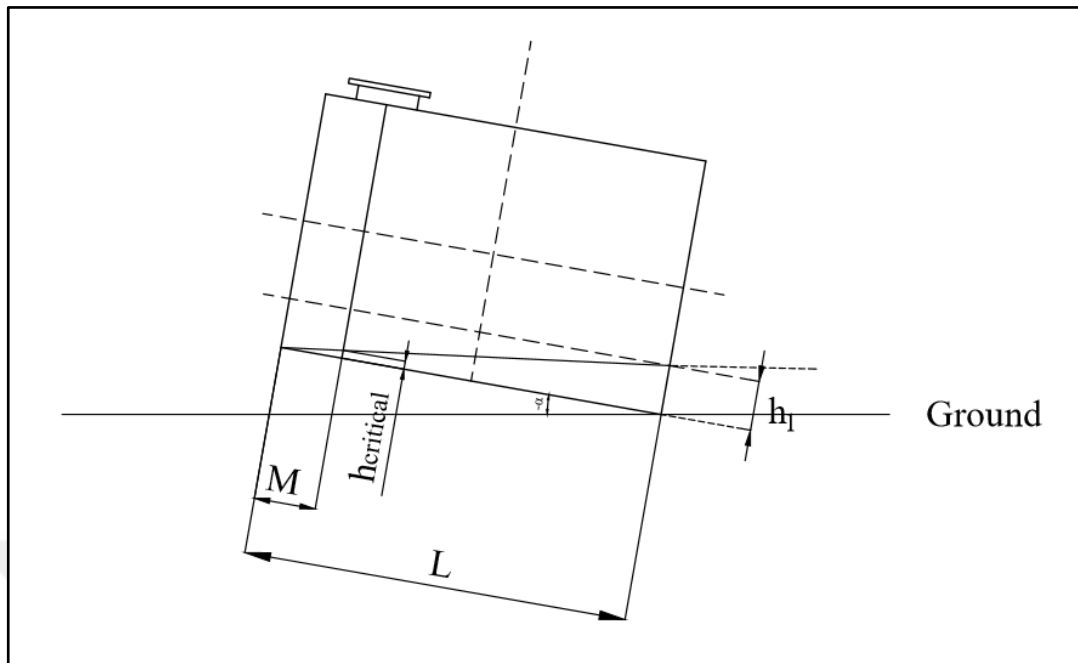


Figure 3.7. Critical fuel level determination for SCT with negative axial tilt

The critical fuel level for the negative axial tilted tank is defined as follows.

$$\tan(-\alpha) = \frac{h_{critical}}{M}$$

$$h_{critical} = M \tan(-\alpha) \quad (3.14)$$

When the critical fuel level is less than the measured fuel level, the fuel volume is calculated using high level negative tilted SCT volume formula. When the critical fuel level is greater than or equal the measured fuel level, the fuel volume is calculated using low level negative tilted SCT volume formula.

$h_{critical} < h_{measured} \rightarrow$ High Fuel Level for Negative Tilted Tank

$h_{critical} \geq h_\alpha \rightarrow$ Low Fuel Level for Negative Tilted Tank

High Level Fuel Volume $\alpha < 0$:

In this case, the measured fuel level is checked according to Eq. 3.14. If it is greater than $h_{critical}$, the tank is classified as ‘high level SCT’ and fuel volume is determined the below manner.

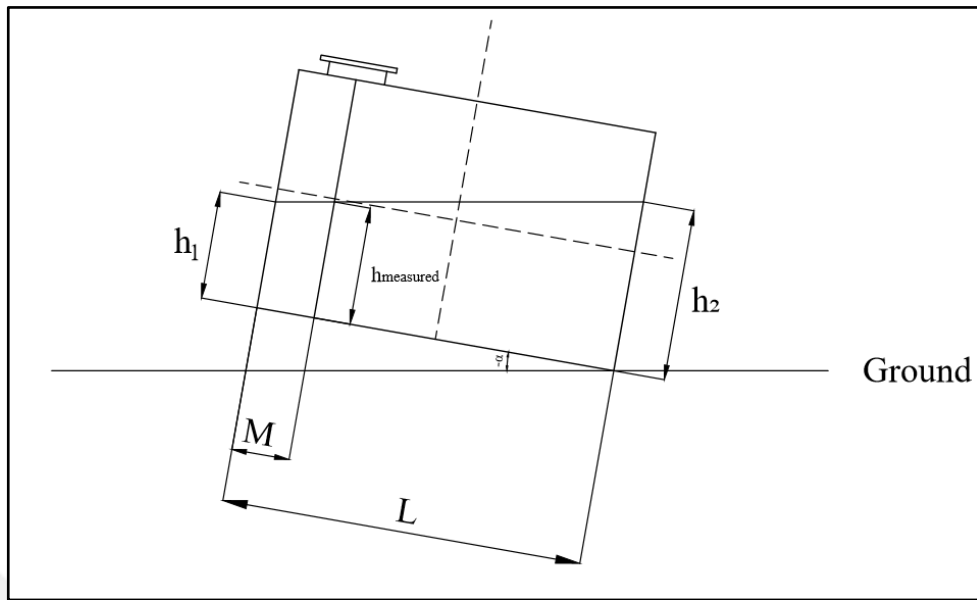


Figure 3.8. High level fuel volume with negative axial tilt

As Figure 3.8 shows that the required parameters to drive the height to volume (h-V) model of this tank are:

h_{measured} : The measured liquid level (This is a known value)

h_1 : The minimum distance of the fuel level to the tank bottom

h_2 : The maximum distance of the fuel level to the tank bottom

h_1 and h_2 are written in terms of the measured fuel level using different geometric relations. The details of the derivation can be seen in Appendix A.5.

$$h_1 = h_{\text{measured}} - M \tan(-\alpha) \quad (3.15)$$

$$h_2 = h_{\text{measured}} + (L - M) \tan(-\alpha) \quad (3.16)$$

After determination of h_1 and h_2 in terms of the measured fuel level (Eq. 3.15 and Eq. 3.16), the fuel volume in the tank is calculated by Eq. 3.1.

$$V(h_1) = L \left[\sqrt{2Rh_1 - h_1^2} (h_1 - R) + R^2 \cos^{-1} \left(1 - \frac{h_1}{R} \right) \right] \quad (3.17)$$

$$V(h_2) = L \left[\sqrt{2Rh_2 - h_2^2} (h_2 - R) + R^2 \cos^{-1} \left(1 - \frac{h_2}{R} \right) \right] \quad (3.18)$$

$$V_{\text{fuel}} = \frac{V(h_1) + V(h_2)}{2} \quad (3.19)$$

Low Level Fuel Volume $\alpha < 0$:

In this case, if the measured fuel level is less than or equal to h_{critical} (Eq. 3.14), the tank is classified as ‘low level SCT’ and fuel volume is determined as follows.

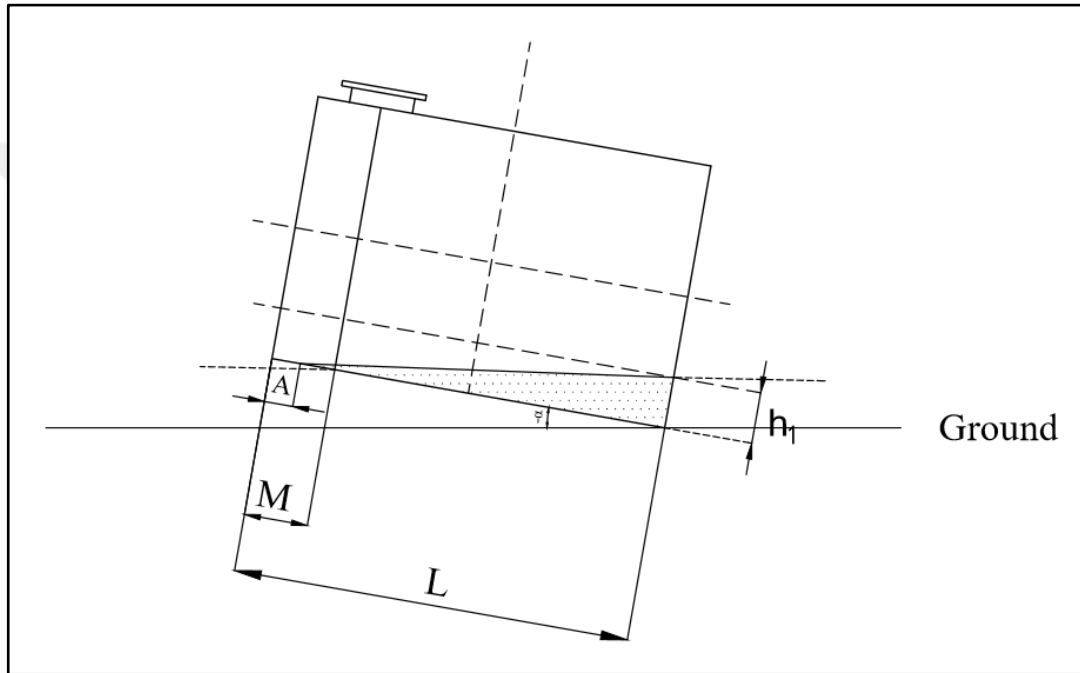


Figure 3.9. Low level fuel volume with negative axial tilt

As Figure 3.9 shows that the required parameters to drive the height to volume (h - V) model of this tank are:

A: The junction point of fuel line and tank bottom

h_1 : The maximum distance from fuel surface to the tank bottom

When “A” equals “M”, the measured fuel level equals to zero. However, tank is full of nonmeasurable fuel volume, V_0 . In other case, “A” can equal minimum zero.

$$0 \leq A < M$$

The slope of the fuel line is determined as follows.

$$\tan(-\alpha) = \frac{h_{\text{measured}}}{M-A}$$

$$A = M - \frac{h_{\text{measured}}}{\tan(-\alpha)} \quad (3.20)$$

h_1 is determined in terms of h_{measured} by Eq. 3.21.

$$\frac{h_{\text{measured}}}{h_1} = \frac{M-A}{L-A}$$

$$h_1 = h_{\text{measured}} + (L-M) \tan(-\alpha) \quad (3.21)$$

The fuel in the tank is calculated using Eq. 3.1 by replacing “ h ” with “ h_1 ”, and “ L ” with $(L-A)$.

$$V_{\text{fuel}} = \frac{(L-A) \left[\sqrt{2Rh_1 - h_1^2} (h_1 - R) + R^2 \cos^{-1} \left(1 - \frac{h_1}{R} \right) \right]}{2} \quad (3.22)$$

This part concludes the derivations for a SCT model. The determinants of SCT volume derivations that are fuel level position with respect to the h_{critical} and tilt type are investigated separately and different relations are obtained. However, the obtained equations or derivations placed into the same equation which is Eq. 3.1, finally.

3.2 CYLINDER TANK WITH DISHED HEAD (CTDH) MODEL

One of the common petroleum storage tank model is a cylindrical tank with dished head (CTDH) in which a simple cylinder body surrounded from its ends by spherical dished head. Figures 3.10, 3.11 (a), and 3.11 (b) show the side view, the front view, and the top view of a cylindrical tank with dished head, respectively.

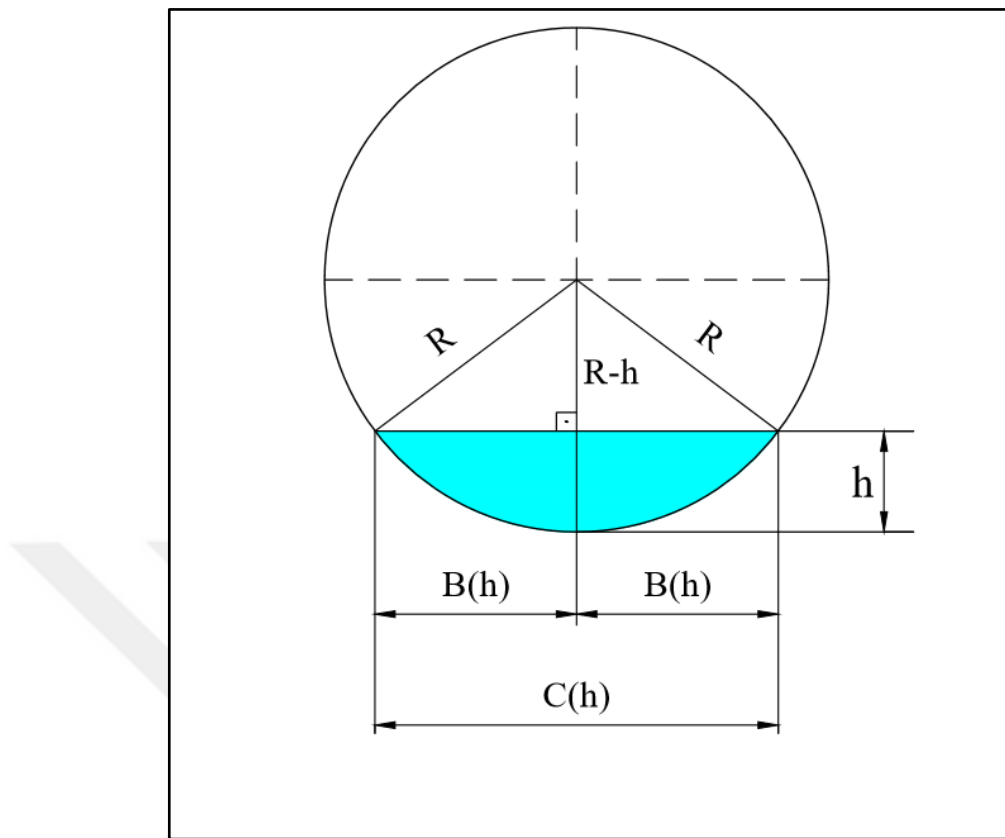


Figure 3.10. The side view of a cylindrical tank with dished head (CTDH)

Here again, the total volume of the tank is found by integrating the chosen segment (i.e. $A(h)$) in the Figure 3.12 along its height. This time, the total volume is the sum of simple cylinder tank volume plus the volume of the dished head. The details of the derivation can be seen in Appendix B.1.

$$V(h) = \int_0^h \left\{ \left[(r^2 - (R-h)^2) \arccos \left(\frac{\sqrt{r^2 - R^2}}{\sqrt{r^2 - (R-h)^2}} \right) \right] - \left[\sqrt{R^2 - (R-h)^2} \sqrt{r^2 - R^2} \right] \right\} dh \quad (3.23)$$

Eq. 3.23 is consistent with [32]

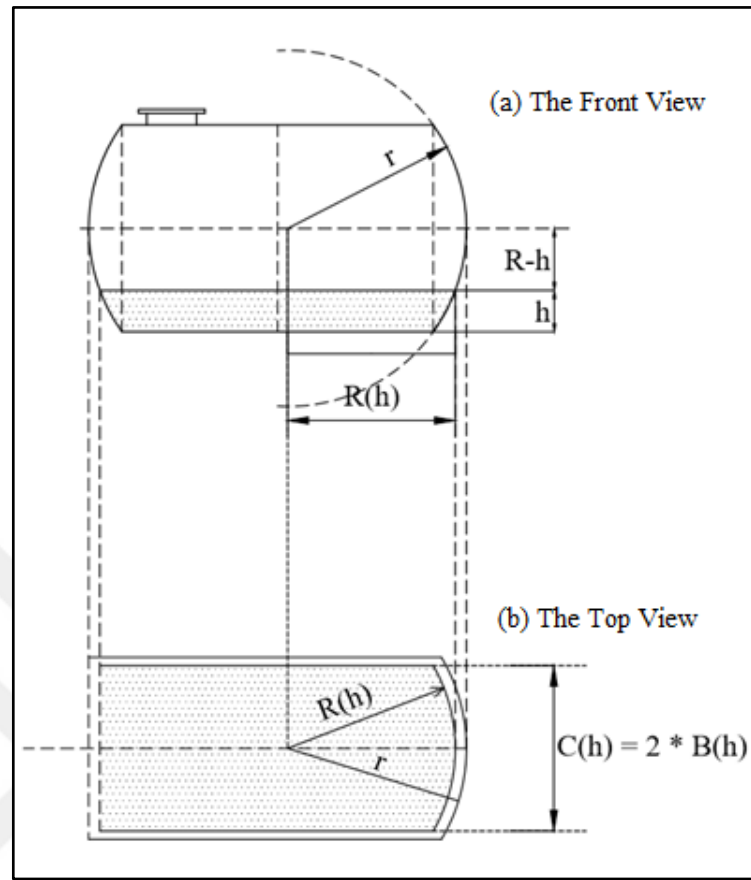


Figure 3.11. (a) The front view of a CTDH (b) The top view of a CTDH

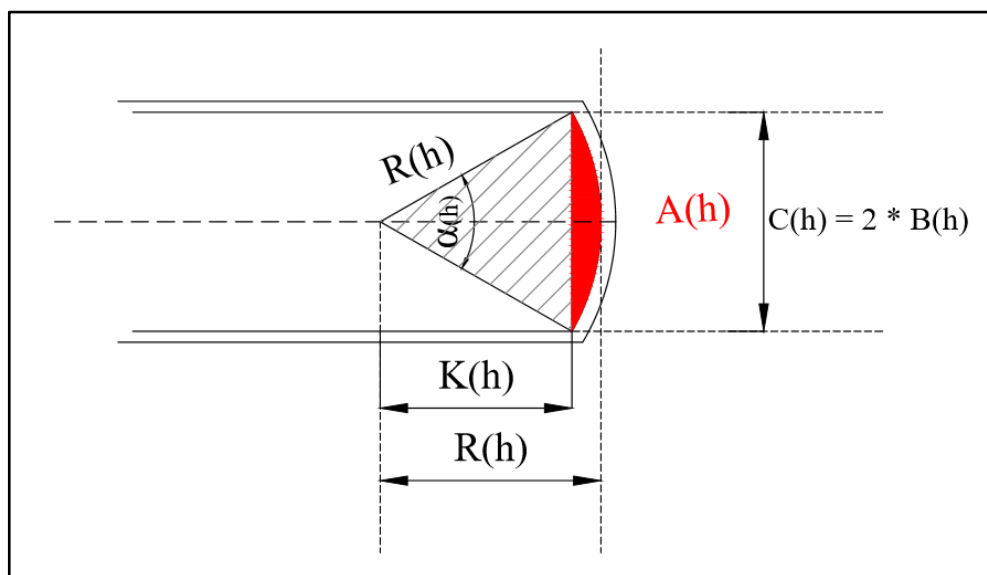


Figure 3.12. The top view of one dished head volume

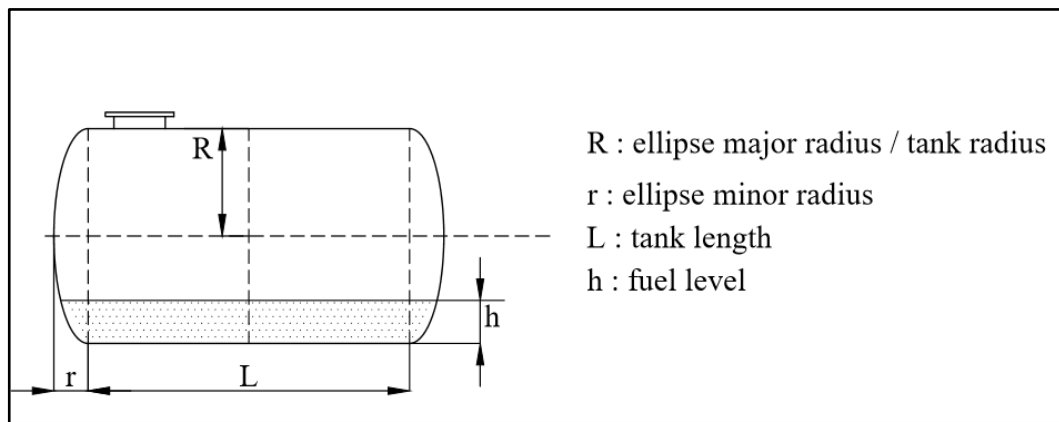


Figure 3.13. Two half-elliptical dished head volume determination

Ellipses have a major (R) and a minor radii (r), where R coincides with the central tank radius. Elliptical end caps (technically, spheroids) have some complex properties. However, for a horizontal tank, computing an end cap's full and partial volumes is often a simple matter of computing a spherical result and scaling the result. Each such end cap is half an oblate spheroid, rotated 90° from the usual convention, and with major (y-axis) radius R equal to the tank's primary radius, and a minor (x-axis) radius r lying in the range $0 \leq r \leq R$. For the half-ellipses at each end of the tank (they can be treated as one spheroid), with major radius R and minor radius r , bisected by content height h , the volume equation can be written as follows [35].

$$V = \frac{\pi r(3R-h)h^2}{3R} \quad (3.24)$$

The sum of the volume of two dished head of the tank is equivalent to the equation below (Eq. 3.25).

$$V_{\text{endcaps}} = \frac{\pi H(3R-h)h^2}{3R} \quad (3.25)$$

As it is seen in the Figure 3.14, the volume of the liquid at level 'h' is the sum of dished head volumes (Eq. 3.25) and the simple cylinder tank volume (Eq. 3.1).

$$V = V_{\text{endcaps}} + V_{\text{cyl}}$$

$$V = \frac{\pi H(3R-h)h^2}{3R} + L \left[\sqrt{2Rh-h^2}(h-R) + R^2 \cos^{-1} \left(1 - \frac{h}{R} \right) \right] \quad (3.26)$$

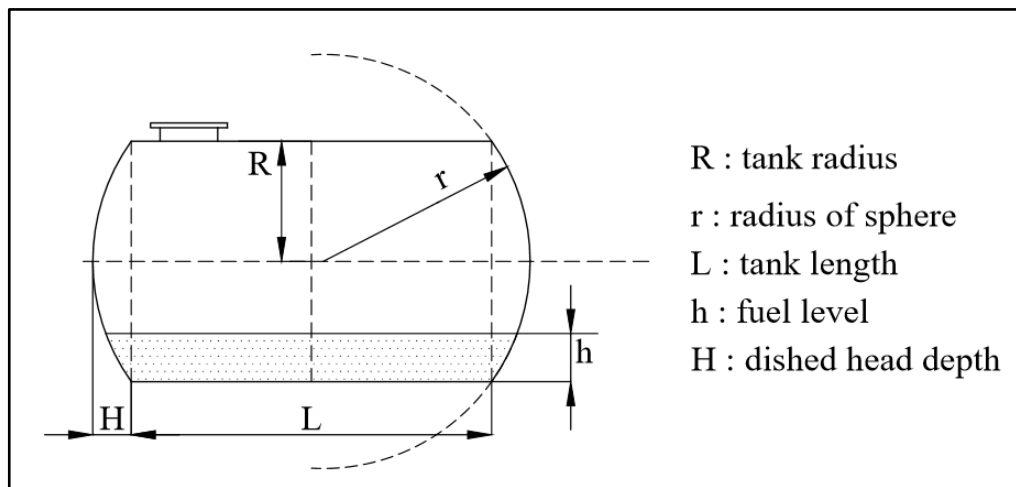


Figure 3.14. Two dished head volume determination

3.2.1 Radial (Horizontal) Tilt

Radial tank tilt effect is applied to the measured fuel level by Eq. 3.2 (β Correction).

$$h = h_{\text{corrected}} = \frac{h'}{\sec \beta} + 2R \sin^2 \beta$$

Where,

R : is the tank radius

h : is the corresponding true liquid height when tank is parallel to the ground

h' : it measured liquid height by probe which produces errors volume

3.2.2 Axial (Vertical) Tilt

Following the radial tilt given above, in this section we will continue with the derivations of the relations in the case of a tilt in axial direction. Unlike the radial tilt case, tilts in $+\alpha$ and $-\alpha$ directions produce different relations because of the asymmetry introduced by the manhole (i.e. probe) position. Another effect of this asymmetry is the position and the volume of the liquid that lies beneath the minimum probe (i.e. measurable) level. Thus, both cases will be treated separately.

Effect of Positive Axial Tilt ($\alpha > 0$):

Nonmeasurable Volume (V_0) $\alpha > 0$:

First, we will derive the relation that gives the nonmeasurable volume (V_0) that lies below the minimum probe level for the positive axial tilt (i.e. $+\alpha$).

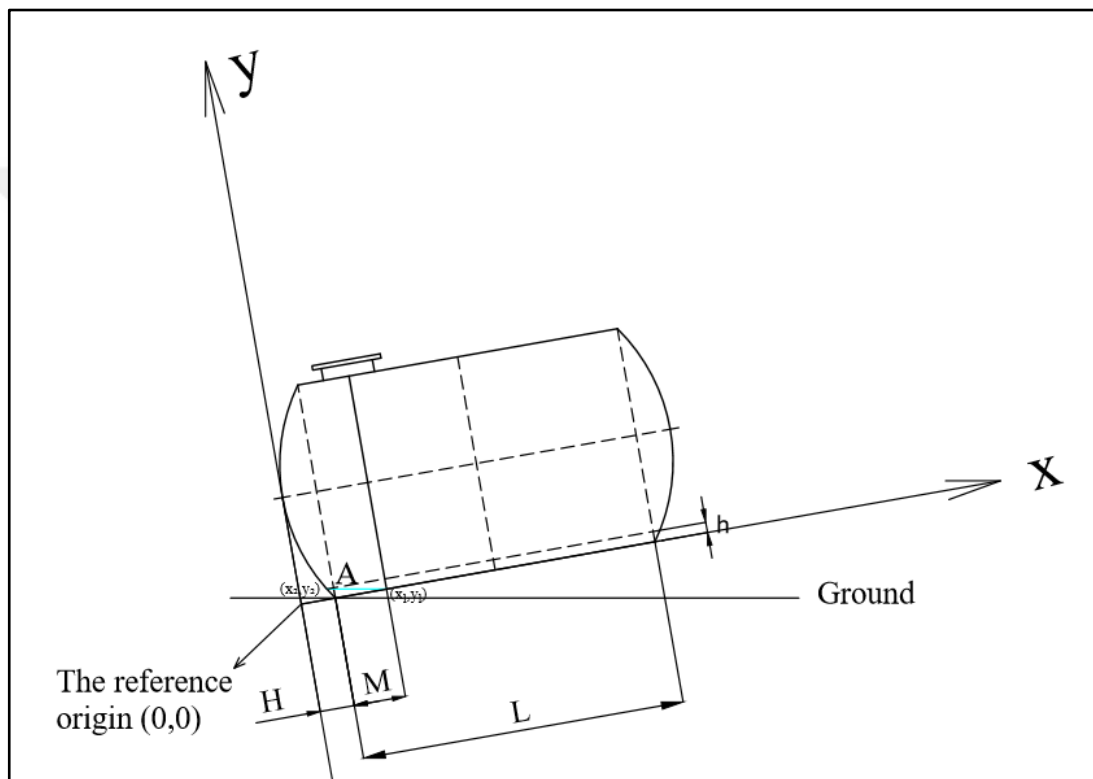


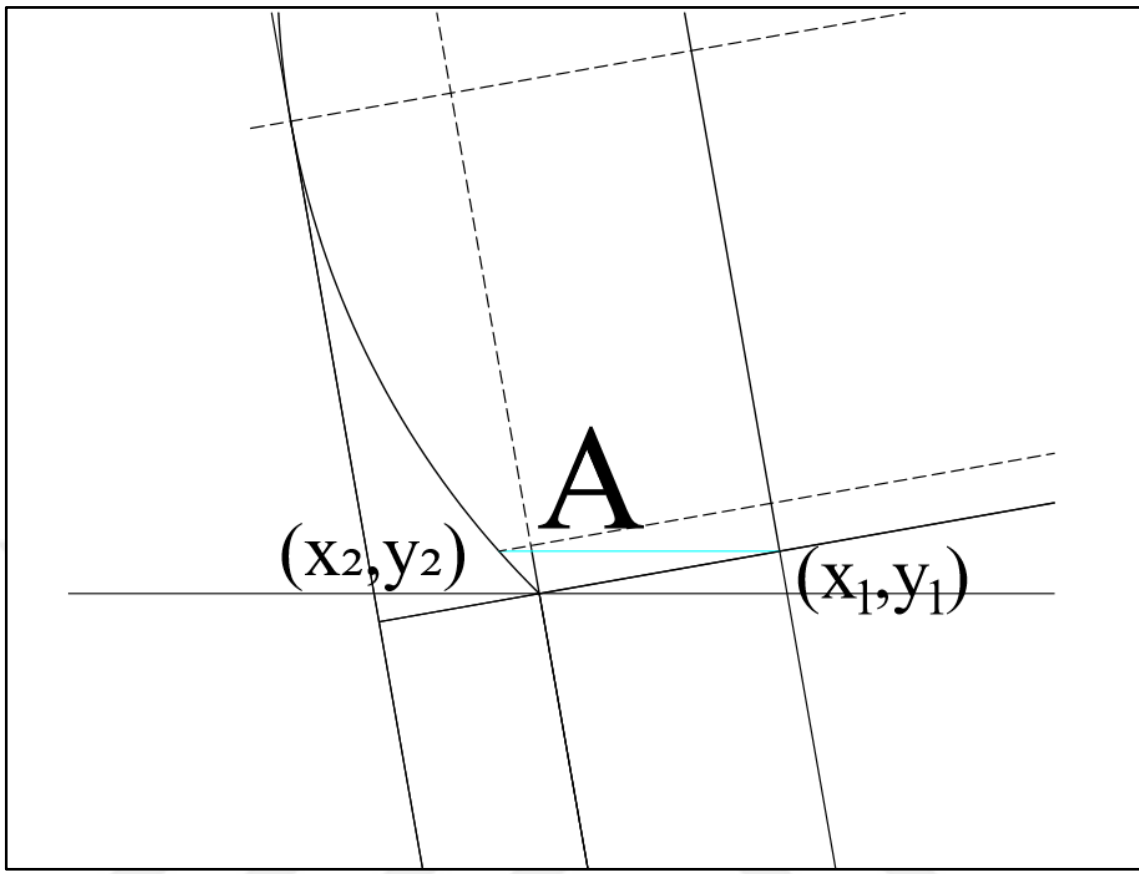
Figure 3.15. Nonmeasurable (V_0) volume of CTDH with positive axial tilt

The relation between point of (x_1, y_1) and point of (x_2, y_2) are determined using simple geometric rules. The details of the derivation can be seen in Appendix B.2.

According to reference origin point, the measured fuel level by the probe equals zero at that point of y_1 . It is seen on the Figure 3.15, y_2 equals "h".

$$x_1 = M + H \quad (3.27)$$

$$y_2 = (x_1 - x_2) \tan \alpha \quad (3.28)$$



Scheme: Focused view of Figure 3.15

Point of (x_2, y_2) is on the left curve of the sphere and the relation between points $(x_2$ and $y_2)$ are as follows Eq. 3.29.

$$(x_2 - r)^2 + (y_2 - R)^2 = r^2 \quad (3.29)$$

After the determination of “ h (or y_2)”, it is put into the Eq. 3.26.

$$V_0 = V_{\text{fuel}} = \frac{\frac{\pi H(3R-h)h^2}{3R} + M \left[\sqrt{2Rh-h^2}(h-R) + R^2 \cos^{-1} \left(1 - \frac{h}{R} \right) \right]}{2}$$

$$V_0 = \frac{\pi H(3R-h)h^2}{6R} + \frac{M \left[\sqrt{2Rh-h^2}(h-R) + R^2 \cos^{-1} \left(1 - \frac{h}{R} \right) \right]}{2} \quad (3.30)$$

Critical Fuel Level (h_{critical}) $\alpha > 0$:

The fuel level in the UST is measured by an automatic tank gauge (ATG) probe. The measured fuel level is transferred into the ATG console and then converted to volume according to calibration chart installed. The equation which will be used for volume calculation is chosen based on the critical fuel level in the underground storage tank.

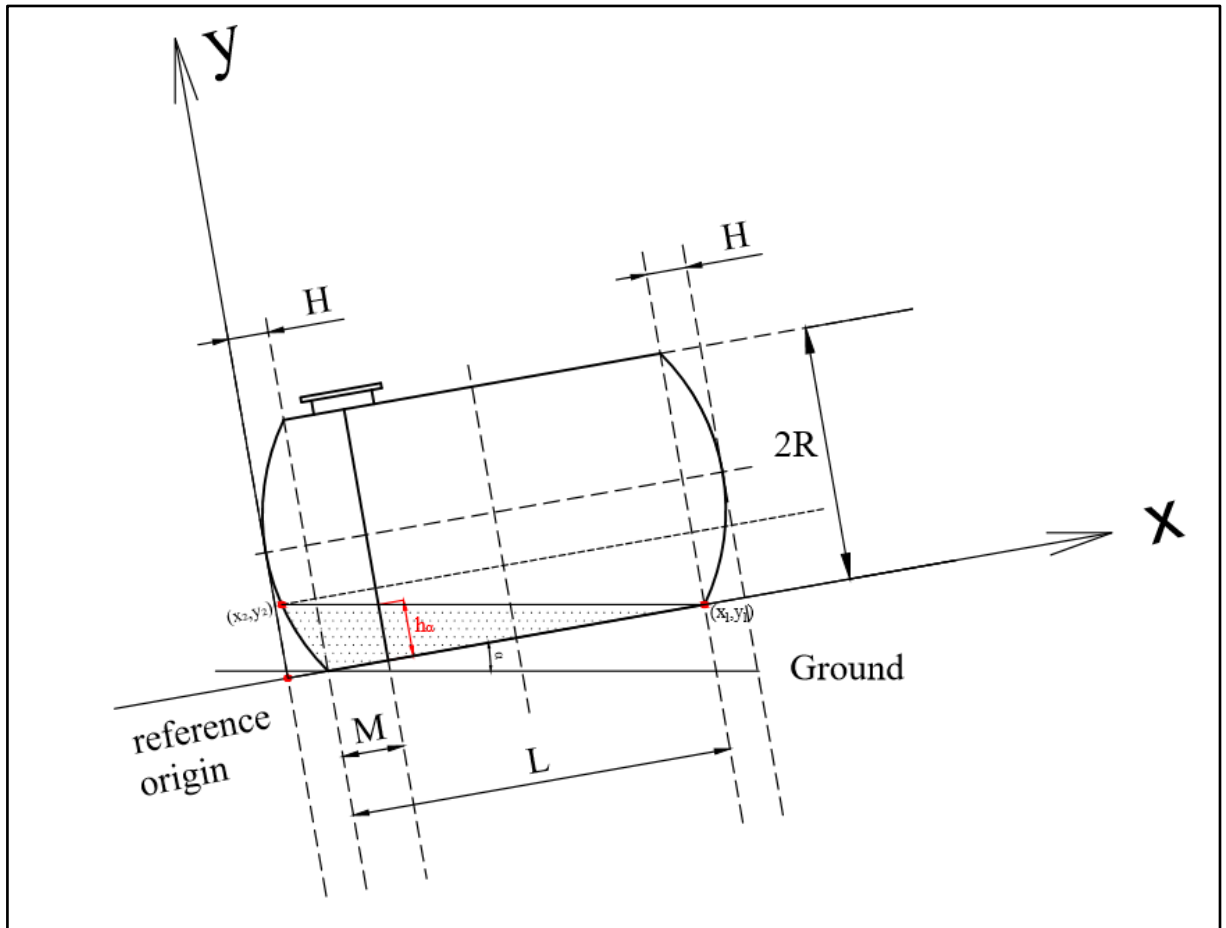


Figure 3.16. Critical fuel level determination for CTDH with positive axial tilt

h_c is the critical fuel level. The point of (x_1, y_1) is determined using below relations (Figure 3.16).

$$x_1 = L + H$$

$$y_1 = 0$$

$$\tan \alpha = \frac{h_c}{x_1 - (M + H)}$$

$$\tan \alpha = \frac{h_c}{L + H - (M + H)}$$

$$\tan \alpha = \frac{h_c}{L-M}$$

$$h_c = (L-M) \tan \alpha \quad (3.31)$$

When the measured fuel level is less than or equal to the critical fuel level (Eq. 3.31), one cap of the tank is full of fuel.

$h_a \leq h_c \rightarrow$ Only one end cap is wet

$h_a > h_c \rightarrow$ Both end caps are wet

Fuel on One Dished Head $\alpha > 0$:

When the measured fuel level is less than or equal to the critical fuel level (Eq. 3.31), one dished head of the tank wet.

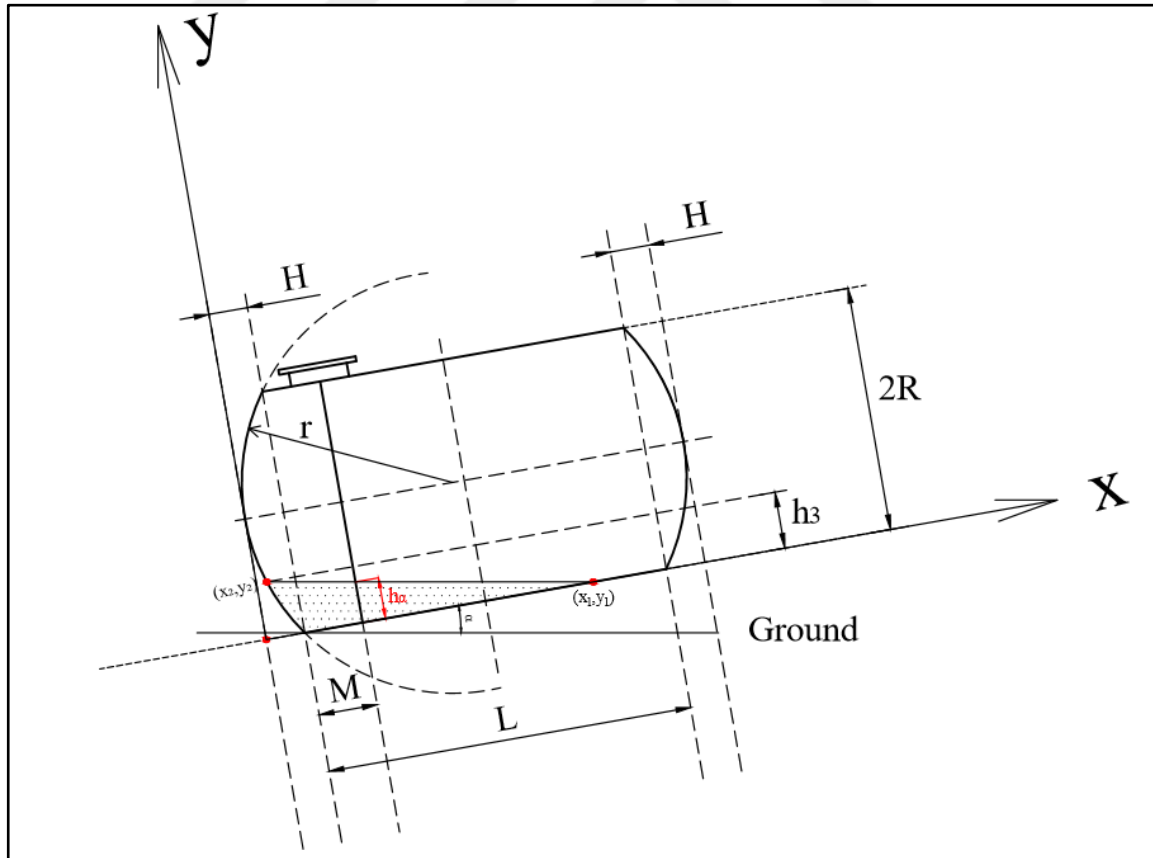


Figure 3.17. Fuel volume for positive axial tilt & wetted one dished head

Figure 3.17 shows that, the point of (x_1, y_1) is on the bottom of the tank and the point of (x_2, y_2) is on the left side of sphere. Also, we can know that y_1 equals zero for all x_1 values.

$$x_1 = \frac{h_a}{\tan \alpha} + (M+H)$$

$$y_1 = 0$$

The general formula of the left sphere is written for the point of (x_2, y_2) according to the reference origin (Point 3).

$$y_2 = (x_1 - x_2) \tan \alpha$$

$$(x_2 - r)^2 + (y_2 - R)^2 = r^2 \quad (3.32)$$

The relation between the h_3 and h_a is determined as follows.

$$y_2 = h_3$$

$$y_2 = h_a + (M+H-x_2) \tan \alpha \quad (3.33)$$

When Eq. 3.32 and Eq. 3.33 are solved simultaneously, “ h_3 (or y_2)” is determined. The details of the derivation can be seen in Appendix B.3.

Determination of h_3 in terms of h_a , it is put into the Eq. 3.26 and fuel volume for this case is calculated according to below equation.

$$V = \frac{V(h_3) - V(h_3)''}{2} \quad (3.34)$$

$$V(h_3) = \frac{\pi H(3R-h_3)h_3^2}{3R} + L \left[\sqrt{(2R-h_3)h_3} (h_3-R) + R^2 \cos^{-1} \left(1 - \frac{h_3}{R} \right) \right] \quad (3.35)$$

$$V(h_3)'' = (L+H-x_1) \left[\sqrt{(2R-h_3)h_3} (h_3-R) + R^2 \cos^{-1} \left(1 - \frac{h_3}{R} \right) \right] \quad (3.36)$$

Fuel on Both Dished Head $\alpha > 0$:

When the measured fuel level is greater than the critical fuel level (Eq. 3.31), both end caps of the tank are wetted.

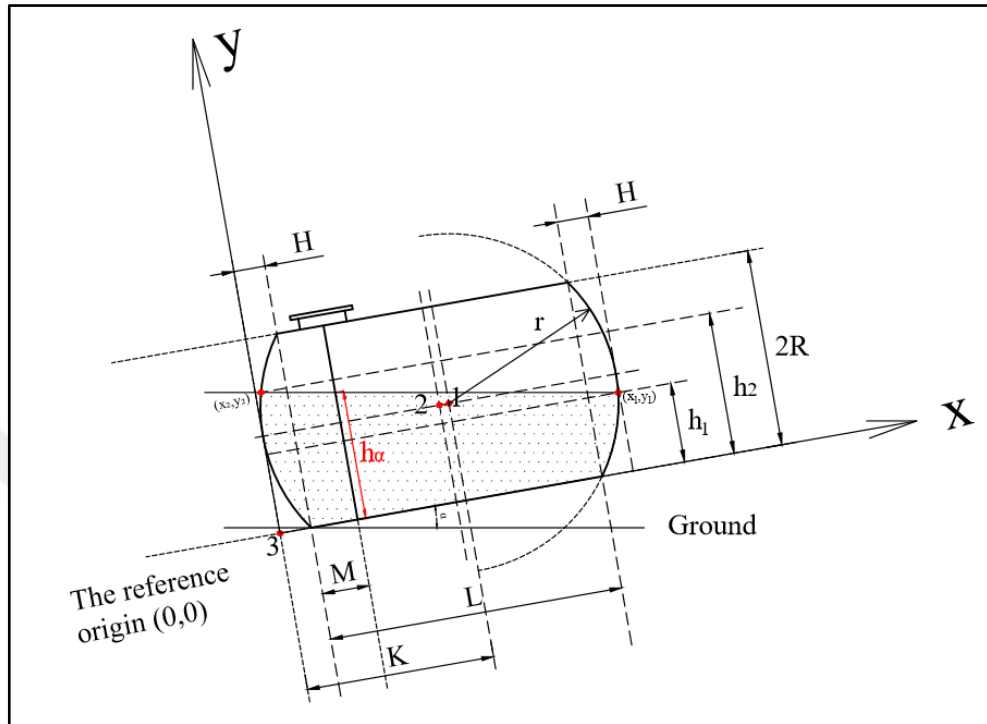


Figure 3.18. Fuel volume for positive axial tilt & wetted two dished head

Point 1: The center of the right sphere of the tank

Point 2: The center of the tank

Point 3: The reference origin of the tank system

K: The horizontal distance between Point 1 and Point 3

h_1 : The minimum distance from fuel surface to the tank bottom

h_2 : The maximum distance from fuel surface to the tank bottom

In this case, fuel surface is in contact with both sides of sphere (i.e. on the right dished head and on the left dished head). In order to determine each point, firstly, the origin of the sphere is shifted from Point 1 to Point 3.

The point of (x_1, y_1) is on the right side of the tank and below equation (Eq. 3.38) is used in order to obtain a relation between x_1 and y_1 as follows (Figure 3.18):

$$y_1 = h_1 \quad (3.37)$$

$$[x_1 - (L + 2H - r)]^2 + [y_1 - R]^2 = r^2 \quad (3.38)$$

The relation between the h_1 and $h\alpha$ is:

$$h_\alpha = h_1 + [(x_1 - M - H) \tan \alpha] \quad (3.39)$$

When Eq. 3.38 and Eq. 3.39 are solved simultaneously, “ h_1 (or y_1)” is calculated. The details of the derivation can be seen in Appendix B.4.

The point of (x_2, y_2) is on the left side of the tank and below equation (Eq. 3.41) is used in order to obtain a relation between x_2 and y_2 as follows. It can be seen in the Figure 3.18.

$$y_2 = h_2 \quad (3.40)$$

$$[x_2 - r]^2 + [y_2 - R]^2 = r^2 \quad (3.41)$$

The relation between the h_2 and $h\alpha$ is determined as follows.

$$y_2 = h_\alpha + (-x_2 + M + H) \tan \alpha \quad (3.42)$$

When Eq. 3.41 and Eq. 3.42 are solved simultaneously, “ h_2 (or y_2)” is calculated. The details of the derivation can be seen in Appendix B.4.

Determination of h_1 and h_2 in terms of $h\alpha$, these fuel levels are put into the Eq. 3.26 and fuel volume for this case is calculated according to below equation.

$$V = \frac{V(h_1) + V(h_2)}{2} \quad (3.43)$$

$$V(h_1) = \frac{\pi H(3R - h_1)h_1^2}{3R} + L \left[\sqrt{(2R - h_1)h_1} (h_1 - R) + R^2 \cos^{-1} \left(1 - \frac{h_1}{R} \right) \right]$$

$$V(h_2) = \frac{\pi H(3R - h_2)h_2^2}{3R} + L \left[\sqrt{(2R - h_2)h_2} (h_2 - R) + R^2 \cos^{-1} \left(1 - \frac{h_2}{R} \right) \right]$$

Effect of Negative Axial Tilt ($\alpha < 0$):

Nonmeasurable Volume (V_0) $\alpha < 0$:

Nonmeasurable fuel volume for the SCT with dished head and with negative axial tilt is determined by assuming the tank in the own coordinate (Figure 3.19).

The reference point is chosen and the distance of the minimum and maximum points where the fuel touch to the tank are determined one by one.

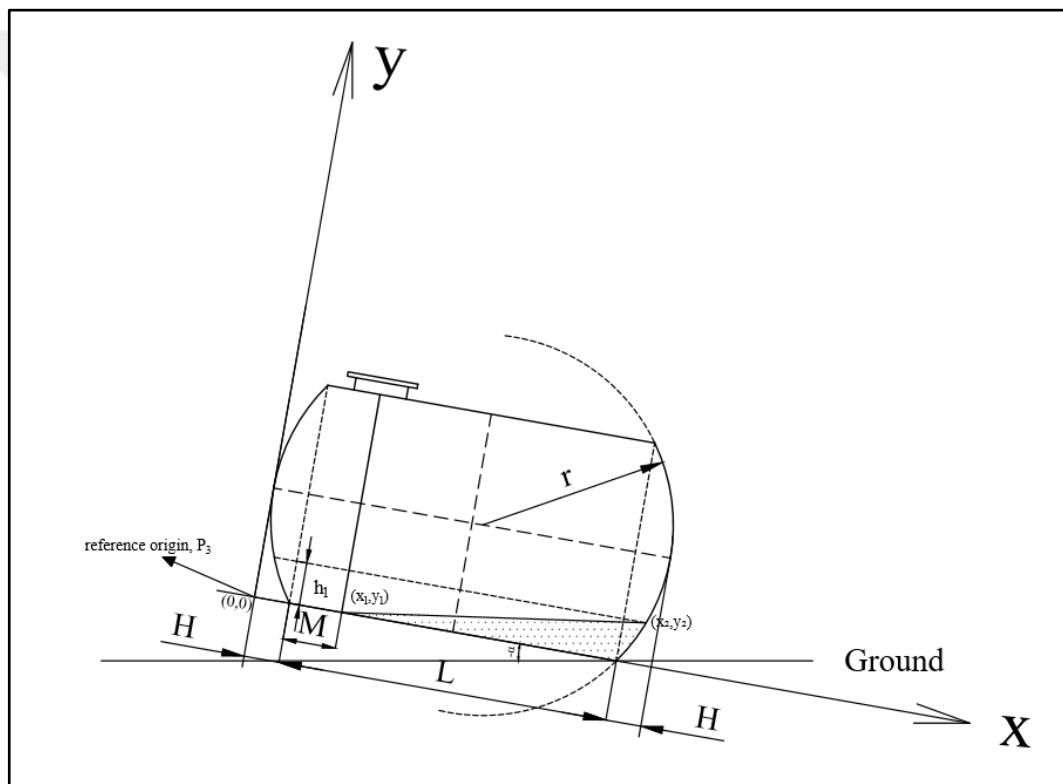


Figure 3.19. Nonmeasurable (V_0) volume of CTDH with negative axial tilt

Point of (x_1, y_1) is on the bottom of the tank and point of (x_2, y_2) is on the right side of the sphere. It is seen in the Figure 3.19, y_1 equals zero for all x values.

$$x_1 = M + H$$

$$y_1 = 0$$

A relation between x_1 , x_2 and y_1 can be written by using the slope of the surface fuel line.

$$y_2 = h_1 \quad (3.44)$$

$$y_2 = (x_2 - x_1) \tan(-\alpha) \quad (3.45)$$

Another relation between x_2 and y_2 is written using general sphere formula for the right curve of the tank.

$$[x_2 - (L + 2H - r)]^2 + [y_2 - R]^2 = r^2 \quad (3.46)$$

There are 3 unknowns and 3 equations (Eq. 3.44, Eq. 3.45 and Eq. 3.46). DOF equals to zero and we can easily solve these equations. The details of the derivation can be seen in Appendix B.5.

Volume of the fuel in the tank, V_{fuel} is calculated using obtained h_1 value by Eq. 3.26.

$$V(h_1) = \frac{\pi H(3R-h_1)h_1^2}{3R} + (L-M) \left[\sqrt{(2R-h_1)h_1} (h_1-R) + R^2 \cos^{-1} \left(1 - \frac{h_1}{R} \right) \right]$$

$$V_{fuel} = \frac{V(h_1)}{2}$$

$$V_0 = V_{fuel} = \frac{\pi H(3R-h_1)h_1^2}{6R} + \frac{L-M}{2} \left[\sqrt{(2R-h_1)h_1} (h_1-R) + R^2 \cos^{-1} \left(1 - \frac{h_1}{R} \right) \right] \quad (3.47)$$

Critical Fuel Level ($h_{critical}$) $\alpha < 0$:

There are two fuel levels in the tank, which wet one end cap or both end caps. The critical fuel level recorded by the probe is the determinant for the calculation of the fuel volume such type of tank and tilt cases.

The slope of the fuel surface line gives a relation between $h_{measured}$ and probe position. This relation can be written as follows by Figure 3.20.

$$\tan(-\alpha) = \frac{h_{measured}}{M}$$

$$h_{measured} = M \tan(-\alpha)$$

$$h_{critical} = M \tan(-\alpha) \quad (3.48)$$

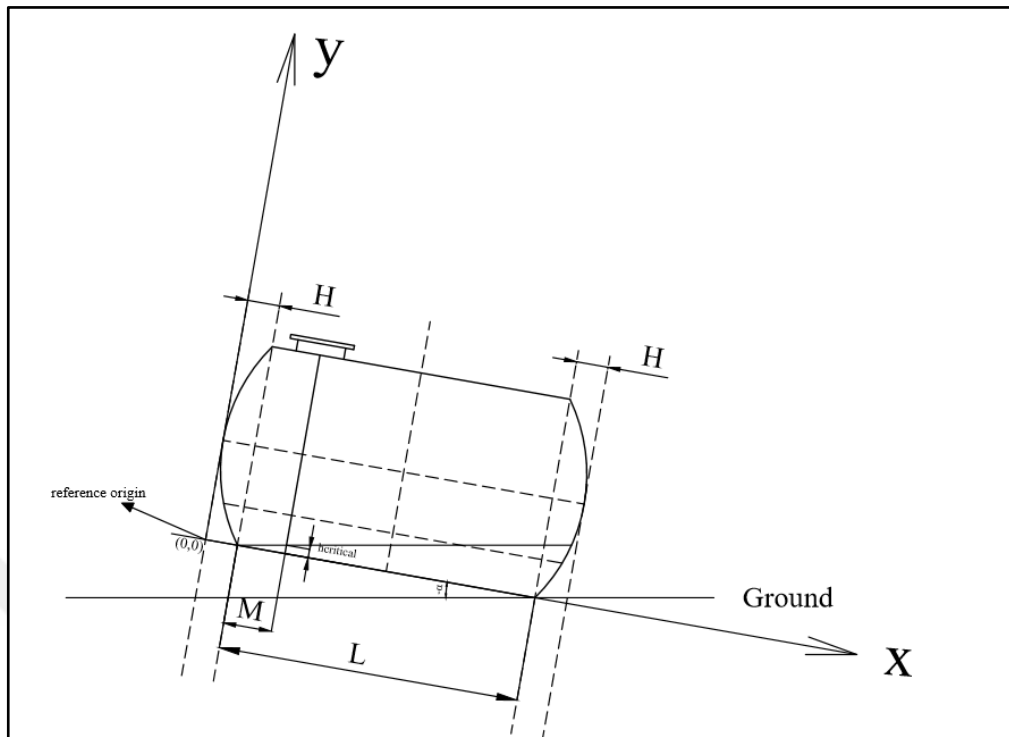


Figure 3.20. Critical fuel level determination for CTDH with negative axial tilt

When the measured fuel level is less than or equal to the critical fuel level (Eq. 3.48), tank one end cap begin to wet. On the other hand, if the measured fuel level is greater than the critical fuel level, tank both end caps wet.

$$h_{\text{measured}} \leq h_{\text{critical}} \rightarrow \text{Only one end cap is wet}$$

$$h_{\text{measured}} > h_{\text{critical}} \rightarrow \text{Both end caps are wet}$$

Fuel on Both Dished Heads $\alpha < 0$:

In this case, the measured fuel level is greater than h_{critical} (Eq. 3.48).

h_1 : The minimum distance of the fuel level to the tank bottom

h_2 : The maximum distance of the fuel level to the tank bottom

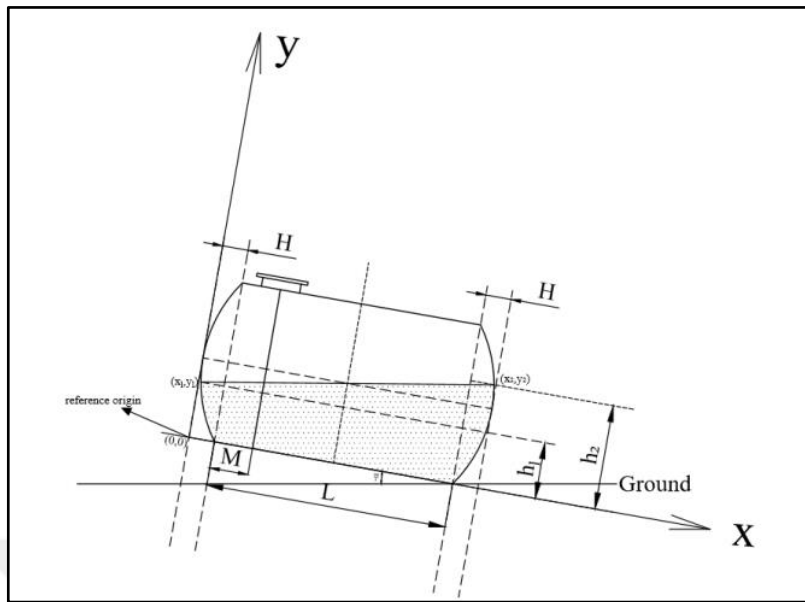


Figure 3.21. Fuel volume for negative axial tilt & wetted both dished head

In this case, there are 2 points are on the tank wall. The point of (x_1, y_1) is on the left curve of sphere and the point of (x_2, y_2) is on the right curve of sphere. The slope of the surface fuel level is gives a relation between points and the measured fuel level. As Figure 3.21 shows:

$$y_1 = h_1$$

$$h_1 = h_{\text{measured}} - (M + H - x_1) \tan(-\alpha) \quad (3.49)$$

The point of (x_1, y_1) is on the left sphere curve of the tank and a relation is written for the left sphere curve.

$$(x_1 - r)^2 + (y_1 - R)^2 = r^2 \quad (3.50)$$

A relation between the point of (x_1, y_1) and the point of (x_2, y_2) is written according to slope equation of the fuel surface level. As it is seen in the Figure 3.21, y_2 point equals to:

$$y_2 = h_2$$

$$h_2 = h_1 + (x_2 - x_1) \tan(-\alpha) \quad (3.51)$$

Another relation between x_2 and y_2 is written using general sphere equation for the right curve of the tank.

$$[x_2 - (L + 2H - r)]^2 + [y_2 - R]^2 = r^2 \quad (3.52)$$

h_1 and h_2 are determined the above derivations and the details of the derivations can be seen in Appendix B.6. Then, using obtained h_1 and h_2 , volume of the fuel in such tank is calculated by Eq. 3.26.

$$V(h_1) = \frac{\pi H(3R-h_1)h_1^2}{3R} + (L) \left[\sqrt{(2R-h_1)h_1} (h_1-R) + R^2 \cos^{-1} \left(1 - \frac{h_1}{R} \right) \right]$$

$$V(h_2) = \frac{\pi H(3R-h_2)h_2^2}{3R} + (L) \left[\sqrt{(2R-h_2)h_2} (h_2-R) + R^2 \cos^{-1} \left(1 - \frac{h_2}{R} \right) \right]$$

$$V_{\text{fuel}} = \frac{V(h_1) + V(h_2)}{2} \quad (3.53)$$

Fuel on One Dished Head $\alpha < 0$

In this case, the measured fuel level is less than or equal to h_{critical} (Eq. 3.48).

There are two points that one of them is on the tank bottom (i.e. point of (x_1, y_1)) and the other is on the right curve of sphere (i.e. point of (x_2, y_2)). Figure 3.22 shows that y_1 equals to 0 (zero) for all x values and y_2 equals to h_1 .

$$y_1 = 0$$

$$y_2 = h_1$$

The slope of the surface fuel line is gives the equations below.

$$h_{\text{measured}} = (M + H - x_1) \tan(-\alpha) \quad (3.54)$$

$$y_2 = (x_2 - x_1) \tan(-\alpha) \quad (3.55)$$

The relation between x_2 and y_2 can be written based on general sphere formula according to the reference origin point (i.e. right curve of sphere).

$$[x_2 - (L + 2H - r)]^2 + (y_2 - R)^2 = r^2 \quad (3.56)$$

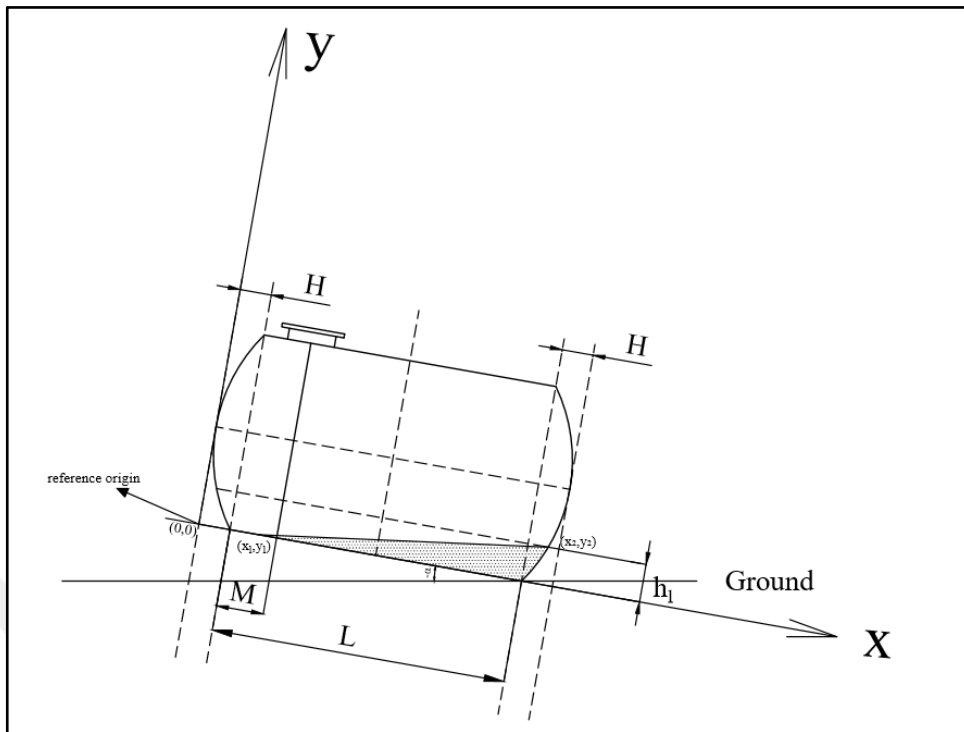


Figure 3.22. Fuel volume for negative axial tilt & wetted one dished head

The equations (Eq. 3.54, Eq. 3.55, and Eq. 3.56) are solved simultaneously and h_1 is determined and the details can be seen in Appendix B.7. Fuel volume (V_{fuel}) is calculated using obtained h_1 placing into Eq. 3.26.

$$V(h_1) = \frac{\pi H(3R-h_1)h_1^2}{3R} + (L+H-x_1) \left[\sqrt{(2R-h_1)h_1} (h_1-R) + R^2 \cos^{-1} \left(1 - \frac{h_1}{R} \right) \right]$$

$$V_{fuel} = \frac{V(h_1)}{2}$$

$$V_{fuel} = \frac{\pi H(3R-h_1)h_1^2}{6R} + \frac{L+H-x_1}{2} \left[\sqrt{(2R-h_1)h_1} (h_1-R) + R^2 \cos^{-1} \left(1 - \frac{h_1}{R} \right) \right] \quad (3.57)$$

This chapter concludes the derivations for a SCT with dished head model. The determinants of SCT with dished head volume derivations that are fuel level position with respect to the $h_{critical}$ and tilt type are investigated separately and different relations are obtained. However, the obtained equations or derivations placed into the same equation which is Eq. 3.26, finally.

3.3 VARIANCE

As defined previously, the variance is the difference between the calculated amount of fuel available in a tank at any given time, and the actual amount of fuel available in the tank. In this study, “correction volume” term is added to that general formula. Correction volume from tank has been represented as $V_{\text{correction}}$.

$$\text{Variance} = \text{Closing Stock} - \text{Book Stock}$$

$$\text{Book Stock} = \text{Initial Stock} + \text{Delivery} - \text{Sales} - \text{Correction} \quad (3.58)$$

$$\text{Variance} = \text{Closing Stock} - (\text{Initial Stock} + \text{Delivery} - \text{Sales} - \text{Correction}) \quad (3.59)$$

At one time or another, operations such as tank cleaning, pump meter calibration or, applications related to wetstock management are performed at the fuel service stations. These operations are known to lead to volume changes. That volume changes have been added to general formula as ‘correction volume’.

There are two types of delivery data which are ATG delivery and invoiced delivery. The amount of delivery measured by tank gauge is called as ‘ATG delivery’ and the amount of delivery measured by terminal gauge with respect to reference temperature ($T_{\text{ref}}=15^\circ$) is called as ‘invoiced delivery’. In order to eliminate the measurement errors of ATG, variance is calculated with respect to the invoiced delivery data in this study.

Initial stock, invoiced delivery, sales, correction and final stock volumes are the primary determinants of fuel variance. One of the targets of this study is to calculate variance accurately. The first step of that calculation is making some assumptions which are listed as follows.

- The tank probe measures correctly the fuel heights.
- The tank probe measures correctly the fuel temperatures.
- The sales data is exact and the pumpmat measures correctly each sales transactions.
- In cases of any operations, correction volume amounts are taken by site owner/operator.

The fuel level measured by ATG probe is transferred into the TLS (Tank Level Sensor) console. Up to that point, there is no error because of the assumption is that the tank probe

measures the fuel level correctly. The measured level datum is converted to volume according to the tank calibration chart at the TLS console. However, level to volume (LV) conversion is incorrect due to inaccurate (or poor) tank calibration chart. Incoming delivery (invoiced), sales and correction volume data is independent from ATG probe and tank calibration chart. In line with these informations, variance formula is revised and incoming data, which is independent from ATG probe and tank calibration chart, is defined as ‘actual volume change’ in the below form.

$$\Delta V_{\text{actual}} = dV_{\text{act}} = V_{\text{sales}} + V_{\text{correction}} - V_{\text{invoiced delivery}}$$

$$\Delta V_{\text{theo}} = dV_{\text{theo}} = V_{\text{final}} - V_{\text{initial}}$$

$$\text{Variance} = \Delta V_{\text{theo}} + \Delta V_{\text{actual}}$$

Actual volume change is the essential point in the variance calculation. The reason is, it can be likened to driving force. For instance, driving force of heat trasfer is temperature gradient. The driving force of variance is volume gradient (actual volume change).

Variance of an ideal system must be equal to the actual volume change with opposite sign. One of the most significant purposes of this study is to obtain an accurate tank calibration or to reduce fuel variances. For that purpose, level and temperature data, which are measured by ATG probe were taken and put into the appropriate theoretical models. Thus, variances are minimized and approximated to zero.

The real-time data include each transaction and frequent readings of inventory level and temperature are used to calculate the accurate volume by using the derived theoretical volume equations. For instance, daily data of a tank inlude initial stock level, initial temperature, final stock level, final temperature, invoiced delivery, sales and correction volume is examined in a detail. According to the above assumptions, actual volume changes are accurate and these data are exactly used in the variance determination. However, due to level to volume conversion is inaccurate in the current chart, theoretical volume change is calculated allowing for the temperature compensation according to the below equation. The details of the derivation of Eq. 3.60 can be seen in the Appendix C.1.

$$dV_{\text{theo}} = V_{\text{final}} - V_{\text{initial}} + [\alpha_{\text{fuel}} \times (T_i - T_f)] \quad (3.60)$$

T_i : Tank initial temperature ($^{\circ}\text{C}$)

T_f : Tank final temperature ($^{\circ}\text{C}$)

α_{fuel} : Fuel thermal expansion coefficient, ($1/\text{ }^{\circ}\text{C}$)

The thermal coefficient of the stored fuel is a significant physical property. Expansion or contraction occurs because of the temperature fluctuations in the stored fuel. The phenomenon causes an apparent volume changes. All volumetric leak detection techniques try to compensate for volume changes by predicting what portion of the total volume change is due to thermal activity. That portion is subtracted from the total volume in order to obtain the actual volume change (the change due to the leak alone). For this reason, the thermal expansion coefficient plays a direct importance in the accurate fuel variance determination. Temperature effect on the fuel volume is calculated using initial temperature, final temperature and thermal expansion coefficient. In this calculation, thermal expansion coefficients of diesel and gasoline are taken as 0.000792 ($1/\text{ }^{\circ}\text{C}$) and 0.001251 ($1/\text{ }^{\circ}\text{C}$), respectively [36].

3.4 VARIANCE MINIMIZATION/REDUCTION

Goal of this study is to minimize or reduce the variance. Several tanks, which are at the different fuel service stations are investigated deeply. The accuracy of level to volume (LV) conversion depends on the current tank calibration chart. In an ideal case, variance should be equal to zero by Eq. 3.61.

$$\text{Var}_{\text{ideal}} = \text{Var}_{\text{theo}} = 0 = V_{\text{final}} - V_{\text{initial}} + dV_{\text{act}} \quad (3.61)$$

There are three cases while minimizing the variances: tank charts that are (i) non-problematic, (ii) requiring uniform adjustment and (iii) requiring non-uniform adjustment. If the variance values with respect to the theoretical tank calibration chart and the current tank calibration chart are similar and near to zero line (Eq. 3.62), that tank calibration chart is classified as non-problematic and it should not require any adjustments.

$$\text{Var}_{\text{theo}} \cong \text{Var}_{\text{chart}} \quad (3.62)$$

3.4.1 Uniform Adjustment

It is mentioned previously that if the variance trend of current chart is equivalent or very near to the ideal tank variance trend, this type chart is classified as non-problematic tank calibration chart and it is not require any adjustment. On the other hand, if the chart is problematic, an adjustment is required in order to obtain an accurate tank calibration chart and prevent its masking effect on real fuel losses. If the variance distribution is uniform, tank calibration chart is corrected by changing the parameters which are tank radius (R), tank length (L), dished head depth (H), probe distance from tank corner (M), axial tank tilt (α) and radial tank tilt (β). Thus, optimum dimensions are obtained for the tank, and the variances are minimized and the masking effect on the real losses is eliminated.

Tank may buckle partially (local buckling) or entirely (nonlocal buckling). The finest characteristic of uniform deformation (i.e. nonlocal buckling) in calibration chart manifests that variance trend has homogeneous distribution in a specific fuel level range or in the whole tank. In other words, this type calibration error shows a repeatable variance pattern and it can be eliminated by an uniform adjustment, which requires to change each parameters. After uniform adjustment, it is seen that current chart curve shifts and the new improved chart established.

3.4.2 Non-uniform Adjustment

In the non-uniform adjustment for the tank whose calibration chart is inaccurate, the variance distribution is non-uniform and there is a big deviation from the ideal tank chart at the some regions. It requires local adjustments or non-uniform adjustment (i.e. correction factor for each tank level).

Contrary the uniform deformation, variance distribution shows gains at a specific level ranges (first deformed region) and loss at a different specific level ranges (second deformed region) unlike over calibrated and under calibrated chart variance pattern. Therefore, a uniform adjusment is non appropriate. For instance, radius is increased and while variances on the first deformed region are reduced, the variances on the second deformed region are increased. Local buckling cases require non-uniform adjusment, which an error function is

defined dependent on fuel level. Each level has a error function, and so that variance trend is adjusted and improved.

It is known that, variance is a function of volume. Besides, volume is the function of fuel level, h .

$$\text{Var} \equiv f(V_i, V_f, dV_{\text{act}})$$

$$V_{\text{chart}} \equiv f(h)$$

$$V_{\text{theo}} \equiv f(h)$$

Thereby, variance is a function of fuel level, h .

$$\text{Var} \equiv f(h)$$

For the ideal tank systems, variance is equivalent to zero, but actual variance is not. The reasons of that deviation may be either wrong dV_{act} value, wrong V_i and V_f , and wrong h_i and h_f . It is assumed at the previous pages that dV_{act} and fuel level measurements (i.e: h_i , h_f) are correct, then the problem is with the poor tank calibration chart. That is:

$$V_{\text{theo}}(h) = \text{accurate volume}$$

$$V_{\text{ch}}(h) = \text{inaccurate volume}$$

In this study, an error term (E), is introduced in order to adjust the tank chart volume (V_{ch}). Correct volume at level, h has been represented as $V_{\text{theo}}(h)$.

$$V_{\text{theo}}(h) = V_{\text{ch}}(h) + E(h) \quad (3.63)$$

Therefore, ideal variance (i.e. $\text{Var}=0$) can be written as follows:

$$\text{Var}_{\text{ideal}} (= 0) = [V_{\text{ch},f} + E_f] - [V_{\text{ch},i} + E_i] + dV_{\text{act}}$$

$$\text{Var}_{\text{ideal}} (= 0) = [V_{\text{ch}}(h_f) - V_{\text{ch}}(h_i) + dV_{\text{act}}] + E(h_f) - E(h_i)$$

$$\text{Var}_{\text{ideal}} (= 0) = \text{Var}_{\text{ch}} + E(h_f) - E(h_i)$$

$$\text{Var}_{\text{ch}} + E_{\text{Var}} = \text{Var}_{\text{ch}} + E(h_f) - E(h_i)$$

$$E_{\text{Var}} = E(h_f) - E(h_i) \quad (3.64)$$

Due to the variance of ideal systems is equal to zero, the above equation can be written as follows:

$$-\text{Var}_{\text{ch}} = E(h_f) - E(h_i)$$

$$\text{Var}_{\text{ch}} = E(h_i) - E(h_f) \quad (3.65)$$

Table 3.1. A sample incoming data sequence

Day	h_i	V_{ch}	h_f	V_{ch}	Sales	Delivery	Correction
1	h ₁	V _{ch,1}	h ₂	V _{ch,2}	V _{S,1}	V _{D,1}	V _{C,1}
2	h ₂	V _{ch,2}	h ₃	V _{ch,3}	V _{S,2}	V _{D,2}	V _{C,2}
3	h ₃	V _{ch,3}	h ₄	V _{ch,4}	V _{S,3}	V _{D,3}	V _{C,3}
4	h ₄	V _{ch,4}	h ₅	V _{ch,5}	V _{S,4}	V _{D,4}	V _{C,4}

It is seen on the above table, the beginning fuel level of day 2 is equal to the end of day 1.

$$E_1 - E_2 = \text{Var}_1$$

$$E_2 - E_3 = \text{Var}_2$$

$$E_3 - E_4 = \text{Var}_3$$

.

.

$$E_{n-1} - E_n = \text{Var}_{n-1}$$

In that system, there are (n) unknowns (i.e: E₁, E₂, E₃, until E_n) and (n-1) equations (Var₁, Var₂, Var₃, until Var_{n-1}). The degree of freedom (DOF) of that system is equal to 1.

$$\text{DOF} = n - (n-1) = 1$$

1 (one) more relation is needed in order to solve the equations of that system. At that point, two method is applied. First method is that an initial guess is made for any of the E_i values to make “DOF=0”. For simplicity, E_1 is assumed as “F”. Second method is that the sum of all relations is added among equations.

$$E_1 - E_n = \sum_{i=1}^{n-1} \text{Var}_i$$

If the 1st method is followed:

$$\left| \begin{array}{ccccccccc|ccc} 1 & 0 & 0 & 0 & \cdot & \cdot & \cdot & \cdot & 0 & 0 & 0 \\ 0 & 1 & -1 & 0 & 0 & \cdot & \cdot & \cdot & 0 & 0 & 0 \\ 0 & 0 & 1 & -1 & 0 & 0 & \cdot & \cdot & 0 & 0 & 0 \\ 0 & 0 & 0 & 1 & -1 & 0 & 0 & \cdot & \cdot & 0 & 0 \\ \cdot & \cdot & \cdot & \cdot & \cdot & \cdot & \cdot & \cdot & \cdot & \cdot & \cdot \\ \cdot & \cdot & \cdot & \cdot & \cdot & \cdot & \cdot & \cdot & \cdot & \cdot & \cdot \\ 0 & 0 & 0 & \cdot & \cdot & 0 & 0 & 1 & -1 & 0 & 0 \\ 0 & 0 & 0 & \cdot & \cdot & 0 & 0 & 1 & -1 & 0 & 0 \\ 0 & 0 & 0 & \cdot & \cdot & \cdot & \cdot & 0 & 0 & 1 & -1 \end{array} \right| = [A]_{n*(n+1)}$$

$$\left| \begin{array}{c} E_1 \\ E_1 \\ E_2 \\ \cdot \\ \cdot \\ \cdot \\ E_n \end{array} \right| = [E]_{(n+1) \times 1}$$

$$\left| \begin{array}{c} F \\ Var_1 \\ Var_2 \\ \cdot \\ \cdot \\ \cdot \\ Var_{n-1} \end{array} \right| = [B]_{(n+1) \times 1}$$

The solution for $[A][E]=[B]$ is:

$$[E] = [A^{-1}][B] \text{ or } [E] = [A] \setminus [B] \quad (3.66)$$

If the 2nd method is followed:

$$\left| \begin{array}{ccccccccc} 1 & -1 & 0 & 0 & \cdot & \cdot & \cdot & \cdot & 0 & 0 & 0 \\ 0 & 1 & -1 & 0 & 0 & \cdot & \cdot & \cdot & 0 & 0 & 0 \\ 0 & 0 & 1 & -1 & 0 & 0 & \cdot & \cdot & 0 & 0 & 0 \\ 0 & 0 & 0 & 1 & -1 & 0 & 0 & \cdot & \cdot & 0 & 0 \\ \cdot & \cdot & \cdot & \cdot & \cdot & \cdot & \cdot & \cdot & \cdot & \cdot & \cdot \\ \cdot & \cdot & \cdot & \cdot & \cdot & \cdot & \cdot & \cdot & \cdot & \cdot & \cdot \\ \cdot & \cdot & \cdot & \cdot & \cdot & \cdot & 0 & 1 & -1 & 0 & 0 \\ 0 & 0 & 0 & \cdot & \cdot & \cdot & 0 & 0 & 1 & -1 & 0 \\ 0 & 0 & 0 & \cdot & \cdot & \cdot & 0 & 0 & 0 & 1 & -1 \\ 0 & 0 & 0 & \cdot & \cdot & \cdot & 0 & 0 & 0 & 0 & 1 \end{array} \right| = [A]_{n \times n}$$

$$\left| \begin{array}{c|c} E_1 & \\ E_2 & \\ E_3 & \\ \cdot & = [E]_{(n+1) \times 1} \\ \cdot & \\ E_n & \\ E_{n+1} & \end{array} \right|$$

$$\begin{array}{c|c} \text{Var}_1 & \\ \text{Var}_2 & \\ \text{Var}_3 & \\ \cdot & = [B]_{(n+1) \times 1} \\ \cdot & \\ \text{Var}_{n-1} & \\ \sum \text{Var}_i & \end{array}$$

The solution of the above matrix system is same with the 1st method solution.

$$[E] = [A^{-1}][B] \text{ or } [E] = [A] \setminus [B]$$

Solving of [E] with either 1st or 2nd method will give a series of “E_i” which are the adjustments of volumes at given “fuel level, h” values. At that point, there is a set of “h-E” pairs. The problem of the set of data is that, the error (E) values between two consecutive fuel levels (h) values are not defined because E values are discrete with respect to h values. This problem can be overcome simply by “curve fitting toolbox” of MATLAB.

Instead of variance values, normalized variances should be used in order to be worked efficiently.

$$\text{Var}^* = \frac{\text{Var}}{dv_{\text{act}}} \quad (3.67)$$

4. RESULTS AND DISCUSSIONS

The aim of this study is to determine the effects of several parameters on the tank calibration chart and to minimize/reduce the extreme variances that lead to inaccuracy and problems in leak detection. In the methodology part, the theoretical models were explained with their level to volume relations. In this section, the effect of each parameter was tested and the real time data, which were gathered from different sites, were used to test the theory and the efficiency of the models on the variance reduction.

UST systems (composed of tanks, associated piping, pumps and dispensers that deliver product to the customers) are examined holistically in wet-stock management. End of the day fuel variance is not a good method to determine the loss or gain of liquid (i.e. variance) within the UST system. Fuel variance is classified in two ways: real variance and apparent variance. Apparent variance is caused by accounting errors and poor tank calibration. It can mask any actual fuel loss, which is not desired. In order to overcome to this problem, poor tank calibration was tackled in this work. The numerous benefits of accurate tank calibration in leak detection are: (i) improved (lowered) variances, (ii) earlier loss and leak detection, (iii) quicker response in case of a leak, (iv) fewer alarms, (v) more precise pump calibration management and (vi) decreased write-offs.

Fuel variance is determined by reconciliation of the present liquid amount in the tank and the calculated amount with respect to sales and delivery volumes. Section I: Introduction addressed the importance of fuel variances in leak detection in detail. In this work, reduction of the variance was aimed, by introducing tank deformation parameters, and therefore obtaining better height to volume relations that would reduce the accounting errors. Thus, variances were minimized/reduced and masking effect of them on the real losses was eliminated.

Effects of uniform or non-uniform deformations can be seen in the variance pattern. Depending on the tank deformation type, it requires either uniform adjustment or non-uniform adjustment. Uniform adjustment technique tries to compensate for a uniform deformation and is based on changing the tank parameter(s) (such as tilt angle or radius). When the tank parameters shift in either positive or negative direction, the tank calibration

chart changes. In a fuel service station, the original (i.e. old) calibration charts are obtained for ideal dimensions with radius, length, dished head depth (if available), horizontal probe position, axial tilt of $\alpha=0^\circ$, and radial tilt of $\beta=0^\circ$. Later on, for instance, if the tank has a radial tilt (or axially tilted, with shorter or lengthier diameter/length/dished head depth/probe offset), the volume measurements would include errors. These kinds of fuel variances are seen extremely high and a wet-stock management analysis can misguidedly point to a leak. The reason of this evaluation comes from variance definition: “For the targets of detecting a leak, it is essential that the quantities of petroleum delivered, stored and dispensed are accurately measured and the difference between gives variance”. In order to eliminate that error, in the ‘uniform variance adjustment part’, a new level to volume (LV) equation is obtained by investigating each parameter and finding the optimal combination (i.e. radial tilt, axial tilt, length, radius, probe position and dished head depth) that reduces the error in liquid volume. Besides uniform deformations, non-uniform deformations may also occur. These type of deformations include partial bucklings at different tank level and require a non-uniform or local adjustment. In this work, we addressed this problem by defining an error function. Therefore, a correction factor for both of the uniform and non-uniform cases, variance trends were improved and their masking effects were prevented.

The major reason for the virtual variances is the error introduced in the conversion of the liquid height to liquid volume because of the inaccuracy or change in tank dimensions. Thus, theoretically, once the correct dimensions and/or the corrections for the changes (such as tilts) are introduced in the volume calculations, the virtual variances should be reduced. In order to test this theory with our derived mathematical models, we have selected five tanks, whose real time data were available from actual sites. These data were obtained from confidential trade sources and will be referred as Site A, Site B, Site C, Site D, and Site E (Table 4.1). The real time data of these specific tanks were gathered for a specific time period (i.e. 4-month) and the results of the study were presented below with discussions. In addition, all raw data are presented in Appendices.

4.1. SIMPLE CYLINDER TANK (SCT)

Although we did not use the SCT equations for variance minimization in this study, in this section, we would like to demonstrate the effects of parameters on a horizontal SCT (i.e. flat

ended horizontal cylindrical tank) through our models. The dimensions of the sample tank from Site A are given in Table 4.1. Initial tank calibration chart was established with no radial nor axial tilt. Volume of the liquid in the tank is calculated with the given tank sizes, which simply consists of radius and length. The effects of six parameters (i.e. R, L, H, M, radial tilt (β) and axial tilt (α)) on SCT liquid volume were examined. Data of each study in this part was presented in Table D.1 and Table D.2 in Appendix D.

Table 4.1. Acquired dimensions of selected tanks

	Total Volume	Radius, R	Length, L	Gauging Point, M	Dished Head Depth, H	Wall Type
	liter	mm	mm	mm	mm	S/D
Site A	10000	1240	2000	400	-	Single
Site B	20000	1250	3750	600	400	Single
Site C	20000	1250	3750	600	400	Single
Site D	30000	1250	6000	600	350	Single
Site E	30000	1240	6000	700	400	Double

4.1.1. Effect of Parameters on SCT Calibration Chart

Eq. 3.1 shows that length and radius are directly proportional to SCT volume (therefore liquid volume) and these were investigated introducing a change of ± 20 mm to radius (R) and a change of ± 40 mm to length. Figure 4.1 shows that greater radius or length imply greater SCT volume, thus that of contained liquid. This introduction for radius is based on the literature, which states: “The diameter can only be changed by a maximum of 2%” [20].

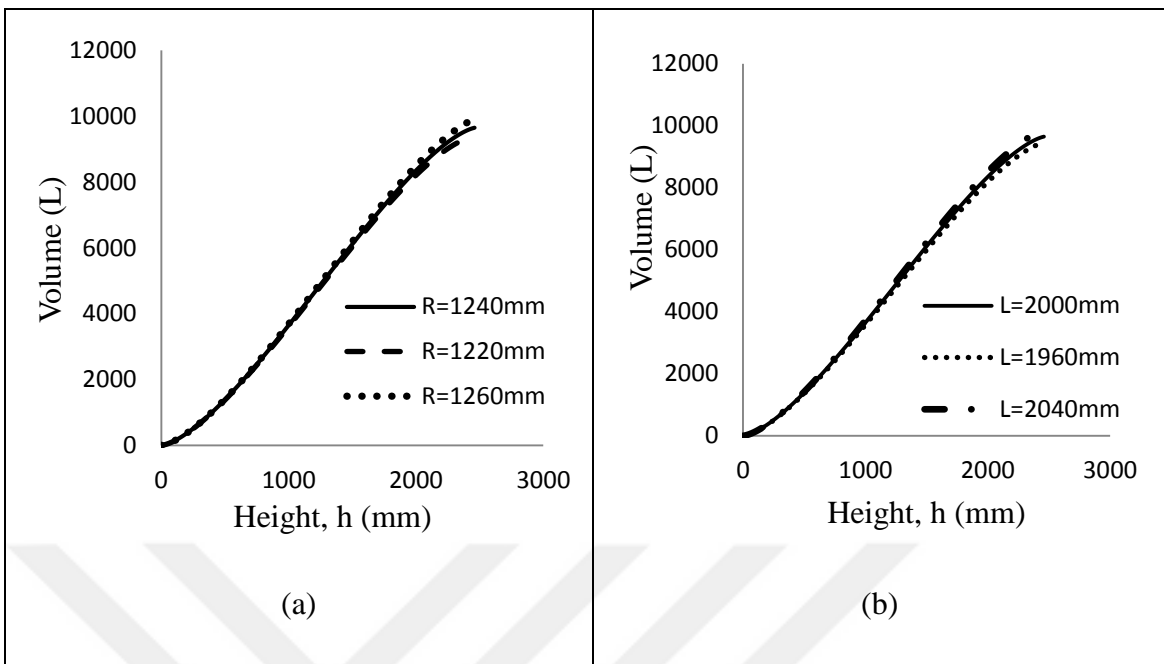


Figure 4.1. (a) Radius and (b) Length effects on the volume of SCT and liquid inside

The chosen tank is SCT (i.e. without dished head), so dished head depth equals to zero (i.e. $H=0$ mm), and has no effect on the volume of the liquid contained in a SCT. Another parameter is the horizontal probe distance from the tank corner (i.e. M) that probe offset is ineffective on calculated volume in the case of no tank tilt. Probe offset of ± 20 mm was introduced and Figure 4.2 shows that probe position has no effect on volume due to tank tilt equals to zero and probe measures the same fuel level at the different offsets.

On this system, a radial tilt of $\Delta\beta = \pm 10^\circ$ was introduced and Figure 4.3 shows the effect of $\pm \beta$ tilt (i.e. radial) on SCT contained liquid volume. It can be seen that positive and negative radial tank tilts have the same effect owing to the symmetry. Figure 4.3 shows that when radial tilt is introduced, although the actual liquid volume does not change, the measured volume increases and the current calibration chart changes.

Next, to observe the effect of the axial tilt, an angle of $\pm 5^\circ$ was introduced. As Figure 4.4 shows, when the tank tilt in either $\pm \alpha$ direction, the tank calibration chart is affected differently. The reason of the selection of axial tilt angle as $\pm 5^\circ$ is based on the following information: “Although this document does not impose any limits on the maximum tank diameter and maximum tank tilt, which this document is applicable, the practical limits would be about 4 m in diameter and 10° in tilt” [37]. In order to demonstrate of axial tilt on SCT volume, the specified angles were used.

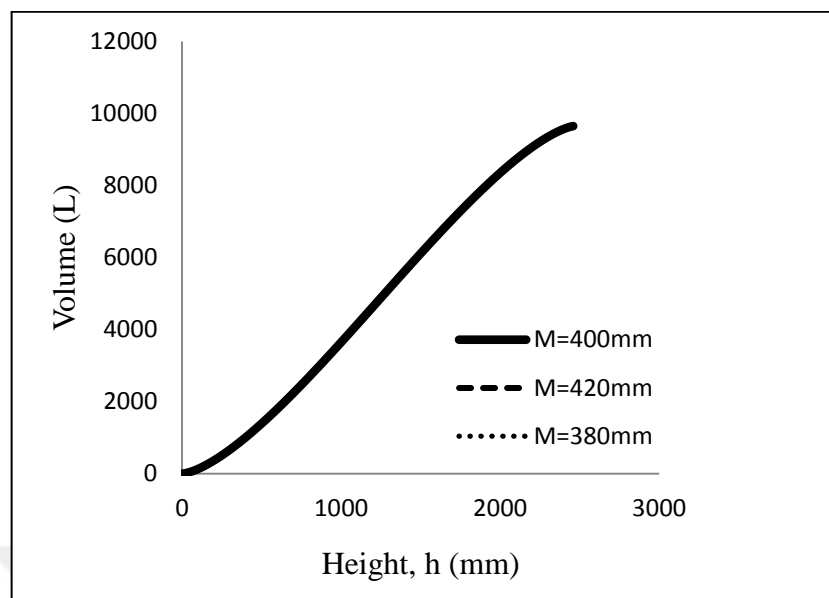


Figure 4.2. Horizontal probe distance from the tank corner (M) effect on SCT volume

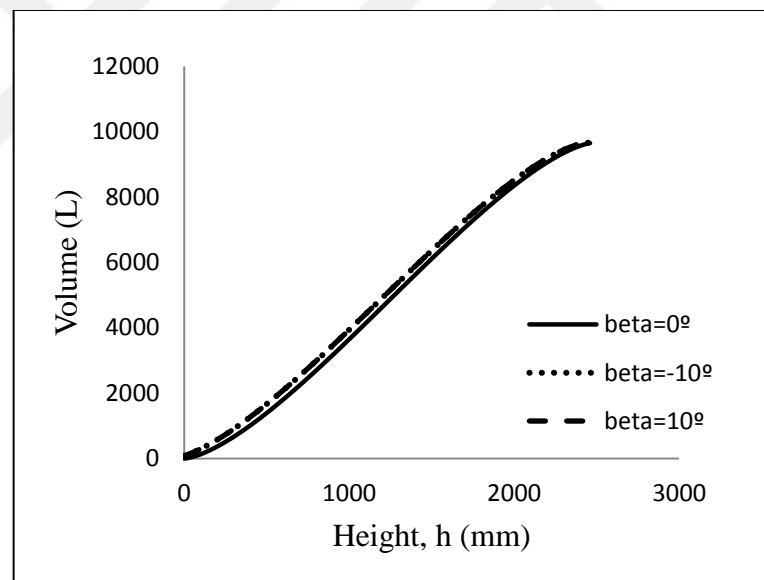


Figure 4.3. Radial (beta) tilt effect on calculated volume in SCT

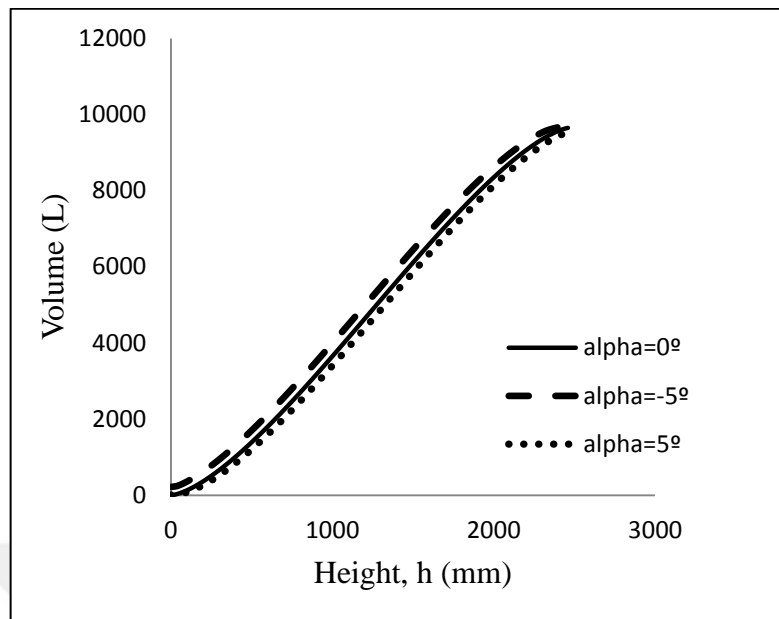


Figure 4.4. Axial (α) tilt effect on SCT volume

Figure 4.1 to 4.4 show that the radius and axial tilt have the strongest effects on the measured volume. In other words, the largest error into the volume calculation is introduced upon the change in tank radius (R) and axial tilt angle (α) even for small changes. As long as $\alpha=0$, the location of the gauging point (where the probe is located (i.e. M)) has no effect on tank level to volume conversion of SCTs, which depends on tank radius, tank length, and instant fuel level.

4.2. CYLINDER TANK WITH DISHED HEAD (CTDH)

To demonstrate the effects of tank parameters on the calibration chart, we have selected the tank in Site B, whose data is given in Table 4.1. Initially, tank calibration chart was prepared with no radial or axial tilts. When no deformation is present, the actual and calculated volumes simply depend on radius (R), length (L), and dished head depth (H). The effects of the six parameters (i.e. R , L , H , M , radial tilt (β) and axial tilt (α)) were investigated and presented below.

4.2.1. Effect of Parameters on CTDH Calibration Chart

The goal of the investigation of axial tilt effect on the volume is to determine an interval that helps us to approach the ideal variance pattern. Figure 4.5 (a) shows that while dashed lines represent the shift in ‘negative alpha’ direction, data with points represent that of ‘positive alpha’. The respective LV relations show that positive alpha case has a smaller effect compared to that of negative alpha, and deviation from the ideal is smaller. Similarly, radial tilt effect was investigated by introducing positive and negative radial tilts. Figure 4.5 (b) shows that while straight line represents ‘no radial tilt’, dashed lines represent ‘positive beta’. As expected, when the tank tilts in either beta direction, the effect is the same due to symmetry.

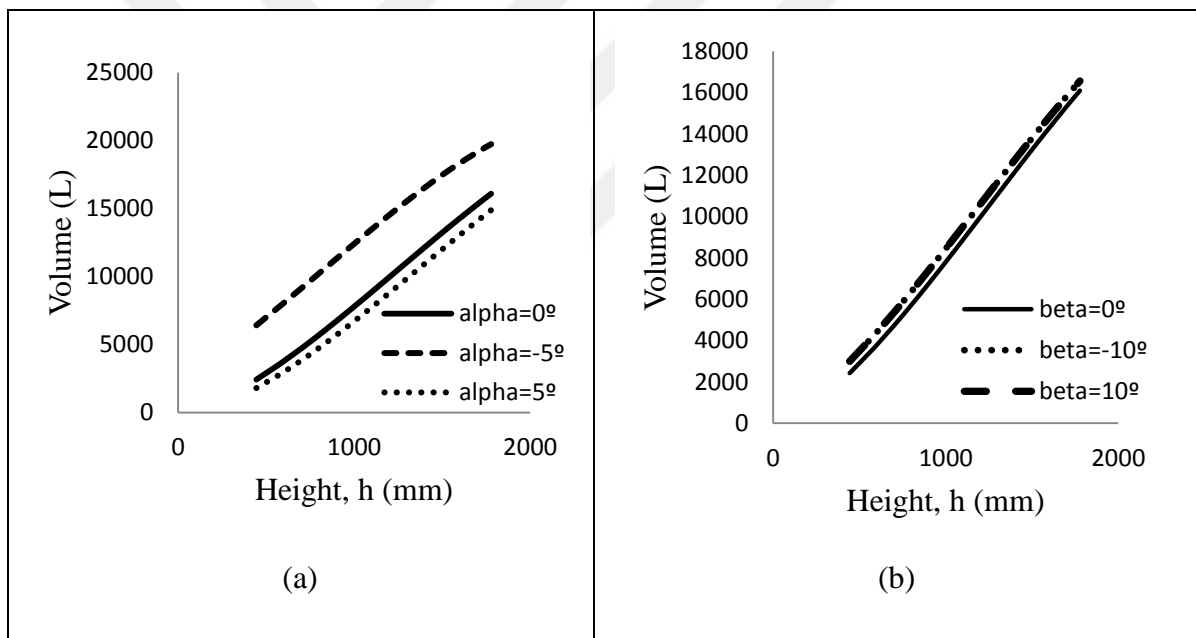


Figure 4.5. (a) Axial tilt (α) effect and (b) Radial tilt (β) effect

Next, the effect of changing tank radius on the calculated volume was investigated. Figure 4.6 (a) shows that when radius is increased, the total volume of tank (therefore the volume of the contained liquid) also increases. According to Figure 4.6 (a) and Eq. 3.26, tank radius and volume are directly proportional. Similarly, Figure 4.6 (b) and Eq. 3.26 show that the effect of varying tank length is similar to that of tank radius.

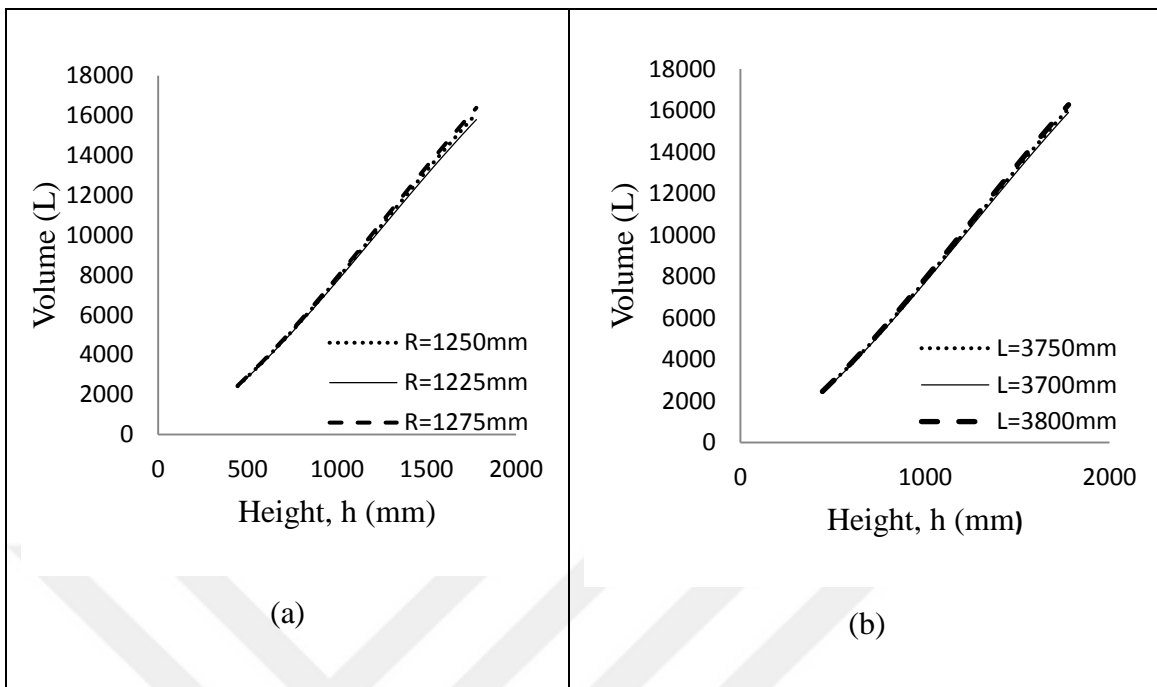


Figure 4.6. (a) Radius (R) and (b) Length (L) effect

The dished head depth (H) effect on the volume is presented in the Figure 4.7 (a). This figure shows that if the dished head depth is increased, the volume also increases. Another parameter is horizontal probe distance from the tank corner (i.e. M). In case of no tank tilt (i.e. radial and/or axial), probe offset in the direction of x-axis has no effect on the calculated volume (for $\alpha=0$) since the probe senses the same fuel height along tank longitudinal axis (i.e. x-axis), which can also be seen in the Figure 4.7 (b).

Figure 4.5 to 4.7 show that the axial tilt has the strongest effect on the measured volume. In other words, the largest error into the volume calculation is introduced upon the axial tilting of the tank. Data of each of the studies in this part were presented in Table D.3, Table D.4, and Table D.5 in Appendix D.

4.3. VARIANCE MINIMIZATION/REDUCTION

The dimensions of tank in their ideal form were obtained from the tank manufacturer(s). The known tank dimensions were placed into the theoretical tank volume equations, which were presented in Section 2: Methodology and the variances were determined. Later on, the derived tank models were used to determine the change in the tank parameters and the new (reduced) variances were calculated. The results are presented below with discussions.

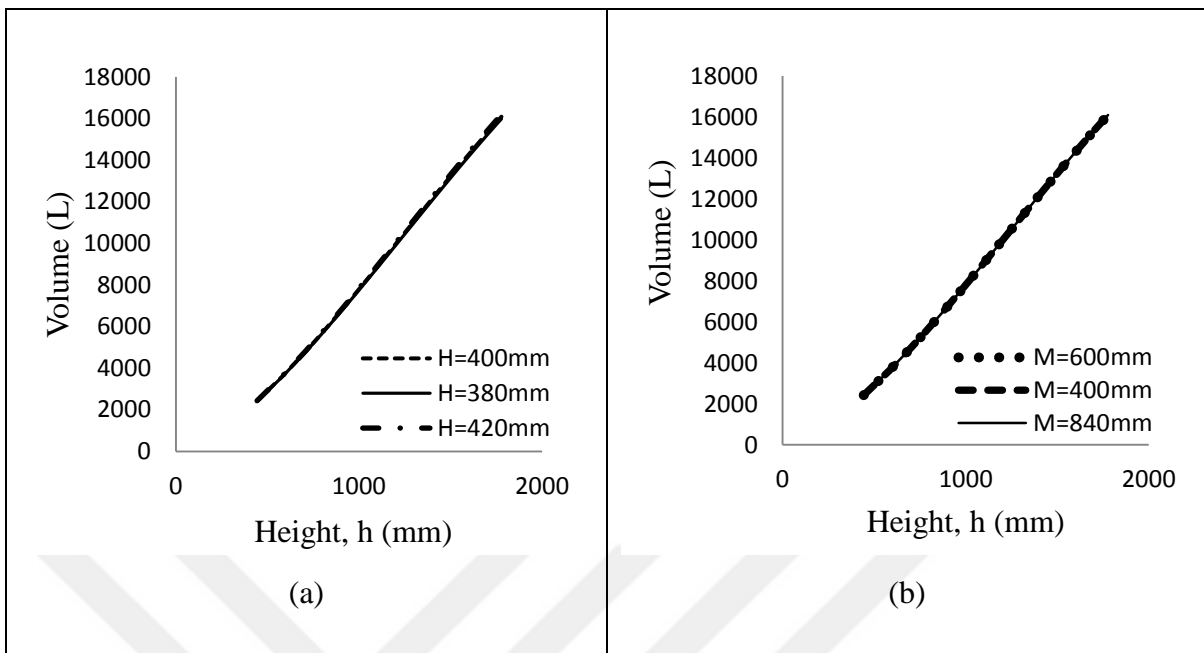


Figure 4.7. (a) Dished head depth (H) and (b) Horizontal probe distance (M) effect

4.3.1. Non-problematic Tank

In this type tank, the chart level to volume conversion should be very close to that of theoretical model. Figure 4.8 clearly shows that, level to volume conversion of the theoretical model chart and currently applied chart (supplied by the tank producer) are very close to each other, and this tank can be classified as “non-problematic tank”. The data was obtained from the tank in Site C and it was tabulated in Table E.1 and E.2 in Appendix E.

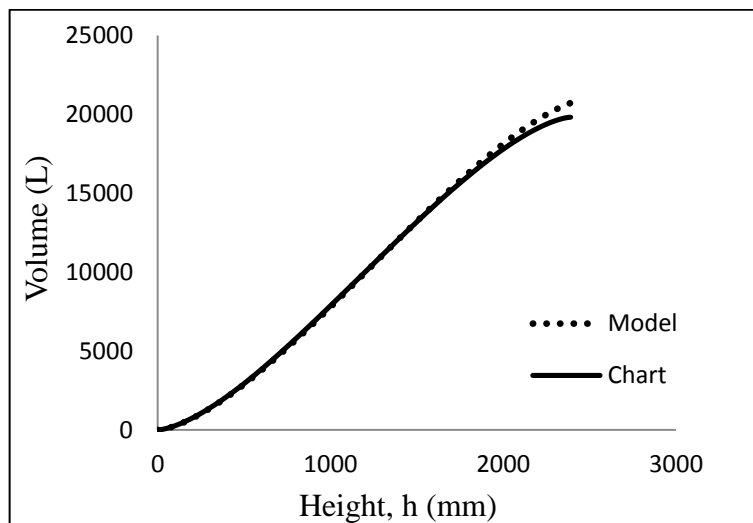


Figure 4.8. Non-problematic current calibration chart of the tank in Site C

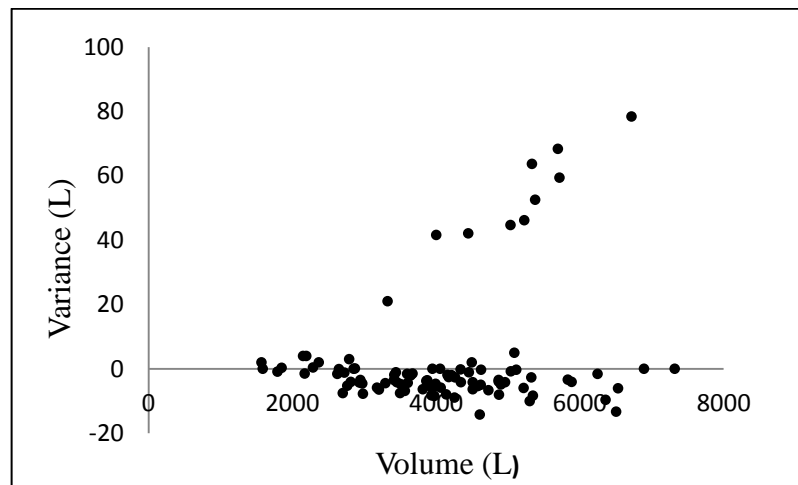


Figure 4.9. Variance vs. volume graph for the tank in Site C

4.3.2. Uniform Variance Adjustment

In this case, tank 4 of Site D (see Table 4.1) was investigated by real time data. The gathered real time data were used and variance vs. fuel height graph was plotted as in Figure 4.10. The nominal variance lies between +20 L to – 200 L. Apart from the extremes caused by missing sales, missing invoice information, or not recorded correction volume, a uniform and linear variance distribution can be seen in Figure 4.10. This implies that, a uniform adjustment is required to minimize the variances.

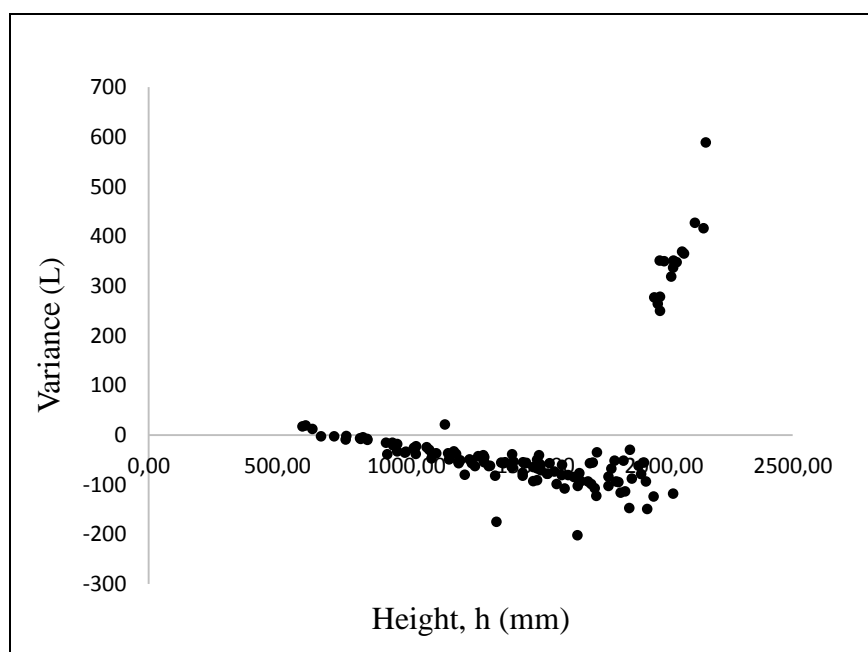


Figure 4.10. Variance distribution of the tank current chart in Site D

Figure 4.10 shows that above the level of 2000 mm, variances are in the form of gain due to the deliveries. We explained the over calibrated tank chart and its variance trend in Section 1.7. Following the idea, this tank chart was classified as “over calibrated”. In addition, the variance shows a linear trend. Therefore, current variance distribution with fuel level can refer to “uniform deformation” and thus requires a uniform adjustment in its one or more parameters.

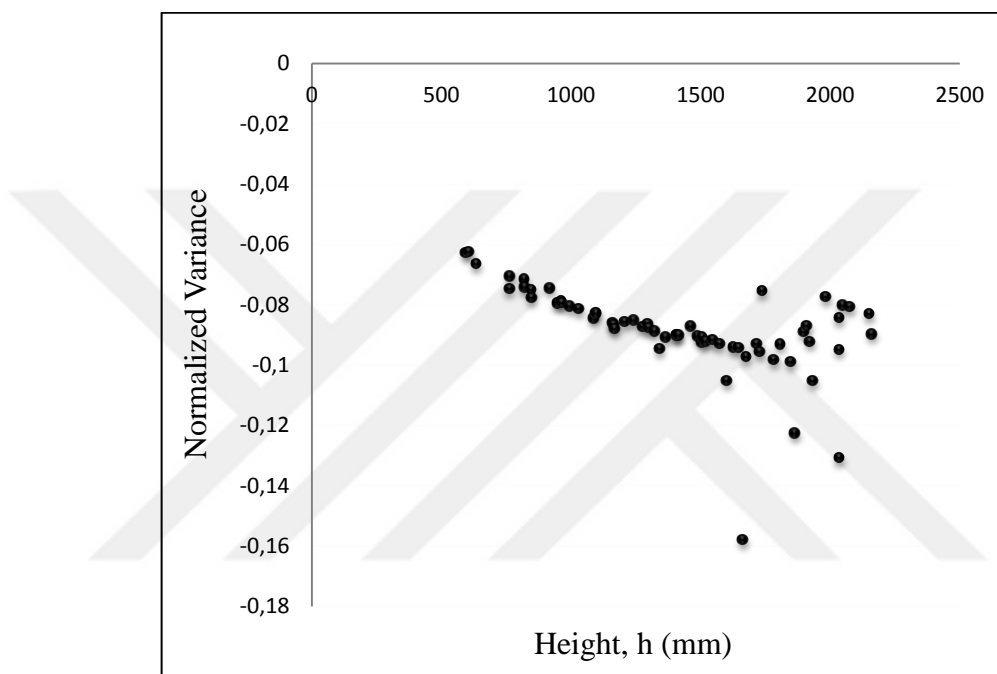


Figure 4.11. Normalized variance distribution of the tank current chart in Site D

Following the determination of current variance trend, normalized variance pattern was obtained by Eq. 3.67 as shown in Figure 4.11 by dividing the variance values by the actual volume change, which is obtained from sales, invoiced delivery and correction volumes. The reason for normalization is to get rid of the scaling in large volume changes. In order to identify the parameter(s) that deviates from ideal we have compared the effect of the parameter changes on the variance with the normalized variance. This is presented in Figure 4.12.

Figure 4.12 showed that the most similar effect is achieved by a (+/-) change in radius and axial tilt. Through following a simple trial and error procedure, whose MATLAB script is given in Appendix F, the deviation of axial tilt, radial tilt, probe offset from their ideal values were determined.

In order to determine the parameters' shift from the ideal value, and to test the validity of our variance reduction approach, the data set was divided into two groups: The first half of the data is used to determine the optimal tank parameters, and the second half is used to check the determined optimal parameters.

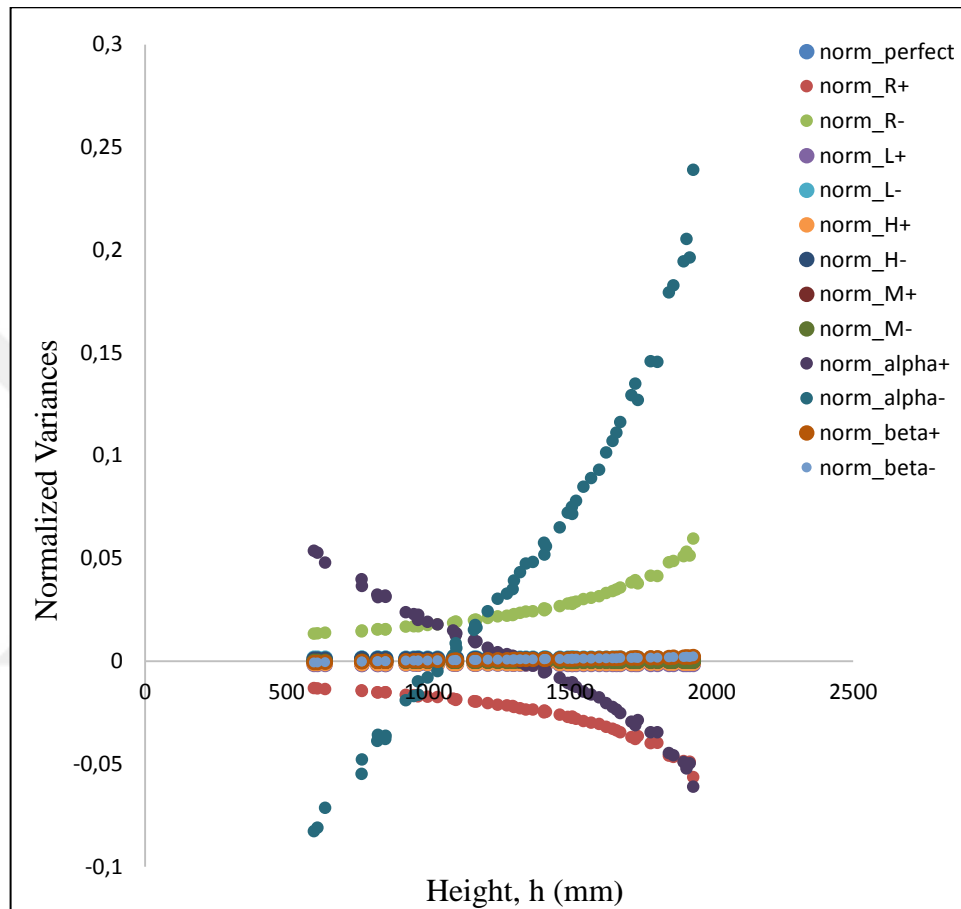


Figure 4.12. All normalized variance distributions of the tank in Site D

Using dished head tanks theoretical volume equation (Eq. 3.26), trials were made with first data set and the optimal parameters are obtained. Then, the obtained parameters were put into the corresponding equation and cross checked with second data set. Each study contains more than one graph that were presented in Figure 4.13, Figure 4.14, and Figure 4.15.

Figure 4.13 shows that variances were reduced by uniform adjustment. Initially, the variance range of current chart is in +20 L to -200 L bar. After the adjustment, this variance bar lowered in +40 L to -20 L. With this improvement, the masking effect is eliminated and physical losses should be detected more easily. The original and optimized parameters of this tank are given in Table 4.2. These parameters are determined by using first group data.

However, at that point, these parameters are not directly accepted as the optimal volume parameters. For this reason, these determined parameters are taken as tank dimensions and using second group data, variances are calculated. Then, it is seen obviously that the determined parameters are appropriate for variance minimization. Figure 4.14 shows that the variance distribution is in ± 40 bar.

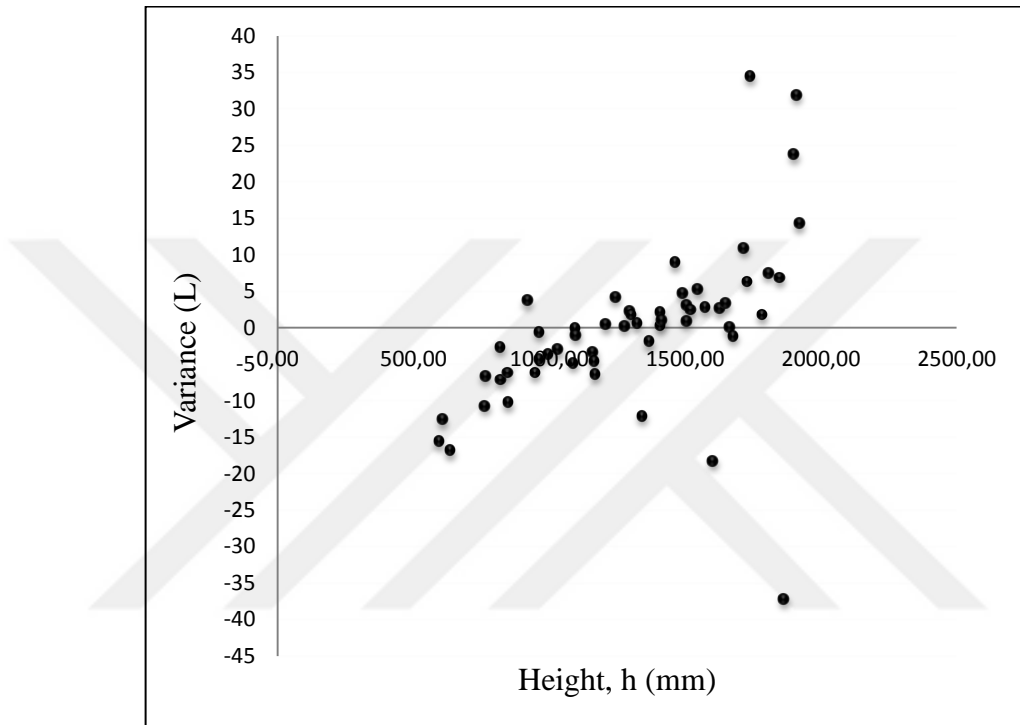


Figure 4.13. First data group variance distribution of the tank in Site D

In ideal case, variance must be equal to zero. That is, the measured closing stock volume and calculated booking stock volume, which is obtained from initial stock, sales and invoiced delivery volumes of liquid in a tank should be equal to each other.

In Figure 4.15, ideal, current chart, and model variance points were compared for all data. It is clearly seen that current variance line was approached to ideal variance line (i.e. 0). Thus, the poor level to volume conversion equation was improved by the correction in the required parameters (R , L , H , M , α , and β), which brings a uniform adjustment. The result is a new accurate tank calibration chart that gives a (more) correct volume for the measured fuel level. In addition, the correct calculation of the volume changes prevents the masking effect of poor calibration chart and enables the detection of even small leaks.

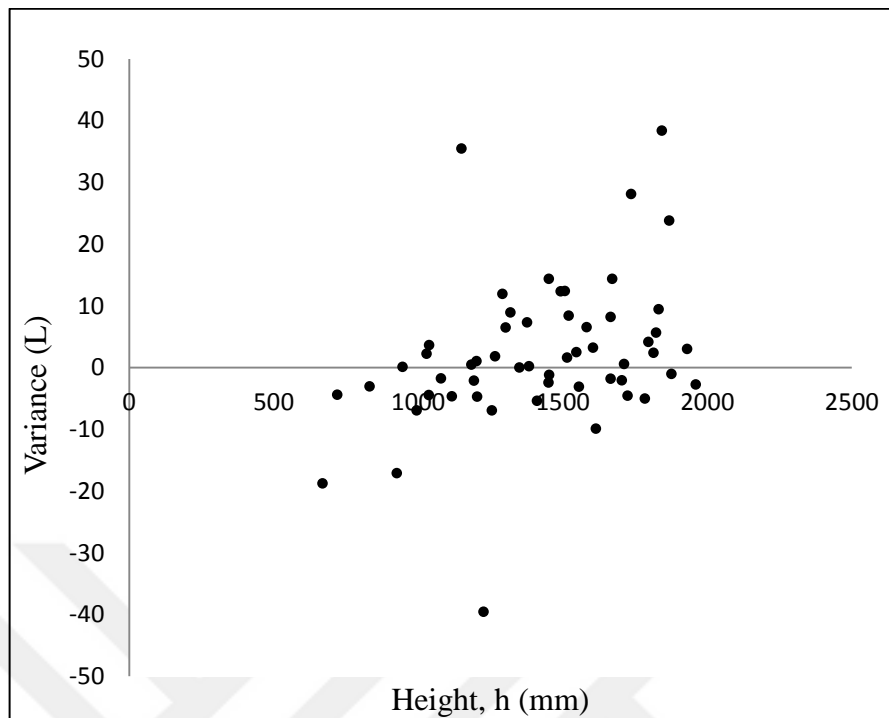


Figure 4.14. Second data group variance distribution of the tank in Site D

The determined optimal tank parameters are tabulated in Table 4.2. When the current chart tank dimensions and model dimensions are compared and Table 4.2 shows that radius is decreased by 0.4% of radius, length is decreased by 0.17% of length, and dished head depth is decreased by 2.86% of dished head depth. The difference between old and new probe offset is 240 mm. In the model tank, the horizontal probe distance from the tank corner is 840 mm. This is possible and viable in the real applications in sites. A sample tank cover drawing is presented in Figure 4.16, which shows there are seven flanges and the ATG probe can be installed into one of them. The horizontal distance between each two flanges is 242.50 mm. The old calibration chart that was established for axial tilt of $\alpha=0^\circ$, and radial tilt of $\beta=0^\circ$. However, the new calibration chart is established for axial tilt of $\alpha=3.75^\circ$, and radial tilt of $\beta=18^\circ$, which shows that tank dimensions and position changed with time. As mentioned in Introduction section, these kinds of deformations/buckles are commonly encountered. Although the changes in the parameters (i.e. R, L, H) are relatively small, owing to the large tank dimensions and total volume, the deviations of the calculated fuel volume makes a large difference. It could be said that the most effective parameters in accurate fuel volume determination for this tank are gauging point (M), axial tilt (α), and radial tilt (β).

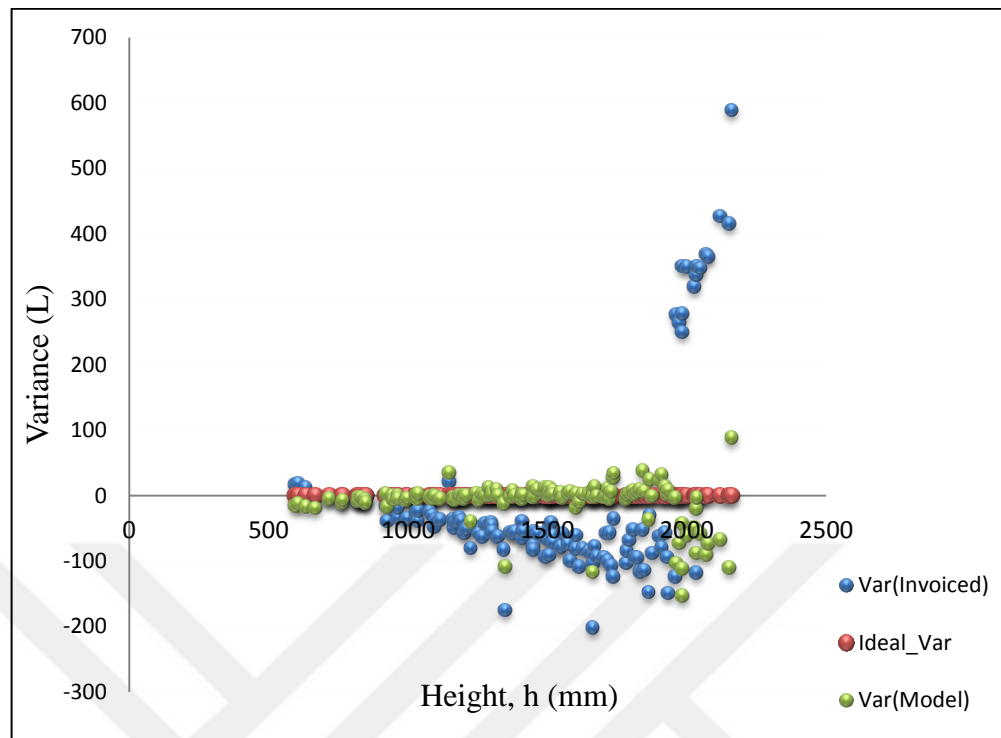


Figure 4.15. Variance comparison of current chart and model with all data groups for the tank in Site D

The sum of the absolute value of each variance in model chart was subtracted from the sum of the absolute value of each variance in the current chart and percentage decrease in variance was obtained. The percentage variance minimization was calculated as 81.3%. Data of this calculation are presented in Appendix E. Furthermore, the real time data and the details of the uniform variance adjustment, variance minimization/reduction controlled with the hourly real time data and related studies can also be seen in Appendix E.

To demonstrate the effects of uniform variance adjustment on the calibration chart, we have selected another tank in Site E with the dimensions given in Table 4.1. Initially, tank calibration chart was established with no radial and axial tilt by the manufacturer. Volume of the tank is calculated with estimated tank sizes, which consist of radius, length, dished head depth. The gathered real time data, which were tabulated in Appendix E was used and variance vs. fuel height graph of the current calibration chart was plotted in Figure 4.17. The variance bar is between +100 L to – 300 L. Here again, variance has a uniform and linear distribution, which can be seen in Figure 4.17.

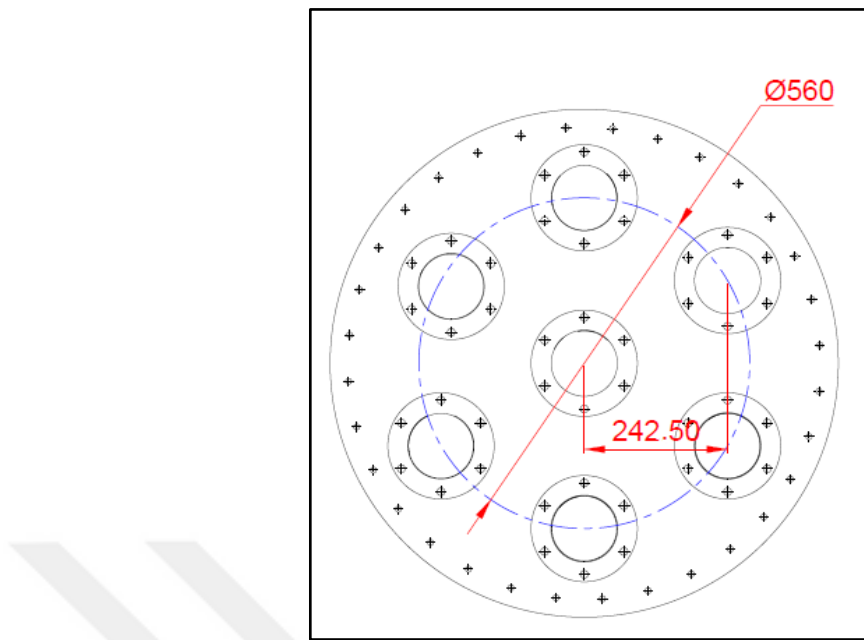


Figure 4.16. A sample of tank cover (unit in mm) [38]

In order to determine the parameters' shift from the ideal value, and to test the validity of our variance reduction approach, the data set of the tank in Site E was again divided into two groups: (i) to determine the optimal tank parameters, and (ii) to check the determined optimal parameters. Using Eq. 3.26, trials were made with first data group and the optimal parameters were obtained. Then, using the obtained parameters in the corresponding equation, and second data set was used to cross check. Results of each study are presented in the form of graphs in Figure 4.18, Figure 4.19, and Figure 4.20.

Figure 4.18 shows that variances were reduced by uniform adjustment. Initially, the variance range of current chart is in +100 L to -300 bar. After the adjustment, this variance range lowered in +20 L to -50 L bar. Thus, the masking effect was eliminated and physical losses should be detected more easily. Through a trial and error procedure the optimal parameters are obtained and presented in Table 4.3. Figure 4.19 clearly shows that the optimum parameters are appropriate for variance minimization through the reduction of the variance distribution into +20 to -40 bar.

Table 4.2. Dimension comparison of provided by manufacturer and obtained by theoretical model for the tank in Site D

Parameters	Manufacturer Tank Dimensions	Model Tank Dimensions	Change (%)
R, mm	1250	1245	5 mm (0.4%)
L, mm	6000	5990	10mm (0.17%)
M, mm	600	840	240 mm (40%)
H, mm	350	340	10 mm (2.86%)
Alpha, Degree	0	3.75	3.75°
Beta, Degree	0	18.00	18°
Capacity, L	30000 (According to teoric tank volume formula, this value equals to 31743)	30675.00	1068 L (3.36%)

The comparison of ideal, current chart (i.e. manufacturer supplied), and model variances are shown in Figure 4.20, which clearly demonstrates that model variance approaches to an ideal case (i.e. 0). Thus, the inaccurate level to volume conversion was improved by uniform adjustment and a new accurate tank calibration chart was established. In addition to these, the masking effect of poor calibration chart was eliminated and the accuracy of LV conversion was increased.

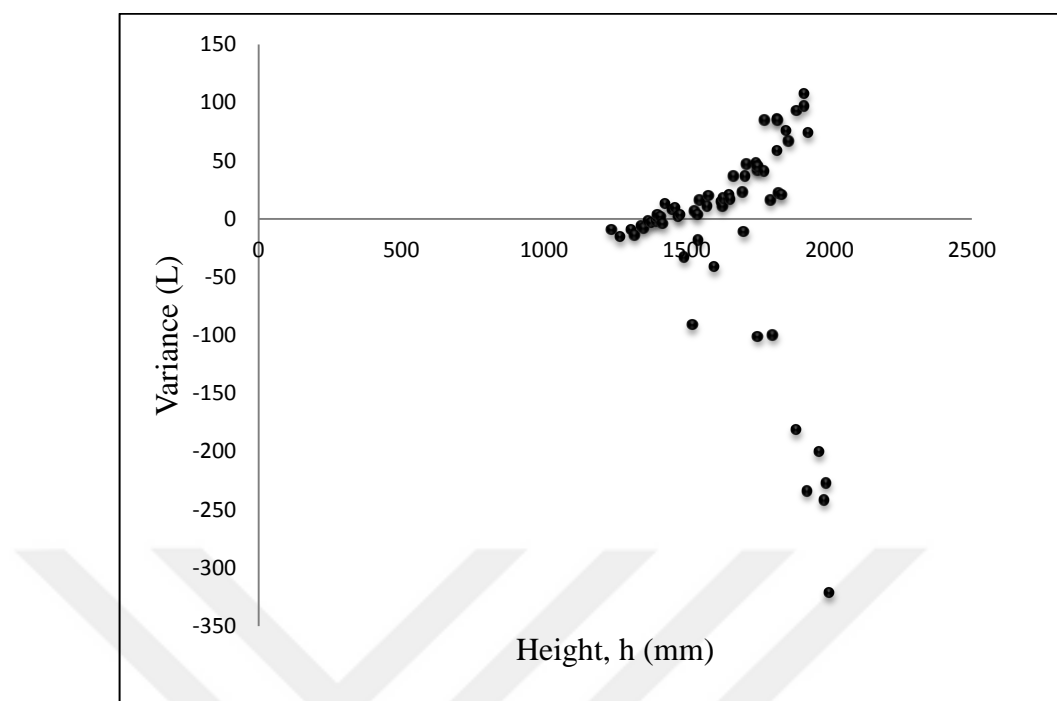


Figure 4.17. Variance distribution of the tank current chart in Site E

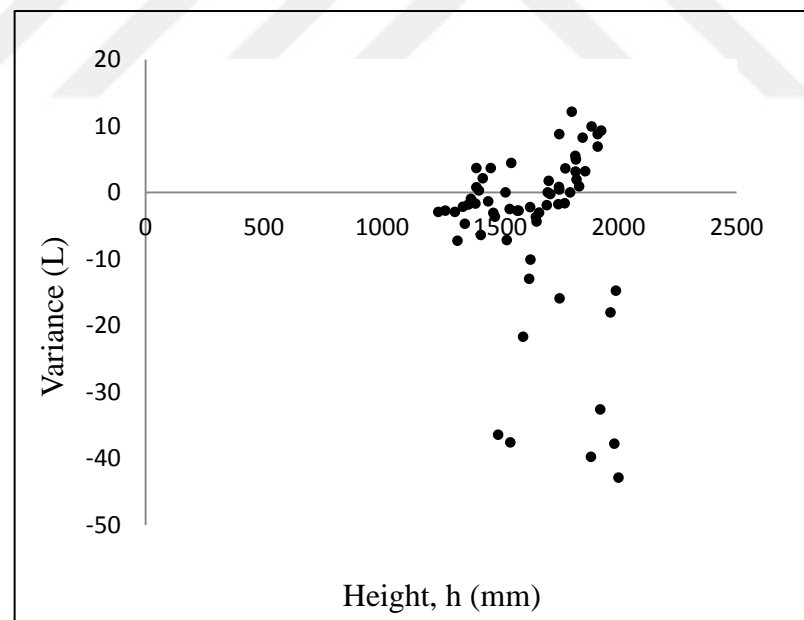


Figure 4.18. First data group variance distribution of the tank in Site E

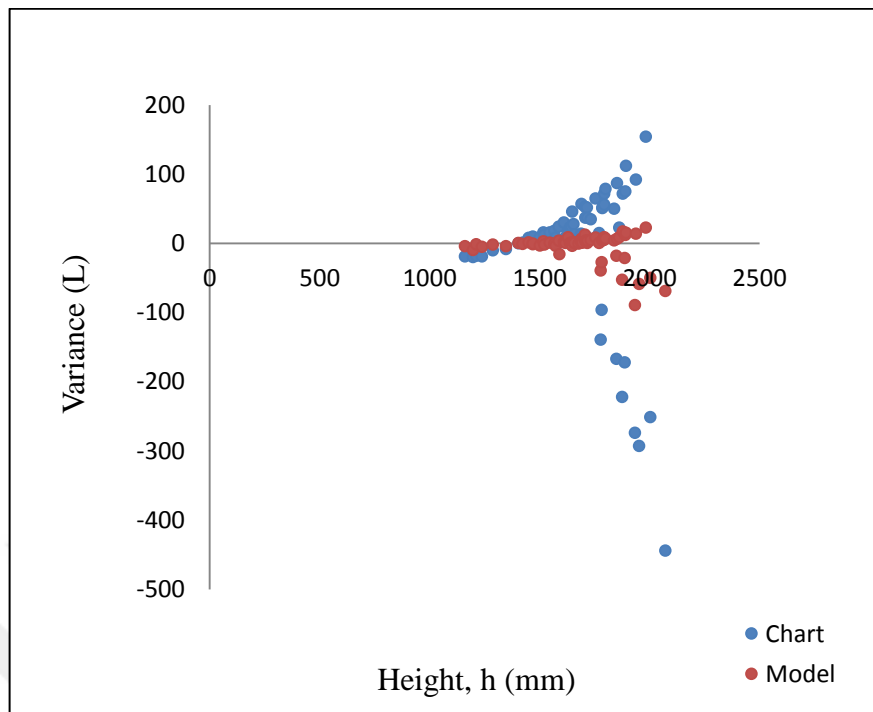


Figure 4.19. Second data group variance distribution of the tank in Site E

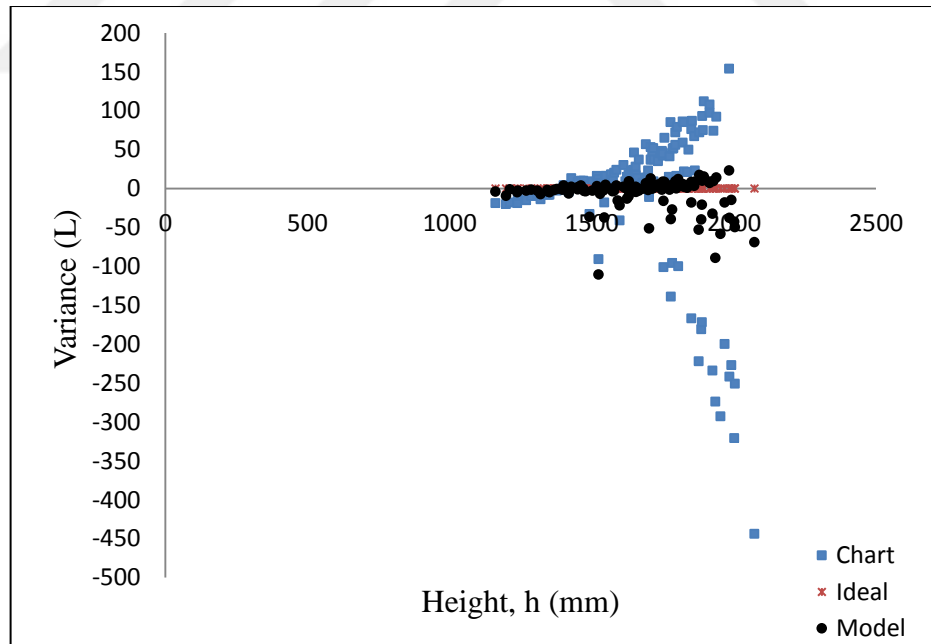


Figure 4.20. Variance comparison of current chart and model with all data groups for the tank in Site E

The current chart and model tank dimensions were compared in Table 4.3. The old calibration chart was made with axial tilt of $\alpha=0^\circ$, and radial tilt of $\beta=0^\circ$. However, our models predict an axial tilt of $\alpha=0.95^\circ$, and radial tilt of $\beta=3.00^\circ$, which is a realistic change

considering an underground tank. As mentioned in Introduction section, these kind of deformations are commonly encountered. Although the changes in the parameters (i.e. α and β) are relatively small, owing to the large tank dimensions and total volume, the deviations of the calculated liquid (fuel) volume makes a large difference.

The sum of the absolute value of each variance in model chart was subtracted from the sum of the absolute value of each variance in the current chart and percentage decrease in variance was obtained. The percentage variance minimization was calculated as 81.1%. Data of this calculation was presented in Appendix E.

4.3.3. Non-uniform Variance Adjustment

At the beginning of the variance minimization in this work, tank 1 in Site B was one of the selected tanks and uniform variance adjustment techniques were applied to this tank. However, we have failed to reduce current chart variance trend by uniform adjustment and realized that the tank has deformed partially at several regions. Unfortunately, we did not have a chance to investigate this underground tank and its deformations. For this reason, to demonstrate a non-uniform deformation case, the selected tank in Site B (see Table 4.1). Figure 4.21 shows that variance trend does not have a specific pattern. Fuel gains and losses are seen at different tank levels and there is no uniformity in the trend. Therefore, it could be said that tank may be deformed in more than one region and an adjustment that brings a uniform correction would fail. The daily real time data of the tank in Site B can be seen in Appendix E.

The time, the incorrect chart of the supplier was corrected by introducing an error term (E) for each level (h) (i.e. $E(h)$). To do this, the variance at the end of a day is calculated by the summation of LV conversion error at the initial fuel level (h_1) and the final fuel level (h_2), as usual. The real time data from the site comes in a sequence, which the beginning volume of second day equals to the end volume of first day. The series of n-days variances form a set of linear equations, as presented in Section 3.4.2. The way to solve this system is that we can write one more relation with the sum of all equations. Both ways enable that the degree of freedom (DOF) equal to zero. The solution of first and second ways is the same (Eq. 3.66).

Table 4.3. Dimension comparison of provided by manufacturer and obtained by theoretical model for the tank in Site E

Parameters	Manufacturer Tank Dimensions	Model Tank Dimensions	Change (%)
R, mm	1240	1220	20 mm (1.61%)
L, mm	6000	5990	10 mm (0.17%)
M, mm	700	600	100 mm (14.3%)
H, mm	400	400	No change
Alpha, Degree	0	0.95	0.95°
Beta, Degree	0	3.00	3.00°
Capacity, L	30000 <i>(According to teoric tank volume formula, this value equals to 31559)</i>	30340.00	1219 L <i>(3.86%)</i>

The variance bar is in +800 L to – 800 L range. Figure 4.21 shows that variance has a non-uniform and non-linear distribution. For this reason, a non-uniform adjustment technique is applied to this tank and the extreme variances and the large variance range were reduced to +15 to -15 range that can be seen in Figure 4.22.

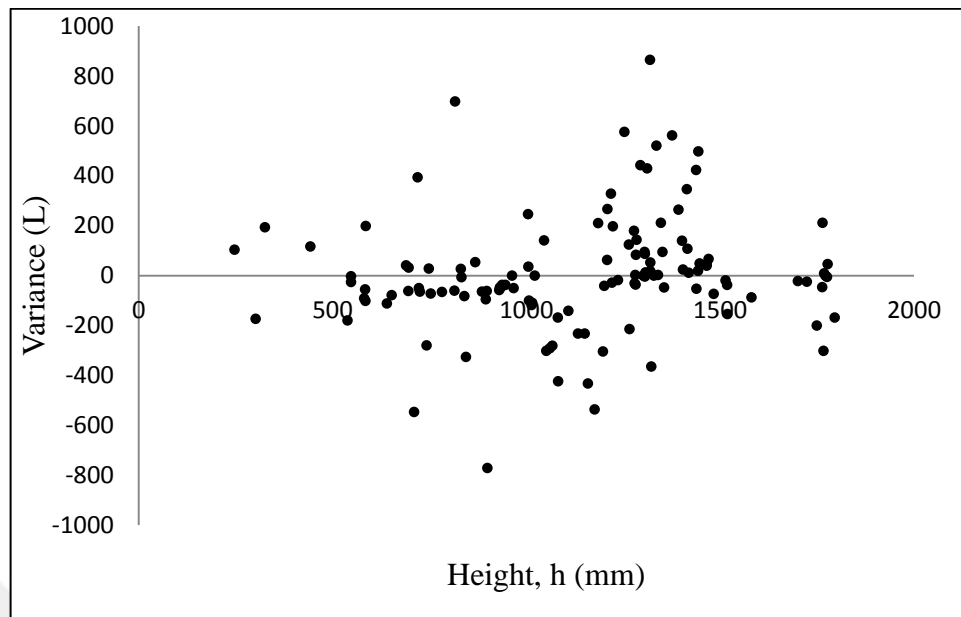


Figure 4.21. Variance distribution of the tank current chart in Site B

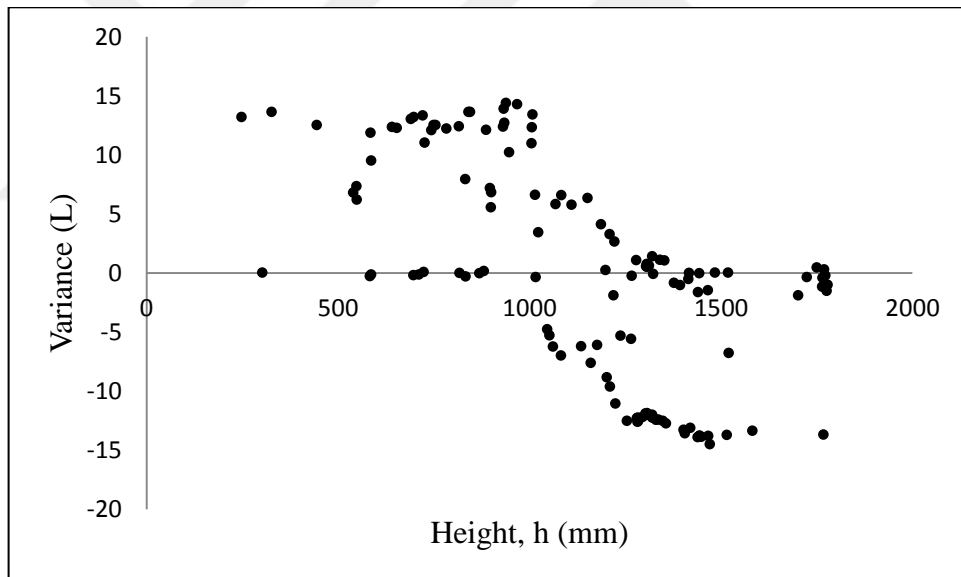


Figure 4.22. Variance distribution of the tank in Site B after non-uniform adjustment

The comparison of ideal, current chart and adjusted variances were presented in Figure 4.23, which shows that existing variance pattern was minimized and approached to the ideal variance line (i.e. 0). Thus, the calibration chart of the tank in Site B was improved by a non-uniform adjustment and the masking effect of inaccurate liquid level to volume relations is prevented.

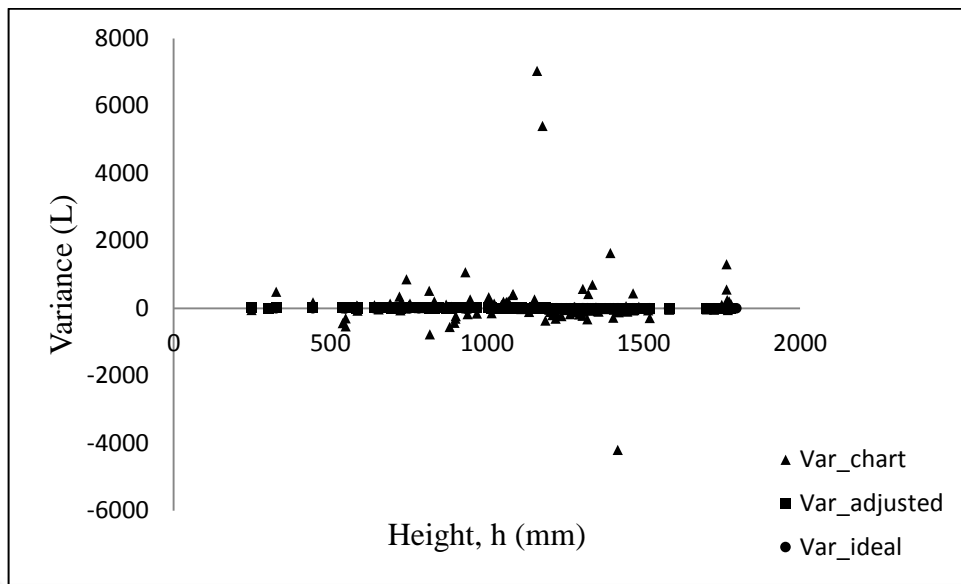


Figure 4.23. Comparison of ideal, current chart and adjusted variances

The sum of the absolute value of each adjusted variances was subtracted from the sum of the absolute value of each current chart variances and the percentage decrease was obtained. The percentage variance minimization was calculated as 97.7% and the data used in this variance minimization were tabulated in Appendix E.

When the variance minimization percentages were compared, it can be seen that the correction factor is near to hundred percent. Although this appears to be advantageous over the parameterized models, it should be kept in mind that non-uniform adjustment is a tank specific technique, which only focuses on the variance minimization and it does not determine the changed tank parameters. In addition, there is only the error (or correction) function and no theoretical tank models involved.

5. CONCLUSIONS

This study aims to improve the wet-stock management and leak detection in USTs through obtaining precise height to volume relations for the liquid contained in. For this goal mathematical models that contain the parameters for the possible deformations were derived and tested with the actual data. The accounted tank deformations are in tank parameters such as radius, length, dished head depth, probe offset and tilt (axial and radial). The analysis of the real time data showed that the deformations can be categorized into two as uniform and non-uniform, both of which require different approaches.

The conclusions of the study are as follows:

- For an undeformed tank the actual volume measurement and the model data matches. This shows that the basic model for the horizontal tanks is valid.
- The analysis of the fuel (volume) variance shows the deformation type of the tank. For a uniform deformation such as tilting of the tank, the variance shows a linear trend that is affected by one or more homogenously changed parameters. On the other hand, for a non-uniform deformation such a buckling in a specific point the variance does not have a specific trend.
- For the uniformly deformed tanks, the parameterized models bring a successful correction in the conversion of the measured liquid heights to prospective volumes.
- For the locally deformed tanks (non-uniform), a similar success was obtained not by the parameterized models, but introducing an error (or corrector) function.
- For both of the approaches (i.e. models or error function) the apparent variance in the stock management reduced considerably in the levels of 80%-100%. By this way, even the small changes in the stock-volume can be accounted for and leaks can be detected.
- This study also shows that obtaining the precise volume measurements by introducing models that account for the deformations in the UST is possible. Moreover, it also proves that this is a valid approach to reducing the apparent variances and improving the leak detection.

6. FUTURE WORK

All studies in this thesis are complete successfully and the results are valid. In order to improve the wet-stock management and leak detection systems for fuel tanks, further developments are possible and it can be moved forward. For this purposes, the below list is formed.

- Shifting of the probe along z-axis may introduce major errors especially if the tank tilts in radial axis. This factor was not parameterized within this work, and will be included in the first improvement.
- Since the parameterized models were successful in predicting the deformations and reducing the fuel variance for the uniform deformations, error functions, as in the case of non-uniform deformations, were not constructed for these cases. However, building and testing the performance of error functions for the uniform cases, and comparing the results with that of parameterized models would give some insight.
- For the improvements in the future, a combination of the model and error function is also considered.
- The major plan for the future is to construct a lab-scale tank system that can simulate the deformations and test the derived models with the controlled case studies.
- In case the method developed reaches to a product level, improvement of the software by introducing artificial-intelligence (AI) is also within consideration. This would remove the human interference as in the case of recognition of the variance patterns and create a fully automated system.

REFERENCES

1. Frankling Fueling System, The Total System Solution The Industry' s Most Comprehensive Product Offering. USA: 2011.
2. The Queensland Work Health and Safety Act, A Guide for Service Station Operators under the Work Health and Safety Act. 2016
3. Energy Regulatory Commission (ERC), Design, Commissioning, Decommissioning and Recommissioning of Petroleum Retail Service Stations. June 2016.
4. Environmental Protection Agency (EPA), Musts for USTs: EPA 510-K-15-001. Washington: November 2015
5. Jiangxi Xiongyu (Group) Co., Ltd. . China 2017 [cited 2017 15 November]; Available from: http://jxygg.en.alibaba.com/product/60580872318-802881950/selling_well_on_the_road_oil_storage_tank_with_ISO_standard_in_factory_price_for_sale_made_in_China.html?spm=a2700.8304367.prewdfa4cf.43.57351a53RU9iHx.
6. Containment Solutions Inc. (CSI), Petroleum Storage Underground Fiberglass Tanks. Texas 2014.
7. EPA, Learn About Underground Storage Tanks (USTs). 2017; [cited 2017 09 November] Available from: <https://www.epa.gov/ust/learn-about-underground-storage-tanks-usts>.
8. TORA Training: Fuel Service Stations Technical Safety. 2016.
9. Health and Safety Authority, Wetstock Reconciliation at Fuel Storage Facilities: An Operator' s Guide. Dublin 2013.
10. AFC International Inc. Combustibles. Gas Detection & Air Monitoring Specialists. 2010; [cited 2017 23 November] Available from: <http://www.afcintl.com/pdfs/applications/combustibles.pdf>.

11. Shinn RC, New Jersey Department of Environmental Protection: A Guide to the Operation and Maintenance of Your Underground Storage Tank System. New Jersey 2001.
12. Texas Commission on Environmental Quality Release Detection and Inventory Control for Petroleum Storage Tanks. Texas 2017.
13. Gorawski M, Gorawska A, Pasterak K, *The TUBE algorithm: Discovering trends in time series for the early detection of fuel leaks from underground storage tanks*. Expert Systems with Applications. 2017;90(Supplement C):356-73.
14. Environmental Protection Agency (EPA), Straight Talk on Tanks: Leak Detection Methods for Petroleum Underground Storage Tanks and Piping. US 2005.
15. Environmental Protection Agency (EPA), Introduction to Statistical Inventory Reconciliation for Underground Storage Tanks. US 1995.
16. Keating JP, Mason RL. *Using statistical models to detect leaks in underground storage tanks*. 2000. 395-412 p.
17. West Yorkshire Fire and Rescue Service, Petrol Stations: Wetstock Control. West Yorkshire 2014.
18. Veeder-Root, Detecting and Reducing Loss in Your Fueling System. 2016.
19. Association for Petroleum and Explosives Administration (APEA), APEA Training Course: Wetstock Management. England 2009.
20. Veeder-Root TLS Foundation Training for TLS Gauge Engineers: Environmental Systems. 2013.
21. Veeder-Root, TLS Magnetostrictive Technology. 2009.
22. Li C, Yuan Y, Song L, Tan Y, Wang G. *Mathematical Model Based on BP Neural Network Algorithm for the Deflection Identification of Storage Tank and Calibration of Tank Capacity Chart* 2013:[13 p.].

23. Khaisongkram W, Banjerdpengchai D. *A combined geometric-volumetric calibration of inclined cylindrical underground storage tanks using the regularized least-squares method* 2004; 1515-20 Vol.2 p.
24. Knyva V, Knyva M. *New Method for Calibration of Horizontal Fuel Tanks*. 2012 [Internet]. 2012; [cited 2017 09 November]. Available from: <http://eejournal.ktu.lt/index.php/elt/article/view/2816>.
25. Wang J, Liu Z, Tong L, Guo L, Bao X, Zhang L. *Precise Measurement on Form of Horizontal Tank Used for Liquid Volume Metrology by Laser Method*. Applied Mechanics and Materials. 2013; 239-240.
26. Mensura 3D Laser Scan Mensura Tech.; 2013; [cited 2017 09 November] Available from: <http://mensura.com.tr/3D.html>.
27. CalibeX 3D Laser Calibration. Asis Otomation 2017; [cited 2017 10 November] Available from: <https://www.youtube.com/watch?v=eIg7wENiQJA>.
28. Gilbarco Veeder-Root, Fuel Management Services (FMS): SIR Environmental. US 2015.
29. Nosach VV. *Calculation of the Calibration Characteristics of Inclined Cylindrical Storage Tanks by a Geometric Method*. Measurement Techniques. 2000;43(10):871-6.
30. Zhipeng Y, Shengshuang C. *Deformation Identification and Tank Capacity Table Calibration of the Storage Tank* Applied Mechanics and Materials 2012; 184-185:[110-3 pp.].
31. Gorawski M, Skrzewski M, Gorawski M, Gorawska A. *Neural Networks in Petrol Station Objects Calibration*. Springer International Publishing; 2015. p. 714-23.
32. Xie W, Wang X, Cui H, Chen J. *Optimization Model of Oil-Volume Marking with Tilted Oil Tank*. Open Journal of Optimization. 2012;Vol.01No.02:5.
33. Li Y, Yang A, Wang X. *Research on Horizontal Tank Position Identification and Capacity Indicator Calibration*. Applied Mechanics and Materials 2014; 443:[662-7 pp.].

34. Sharma YK, Majhi A, Kukreti VS, Garg MO. *Stock loss studies on breathing loss of gasoline*. Fuel. 2010;89(7):1695-9.
35. Lutus P. Storage Container Mathematics. 2015.
36. Maresca JW Hillger RW. *Chemical Stored in USTs: Characteristics and Leak Detection* New Jersey EPA Press. 1991.
37. BS ISO 12917-1: 2017 *Petroleum and Liquid Petroleum Products - Calibration of Horizontal Cylindrical Tanks - Part 1: Manual Methods* 2017.
38. Tora Drawing Trainings: Tank Cover Drawings. 2016.

APPENDIX A: DETAILS OF SCT VOLUME DERIVATIONS

A.1. Simple Cylinder Tank Model

The first case, we will consider is a simple cylinder tank as known in Figure 3.1. (a) and Figure 3.1. (b), in view of side and front, respectively. The volume of the liquid of height “h” in a simple cylinder tank is determined by integrating the chosen slice along the tank height (h).

$$R^2 = (R-y)^2 + a^2$$

$$a^2 = R^2 - (R-y)^2$$

$$a = \sqrt{R^2 - (R-y)^2}$$

$$2a = 2\sqrt{R^2 - (R-y)^2}$$

The area of the infinitesimal slice is calculated as follows.

$$dA = 2ady$$

The volume of the infinitesimal slice is calculated as follows.

$$dV = LdA$$

$$dV = 2aLdy$$

$$dV = 2L\sqrt{R^2 - (R-y)^2} dy$$

$$dV = 2L\sqrt{R^2 - (R^2 - 2Ry + y^2)} dy$$

$$dV = 2L\sqrt{2Ry - y^2} dy$$

$$dV = 2L\sqrt{y(2R-y)} dy$$

$$V_c = \int_0^h 2L \sqrt{2Ry - y^2} dy$$

$$V_c = L \int_0^h 2 \sqrt{R^2 - (R-h)^2} dh$$

$$V_c = L \int_0^h 2 \sqrt{2Rh - h^2} dh$$

The surface area of the tank is multiplied by the tank's length to acquire a volume equation. Using following integral formula, the above equation is integrated.

$$\int \sqrt{2au-u^2} du = \frac{u-a}{2} \sqrt{2au-u^2} + \frac{a^2}{2} \cos^{-1}\left(\frac{a-u}{a}\right) + c$$

$$V_c = 2L * \left[\frac{y-R}{2} \sqrt{2Ry-y^2} + \frac{R^2}{2} \cos^{-1}\left(\frac{R-y}{R}\right) \right]_0^h$$

$$V_c = 2L \left[\left[\frac{h-R}{2} \sqrt{2Rh-h^2} + \frac{R^2}{2} \cos^{-1}\left(\frac{R-h}{R}\right) \right] - [0] \right]$$

$$V_c = 2L \left[\frac{h-R}{2} \sqrt{2Rh-h^2} + \frac{R^2}{2} \cos^{-1}\left(\frac{R-h}{R}\right) \right]$$

$$V_c = L \left[\sqrt{2Rh-h^2}(h-R) + R^2 \cos^{-1}\left(1-\frac{h}{R}\right) \right]$$

A.2. Radial (Horizontal) Tilt

Using simple geometric rules and Figure 3.2, the relation between the measured fuel level and the true fuel level is determined as follows.

$$m^2 + h^2 = (h')^2 + (2l)^2$$

$$m^2 + (2R-h)^2 = (2R'-h')^2$$

$$m^2 + (R-h)^2 = (R'-h')^2 + l^2$$

$$(R')^2 + l^2 = R^2$$

$$R' = R \cos \beta$$

$$(R \cos \beta)^2 + l^2 = R^2$$

$$R^2 \cos^2 \beta + l^2 = R^2$$

$$l^2 = R^2 - R^2 \cos^2 \beta$$

$$l^2 = R^2(1 - \cos^2 \beta)$$

$$l^2 = R^2 \sin^2 \beta$$

$$(h')^2 + (2l)^2 = m^2 + h^2$$

$$(h')^2 + (2l)^2 = (2R' - h')^2 - (2R - h)^2 + h^2$$

$$(h')^2 + 4l^2 = 4(R')^2 - 4R'h' + (h')^2 - (4R^2 - 4Rh + h^2) + h^2$$

$$4(R^2 \sin^2 \beta) = 4(R')^2 - 4R'h' - 4R^2 + 4Rh$$

$$4R^2 \sin^2 \beta + 4R^2 = 4(R')^2 - 4R'h' + 4Rh$$

$$R^2 \sin^2 \beta + R^2 = (R')^2 - R'h' + Rh$$

$$R^2 \sin^2 \beta + R^2 = (R \cos \beta)^2 - (R \cos \beta h') + Rh$$

$$R^2 \sin^2 \beta + R^2 = R^2 \cos^2 \beta - (h'R \cos \beta) + Rh$$

$$R^2 (\sin^2 \beta + 1 - \cos^2 \beta) = hR - h'R \cos \beta$$

$$R^2 (\sin^2 \beta - \cos^2 \beta + (\sin^2 \beta + \cos^2 \beta)) = R(h - h' \cos \beta)$$

$$R(2 \sin^2 \beta) = h - h' \cos \beta$$

$$h' = \frac{h - 2R\sin^2\beta}{\cos\beta}$$

$$h' = (h - 2R\sin^2\beta) \sec\beta$$

Or it can be written as follows:

$$h = h_{\text{corrected}} = \frac{h'}{\sec\beta} + 2R\sin^2\beta$$

A.3. High Level Fuel Volume for Positive Axial Tilted Tank

In this case, the measured fuel level is checked according to Eq. 3.6. If it is greater than h_{critical} , the tank is classified as high level simple cylinder tank and fuel volume is determined the below manner. The relations between h_1 and h_2 in the Figure 3.4 are written using general slope formula.

$$\tan\alpha = \frac{h_2 - h_1}{L}$$

$$\frac{h_a - h_1}{h_2 - h_1} = \frac{L - M}{L}$$

$$(h_a - h_1) \times L = (h_2 - h_1) \times (L - M)$$

$$(h_a - h_1)L = L \tan\alpha (L - M)$$

$$h_a = \tan\alpha (L - M) + h_1$$

$$h_1 = h_a - (L - M) \tan\alpha$$

Another slope equation of the surface fuel line is as follows.

$$\tan\alpha = \frac{h_2 - h_a}{M}$$

$$h_2 = h_a + M \tan\alpha$$

Using obtained relations, h_1 and h_2 can be determined. Then, these levels are put into the simple cylindrical tank volume formula.

$$V_{\text{total}} = \frac{V(h_1) + V(h_2)}{2}$$

A.4. Low Level Fuel Volume for Positive Axial Tilted Tank

In this case, if the measured fuel level is greater than h_{critical} (Eq. 3.6), the tank is classified as low level simple cylinder tank and fuel volume is determined the below manner. The slope of the surface fuel line is as follows (Figure 3.5).

$$\frac{h_a}{F-M} = \tan \alpha$$

$$(F-M) \tan \alpha = h_a$$

$$F = \frac{h_a}{\tan \alpha} + M$$

Another slope of the surface fuel line is written as follows.

$$\frac{h_a}{h_3} = \frac{F-M}{F}$$

$$h_a = \left(\frac{F-M}{F} \right) h_3$$

$$h_a = \left(1 - \frac{M}{F} \right) h_3$$

$$h_a = \left(1 - \frac{M}{\frac{h_a}{\tan \alpha} + M} \right) h_3$$

$$h_a = \left(\frac{\frac{h_a}{\tan \alpha} + M - M}{\frac{h_a}{\tan \alpha} + M} \right) h_3$$

$$h_a = \left(\frac{\frac{h_a}{\tan \alpha}}{\frac{h_a}{\tan \alpha} + M \tan \alpha} \right) h_3$$

$$h_{\alpha} = \left(\frac{h_{\alpha}}{h_{\alpha} + M \tan \alpha} \right) h_3$$

$$h_3 = h_{\alpha} + M \tan \alpha$$

The fuel volume is determined by the below equation.

$$V = \frac{F \left[\sqrt{(2R-h_3)h_3} (h_3 - R) + R^2 \cos^{-1} \left(1 - \frac{h_3}{R} \right) \right]}{2}$$

A.5. High Level Fuel Volume for Negative Axial Tilted Tank

In this case, the measured fuel level is checked according to Eq. 3.14. If it is greater than $h_{critical}$, the tank is classified as high level simple cylinder tank and fuel volume is determined the below manner. The slope of the fuel line can be calculated by using different geometric relations (Figure 3.8).

$$\tan(-\alpha) = \frac{h_2 - h_1}{L}$$

$$\tan(-\alpha) = \frac{h_{measured} - h_1}{M}$$

$$\frac{h_{measured} - h_1}{h_2 - h_1} = \frac{M}{L}$$

The following equation gives the relation between the h_1 and $h_{measured}$.

$$h_1 = h_{measured} - M \tan(-\alpha)$$

The relation between h_1 and h_2 is determined as follows.

$$h_2 - h_1 = L \tan(-\alpha)$$

$$h_2 = h_{measured} + (L - M) \tan(-\alpha)$$

After determination of the fuel level of h_1 and h_2 , the fuel volume in the tank is calculated using simple cylinder tank volume equation.

$$V_{cyl} = L \left[\sqrt{2Rh - h^2} (h - R) + R^2 \cos^{-1} \left(1 - \frac{h}{R} \right) \right]$$

$$V(h_1) = L \left[\sqrt{2Rh_1 - h_1^2} (h_1 - R) + R^2 \cos^{-1} \left(1 - \frac{h_1}{R} \right) \right]$$

$$V(h_2) = L \left[\sqrt{2Rh_2 - h_2^2} (h_2 - R) + R^2 \cos^{-1} \left(1 - \frac{h_2}{R} \right) \right]$$

$$V_{\text{fuel}} = \frac{V(h_1) + V(h_2)}{2}$$



APPENDIX B: DETAILS OF CTDH VOLUME DERIVATIONS

B.1. Simple Cylinder Tank with Dished Head Model

The side view, the front view, and the top view of a cylindrical tank with dished head are drawn in the Figures 3.10, 3.11 (a), and 3.11 (b). The geometric relations are used in order to determine tank one dished head volume.

$$B(h) = \sqrt{R^2 - (R-h)^2}$$

$$C(h) = 2 * B(h)$$

$$C(h) = 2\sqrt{R^2 - (R-h)^2}$$

$$R(h) = \sqrt{r^2 - (R-h)^2}$$

$$K(h) = \sqrt{(R(h))^2 - \left(\frac{C(h)}{2}\right)^2}$$

$$K(h) = \sqrt{\left(\sqrt{r^2 - (R-h)^2}\right)^2 - \left(\frac{2\sqrt{R^2 - (R-h)^2}}{2}\right)^2}$$

$$K(h) = \sqrt{(r^2 - (R-h)^2) - (R^2 - (R-h)^2)}$$

$$K(h) = \sqrt{r^2 - R^2}$$

$\alpha(h)$ Calculation:

$$\cos\left(\frac{\alpha}{2}\right) = \frac{K(h)}{R(h)}$$

$$\frac{\alpha}{2} = \arccos\left(\frac{K(h)}{R(h)}\right)$$

$$\alpha(h) = 2 \arccos\left(\frac{K(h)}{R(h)}\right)$$

$A(h)$ = Area of Sphere Segment of $\alpha(h)$ – Triangle Area

$$A(h) = \left[\pi(R(h))^2 \frac{\alpha(h)}{2\pi} \right] - \left[\frac{C(h)K(h)}{2} \right]$$

$$A(h) = \left[\pi \left(\sqrt{r^2 - (R-h)^2} \right)^2 \frac{2 \arccos\left(\frac{\sqrt{r^2 - R^2}}{\sqrt{r^2 - (R-h)^2}}\right)}{2\pi} \right] - \left[\frac{2\sqrt{R^2 - (R-h)^2} \sqrt{r^2 - R^2}}{2} \right]$$

$$A(h) = \left[(r^2 - (R-h)^2) \arccos\left(\frac{\sqrt{r^2 - R^2}}{\sqrt{r^2 - (R-h)^2}}\right) \right] - \left[\sqrt{R^2 - (R-h)^2} \sqrt{r^2 - R^2} \right]$$

$$V(h) = \int_0^h A(h) dh$$

$$V(h) = \int_0^h \left\{ \left[(r^2 - (R-h)^2) \arccos\left(\frac{\sqrt{r^2 - R^2}}{\sqrt{r^2 - (R-h)^2}}\right) \right] - \left[\sqrt{R^2 - (R-h)^2} \sqrt{r^2 - R^2} \right] \right\} dh$$

For the half-ellipses at each end of the tank (they can be treated as one spheroid), with major radius R and minor radius r , bisected by content height h , the volume equation can be written as follows.

$$v = \frac{\pi r (3R-h) h^2}{3R}$$

The sum of the volume of two dished head of the tank is equivalent to the below equation which is written based on tank terminology used in this study.

$$v = \frac{\pi H (3R-h) h^2}{3R}$$

$$V = \frac{\pi H (3R-h) h^2}{3R} + L \left[\sqrt{2Rh-h^2}(h-R) + R^2 \cos^{-1}\left(1-\frac{h}{R}\right) \right]$$

B.2. Nonmeasurable Volume, V_0 Determination

First, we will drive the relation that gives the nonmeasurable volume (V_0) that lies below the minimum probe level for the positive axial tilt (i.e. $+\alpha$) (Figure 3.14 and 3.15). According to reference origin point, x_1 can be written as follows.

$$x_1 = M + H$$

The measured fuel level by the probe equals zero at that point of y_1 .

$$y_1 = 0$$

The slope of the line is determined by the below equation.

$$\tan \alpha = \frac{A}{M}$$

$$A = M \tan \alpha$$

Point of (x_2, y_2) :

$$\tan \alpha = \frac{y_2 - y_1}{x_1 - x_2}$$

It is seen in the figure, $y_1 = 0$. Then,

$$\tan \alpha = \frac{y_2}{x_1 - x_2}$$

$$y_2 = (x_1 - x_2) \tan \alpha$$

Also known, $x_1 = M + H$

$$y_2 = (M + H - x_2) \tan \alpha$$

$$x_2 = M + H - \frac{y_2}{\tan \alpha}$$

Determination of y_2 :

$$(x_2 - r)^2 + (y_2 - R)^2 = r^2$$

$$x_2^2 - 2x_2r + r^2 + y_2^2 - 2y_2R + R^2 - r^2 = 0$$

It is known that:

$$y_2 = (M+H-x_2) \tan \alpha$$

$$x_2^2 - 2x_2r + r^2 + [(M+H)^2 - 2(M+H)x_2 + x_2^2] \tan^2 \alpha - 2R(M+H) \tan \alpha + 2Rx_2 \tan \alpha + R^2 - r^2 = 0$$

$$x_2^2(1+\tan^2 \alpha) + x_2(-2r-2(M+H)\tan^2 \alpha + 2R \tan \alpha) + (M+H)^2 \tan^2 \alpha - 2R(M+H) \tan \alpha + R^2 = 0$$

The above equation is in the form of $ax_2^2 + bx_2 + c = 0$.

$$ax_2^2 + bx_2 + c = 0$$

$$a = 1 + \tan^2 \alpha$$

$$b = -2r - 2(M+H)\tan^2 \alpha + 2R \tan \alpha$$

$$c = (M+H)^2 \tan^2 \alpha - 2R(M+H) \tan \alpha + R^2$$

Using Matlab, a, b, and c are solved easily. After determination of the a, b and c coefficients, y_2 is calculated. For the fuel volume determination, the below formula is used.

$$V_{\text{fuel}} = \frac{V(h)}{2}$$

$$V(h) = \frac{\pi H(3R-h)h^2}{3R} + M \left[\sqrt{2Rh-h^2}(h-R) + R^2 \cos^{-1} \left(1 - \frac{h}{R} \right) \right]$$

$$V_0 = V_{\text{fuel}} = \frac{\frac{\pi H(3R-h)h^2}{3R} + M \left[\sqrt{2Rh-h^2}(h-R) + R^2 \cos^{-1} \left(1 - \frac{h}{R} \right) \right]}{2}$$

$$V_0 = \frac{\pi H(3R-h)h^2}{6R} + \frac{M \left[\sqrt{2Rh-h^2}(h-R) + R^2 \cos^{-1} \left(1 - \frac{h}{R} \right) \right]}{2}$$

B.3. Fuel on One Dished Head

When the measured fuel level is less than or equal to the critical fuel level (Eq. 3.31), one dished head of the tank is full of fuel. It is seen in the Figure 3.17, y_1 equals to zero for all x_1 values.

$$\tan \alpha = \frac{h_a - y_1}{x_1 - (M+H)}$$

$$h_a - 0 = [x_1 - (M + H)] \tan \alpha$$

$$0 = y_1 = h_a - [x_1 - (M + H)] \tan \alpha$$

$$X_1 = \frac{h_a}{\tan \alpha} + (M + H)$$

$$y_1 = 0$$

Below relation can be written for the point of (x_2, y_2) by using fuel line slope.

$$\tan \alpha = \frac{y_2 - y_1}{x_1 - x_2}$$

$$\tan \alpha = \frac{y_2 - 0}{x_1 - x_2}$$

$$y_2 = (x_1 - x_2) \tan \alpha$$

$$y_2 = \left[\left(\frac{h_a}{\tan \alpha} + (M + H) \right) - x_2 \right] \tan \alpha$$

$$y_2 = h_a + (M + H - x_2) \tan \alpha$$

$$y_2 = h_3$$

The relation between h_3 and h_a is determined as follows.

$$(x_1 - x_2) \tan \alpha = y_2 = h_3$$

$$\left[\left(\frac{h_a}{\tan \alpha} + (M + H) \right) - x_2 \right] \tan \alpha = h_3$$

$$\left(\frac{h_a}{\tan \alpha} + (M + H) \right) - x_2 = \frac{h_3}{\tan \alpha}$$

$$\left(\frac{h_a}{\tan \alpha} + (M + H) \right) = \frac{h_3}{\tan \alpha} + x_2$$

$$\frac{h_a}{\tan \alpha} = \frac{h_3}{\tan \alpha} + x_2 - M - H$$

$$h_a = h_3 + (x_2 - M - H) \tan \alpha$$

The general formula of the left sphere is written according to the reference origin (Point 3).

$$(x-r)^2 + (y-R)^2 = r^2$$

Equations are solved simultaneously and x_2 is determined.

$$(x_2 - r)^2 + (y_2 - R)^2 = r^2$$

$$(x_2 - r)^2 + (h_3 - R)^2 = r^2$$

$$(x_2 - r)^2 = r^2 - (h_3 - R)^2$$

$$x_2 - r = \sqrt{r^2 - (h_3 - R)^2}$$

$$x_2 = \sqrt{r^2 - (h_3 - R)^2} + r$$

$$x_2 = \sqrt{r^2 - (h_3^2 - 2h_3R + R^2)} + r$$

$$x_2 = \sqrt{r^2 - R^2 + 2h_3R - h_3^2} + r$$

The general volume formula of the simple cylindrical tank is as follows.

$$V(h) = L \left[\sqrt{(2R-h)h} (h-R) + R^2 \cos^{-1} \left(1 - \frac{h}{R} \right) \right]$$

The general volume formula of the simple cylindrical tank with dished head is as follows.

$$V(h) = \frac{\pi H(3R-h)h^2}{3R} + L \left[\sqrt{(2R-h)h} (h-R) + R^2 \cos^{-1} \left(1 - \frac{h}{R} \right) \right]$$

The fuel volume in the tank is calculated according to below equation.

$$V = \frac{V(h_3) - V(h_3'')}{2}$$

$$V(h_3) = \frac{\pi H(3R-h_3)h_3^2}{3R} + L \left[\sqrt{(2R-h_3)h_3} (h_3-R) + R^2 \cos^{-1} \left(1 - \frac{h_3}{R} \right) \right]$$

$$V(h_3)'' = (L+H-x_1) \left[\sqrt{(2R-h_3)h_3} (h_3-R) + R^2 \cos^{-1} \left(1 - \frac{h_3}{R} \right) \right]$$

In order to solve the unknowns, the derived equations are formed in the below way.

$$h_3 = y_2 = h_a + (M+H-x_2) \tan \alpha$$

$$y_2 = C_1 x_2 + C_2$$

$$(x_2-r)^2 + (h_3-R)^2 = r^2$$

$$(x_2-C_3)^2 + (h_3-R)^2 = r^2$$

$$(x_2-C_3)^2 + (C_1 x_2 + C_2 - R)^2 = r^2$$

$$(x_2-C_3)^2 + (C_1 x_2 + C_4)^2 = r^2$$

$$x_2^2 - 2x_2 C_3 + C_3^2 + (C_1 x_2)^2 + 2C_1 x_2 C_4 + C_4^2 = r^2$$

$$x_2^2 (1+C_1^2) + x_2 (-2C_3 + 2C_1 C_4) + C_4^2 + C_3^2 - r^2 = 0$$

$$a = 1 + C_1^2$$

$$b = -2C_3 + 2C_1 C_4$$

$$c = C_4^2 + C_3^2 - r^2$$

$$C_1 = -\tan \alpha$$

$$C_2 = h_a + M \tan \alpha + H \tan \alpha$$

$$C_3 = r$$

$$C_4 = h_a + M \tan \alpha + H \tan \alpha - R$$

B.4. Fuel on Both Dished Head

When the measured fuel level is greater than the critical fuel level (Eq. 3.31), both end caps of the tank are full of fuel. It can be seen in the Figure 3.18. The origin of the sphere is shifted from Point 1 to Point 3.

$$K = H + \frac{L}{2} + \left[\frac{L}{2} - (r - H) \right]$$

$$K = L + 2H - r$$

The general formula of the right sphere is as follows.

$$[x - (L + 2H - r)]^2 + [y - R]^2 = r^2$$

The point of (x_1, y_1) :

$$\tan \alpha = \frac{h_\alpha - y_1}{x_1 - (M + H)}$$

$$h_\alpha - y_1 = (x_1 - M - H) \tan \alpha$$

$$y_1 = h_\alpha - [(x_1 - M - H) \tan \alpha]$$

It is seen in the Figure 3.18 that:

$$y_1 = h_1$$

$$[x_1 - (L + 2H - r)]^2 + [y_1 - R]^2 = r^2$$

The relation between the h_1 and h_α is determined as follows.

$$h_\alpha - [(x_1 - M - H) \tan \alpha] = h_1$$

$$h_\alpha = h_1 + [(x_1 - M - H) \tan \alpha]$$

Equations are solved simultaneously in the below.

$$[x_1 - (L + 2H - r)]^2 + [y_1 - R]^2 = r^2$$

$$[x_1 - (L + 2H - r)]^2 + [h_1 - R]^2 = r^2$$

$$[x_1 - (L + 2H - r)]^2 = r^2 - [h_1 - R]^2$$

$$x_1 - (L + 2H - r) = \sqrt[r^2 - [h_1 - R]^2]{}$$

$$x_1 = \sqrt[r^2 - [h_1 - R]^2]{r^2} + (L + 2H - r)$$

$$x_1 = \sqrt[2]{r^2 - (h_1^2 - 2h_1R + R^2) + (L+2H-r)}$$

$$x_1 = \sqrt[2]{r^2 - R^2 + 2h_1R - h_1^2} + (L+2H-r)$$

$$h_1 = y_1 = h_\alpha - [(x_1 - M - H) \tan \alpha]$$

$$y_1 = C_1 x_1 + C_2$$

$$[x_1 - (L+2H-r)]^2 + [h_1 - R]^2 = r^2$$

$$[x_1 - C_3]^2 + [h_1 - R]^2 = r^2$$

$$[x_1 - C_3]^2 + [C_1 x_1 + C_2 - R]^2 = r^2$$

$$[x_1 - C_3]^2 + [C_1 x_1 + C_4]^2 = r^2$$

$$x_1^2 - 2x_1 C_3 + C_3^2 + (C_1 x_1)^2 + 2C_1 x_1 C_4 + C_4^2 = r^2$$

$$x_1^2 (1 + C_1^2) + x_1 (-2C_3 + 2C_1 C_4) + C_4^2 + C_3^2 - r^2 = 0$$

The above equation is in the form of $ax^2 + bx + c$.

$$a = 1 + C_1^2$$

$$b = -2C_3 + 2C_1 C_4$$

$$c = C_4^2 + C_3^2 - r^2$$

$$C_1 = -\tan \alpha$$

$$C_2 = h_\alpha + M \tan \alpha + H \tan \alpha$$

$$C_3 = L + 2H - r$$

$$C_4 = h_\alpha + M \tan \alpha + H \tan \alpha - R$$

The point of (x_2, y_2) :

$$\tan \alpha = \frac{y_2 - y_1}{x_2 - x_1} = \frac{h_\alpha - y_1}{x_1 - (M + H)}$$

$$\begin{aligned}
 & \frac{y_2 - (h_a - [(x_1 - M - H) \tan \alpha])}{\left(\sqrt{r^2 - R^2 + 2h_1 R - h_1^2} + (L + 2H - r) \right) - x_2} = \tan \alpha \\
 y_2 &= \left[\left(\sqrt{r^2 - R^2 + 2h_1 R - h_1^2} + (L + 2H - r) \right) - x_2 \right] \tan \alpha + (h_a - [(x_1 - M - H) \tan \alpha]) \\
 y_2 &= (x_1 - x_2) \tan \alpha + (h_a - [(x_1 - M - H) \tan \alpha]) \\
 y_2 &= x_1 \tan \alpha - x_2 \tan \alpha + h_a - x_1 \tan \alpha + M \tan \alpha + H \tan \alpha \\
 y_2 &= h_a + (-x_2 + M + H) \tan \alpha
 \end{aligned}$$

It is seen in Figure 3.18 that:

$$y_2 = h_2$$

The general formula of the left sphere is as follows.

$$(x - r)^2 + (y - R)^2 = r^2$$

The point of (x_2, y_2) is on the left sphere of the tank.

$$(x_2 - r)^2 + [y_2 - R]^2 = r^2$$

It is known that, $y_2 = h_2$.

$$(x_2 - r)^2 + (h_2 - R)^2 = r^2$$

$$(x_2 - r)^2 = r^2 - (h_2 - R)^2$$

$$x_2 - r = \sqrt{r^2 - (h_2 - R)^2}$$

$$x_2 = \sqrt{r^2 - (h_2 - R)^2} + r$$

$$x_2 = \sqrt{r^2 - R^2 + 2h_2 R - h_2^2} + r$$

$$h_2 = y_2 = h_a + [(-x_2 + M + H) \tan \alpha]$$

$$y_2 = C_1 x_2 + C_2$$

$$(x_2 - r)^2 + (h_2 - R)^2 = r^2$$

$$[x_2 - C_3]^2 + [h_2 - R]^2 = r^2$$

$$[x_2 - C_3]^2 + [C_1 x_2 + C_2 - R]^2 = r^2$$

$$[x_2 - C_3]^2 + [C_1 x_2 + C_4]^2 = r^2$$

$$x_2^2 - 2x_2 C_3 + C_3^2 + (C_1 x_2)^2 + 2C_1 x_2 C_4 + C_4^2 = r^2$$

$$x_2^2 (1 + C_1^2) + x_2 (-2C_3 + 2C_1 C_4) + C_4^2 + C_3^2 - r^2 = 0$$

$$a = 1 + C_1^2$$

$$b = -2C_3 + 2C_1 C_4$$

$$c = C_4^2 + C_3^2 - r^2$$

$$C_1 = -\tan \alpha$$

$$C_2 = h_\alpha + M \tan \alpha + H \tan \alpha$$

$$C_3 = r$$

$$C_4 = h_\alpha + M \tan \alpha + H \tan \alpha - R$$

The general volume formula of the cylindrical tank with dished head is as follows.

$$V(h) = \frac{\pi H(3R-h)h^2}{3R} + L \left[\sqrt{(2R-h)h} (h-R) + R^2 \cos^{-1} \left(1 - \frac{h}{R} \right) \right]$$

The fuel volume in the tank is calculated according to below equation.

$$V = \frac{V(h_1) + V(h_2)}{2}$$

$$V(h_1) = \frac{\pi H(3R-h_1)h_1^2}{3R} + L \left[\sqrt{(2R-h_1)h_1} (h_1-R) + R^2 \cos^{-1} \left(1 - \frac{h_1}{R} \right) \right]$$

$$V(h_2) = \frac{\pi H(3R-h_2)h_2^2}{3R} + L \left[\sqrt{(2R-h_2)h_2} (h_2-R) + R^2 \cos^{-1} \left(1 - \frac{h_2}{R} \right) \right]$$

B.5. Nonmeasurable Volume, V_0 Determination

Nonmeasurable fuel volume for the simple cylinder tank with dished head and with negative axial tilt is determined by assuming the tank in the own coordinate (Figure 3.19).

The reference point is chosen and the distance of the minimum and maximum points where the fuel touch to the tank are determined one by one. Point of (x_1, y_1) : It is seen in the Figure 3.16, y_1 equals zero for all x values.

$$x_1 = M + H$$

$$y_1 = 0$$

Point of (x_2, y_2) : The slope of the surface fuel line is determined according to the below equation.

$$\tan(-\alpha) = \frac{y_2 - y_1}{x_2 - x_1}$$

It is known that $y_1 = 0$.

$$\tan(-\alpha) = \frac{y_2}{x_2 - x_1}$$

$$y_2 = (x_2 - x_1) \tan(-\alpha)$$

Another relation between the x_2 and y_2 is written using general sphere formula for the right curve of the tank.

$$[x_2 - (L + 2H - r)]^2 + [y_2 - R]^2 = r^2$$

$$[x_2 - (L + 2H - r)]^2 + [h_1 - R]^2 = r^2$$

$$[x_2 - (L + 2H - r)]^2 = r^2 - (h_1 - R)^2$$

$$x_2 - (L + 2H - r) = \sqrt{r^2 - (h_1 - R)^2}$$

$$x_2 = \sqrt{r^2 - (h_1 - R)^2} + L + 2H - r$$

$$h_1 = y_2 = (x_2 - x_1) \tan(-\alpha)$$

Equations are solved simultaneously.

$$h_1 = y_2 = x_2 \tan(-\alpha) - x_1 \tan(-\alpha)$$

$$y_2 = C_1 x_2 + C_2$$

$$[x_2 - (L + 2H - r)]^2 + [h_1 - R]^2 = r^2$$

$$[x_2 - C_3]^2 + [h_1 - R]^2 = r^2$$

$$[x_2 - C_3]^2 + [C_1 x_2 + C_2 - R]^2 = r^2$$

$$[x_2 - C_3]^2 + [C_1 x_2 + C_4]^2 = r^2$$

$$x_2^2 - 2x_2 C_3 + C_3^2 + (C_1 x_2)^2 + 2C_1 x_2 C_4 + C_4^2 = r^2$$

$$x_2^2 (1 + C_1^2) + x_2 (-2C_3 + 2C_1 C_4) + C_4^2 + C_3^2 - r^2 = 0$$

$$a = 1 + C_1^2$$

$$b = -2C_3 + 2C_1 C_4$$

$$c = C_4^2 + C_3^2 - r^2$$

$$C_1 = \tan(-\alpha)$$

$$C_2 = -(M + H) \tan(-\alpha)$$

$$C_3 = L + 2H - r$$

$$C_4 = -R - (M + H) \tan(-\alpha)$$

Volume of the fuel in the tank, V_{fuel} is calculated using obtained h_1 value. General formula of the simple cylindrical tank with end caps is as follows.

$$V(h) = \frac{\pi H (3R - h) h^2}{3R} + L \left[\sqrt{(2R - h)h} (h - R) + R^2 \cos^{-1} \left(1 - \frac{h}{R} \right) \right]$$

$$V(h_1) = \frac{\pi H (3R - h_1) h_1^2}{3R} + (L - M) \left[\sqrt{(2R - h_1)h_1} (h_1 - R) + R^2 \cos^{-1} \left(1 - \frac{h_1}{R} \right) \right]$$

$$V_{fuel} = \frac{V(h_1)}{2}$$

$$V_0 - V_{\text{fuel}} = \frac{\frac{\pi H(3R-h_1)h_1^2}{3R} + (L-M)\left[\sqrt{(2R-h_1)h_1}(h_1-R) + R^2 \cos^{-1}\left(1-\frac{h_1}{R}\right)\right]}{2}$$

$$V_0 = \frac{\pi H(3R-h_1)h_1^2}{6R} + \frac{L-M}{2}\left[\sqrt{(2R-h_1)h_1}(h_1-R) + R^2 \cos^{-1}\left(1-\frac{h_1}{R}\right)\right]$$

B.6. Fuel on Both Dished Head

In this case, the measured fuel level is greater than h_{critical} (Eq. 3.48). The Point of (x_1, y_1) : The slope of the surface fuel level is determined according to the below formula.

$$\tan(-\alpha) = \frac{h_{\text{measured}} - y_1}{M + (H - x_1)}$$

As it is seen in the Figure 3.21,

$$y_1 = h_1$$

$$\tan(-\alpha) = \frac{h_{\text{measured}} - h_1}{M + (H - x_1)}$$

$$h_1 = h_{\text{measured}} - (M + H - x_1) \tan(-\alpha)$$

The point of (x_1, y_1) is on the left sphere curve of the tank and a relation is written for the left sphere curve.

$$(x_1 - r)^2 + (y_1 - R)^2 = r^2$$

$$(x_1 - r)^2 = r^2 - (h_1 - R)^2$$

$$x_1 - r = \sqrt{r^2 - (h_1 - R)^2}$$

$$x_1 = \sqrt{r^2 - (h_1 - R)^2} + r$$

$$h_1 = y_1 = h_{\text{measured}} - (M + H - x_1) \tan(-\alpha)$$

$$y_1 = C_1 x_1 + C_2$$

$$[x_1 - r]^2 + [h_1 - R]^2 = r^2$$

$$[x_1 - C_3]^2 + [h_1 - R]^2 = r^2$$

$$[x_1 - C_3]^2 + [C_1 x_1 + C_2 - R]^2 = r^2$$

$$[x_1 - C_3]^2 + [C_1 x_1 + C_4]^2 = r^2$$

$$x_1^2 - 2x_1 C_3 + C_3^2 + (C_1 x_1)^2 + 2C_1 x_1 C_4 + C_4^2 = r^2$$

$$x_1^2 (1 + C_1^2) + x_1 (-2C_3 + 2C_1 C_4) + C_4^2 + C_3^2 - r^2 = 0$$

$$a = 1 + C_1^2$$

$$b = -2C_3 + 2C_1 C_4$$

$$c = C_4^2 + C_3^2 - r^2$$

$$C_1 = \tan(-\alpha)$$

$$C_2 = h_{\text{measured}} - (M + H) \tan(-\alpha)$$

$$C_3 = r$$

$$C_4 = h_{\text{measured}} - R - (M + H) \tan(-\alpha)$$

The Point of (x_2, y_2) : The slope of the surface fuel level is determined according to the below formula.

$$\tan(-\alpha) = \frac{y_2 - y_1}{x_2 - x_1}$$

As it is seen in the Figure 3.21,

$$y_1 = h_1$$

$$y_2 = h_2$$

After inserting terms, the slope becomes:

$$\tan(-\alpha) = \frac{h_2 - h_1}{x_2 - x_1}$$

$$h_2 - h_1 = (x_2 - x_1) \tan(-\alpha)$$

$$h_2 = h_1 + (x_2 - x_1) \tan(-\alpha)$$

The point of (x_2, y_2) is on the right sphere curve of the tank and a relation is written for the right sphere curve.

$$[x_2 - (L+2H-r)]^2 + (y_2 - R)^2 = r^2$$

$$[x_2 - (L+2H-r)]^2 + (h_2 - R)^2 = r^2$$

$$[x_2 - (L+2H-r)]^2 = r^2 - (h_2 - R)^2$$

$$x_2 - (L+2H-r) = \sqrt{r^2 - (h_2 - R)^2}$$

$$x_2 = \sqrt{r^2 - (h_2 - R)^2} + L + 2H - r$$

$$x_2 = \sqrt{r^2 - R^2 + 2h_2R - h_2^2} + L + 2H - r$$

The equations are solved simultaneously.

$$h_2 = y_2 = h_1 + x_2 \tan(-\alpha) - x_1 \tan(-\alpha)$$

$$h_2 = y_2 = h_{\text{measured}} - (M + H - x_1) \tan(-\alpha) + x_2 \tan(-\alpha) - x_1 \tan(-\alpha)$$

$$h_2 = y_2 = h_{\text{measured}} - M \tan(-\alpha) - H \tan(-\alpha) + x_1 \tan(-\alpha) + x_2 \tan(-\alpha) - x_1 \tan(-\alpha)$$

$$h_2 = y_2 = h_{\text{measured}} - M \tan(-\alpha) - H \tan(-\alpha) + x_2 \tan(-\alpha)$$

$$y_2 = C_1 x_2 + C_2$$

$$[x_2 - (L+2H-r)]^2 + [y_2 - R]^2 = r^2$$

$$[x_2 - C_3]^2 + [h_2 - R]^2 = r^2$$

$$[x_2 - C_3]^2 + [C_1 x_2 + C_2 - R]^2 = r^2$$

$$[x_2 - C_3]^2 + [C_1 x_2 + C_4]^2 = r^2$$

$$x_2^2 - 2x_2 C_3 + C_3^2 + (C_1 x_2)^2 + 2C_1 x_2 C_4 + C_4^2 = r^2$$

$$x_2^2 (1 + C_1^2) + x_2 (-2C_3 + 2C_1 C_4) + C_4^2 + C_3^2 - r^2 = 0$$

$$a=1+C_1^2$$

$$b=-2C_3+2C_1C_4$$

$$c=C_4^2+C_3^2-r^2$$

$$C_1=\tan(-\alpha)$$

$$C_2=h_{\text{measured}}-M \tan(-\alpha) - H \tan(-\alpha)$$

$$C_3=L+2H-r$$

$$C_4=h_{\text{measured}}-R-(M+H) \tan(-\alpha)$$

Volume of the fuel in the tank, V_{fuel} is calculated using obtained h_1 and h_2 values. General formula of the simple cylindrical tank with end caps is as follows.

$$V(h)=\frac{\pi H(3R-h)h^2}{3R} + L \left[\sqrt{(2R-h)h} (h-R) + R^2 \cos^{-1} \left(1 - \frac{h}{R} \right) \right]$$

$$V(h_1)=\frac{\pi H(3R-h_1)h_1^2}{3R} + (L) \left[\sqrt{(2R-h_1)h_1} (h_1-R) + R^2 \cos^{-1} \left(1 - \frac{h_1}{R} \right) \right]$$

$$V(h_2)=\frac{\pi H(3R-h_2)h_2^2}{3R} + (L) \left[\sqrt{(2R-h_2)h_2} (h_2-R) + R^2 \cos^{-1} \left(1 - \frac{h_2}{R} \right) \right]$$

$$V_{\text{fuel}}=\frac{V(h_1)+V(h_2)}{2}$$

B.7. Fuel on One Dished Head

In this case, the measured fuel level is less than or equal to h_{critical} (Eq. 3.48). Point of (x_1, y_1) : The slope of the surface fuel line is determined as follows.

$$\tan(-\alpha)=\frac{h_{\text{measured}}}{M-(x_1-H)}$$

$$h_{\text{measured}}=(M+H-x_1) \tan(-\alpha)$$

$$x_1 = M + H - \frac{h_{\text{measured}}}{\tan(-\alpha)}$$

It is seen in the Figure 3.22 that y_1 equals zero according to the reference origin point for all x values.

$$y_1 = 0$$

Point of (x_2, y_2) : The slope of the fuel surface line is also determined using the specific two point on the line.

$$\tan(-\alpha) = \frac{y_2 - y_1}{x_2 - x_1}$$

As it is seen in the Figure 3.22,

$$y_1 = 0$$

$$\tan(-\alpha) = \frac{y_2}{x_2 - x_1}$$

$$y_2 = (x_2 - x_1) \tan(-\alpha)$$

$$h_1 = y_2 = (x_2 - x_1) \tan(-\alpha)$$

The point of (x_2, y_2) is on the curve of the right sphere of the tank. The relation between x_2 and y_2 can be written based on general sphere formula according to the reference origin point.

$$[x_2 - (L + 2H - r)]^2 + (y_2 - R)^2 = r^2$$

$$[x_2 - (L + 2H - r)]^2 + (h_1 - R)^2 = r^2$$

$$[x_2 - (L + 2H - r)]^2 = r^2 - (h_1 - R)^2$$

$$x_2 - (L + 2H - r) = \sqrt{r^2 - (h_1 - R)^2}$$

$$x_2 = \sqrt{r^2 - (h_1 - R)^2} + L + 2H - r$$

$$x_2 = \sqrt{r^2 - R^2 + 2h_1R - h_1^2} + L + 2H - r$$

Equations are solved simultaneously.

$$h_1 = y_2 = x_2 \tan(-\alpha) - x_1 \tan(-\alpha)$$

$$y_2 = C_1 x_2 + C_2$$

$$[x_2 - (L + 2H - r)]^2 + [h_1 - R]^2 = r^2$$

$$[x_2 - C_3]^2 + [h_1 - R]^2 = r^2$$

$$[x_2 - C_3]^2 + [C_1 x_2 + C_2 - R]^2 = r^2$$

$$[x_2 - C_3]^2 + [C_1 x_2 + C_4]^2 = r^2$$

$$x_2^2 - 2x_2 C_3 + C_3^2 + (C_1 x_2)^2 + 2C_1 x_2 C_4 + C_4^2 = r^2$$

$$x_2^2 (1 + C_1^2) + x_2 (-2C_3 + 2C_1 C_4) + C_4^2 + C_3^2 - r^2 = 0$$

$$a = 1 + C_1^2$$

$$b = -2C_3 + 2C_1 C_4$$

$$c = C_4^2 + C_3^2 - r^2$$

$$C_1 = \tan(-\alpha)$$

$$C_2 = h_{\text{measured}} - (M + H) \tan(-\alpha)$$

$$C_3 = L + 2H - r$$

$$C_4 = h_{\text{measured}} - R - (M + H) \tan(-\alpha)$$

Volume of the fuel in the tank, V_{fuel} is calculated using obtained h_1 value. General formula of the simple cylindrical tank with end caps is as follows.

$$V(h) = \frac{\pi H (3R - h) h^2}{3R} + L \left[\sqrt{(2R - h)h} (h - R) + R^2 \cos^{-1} \left(1 - \frac{h}{R} \right) \right]$$

$$V(h_1) = \frac{\pi H (3R - h_1) h_1^2}{3R} + (L + H - x_1) \left[\sqrt{(2R - h_1)h_1} (h_1 - R) + R^2 \cos^{-1} \left(1 - \frac{h_1}{R} \right) \right]$$

$$V_{\text{fuel}} = \frac{V(h_1)}{2}$$

$$V_{\text{fuel}} = \frac{\frac{\pi H(3R-h_1)h_1^2}{3R} + (L+H-x_1) \left[\sqrt{(2R-h_1)h_1} (h_1-R) + R^2 \cos^{-1} \left(1 - \frac{h_1}{R} \right) \right]}{2}$$

$$V_{\text{fuel}} = \frac{\pi H(3R-h_1)h_1^2}{6R} + \frac{L+H-x_1}{2} \left[\sqrt{(2R-h_1)h_1} (h_1-R) + R^2 \cos^{-1} \left(1 - \frac{h_1}{R} \right) \right]$$



APPENDIX C: DETAILS OF TEMPERATURE COMPENSATION

C.1. Variance

Theoretical volume change is calculated allowing for the temperature compensation according to the below derivation.

$$\Delta V_{\text{theo}} = V_{\text{final stock}} - V_{\text{initial stock}}$$

$$\Delta V_{\text{theo}} = (V_{\text{final}} - \Delta V_{\text{temp,f}}) - (V_{\text{initial}} - \Delta V_{\text{temp,i}})$$

$$\Delta V_{\text{theo}} = [V_{\text{final}} - ((T_f - T_{\text{ref}}) \times \alpha_{\text{fuel}})] - [V_{\text{initial}} - ((T_i - T_{\text{ref}}) \times \alpha_{\text{fuel}})]$$

$$\Delta V_{\text{theo}} = V_{\text{final}} - ((T_f - T_{\text{ref}}) \times \alpha_{\text{fuel}}) - V_{\text{initial}} + ((T_i - T_{\text{ref}}) \times \alpha_{\text{fuel}})]$$

$$\Delta V_{\text{theo}} = V_{\text{final}} - V_{\text{initial}} + [\alpha_{\text{fuel}} \times (T_i - T_{\text{ref}} - T_f + T_{\text{ref}})]$$

$$\Delta V_{\text{theo}} = V_{\text{final}} - V_{\text{initial}} + [\alpha_{\text{fuel}} \times (T_i - T_f)]$$

T_i and T_f are tank initial and final temperatures ($^{\circ}\text{C}$), respectively. α_{fuel} is fuel thermal expansion coefficient ($1/^{\circ}\text{C}$).

APPENDIX D: EFFECT OF PARAMETERS ON LIQUID VOLUME

D1. Effect of Parameters on SCT Volume

Table D.1. The tank in Site A parameters data set – I

h (mm)	R=1240mm	R=1220mm	R=1260mm	L=2000mm	L=1960mm	L=2040mm
0	0.00	0.00	0.00	0.00	0.00	0.00
10	4.19	4.16	4.23	4.19	4.11	4.28
20	11.85	11.75	11.94	11.85	11.61	12.09
30	21.74	21.56	21.92	21.74	21.31	22.18
40	33.43	33.16	33.70	33.43	32.76	34.10
50	46.67	46.28	47.05	46.67	45.73	47.60
60	61.27	60.77	61.77	61.27	60.04	62.49
70	77.11	76.48	77.74	77.11	75.57	78.66
80	94.10	93.32	94.87	94.10	92.22	95.98
90	112.14	111.21	113.06	112.14	109.90	114.39
100	131.18	130.09	132.26	131.18	128.56	133.80
110	151.15	149.90	152.40	151.15	148.13	154.18
120	172.01	170.58	173.44	172.01	168.57	175.45
130	193.71	192.09	195.32	193.71	189.84	197.59
140	216.22	214.41	218.02	216.22	211.89	220.54
150	239.49	237.48	241.49	239.49	234.70	244.28
160	263.50	261.28	265.70	263.50	258.23	268.77
170	288.22	285.79	290.64	288.22	282.46	293.99
180	313.63	310.97	316.26	313.63	307.35	319.90
190	339.69	336.81	342.55	339.69	332.90	346.48
200	366.39	363.27	369.48	366.39	359.06	373.72
210	393.71	390.35	397.04	393.71	385.83	401.58
220	421.62	418.01	425.20	421.62	413.19	430.05
230	450.11	446.25	453.94	450.11	441.11	459.11
240	479.16	475.04	483.25	479.16	469.58	488.75
250	508.76	504.37	513.11	508.76	498.59	518.94
260	538.89	534.23	543.51	538.89	528.11	549.67
270	569.54	564.60	574.43	569.54	558.14	580.93
280	600.68	595.46	605.86	600.68	588.67	612.70
290	632.32	626.81	637.78	632.32	619.67	644.97
300	664.43	658.63	670.19	664.43	651.14	677.72
310	697.01	690.90	703.07	697.01	683.07	710.95
320	730.04	723.63	736.40	730.04	715.44	744.65
330	763.52	756.79	770.19	763.52	748.25	778.79

340	797.43	790.38	804.41	797.43	781.48	813.37
350	831.76	824.39	839.06	831.76	815.12	848.39
360	866.50	858.80	874.12	866.50	849.17	883.83
370	901.64	893.61	909.60	901.64	883.61	919.67
380	937.18	928.81	945.47	937.18	918.44	955.92
390	973.10	964.39	981.74	973.10	953.64	992.57
400	1009.40	1000.34	1018.39	1009.40	989.22	1029.59
410	1046.07	1036.65	1055.41	1046.07	1025.15	1066.99
420	1083.10	1073.32	1092.79	1083.10	1061.44	1104.76
430	1120.48	1110.34	1130.54	1120.48	1098.07	1142.89
440	1158.21	1147.69	1168.63	1158.21	1135.04	1181.37
450	1196.27	1185.38	1207.07	1196.27	1172.35	1220.20
460	1234.67	1223.40	1245.84	1234.67	1209.97	1259.36
470	1273.39	1261.73	1284.94	1273.39	1247.92	1298.85
480	1312.42	1300.37	1324.36	1312.42	1286.17	1338.67
490	1351.77	1339.32	1364.10	1351.77	1324.73	1378.80
500	1391.42	1378.57	1404.15	1391.42	1363.59	1419.25
510	1431.37	1418.11	1444.50	1431.37	1402.74	1459.99
520	1471.60	1457.94	1485.14	1471.60	1442.17	1501.04
530	1512.13	1498.05	1526.08	1512.13	1481.89	1542.37
540	1552.93	1538.43	1567.30	1552.93	1521.87	1583.99
550	1594.01	1579.08	1608.80	1594.01	1562.13	1625.89
560	1635.35	1619.99	1650.57	1635.35	1602.65	1668.06
570	1676.96	1661.16	1692.61	1676.96	1643.42	1710.50
580	1718.82	1702.58	1734.91	1718.82	1684.45	1753.20
590	1760.94	1744.25	1777.47	1760.94	1725.72	1796.16
600	1803.30	1786.16	1820.28	1803.30	1767.23	1839.37
610	1845.90	1828.31	1863.33	1845.90	1808.98	1882.82
620	1888.74	1870.68	1906.63	1888.74	1850.97	1926.52
630	1931.81	1913.28	1950.16	1931.81	1893.17	1970.45
640	1975.11	1956.11	1993.92	1975.11	1935.60	2014.61
650	2018.62	1999.15	2037.91	2018.62	1978.25	2059.00
660	2062.36	2042.40	2082.12	2062.36	2021.11	2103.60
670	2106.30	2085.86	2126.55	2106.30	2064.17	2148.43
680	2150.45	2129.52	2171.18	2150.45	2107.44	2193.46
690	2194.81	2173.37	2216.03	2194.81	2150.91	2238.70
700	2239.36	2217.42	2261.08	2239.36	2194.57	2284.15
710	2284.10	2261.66	2306.33	2284.10	2238.42	2329.79
720	2329.04	2306.09	2351.77	2329.04	2282.46	2375.62
730	2374.16	2350.69	2397.40	2374.16	2326.68	2421.64
740	2419.46	2395.47	2443.22	2419.46	2371.07	2467.85
750	2464.94	2440.42	2489.21	2464.94	2415.64	2514.23
760	2510.58	2485.53	2535.39	2510.58	2460.37	2560.80
770	2556.40	2530.81	2581.74	2556.40	2505.27	2607.53

780	2602.38	2576.25	2628.25	2602.38	2550.33	2654.43
790	2648.52	2621.84	2674.93	2648.52	2595.55	2701.49
800	2694.82	2667.58	2721.78	2694.82	2640.92	2748.71
810	2741.26	2713.47	2768.77	2741.26	2686.44	2796.09
820	2787.86	2759.51	2815.93	2787.86	2732.10	2843.62
830	2834.60	2805.68	2863.23	2834.60	2777.91	2891.29
840	2881.48	2851.98	2910.67	2881.48	2823.85	2939.11
850	2928.50	2898.42	2958.26	2928.50	2869.93	2987.07
860	2975.64	2944.99	3005.99	2975.64	2916.13	3035.16
870	3022.92	2991.67	3053.85	3022.92	2962.46	3083.38
880	3070.32	3038.48	3101.83	3070.32	3008.92	3131.73
890	3117.85	3085.41	3149.95	3117.85	3055.49	3180.20
900	3165.49	3132.44	3198.19	3165.49	3102.18	3228.80
910	3213.24	3179.59	3246.55	3213.24	3148.98	3277.51
920	3261.11	3226.84	3295.02	3261.11	3195.89	3326.33
930	3309.08	3274.19	3343.61	3309.08	3242.90	3375.26
940	3357.16	3321.64	3392.30	3357.16	3290.02	3424.30
950	3405.33	3369.18	3441.10	3405.33	3337.23	3473.44
960	3453.61	3416.82	3490.00	3453.61	3384.53	3522.68
970	3501.97	3464.54	3539.00	3501.97	3431.93	3572.01
980	3550.43	3512.35	3588.09	3550.43	3479.42	3621.43
990	3598.97	3560.23	3637.28	3598.97	3526.99	3670.94
1000	3647.59	3608.19	3686.55	3647.59	3574.64	3720.54
1010	3696.29	3656.23	3735.91	3696.29	3622.36	3770.21
1020	3745.06	3704.34	3785.35	3745.06	3670.16	3819.97
1030	3793.91	3752.51	3834.86	3793.91	3718.04	3869.79
1040	3842.83	3800.74	3884.45	3842.83	3765.97	3919.69
1050	3891.81	3849.04	3934.11	3891.81	3813.98	3969.65
1060	3940.86	3897.39	3983.84	3940.86	3862.04	4019.68
1070	3989.96	3945.79	4033.63	3989.96	3910.16	4069.76
1080	4039.12	3994.25	4083.49	4039.12	3958.34	4119.90
1090	4088.33	4042.75	4133.40	4088.33	4006.56	4170.10
1100	4137.59	4091.29	4183.36	4137.59	4054.84	4220.34
1110	4186.90	4139.87	4233.38	4186.90	4103.16	4270.63
1120	4236.24	4188.49	4283.45	4236.24	4151.52	4320.97
1130	4285.63	4237.15	4333.56	4285.63	4199.92	4371.34
1140	4335.05	4285.83	4383.71	4335.05	4248.35	4421.75
1150	4384.51	4334.53	4433.90	4384.51	4296.82	4472.20
1160	4433.99	4383.26	4484.12	4433.99	4345.31	4522.67
1170	4483.50	4432.01	4534.38	4483.50	4393.83	4573.17
1180	4533.03	4480.78	4584.66	4533.03	4442.37	4623.69
1190	4582.58	4529.56	4634.97	4582.58	4490.93	4674.23
1200	4632.15	4578.35	4685.31	4632.15	4539.50	4724.79
1210	4681.73	4627.15	4735.66	4681.73	4588.09	4775.36

1220	4731.32	4675.95	4786.03	4731.32	4636.69	4825.94
1230	4780.91	4724.75	4836.41	4780.91	4685.30	4876.53
1240	4830.51	4773.54	4886.80	4830.51	4733.90	4927.12
1250	4880.11	4822.33	4937.19	4880.11	4782.51	4977.71
1260	4929.71	4871.11	4987.59	4929.71	4831.11	5028.30
1270	4979.30	4919.88	5037.99	4979.30	4879.71	5078.88
1280	5028.88	4968.63	5088.39	5028.88	4928.30	5129.46
1290	5078.45	5017.36	5138.78	5078.45	4976.88	5180.01
1300	5128.00	5066.07	5189.16	5128.00	5025.44	5230.56
1310	5177.53	5114.75	5239.53	5177.53	5073.98	5281.08
1320	5227.04	5163.40	5289.88	5227.04	5122.50	5331.58
1330	5276.52	5212.02	5340.21	5276.52	5170.99	5382.05
1340	5325.97	5260.60	5390.52	5325.97	5219.46	5432.49
1350	5375.40	5309.14	5440.81	5375.40	5267.89	5482.90
1360	5424.78	5357.64	5491.06	5424.78	5316.29	5533.28
1370	5474.13	5406.10	5541.29	5474.13	5364.65	5583.61
1380	5523.43	5454.50	5591.48	5523.43	5412.97	5633.90
1390	5572.69	5502.85	5641.63	5572.69	5461.24	5684.15
1400	5621.91	5551.15	5691.74	5621.91	5509.47	5734.34
1410	5671.06	5599.38	5741.80	5671.06	5557.64	5784.49
1420	5720.17	5647.56	5791.82	5720.17	5605.76	5834.57
1430	5769.21	5695.66	5841.79	5769.21	5653.83	5884.60
1440	5818.19	5743.70	5891.70	5818.19	5701.83	5934.56
1450	5867.11	5791.66	5941.55	5867.11	5749.77	5984.45
1460	5915.96	5839.55	5991.34	5915.96	5797.64	6034.28
1470	5964.74	5887.35	6041.07	5964.74	5845.44	6084.03
1480	6013.44	5935.08	6090.73	6013.44	5893.17	6133.71
1490	6062.06	5982.71	6140.32	6062.06	5940.82	6183.30
1500	6110.60	6030.25	6189.84	6110.60	5988.39	6232.81
1510	6159.05	6077.70	6239.28	6159.05	6035.87	6282.24
1520	6207.42	6125.06	6288.63	6207.42	6083.27	6331.57
1530	6255.69	6172.31	6337.91	6255.69	6130.58	6380.80
1540	6303.87	6219.45	6387.09	6303.87	6177.79	6429.94
1550	6351.94	6266.49	6436.18	6351.94	6224.90	6478.98
1560	6399.92	6313.41	6485.18	6399.92	6271.92	6527.91
1570	6447.78	6360.22	6534.08	6447.78	6318.83	6576.74
1580	6495.54	6406.91	6582.88	6495.54	6365.63	6625.45
1590	6543.18	6453.47	6631.58	6543.18	6412.31	6674.04
1600	6590.70	6499.91	6680.16	6590.70	6458.89	6722.52
1610	6638.10	6546.22	6728.64	6638.10	6505.34	6770.87
1620	6685.38	6592.39	6777.00	6685.38	6551.67	6819.09
1630	6732.53	6638.42	6825.23	6732.53	6597.88	6867.18
1640	6779.55	6684.31	6873.35	6779.55	6643.96	6915.14
1650	6826.43	6730.05	6921.34	6826.43	6689.90	6962.95

1660	6873.17	6775.64	6969.20	6873.17	6735.70	7010.63
1670	6919.76	6821.08	7016.92	6919.76	6781.37	7058.16
1680	6966.21	6866.36	7064.51	6966.21	6826.88	7105.53
1690	7012.50	6911.48	7111.96	7012.50	6872.25	7152.75
1700	7058.64	6956.43	7159.26	7058.64	6917.47	7199.82
1710	7104.62	7001.20	7206.41	7104.62	6962.53	7246.72
1720	7150.44	7045.81	7253.41	7150.44	7007.43	7293.45
1730	7196.09	7090.23	7300.25	7196.09	7052.17	7340.01
1740	7241.57	7134.47	7346.93	7241.57	7096.73	7386.40
1750	7286.87	7178.52	7393.45	7286.87	7141.13	7432.60
1760	7331.99	7222.38	7439.80	7331.99	7185.35	7478.63
1770	7376.92	7266.04	7485.97	7376.92	7229.38	7524.46
1780	7421.67	7309.49	7531.97	7421.67	7273.23	7570.10
1790	7466.22	7352.74	7577.79	7466.22	7316.89	7615.54
1800	7510.57	7395.78	7623.42	7510.57	7360.36	7660.78
1810	7554.72	7438.61	7668.86	7554.72	7403.63	7705.82
1820	7598.67	7481.21	7714.11	7598.67	7446.70	7750.64
1830	7642.40	7523.59	7759.15	7642.40	7489.55	7795.25
1840	7685.92	7565.73	7804.00	7685.92	7532.20	7839.64
1850	7729.21	7607.64	7848.64	7729.21	7574.63	7883.80
1860	7772.28	7649.31	7893.06	7772.28	7616.84	7927.73
1870	7815.12	7690.73	7937.27	7815.12	7658.82	7971.43
1880	7857.73	7731.90	7981.26	7857.73	7700.57	8014.88
1890	7900.09	7772.82	8025.03	7900.09	7742.09	8058.09
1900	7942.20	7813.47	8068.56	7942.20	7783.36	8101.05
1910	7984.07	7853.85	8111.85	7984.07	7824.39	8143.75
1920	8025.67	7893.95	8154.91	8025.67	7865.16	8186.19
1930	8067.02	7933.78	8197.72	8067.02	7905.68	8228.36
1940	8108.09	7973.32	8240.27	8108.09	7945.93	8270.26
1950	8148.90	8012.57	8282.57	8148.90	7985.92	8311.88
1960	8189.42	8051.52	8324.61	8189.42	8025.63	8353.21
1970	8229.66	8090.16	8366.39	8229.66	8065.07	8394.25
1980	8269.61	8128.50	8407.88	8269.61	8104.22	8435.00
1990	8309.26	8166.51	8449.11	8309.26	8143.07	8475.44
2000	8348.60	8204.20	8490.04	8348.60	8181.63	8515.58
2010	8387.64	8241.55	8530.69	8387.64	8219.89	8555.39
2020	8426.36	8278.57	8571.04	8426.36	8257.83	8594.88
2030	8464.75	8315.24	8611.08	8464.75	8295.46	8634.05
2040	8502.82	8351.55	8650.82	8502.82	8332.76	8672.87
2050	8540.54	8387.50	8690.25	8540.54	8369.73	8711.35
2060	8577.92	8423.08	8729.35	8577.92	8406.37	8749.48
2070	8614.95	8458.28	8768.12	8614.95	8442.65	8787.25
2080	8651.62	8493.09	8806.56	8651.62	8478.59	8824.65
2090	8687.92	8527.50	8844.65	8687.92	8514.16	8861.68

2100	8723.85	8561.51	8882.39	8723.85	8549.37	8898.32
2110	8759.38	8595.10	8919.78	8759.38	8584.20	8934.57
2120	8794.53	8628.26	8956.80	8794.53	8618.64	8970.42
2130	8829.27	8660.99	8993.45	8829.27	8652.68	9005.86
2140	8863.60	8693.27	9029.71	8863.60	8686.33	9040.87
2150	8897.51	8725.08	9065.59	8897.51	8719.56	9075.46
2160	8930.98	8756.43	9101.06	8930.98	8752.36	9109.60
2170	8964.01	8787.30	9136.13	8964.01	8784.73	9143.29
2180	8996.59	8817.66	9170.78	8996.59	8816.66	9176.52
2190	9028.71	8847.52	9205.00	9028.71	8848.13	9209.28
2200	9060.34	8876.85	9238.78	9060.34	8879.14	9241.55
2210	9091.49	8905.65	9272.12	9091.49	8909.66	9273.32
2220	9122.14	8933.88	9305.00	9122.14	8939.69	9304.58
2230	9152.26	8961.55	9337.40	9152.26	8969.22	9335.31
2240	9181.86	8988.62	9369.33	9181.86	8998.23	9365.50
2250	9210.92	9015.09	9400.75	9210.92	9026.70	9395.13
2260	9239.41	9040.92	9431.67	9239.41	9054.62	9424.20
2270	9267.32	9066.10	9462.07	9267.32	9081.97	9452.67
2280	9294.64	9090.61	9491.94	9294.64	9108.74	9480.53
2290	9321.34	9114.41	9521.25	9321.34	9134.91	9507.76
2300	9347.40	9137.49	9549.99	9347.40	9160.45	9534.35
2310	9372.80	9159.80	9578.15	9372.80	9185.35	9560.26
2320	9397.52	9181.32	9605.70	9397.52	9209.57	9585.47
2330	9421.53	9202.00	9632.64	9421.53	9233.10	9609.97
2340	9444.81	9221.80	9658.92	9444.81	9255.91	9633.70
2350	9467.31	9240.68	9684.55	9467.31	9277.97	9656.66
2360	9489.01	9258.57	9709.48	9489.01	9299.23	9678.79
2370	9509.87	9275.41	9733.70	9509.87	9319.67	9700.07
2380	9529.84	9291.13	9757.17	9529.84	9339.25	9720.44
2390	9548.88	9305.61	9779.87	9548.88	9357.90	9739.86
2400	9566.93	9318.73	9801.75	9566.93	9375.59	9758.27
2410	9583.91	9330.33	9822.78	9583.91	9392.23	9775.59
2420	9599.76	9340.14	9842.92	9599.76	9407.76	9791.75
2430	9614.36	9347.73	9862.12	9614.36	9422.07	9806.65
2440	9627.59	9351.89	9880.32	9627.59	9435.04	9820.14
2450	9639.28	9351.89	9897.44	9639.28	9446.50	9832.07
2460	9649.18	9351.89	9913.42	9649.18	9456.19	9842.16

Table D.2. The tank in Site A parameters data set - II

alpha=0°	alpha=-5°	alpha=5°	beta=0°	beta=-10°	beta=10°	M=400mm	M=380mm	M=420mm
0.00	216.18	5.48	0.00	85.10	85.10	0.00	0.00	0.00
4.19	223.30	7.86	4.19	102.32	102.32	4.19	4.19	4.19
11.85	229.49	11.19	11.85	120.55	120.55	11.85	11.85	11.85
21.74	234.67	15.56	21.74	139.71	139.71	21.74	21.74	21.74
33.43	244.00	21.05	33.43	159.75	159.75	33.43	33.43	33.43
46.67	260.14	27.75	46.67	180.64	180.64	46.67	46.67	46.67
61.27	277.92	35.73	61.27	202.33	202.33	61.27	61.27	61.27
77.11	296.99	45.05	77.11	224.78	224.78	77.11	77.11	77.11
94.10	317.19	55.80	94.10	247.97	247.97	94.10	94.10	94.10
112.14	338.41	68.01	112.14	271.86	271.86	112.14	112.14	112.14
131.18	360.55	81.76	131.18	296.44	296.44	131.18	131.18	131.18
151.15	383.56	97.10	151.15	321.66	321.66	151.15	151.15	151.15
172.01	407.39	114.08	172.01	347.52	347.52	172.01	172.01	172.01
193.71	431.99	132.75	193.71	373.99	373.99	193.71	193.71	193.71
216.22	457.31	153.15	216.22	401.06	401.06	216.22	216.22	216.22
239.49	483.34	168.12	239.49	428.69	428.69	239.49	239.49	239.49
263.50	510.04	185.14	263.50	456.89	456.89	263.50	263.50	263.50
288.22	537.39	203.60	288.22	485.62	485.62	288.22	288.22	288.22
313.63	565.35	223.25	313.63	514.88	514.88	313.63	313.63	313.63
339.69	593.91	243.97	339.69	544.66	544.66	339.69	339.69	339.69
366.39	623.05	265.66	366.39	574.93	574.93	366.39	366.39	366.39
393.71	652.74	288.25	393.71	605.68	605.68	393.71	393.71	393.71
421.62	682.98	311.68	421.62	636.91	636.91	421.62	421.62	421.62
450.11	713.75	335.89	450.11	668.60	668.60	450.11	450.11	450.11
479.16	745.02	360.86	479.16	700.74	700.74	479.16	479.16	479.16
508.76	776.79	386.55	508.76	733.32	733.32	508.76	508.76	508.76
538.89	809.04	412.91	538.89	766.32	766.32	538.89	538.89	538.89
569.54	841.76	439.94	569.54	799.74	799.74	569.54	569.54	569.54
600.68	874.94	467.60	600.68	833.58	833.58	600.68	600.68	600.68
632.32	908.56	495.86	632.32	867.81	867.81	632.32	632.32	632.32
664.43	942.62	524.71	664.43	902.43	902.43	664.43	664.43	664.43
697.01	977.10	554.13	697.01	937.44	937.44	697.01	697.01	697.01
730.04	1012.00	584.10	730.04	972.81	972.81	730.04	730.04	730.04
763.52	1047.29	614.61	763.52	1008.56	1008.56	763.52	763.52	763.52
797.43	1082.99	645.63	797.43	1044.66	1044.66	797.43	797.43	797.43
831.76	1119.06	677.15	831.76	1081.11	1081.11	831.76	831.76	831.76
866.50	1155.51	709.17	866.50	1117.90	1117.90	866.50	866.50	866.50
901.64	1192.33	741.66	901.64	1155.03	1155.03	901.64	901.64	901.64
937.18	1229.51	774.61	937.18	1192.48	1192.48	937.18	937.18	937.18
973.10	1267.04	808.01	973.10	1230.26	1230.26	973.10	973.10	973.10
1009.40	1304.92	841.85	1009.40	1268.35	1268.35	1009.40	1009.40	1009.40

1046.07	1343.13	876.12	1046.07	1306.75	1306.75	1046.07	1046.07	1046.07
1083.10	1381.66	910.81	1083.10	1345.45	1345.45	1083.10	1083.10	1083.10
1120.48	1420.52	945.91	1120.48	1384.45	1384.45	1120.48	1120.48	1120.48
1158.21	1459.70	981.41	1158.21	1423.74	1423.74	1158.21	1158.21	1158.21
1196.27	1499.18	1017.29	1196.27	1463.31	1463.31	1196.27	1196.27	1196.27
1234.67	1538.96	1053.56	1234.67	1503.16	1503.16	1234.67	1234.67	1234.67
1273.39	1579.04	1090.20	1273.39	1543.28	1543.28	1273.39	1273.39	1273.39
1312.42	1619.41	1127.20	1312.42	1583.67	1583.67	1312.42	1312.42	1312.42
1351.77	1660.06	1164.55	1351.77	1624.32	1624.32	1351.77	1351.77	1351.77
1391.42	1700.99	1202.26	1391.42	1665.22	1665.22	1391.42	1391.42	1391.42
1431.37	1742.18	1240.30	1431.37	1706.38	1706.38	1431.37	1431.37	1431.37
1471.60	1783.65	1278.67	1471.60	1747.78	1747.78	1471.60	1471.60	1471.60
1512.13	1825.37	1317.37	1512.13	1789.42	1789.42	1512.13	1512.13	1512.13
1552.93	1867.34	1356.39	1552.93	1831.29	1831.29	1552.93	1552.93	1552.93
1594.01	1909.57	1395.72	1594.01	1873.40	1873.40	1594.01	1594.01	1594.01
1635.35	1952.03	1435.36	1635.35	1915.73	1915.73	1635.35	1635.35	1635.35
1676.96	1994.74	1475.29	1676.96	1958.29	1958.29	1676.96	1676.96	1676.96
1718.82	2037.68	1515.51	1718.82	2001.06	2001.06	1718.82	1718.82	1718.82
1760.94	2080.84	1556.02	1760.94	2044.04	2044.04	1760.94	1760.94	1760.94
1803.30	2124.23	1596.81	1803.30	2087.23	2087.23	1803.30	1803.30	1803.30
1845.90	2167.84	1637.88	1845.90	2130.62	2130.62	1845.90	1845.90	1845.90
1888.74	2211.66	1679.21	1888.74	2174.21	2174.21	1888.74	1888.74	1888.74
1931.81	2255.68	1720.80	1931.81	2217.99	2217.99	1931.81	1931.81	1931.81
1975.11	2299.91	1762.65	1975.11	2261.97	2261.97	1975.11	1975.11	1975.11
2018.62	2344.35	1804.75	2018.62	2306.13	2306.13	2018.62	2018.62	2018.62
2062.36	2388.97	1847.10	2062.36	2350.47	2350.47	2062.36	2062.36	2062.36
2106.30	2433.79	1889.68	2106.30	2394.99	2394.99	2106.30	2106.30	2106.30
2150.45	2478.79	1932.50	2150.45	2439.68	2439.68	2150.45	2150.45	2150.45
2194.81	2523.97	1975.56	2194.81	2484.54	2484.54	2194.81	2194.81	2194.81
2239.36	2569.33	2018.83	2239.36	2529.56	2529.56	2239.36	2239.36	2239.36
2284.10	2614.86	2062.33	2284.10	2574.75	2574.75	2284.10	2284.10	2284.10
2329.04	2660.56	2106.05	2329.04	2620.09	2620.09	2329.04	2329.04	2329.04
2374.16	2706.43	2149.97	2374.16	2665.59	2665.59	2374.16	2374.16	2374.16
2419.46	2752.45	2194.10	2419.46	2711.24	2711.24	2419.46	2419.46	2419.46
2464.94	2798.64	2238.43	2464.94	2757.03	2757.03	2464.94	2464.94	2464.94
2510.58	2844.97	2282.96	2510.58	2802.97	2802.97	2510.58	2510.58	2510.58
2556.40	2891.45	2327.68	2556.40	2849.04	2849.04	2556.40	2556.40	2556.40
2602.38	2938.08	2372.59	2602.38	2895.25	2895.25	2602.38	2602.38	2602.38
2648.52	2984.85	2417.68	2648.52	2941.59	2941.59	2648.52	2648.52	2648.52
2694.82	3031.75	2462.96	2694.82	2988.05	2988.05	2694.82	2694.82	2694.82
2741.26	3078.79	2508.40	2741.26	3034.64	3034.64	2741.26	2741.26	2741.26
2787.86	3125.96	2554.02	2787.86	3081.36	3081.36	2787.86	2787.86	2787.86
2834.60	3173.25	2599.80	2834.60	3128.18	3128.18	2834.60	2834.60	2834.60
2881.48	3220.66	2645.75	2881.48	3175.12	3175.12	2881.48	2881.48	2881.48

2928.50	3268.19	2691.86	2928.50	3222.18	3222.18	2928.50	2928.50	2928.50
2975.64	3315.84	2738.11	2975.64	3269.33	3269.33	2975.64	2975.64	2975.64
3022.92	3363.59	2784.52	3022.92	3316.60	3316.60	3022.92	3022.92	3022.92
3070.32	3411.45	2831.08	3070.32	3363.96	3363.96	3070.32	3070.32	3070.32
3117.85	3459.42	2877.78	3117.85	3411.41	3411.41	3117.85	3117.85	3117.85
3165.49	3507.49	2924.61	3165.49	3458.96	3458.96	3165.49	3165.49	3165.49
3213.24	3555.65	2971.59	3213.24	3506.60	3506.60	3213.24	3213.24	3213.24
3261.11	3603.90	3018.69	3261.11	3554.33	3554.33	3261.11	3261.11	3261.11
3309.08	3652.24	3065.92	3309.08	3602.13	3602.13	3309.08	3309.08	3309.08
3357.16	3700.67	3113.27	3357.16	3650.02	3650.02	3357.16	3357.16	3357.16
3405.33	3749.18	3160.74	3405.33	3697.99	3697.99	3405.33	3405.33	3405.33
3453.61	3797.77	3208.33	3453.61	3746.02	3746.02	3453.61	3453.61	3453.61
3501.97	3846.44	3256.03	3501.97	3794.13	3794.13	3501.97	3501.97	3501.97
3550.43	3895.18	3303.84	3550.43	3842.31	3842.31	3550.43	3550.43	3550.43
3598.97	3943.98	3351.76	3598.97	3890.54	3890.54	3598.97	3598.97	3598.97
3647.59	3992.85	3399.77	3647.59	3938.84	3938.84	3647.59	3647.59	3647.59
3696.29	4041.78	3447.89	3696.29	3987.20	3987.20	3696.29	3696.29	3696.29
3745.06	4090.77	3496.10	3745.06	4035.60	4035.60	3745.06	3745.06	3745.06
3793.91	4139.82	3544.39	3793.91	4084.06	4084.06	3793.91	3793.91	3793.91
3842.83	4188.92	3592.78	3842.83	4132.57	4132.57	3842.83	3842.83	3842.83
3891.81	4238.06	3641.25	3891.81	4181.12	4181.12	3891.81	3891.81	3891.81
3940.86	4287.25	3689.80	3940.86	4229.71	4229.71	3940.86	3940.86	3940.86
3989.96	4336.48	3738.43	3989.96	4278.34	4278.34	3989.96	3989.96	3989.96
4039.12	4385.75	3787.13	4039.12	4327.01	4327.01	4039.12	4039.12	4039.12
4088.33	4435.06	3835.90	4088.33	4375.71	4375.71	4088.33	4088.33	4088.33
4137.59	4484.39	3884.74	4137.59	4424.43	4424.43	4137.59	4137.59	4137.59
4186.90	4533.76	3933.64	4186.90	4473.19	4473.19	4186.90	4186.90	4186.90
4236.24	4583.15	3982.60	4236.24	4521.96	4521.96	4236.24	4236.24	4236.24
4285.63	4632.56	4031.62	4285.63	4570.76	4570.76	4285.63	4285.63	4285.63
4335.05	4681.99	4080.69	4335.05	4619.57	4619.57	4335.05	4335.05	4335.05
4384.51	4731.44	4129.82	4384.51	4668.39	4668.39	4384.51	4384.51	4384.51
4433.99	4780.90	4178.98	4433.99	4717.22	4717.22	4433.99	4433.99	4433.99
4483.50	4830.37	4228.20	4483.50	4766.06	4766.06	4483.50	4483.50	4483.50
4533.03	4879.84	4277.45	4533.03	4814.91	4814.91	4533.03	4533.03	4533.03
4582.58	4929.32	4326.73	4582.58	4863.76	4863.76	4582.58	4582.58	4582.58
4632.15	4978.79	4376.06	4632.15	4912.60	4912.60	4632.15	4632.15	4632.15
4681.73	5028.27	4425.41	4681.73	4961.44	4961.44	4681.73	4681.73	4681.73
4731.32	5077.73	4474.79	4731.32	5010.27	5010.27	4731.32	4731.32	4731.32
4780.91	5127.18	4524.19	4780.91	5059.09	5059.09	4780.91	4780.91	4780.91
4830.51	5176.62	4573.61	4830.51	5107.89	5107.89	4830.51	4830.51	4830.51
4880.11	5226.04	4623.05	4880.11	5156.68	5156.68	4880.11	4880.11	4880.11
4929.71	5275.45	4672.50	4929.71	5205.45	5205.45	4929.71	4929.71	4929.71
4979.30	5324.83	4721.97	4979.30	5254.19	5254.19	4979.30	4979.30	4979.30
5028.88	5374.18	4771.44	5028.88	5302.91	5302.91	5028.88	5028.88	5028.88

5078.45	5423.50	4820.91	5078.45	5351.59	5351.59	5078.45	5078.45	5078.45
5128.00	5472.79	4870.39	5128.00	5400.25	5400.25	5128.00	5128.00	5128.00
5177.53	5522.04	4919.86	5177.53	5448.87	5448.87	5177.53	5177.53	5177.53
5227.04	5571.25	4969.33	5227.04	5497.44	5497.44	5227.04	5227.04	5227.04
5276.52	5620.42	5018.79	5276.52	5545.98	5545.98	5276.52	5276.52	5276.52
5325.97	5669.54	5068.24	5325.97	5594.47	5594.47	5325.97	5325.97	5325.97
5375.40	5718.61	5117.67	5375.40	5642.91	5642.91	5375.40	5375.40	5375.40
5424.78	5767.63	5167.08	5424.78	5691.30	5691.30	5424.78	5424.78	5424.78
5474.13	5816.59	5216.47	5474.13	5739.63	5739.63	5474.13	5474.13	5474.13
5523.43	5865.49	5265.84	5523.43	5787.91	5787.91	5523.43	5523.43	5523.43
5572.69	5914.33	5315.18	5572.69	5836.13	5836.13	5572.69	5572.69	5572.69
5621.91	5963.10	5364.48	5621.91	5884.28	5884.28	5621.91	5621.91	5621.91
5671.06	6011.80	5413.75	5671.06	5932.36	5932.36	5671.06	5671.06	5671.06
5720.17	6060.43	5462.98	5720.17	5980.37	5980.37	5720.17	5720.17	5720.17
5769.21	6108.98	5512.17	5769.21	6028.31	6028.31	5769.21	5769.21	5769.21
5818.19	6157.45	5561.32	5818.19	6076.17	6076.17	5818.19	5818.19	5818.19
5867.11	6205.84	5610.42	5867.11	6123.95	6123.95	5867.11	5867.11	5867.11
5915.96	6254.14	5659.46	5915.96	6171.64	6171.64	5915.96	5915.96	5915.96
5964.74	6302.35	5708.45	5964.74	6219.25	6219.25	5964.74	5964.74	5964.74
6013.44	6350.46	5757.38	6013.44	6266.76	6266.76	6013.44	6013.44	6013.44
6062.06	6398.48	5806.25	6062.06	6314.19	6314.19	6062.06	6062.06	6062.06
6110.60	6446.39	5855.06	6110.60	6361.51	6361.51	6110.60	6110.60	6110.60
6159.05	6494.20	5903.79	6159.05	6408.73	6408.73	6159.05	6159.05	6159.05
6207.42	6541.90	5952.46	6207.42	6455.85	6455.85	6207.42	6207.42	6207.42
6255.69	6589.49	6001.05	6255.69	6502.87	6502.87	6255.69	6255.69	6255.69
6303.87	6636.96	6049.56	6303.87	6549.77	6549.77	6303.87	6303.87	6303.87
6351.94	6684.32	6097.99	6351.94	6596.55	6596.55	6351.94	6351.94	6351.94
6399.92	6731.55	6146.33	6399.92	6643.22	6643.22	6399.92	6399.92	6399.92
6447.78	6778.65	6194.59	6447.78	6689.77	6689.77	6447.78	6447.78	6447.78
6495.54	6825.62	6242.75	6495.54	6736.19	6736.19	6495.54	6495.54	6495.54
6543.18	6872.46	6290.81	6543.18	6782.48	6782.48	6543.18	6543.18	6543.18
6590.70	6919.15	6338.78	6590.70	6828.64	6828.64	6590.70	6590.70	6590.70
6638.10	6965.71	6386.64	6638.10	6874.67	6874.67	6638.10	6638.10	6638.10
6685.38	7012.12	6434.40	6685.38	6920.55	6920.55	6685.38	6685.38	6685.38
6732.53	7058.38	6482.04	6732.53	6966.29	6966.29	6732.53	6732.53	6732.53
6779.55	7104.48	6529.57	6779.55	7011.88	7011.88	6779.55	6779.55	6779.55
6826.43	7150.43	6576.99	6826.43	7057.33	7057.33	6826.43	6826.43	6826.43
6873.17	7196.21	6624.28	6873.17	7102.61	7102.61	6873.17	6873.17	6873.17
6919.76	7241.83	6671.44	6919.76	7147.74	7147.74	6919.76	6919.76	6919.76
6966.21	7287.28	6718.48	6966.21	7192.71	7192.71	6966.21	6966.21	6966.21
7012.50	7332.55	6765.39	7012.50	7237.51	7237.51	7012.50	7012.50	7012.50
7058.64	7377.64	6812.15	7058.64	7282.14	7282.14	7058.64	7058.64	7058.64
7104.62	7422.55	6858.78	7104.62	7326.59	7326.59	7104.62	7104.62	7104.62
7150.44	7467.27	6905.26	7150.44	7370.87	7370.87	7150.44	7150.44	7150.44

7196.09	7511.80	6951.60	7196.09	7414.96	7414.96	7196.09	7196.09	7196.09
7241.57	7556.13	6997.78	7241.57	7458.87	7458.87	7241.57	7241.57	7241.57
7286.87	7600.26	7043.81	7286.87	7502.58	7502.58	7286.87	7286.87	7286.87
7331.99	7644.19	7089.67	7331.99	7546.10	7546.10	7331.99	7331.99	7331.99
7376.92	7687.90	7135.37	7376.92	7589.42	7589.42	7376.92	7376.92	7376.92
7421.67	7731.40	7180.90	7421.67	7632.53	7632.53	7421.67	7421.67	7421.67
7466.22	7774.68	7226.26	7466.22	7675.44	7675.44	7466.22	7466.22	7466.22
7510.57	7817.73	7271.45	7510.57	7718.13	7718.13	7510.57	7510.57	7510.57
7554.72	7860.55	7316.45	7554.72	7760.61	7760.61	7554.72	7554.72	7554.72
7598.67	7903.14	7361.26	7598.67	7802.86	7802.86	7598.67	7598.67	7598.67
7642.40	7945.48	7405.89	7642.40	7844.88	7844.88	7642.40	7642.40	7642.40
7685.92	7987.59	7450.32	7685.92	7886.67	7886.67	7685.92	7685.92	7685.92
7729.21	8029.44	7494.55	7729.21	7928.23	7928.23	7729.21	7729.21	7729.21
7772.28	8071.03	7538.58	7772.28	7969.54	7969.54	7772.28	7772.28	7772.28
7815.12	8112.36	7582.40	7815.12	8010.61	8010.61	7815.12	7815.12	7815.12
7857.73	8153.42	7626.00	7857.73	8051.42	8051.42	7857.73	7857.73	7857.73
7900.09	8194.21	7669.39	7900.09	8091.97	8091.97	7900.09	7900.09	7900.09
7942.20	8234.72	7712.56	7942.20	8132.27	8132.27	7942.20	7942.20	7942.20
7984.07	8274.94	7755.49	7984.07	8172.29	8172.29	7984.07	7984.07	7984.07
8025.67	8314.88	7798.20	8025.67	8212.04	8212.04	8025.67	8025.67	8025.67
8067.02	8354.51	7840.67	8067.02	8251.51	8251.51	8067.02	8067.02	8067.02
8108.09	8393.84	7882.89	8108.09	8290.69	8290.69	8108.09	8108.09	8108.09
8148.90	8432.86	7924.87	8148.90	8329.58	8329.58	8148.90	8148.90	8148.90
8189.42	8471.56	7966.59	8189.42	8368.18	8368.18	8189.42	8189.42	8189.42
8229.66	8509.93	8008.05	8229.66	8406.47	8406.47	8229.66	8229.66	8229.66
8269.61	8547.98	8049.25	8269.61	8444.45	8444.45	8269.61	8269.61	8269.61
8309.26	8585.68	8090.17	8309.26	8482.11	8482.11	8309.26	8309.26	8309.26
8348.60	8623.04	8130.82	8348.60	8519.45	8519.45	8348.60	8348.60	8348.60
8387.64	8660.04	8171.19	8387.64	8556.45	8556.45	8387.64	8387.64	8387.64
8426.36	8696.67	8211.27	8426.36	8593.12	8593.12	8426.36	8426.36	8426.36
8464.75	8732.94	8251.05	8464.75	8629.45	8629.45	8464.75	8464.75	8464.75
8502.82	8768.83	8290.54	8502.82	8665.42	8665.42	8502.82	8502.82	8502.82
8540.54	8804.32	8329.71	8540.54	8701.03	8701.03	8540.54	8540.54	8540.54
8577.92	8839.42	8368.57	8577.92	8736.28	8736.28	8577.92	8577.92	8577.92
8614.95	8874.11	8407.11	8614.95	8771.14	8771.14	8614.95	8614.95	8614.95
8651.62	8908.38	8445.32	8651.62	8805.62	8805.62	8651.62	8651.62	8651.62
8687.92	8942.22	8483.19	8687.92	8839.71	8839.71	8687.92	8687.92	8687.92
8723.85	8975.63	8520.72	8723.85	8873.40	8873.40	8723.85	8723.85	8723.85
8759.38	9008.58	8557.90	8759.38	8906.67	8906.67	8759.38	8759.38	8759.38
8794.53	9041.07	8594.72	8794.53	8939.53	8939.53	8794.53	8794.53	8794.53
8829.27	9073.08	8631.17	8829.27	8971.95	8971.95	8829.27	8829.27	8829.27
8863.60	9104.60	8667.25	8863.60	9003.92	9003.92	8863.60	8863.60	8863.60
8897.51	9135.63	8702.94	8897.51	9035.45	9035.45	8897.51	8897.51	8897.51
8930.98	9166.13	8738.24	8930.98	9066.51	9066.51	8930.98	8930.98	8930.98

8964.01	9196.10	8773.13	8964.01	9097.09	9097.09	8964.01	8964.01	8964.01
8996.59	9225.52	8807.61	8996.59	9127.18	9127.18	8996.59	8996.59	8996.59
9028.71	9254.37	8841.67	9028.71	9156.77	9156.77	9028.71	9028.71	9028.71
9060.34	9282.64	8875.29	9060.34	9185.84	9185.84	9060.34	9060.34	9060.34
9091.49	9310.29	8908.47	9091.49	9214.38	9214.38	9091.49	9091.49	9091.49
9122.14	9337.32	8941.19	9122.14	9242.38	9242.38	9122.14	9122.14	9122.14
9152.26	9363.69	8973.44	9152.26	9269.81	9269.81	9152.26	9152.26	9152.26
9181.86	9389.37	9005.21	9181.86	9296.66	9296.66	9181.86	9181.86	9181.86
9210.92	9414.34	9036.49	9210.92	9322.91	9322.91	9210.92	9210.92	9210.92
9239.41	9438.56	9067.25	9239.41	9348.55	9348.55	9239.41	9239.41	9239.41
9267.32	9461.98	9097.49	9267.32	9373.54	9373.54	9267.32	9267.32	9267.32
9294.64	9484.57	9127.19	9294.64	9397.87	9397.87	9294.64	9294.64	9294.64
9321.34	9506.26	9156.33	9321.34	9421.51	9421.51	9321.34	9321.34	9321.34
9347.40	9526.98	9184.89	9347.40	9444.44	9444.44	9347.40	9347.40	9347.40
9372.80	9546.64	9212.85	9372.80	9466.62	9466.62	9372.80	9372.80	9372.80
9397.52	9565.09	9240.19	9397.52	9488.02	9488.02	9397.52	9397.52	9397.52
9421.53	9582.11	9266.89	9421.53	9508.61	9508.61	9421.53	9421.53	9421.53
9444.81	9597.08	9292.92	9444.81	9528.34	9528.34	9444.81	9444.81	9444.81
9467.31	9609.61	9318.25	9467.31	9547.17	9547.17	9467.31	9467.31	9467.31
9489.01	9621.80	9342.85	9489.01	9565.04	9565.04	9489.01	9489.01	9489.01
9509.87	9633.62	9366.67	9509.87	9581.89	9581.89	9509.87	9509.87	9509.87
9529.84	9645.07	9389.68	9529.84	9597.65	9597.65	9529.84	9529.84	9529.84
9548.88	9656.12	9411.83	9548.88	9612.21	9612.21	9548.88	9548.88	9548.88
9566.93	9666.76	9433.04	9566.93	9625.47	9625.47	9566.93	9566.93	9566.93
9583.91	9676.97	9453.24	9583.91	9637.27	9637.27	9583.91	9583.91	9583.91
9599.76	9686.73	9472.32	9599.76	9647.37	9647.37	9599.76	9599.76	9599.76
9614.36	9696.00	9490.09	9614.36	9655.42	9655.42	9614.36	9614.36	9614.36
9627.59	9704.77	9506.23	9627.59	9660.57	9660.57	9627.59	9627.59	9627.59
9639.28	9712.98	9519.67	9639.28	9661.03	9661.03	9639.28	9639.28	9639.28
9649.18	9720.60	9532.03	9649.18	9661.03	9661.03	9649.18	9649.18	9649.18

D2. Effect of Parameters on SCT with Dished Head Volume

Table D.3. The tank in Site B parameters data set – I

h (mm)	R=1250mm	R=1225mm	R=1275mm	L=3750mm	L=3700mm	L=3800mm
443.83	2427.05	2401.55	2452.24	2427.05	2397.60	2456.50
582.55	3618.35	3578.80	3657.40	3618.35	3574.91	3661.79
584.63	3637.13	3597.35	3676.41	3637.13	3593.47	3680.80
586.38	3653.01	3613.03	3692.48	3653.01	3609.16	3696.85
696.44	4685.61	4632.49	4738.01	4685.61	4629.75	4741.46
710.72	4824.07	4769.13	4878.28	4824.07	4766.61	4881.53
720.31	4917.67	4861.48	4973.11	4917.67	4859.13	4976.22
723.34	4947.32	4890.73	5003.15	4947.32	4888.43	5006.21
749.29	5203.02	5142.98	5262.25	5203.02	5141.17	5264.87
782.76	5537.03	5472.38	5600.78	5537.03	5471.32	5602.73
815.16	5864.53	5795.27	5932.83	5864.53	5795.05	5934.02
816.73	5880.50	5811.00	5949.02	5880.50	5810.83	5950.16
831.56	6031.84	5960.18	6102.50	6031.84	5960.44	6103.25
833.10	6047.61	5975.71	6118.49	6047.61	5976.02	6119.20
840.58	6124.21	6051.21	6196.18	6124.21	6051.74	6196.68
868.77	6414.81	6337.54	6490.96	6414.81	6338.99	6490.62
880.75	6539.00	6459.88	6616.97	6539.00	6461.75	6616.24
896.18	6699.77	6618.24	6780.11	6699.77	6620.68	6778.86
898.84	6727.49	6645.54	6808.25	6727.49	6648.08	6806.90
900.00	6739.57	6657.44	6820.51	6739.57	6660.02	6819.12
932.58	7081.47	6994.10	7167.56	7081.47	6998.00	7164.95
946.09	7224.04	7134.44	7312.31	7224.04	7138.93	7309.15
967.70	7453.05	7359.83	7544.88	7453.05	7365.32	7540.79
1006.00	7861.58	7761.74	7959.90	7861.58	7769.17	7954.00
1013.92	7946.43	7845.20	8046.12	7946.43	7853.05	8039.82
1051.77	8353.53	8245.45	8459.92	8353.53	8255.48	8451.57
1067.95	8528.28	8417.20	8637.60	8528.28	8428.23	8628.32
1081.62	8676.21	8562.57	8788.06	8676.21	8574.48	8777.95
1082.34	8684.02	8570.24	8796.00	8684.02	8582.19	8785.84
1109.05	8973.82	8854.92	9090.81	8973.82	8868.68	9078.95
1151.31	9433.92	9306.65	9559.12	9433.92	9323.53	9544.32
1186.05	9813.25	9678.84	9945.42	9813.25	9698.52	9927.98
1209.00	10064.20	9924.95	10201.11	10064.20	9946.61	10181.79
1210.08	10076.01	9936.53	10213.14	10076.01	9958.28	10193.74
1221.63	10202.38	10060.42	10341.94	10202.38	10083.21	10321.55
1253.94	10556.01	10406.97	10702.48	10556.01	10432.79	10679.22

1265.24	10679.69	10528.13	10828.63	10679.69	10555.06	10804.31
1266.68	10695.45	10543.57	10844.71	10695.45	10570.65	10820.25
1278.37	10823.38	10668.85	10975.22	10823.38	10697.12	10949.64
1283.04	10874.48	10718.89	11027.36	10874.48	10747.63	11001.33
1304.57	11109.98	10949.42	11267.71	11109.98	10980.44	11239.51
1305.72	11122.55	10961.73	11280.54	11122.55	10992.87	11252.23
1306.54	11131.51	10970.50	11289.69	11131.51	11001.73	11261.30
1308.11	11148.68	10987.30	11307.22	11148.68	11018.70	11278.66
1312.13	11192.63	11030.30	11352.08	11192.63	11062.14	11323.11
1320.46	11283.66	11119.37	11445.03	11283.66	11152.13	11415.18
1322.84	11309.66	11144.81	11471.58	11309.66	11177.84	11441.48
1335.92	11452.49	11284.53	11617.46	11452.49	11319.04	11585.94
1340.44	11501.83	11332.78	11667.85	11501.83	11367.82	11635.84
1347.55	11579.41	11408.64	11747.10	11579.41	11444.51	11714.31
1356.00	11671.55	11498.73	11841.25	11671.55	11535.59	11807.50
1393.00	12074.22	11892.21	12252.88	12074.22	11933.66	12214.77
1414.71	12309.78	12122.24	12493.85	12309.78	12166.53	12453.03
1419.83	12365.25	12176.38	12550.60	12365.25	12221.37	12509.13
1438.91	12571.63	12377.78	12761.84	12571.63	12425.39	12717.87
1443.18	12617.74	12422.76	12809.05	12617.74	12470.97	12764.51
1466.00	12863.68	12662.60	13060.92	12863.68	12714.09	13013.26
1470.49	12911.96	12709.67	13110.39	12911.96	12761.82	13062.10
1519.71	13438.74	13222.79	13650.46	13438.74	13282.57	13594.91
1581.56	14093.01	13858.98	14322.29	14093.01	13929.33	14256.68
1700.94	15324.48	15052.42	15590.63	15324.48	15146.64	15502.32
1776.03	16072.23	15773.87	16363.81	16072.23	15885.76	16258.71
1778.37	16095.14	15795.93	16387.53	16095.14	15908.40	16281.88

Table D.4. The tank in Site B parameters data set – II

M=600mm	M=400mm	M=840mm	H=400mm	H=380mm	H=420mm
2427.05	2427.05	2427.05	2427.05	2416.14	2437.96
3618.35	3618.35	3618.35	3618.35	3600.34	3636.36
3637.13	3637.13	3637.13	3637.13	3619.01	3655.26
3653.01	3653.01	3653.01	3653.01	3634.78	3671.23
4685.61	4685.61	4685.61	4685.61	4660.79	4710.42
4824.07	4824.07	4824.07	4824.07	4798.35	4849.79
4917.67	4917.67	4917.67	4917.67	4891.33	4944.01
4947.32	4947.32	4947.32	4947.32	4920.78	4973.85
5203.02	5203.02	5203.02	5203.02	5174.79	5231.25
5537.03	5537.03	5537.03	5537.03	5506.56	5567.49

5864.53	5864.53	5864.53	5864.53	5831.86	5897.21
5880.50	5880.50	5880.50	5880.50	5847.71	5913.28
6031.84	6031.84	6031.84	6031.84	5998.03	6065.66
6047.61	6047.61	6047.61	6047.61	6013.69	6081.53
6124.21	6124.21	6124.21	6124.21	6089.77	6158.65
6414.81	6414.81	6414.81	6414.81	6378.37	6451.24
6539.00	6539.00	6539.00	6539.00	6501.70	6576.29
6699.77	6699.77	6699.77	6699.77	6661.37	6738.17
6727.49	6727.49	6727.49	6727.49	6688.89	6766.08
6739.57	6739.57	6739.57	6739.57	6700.89	6778.25
7081.47	7081.47	7081.47	7081.47	7040.42	7122.53
7224.04	7224.04	7224.04	7224.04	7181.99	7266.09
7453.05	7453.05	7453.05	7453.05	7409.40	7496.71
7861.58	7861.58	7861.58	7861.58	7815.05	7908.11
7946.43	7946.43	7946.43	7946.43	7899.31	7993.56
8353.53	8353.53	8353.53	8353.53	8303.52	8403.54
8528.28	8528.28	8528.28	8528.28	8477.02	8579.53
8676.21	8676.21	8676.21	8676.21	8623.91	8728.52
8684.02	8684.02	8684.02	8684.02	8631.66	8736.38
8973.82	8973.82	8973.82	8973.82	8919.39	9028.24
9433.92	9433.92	9433.92	9433.92	9376.21	9491.64
9813.25	9813.25	9813.25	9813.25	9752.82	9873.68
10064.20	10064.20	10064.20	10064.20	10001.97	10126.43
10076.01	10076.01	10076.01	10076.01	10013.69	10138.32
10202.38	10202.38	10202.38	10202.38	10139.16	10265.60
10556.01	10556.01	10556.01	10556.01	10490.25	10621.76
10679.69	10679.69	10679.69	10679.69	10613.04	10746.33
10695.45	10695.45	10695.45	10695.45	10628.69	10762.21
10823.38	10823.38	10823.38	10823.38	10755.70	10891.06
10874.48	10874.48	10874.48	10874.48	10806.44	10942.52
11109.98	11109.98	11109.98	11109.98	11040.24	11179.71
11122.55	11122.55	11122.55	11122.55	11052.72	11192.37
11131.51	11131.51	11131.51	11131.51	11061.63	11201.40
11148.68	11148.68	11148.68	11148.68	11078.67	11218.69
11192.63	11192.63	11192.63	11192.63	11122.30	11262.95
11283.66	11283.66	11283.66	11283.66	11212.68	11354.63
11309.66	11309.66	11309.66	11309.66	11238.50	11380.82
11452.49	11452.49	11452.49	11452.49	11380.31	11524.68
11501.83	11501.83	11501.83	11501.83	11429.29	11574.37
11579.41	11579.41	11579.41	11579.41	11506.31	11652.50
11671.55	11671.55	11671.55	11671.55	11597.79	11745.30
12074.22	12074.22	12074.22	12074.22	11997.59	12150.85

12309.78	12309.78	12309.78	12309.78	12231.47	12388.09
12365.25	12365.25	12365.25	12365.25	12286.55	12443.96
12571.63	12571.63	12571.63	12571.63	12491.46	12651.80
12617.74	12617.74	12617.74	12617.74	12537.24	12698.24
12863.68	12863.68	12863.68	12863.68	12781.43	12945.92
12911.96	12911.96	12911.96	12911.96	12829.37	12994.55
13438.74	13438.74	13438.74	13438.74	13352.44	13525.05
14093.01	14093.01	14093.01	14093.01	14002.13	14183.89
15324.48	15324.48	15324.48	15324.48	15225.15	15423.81
16072.23	16072.23	16072.23	16072.23	15967.91	16176.56
16095.14	16095.14	16095.14	16095.14	15990.67	16199.62

Table D.5. The tank in Site B parameters data set – III

alpha=0°	alpha=-5°	alpha=5°	beta=0°	beta=-10°	beta=10°
2427.05	6418.24	1804.76	2427.05	2999.74	2999.74
3618.35	7877.55	2841.92	3618.35	4233.34	4233.34
3637.13	7899.73	2858.67	3637.13	4252.61	4252.61
3653.01	7918.45	2872.82	3653.01	4268.89	4268.89
4685.61	9106.11	3806.41	4685.61	5321.81	5321.81
4824.07	9261.27	3933.19	4824.07	5462.18	5462.18
4917.67	9365.66	4019.07	4917.67	5556.98	5556.98
4947.32	9398.64	4046.31	4947.32	5587.00	5587.00
5203.02	9681.52	4281.77	5203.02	5845.54	5845.54
5537.03	10046.91	4590.78	5537.03	6182.50	6182.50
5864.53	10400.90	4895.26	5864.53	6512.13	6512.13
5880.50	10418.04	4910.13	5880.50	6528.18	6528.18
6031.84	10580.17	5051.32	6031.84	6680.25	6680.25
6047.61	10597.00	5066.05	6047.61	6696.08	6696.08
6124.21	10678.69	5137.63	6124.21	6772.98	6772.98
6414.81	10986.69	5409.80	6414.81	7064.39	7064.39
6539.00	11117.41	5526.40	6539.00	7188.77	7188.77
6699.77	11285.85	5677.60	6699.77	7349.66	7349.66
6727.49	11314.81	5703.69	6727.49	7377.39	7377.39
6739.57	11327.42	5715.07	6739.57	7389.47	7389.47
7081.47	11682.33	6037.64	7081.47	7731.08	7731.08
7224.04	11829.19	6172.48	7224.04	7873.34	7873.34
7453.05	12063.76	6389.50	7453.05	8101.65	8101.65
7861.58	12478.16	6777.83	7861.58	8508.28	8508.28
7946.43	12563.59	6858.67	7946.43	8592.64	8592.64
8353.53	12970.47	7247.39	8353.53	8996.92	8996.92

8528.28	13143.62	7414.67	8528.28	9170.23	9170.23
8676.21	13289.51	7556.48	8676.21	9316.85	9316.85
8684.02	13297.19	7563.97	8684.02	9324.59	9324.59
8973.82	13581.07	7842.30	8973.82	9611.53	9611.53
9433.92	14026.84	8285.55	9433.92	10066.42	10066.42
9813.25	14389.81	8652.19	9813.25	10440.81	10440.81
10064.20	14627.70	8895.34	10064.20	10688.20	10688.20
10076.01	14638.85	8906.79	10076.01	10699.83	10699.83
10202.38	14757.92	9029.43	10202.38	10824.31	10824.31
10556.01	15088.71	9373.22	10556.01	11172.33	11172.33
10679.69	15203.56	9493.67	10679.69	11293.95	11293.95
10695.45	15218.17	9509.03	10695.45	11309.44	11309.44
10823.38	15336.45	9633.76	10823.38	11435.17	11435.17
10874.48	15383.56	9683.62	10874.48	11485.37	11485.37
11109.98	15599.71	9913.62	11109.98	11716.61	11716.61
11122.55	15611.20	9925.91	11122.55	11728.95	11728.95
11131.51	15619.39	9934.68	11131.51	11737.75	11737.75
11148.68	15635.08	9951.46	11148.68	11754.60	11754.60
11192.63	15675.18	9994.44	11192.63	11797.72	11797.72
11283.66	15758.08	10083.51	11283.66	11887.02	11887.02
11309.66	15781.72	10108.97	11309.66	11912.53	11912.53
11452.49	15911.20	10248.88	11452.49	12052.58	12052.58
11501.83	15955.78	10297.24	11501.83	12100.94	12100.94
11579.41	16025.73	10373.32	11579.41	12176.96	12176.96
11671.55	16108.59	10463.74	11671.55	12267.23	12267.23
12074.22	16467.69	10859.63	12074.22	12661.35	12661.35
12309.78	16675.46	11091.80	12309.78	12891.65	12891.65
12365.25	16724.13	11146.53	12365.25	12945.85	12945.85
12571.63	16904.37	11350.36	12571.63	13147.41	13147.41
12617.74	16944.46	11395.94	12617.74	13192.42	13192.42
12863.68	17157.09	11639.36	12863.68	13432.38	13432.38
12911.96	17198.60	11687.21	12911.96	13479.46	13479.46
13438.74	17646.41	12210.42	13438.74	13992.58	13992.58
14093.01	18188.87	12863.46	14093.01	14628.43	14628.43
15324.48	19163.14	14103.29	15324.48	15820.50	15820.50
16072.23	19719.11	14863.93	16072.23	16540.93	16540.93
16095.14	19735.64	14887.34	16095.14	16562.95	16562.95

APPENDIX E: VARIANCE MINIMIZATION/REDUCTION

E.1. A Sample of Non-problematic Tank

Table E.1. The tank in Site C level to volume data of model and chart

h (mm)	Model Volume	Chart Volume	h (mm)	Model Volume	Chart Volume
0	0	0	320	1492.51	1524
10	8.02	9	330	1562.67	1595
20	22.81	24	340	1633.83	1667
30	42.05	45	350	1705.97	1740
40	64.93	69	360	1779.07	1813
50	90.96	96	370	1853.11	1889
60	119.80	126	380	1928.08	1965
70	151.22	158	390	2003.94	2042
80	185.03	193	400	2080.69	2120
90	221.07	230	410	2158.30	2199
100	259.21	269	420	2236.76	2278
110	299.34	310	430	2316.06	2358
120	341.38	353	440	2396.17	2439
130	385.22	398	450	2477.09	2521
140	430.81	445	460	2558.79	2603
150	478.06	494	470	2641.26	2686
160	526.93	544	480	2724.48	2770
170	577.36	595	490	2808.45	2856
180	629.29	648	500	2893.14	2943
190	682.67	703	510	2978.55	3030
200	737.47	758	520	3064.66	3118
210	793.64	815	530	3151.45	3207
220	851.15	873	540	3238.92	3296
230	909.95	933	550	3327.04	3386
240	970.02	993	560	3415.82	3476
250	1031.32	1056	570	3505.23	3567
260	1093.82	1120	580	3595.26	3659
270	1157.49	1185	590	3685.91	3751
280	1222.31	1251	600	3777.15	3843
290	1288.24	1318	610	3868.98	3937
300	1355.27	1385	620	3961.39	4031
310	1423.37	1454	630	4054.36	4125

h (mm)	Model Volume	Chart Volume	h (mm)	Model Volume	Chart Volume
640	4147.88	4220	1050	8334.43	8407
650	4241.94	4315	1060	8442.36	8514
660	4336.54	4411	1070	8550.44	8621
670	4431.66	4508	1080	8658.67	8728
680	4527.28	4604	1090	8767.03	8834
690	4623.41	4702	1100	8875.53	8941
700	4720.02	4799	1110	8984.14	9048
710	4817.11	4897	1120	9092.86	9154
720	4914.67	4996	1130	9201.70	9261
730	5012.69	5094	1140	9310.62	9368
740	5111.16	5193	1150	9419.64	9475
750	5210.06	5293	1160	9528.73	9582
760	5309.39	5393	1170	9637.90	9689
770	5409.14	5493	1180	9747.13	9796
780	5509.29	5594	1190	9856.42	9903
790	5609.85	5695	1200	9965.76	10010
800	5710.79	5796	1210	10075.14	10117
810	5812.12	5897	1220	10184.54	10225
820	5913.81	5999	1230	10293.98	10333
830	6015.87	6101	1240	10403.43	10440
840	6118.28	6204	1250	10512.88	10548
850	6221.03	6307	1260	10622.34	10655
860	6324.12	6410	1270	10731.79	10763
870	6427.53	6513	1280	10841.22	10870
880	6531.25	6616	1290	10950.63	10977
890	6635.28	6720	1300	11060.00	11085
900	6739.61	6824	1310	11169.34	11192
910	6844.23	6928	1320	11278.63	11299
920	6949.13	7032	1330	11387.86	11405
930	7054.31	7137	1340	11497.03	11512
940	7159.74	7242	1350	11606.13	11619
950	7265.43	7347	1360	11715.14	11725
960	7371.36	7452	1370	11824.07	11831
970	7477.54	7558	1380	11932.90	11937
980	7583.94	7663	1390	12041.62	12043
990	7690.56	7769	1400	12150.24	12149
1000	7797.39	7875	1410	12258.73	12255
1010	7904.42	7981	1420	12367.09	12361
1020	8011.66	8088	1430	12475.32	12466
1030	8119.07	8194	1440	12583.40	12571
1040	8226.67	8301	1450	12691.33	12676

h (mm)	Model Volume	Chart Volume	h (mm)	Model Volume	Chart Volume
1460	12799.09	12780	1870	16971.41	16738
1470	12906.69	12884	1880	17064.38	16825
1480	13014.11	12988	1890	17156.78	16910
1490	13121.34	13092	1900	17248.61	16996
1500	13228.37	13196	1910	17339.86	17080
1510	13335.21	13299	1920	17430.50	17163
1520	13441.83	13402	1930	17520.53	17246
1530	13548.23	13505	1940	17609.94	17327
1540	13654.40	13608	1950	17698.72	17408
1550	13760.33	13710	1960	17786.85	17488
1560	13866.02	13812	1970	17874.31	17568
1570	13971.46	13912	1980	17961.11	17647
1580	14076.63	14013	1990	18047.21	17725
1590	14181.53	14113	2000	18132.62	17802
1600	14286.15	14213	2010	18217.32	17878
1610	14390.48	14313	2020	18301.28	17954
1620	14494.51	14412	2030	18384.51	18029
1630	14598.24	14511	2040	18466.98	18102
1640	14701.65	14609	2050	18548.68	18174
1650	14804.73	14708	2060	18629.59	18245
1660	14907.48	14805	2070	18709.70	18315
1670	15009.89	14903	2080	18789.00	18385
1680	15111.95	14999	2090	18867.46	18453
1690	15213.64	15095	2100	18945.08	18520
1700	15314.97	15190	2110	19021.82	18587
1710	15415.91	15284	2120	19097.69	18652
1720	15516.47	15379	2130	19172.65	18716
1730	15616.63	15473	2140	19246.69	18780
1740	15716.38	15566	2150	19319.79	18842
1750	15815.71	15659	2160	19391.93	18902
1760	15914.61	15752	2170	19463.10	18961
1770	16013.07	15844	2180	19533.26	19019
1780	16111.09	15935	2190	19602.40	19075
1790	16208.65	16026	2200	19670.49	19130
1800	16305.74	16117	2210	19737.52	19184
1810	16402.35	16207	2220	19803.46	19237
1820	16498.48	16297	2230	19868.27	19288
1830	16594.11	16387	2240	19931.94	19337
1840	16689.22	16475	2250	19994.45	19385
1850	16783.82	16564	2260	20055.74	19432
1860	16877.88	16651	2270	20115.81	19477

h (mm)	Model Volume	Chart Volume
2280	20174.62	19519
2290	20232.12	19560
2300	20288.29	19599
2310	20343.09	19635
2320	20396.48	19670
2330	20448.41	19702
2340	20498.83	19732
2350	20547.70	19759
2360	20594.96	19783
2370	20640.54	19803
2380	20684.39	19818
2390	20726.42	19827

Table E.2. Variance determination data for the tank in Site C

Day	Initial Volume (L)	Invoiced Delivery (L)	Correction Volume (L)	Sales (L)	Final Volume (L)	Variance (L)
1	4321	0	0	0	3952	0
2	3952	0	0	352	3598	-2
3	3598	0	0	383	3208	-6
4	3208	0	0	419	2792	3
5	2792	0	0	645	2151	4
6	2151	5711	0	643	7322	104
7	7322	0	0	800	6509	-13
8	6510	0	0	1194	5305	-10
9	5305	0	0	1040	4257	-9
10	4257	0	0	747	3502	-8
11	3502	0	0	790	2705	-8
12	2705	2170	0	469	4448	42
13	4448	0	0	502	3938	-8
14	3938	0	0	478	3456	-4
15	3456	0	0	501	2951	-4
16	2951	0	0	585	2368	2
17	2368	0	0	514	1854	0
18	1854	1966	0	514	3328	21
19	3328	0	0	675	2653	0
20	2653	3150	0	530	5336	64
21	5336	0	0	372	4960	-4
22	4960	0	0	330	4624	-5
23	4624	0	0	658	3961	-6
24	3961	0	0	540	3417	-3
25	3417	0	0	596	2817	-4
26	2817	0	0	640	2175	-2

27	2175	0	0	604	1573	2
28	1573	3048	0	716	4057	152
29	4057	0	0	482	3568	-7
30	3568	0	0	628	2936	-4
31	2936	0	0	743	2197	4
32	2197	0	0	560	1592	-45
33	1592	5750	0	500	6894	52
34	6894	0	0	523	6362	-10
35	6362	0	0	522	5837	-3
36	5837	0	0	477	5351	-8
37	5351	0	0	475	4872	-3
38	4872	0	0	356	4512	-4
39	4512	0	0	333	4177	-3
40	4177	0	0	176	3997	-5
41	3997	0	0	344	3650	-2
42	3650	0	0	351	3295	-5
43	3295	2158	0	269	5230	46
44	5230	0	0	186	5043	-1
45	5043	0	0	456	4582	-5
46	4582	0	0	239	4343	0
47	4343	0	0	182	4160	-2
48	4160	0	0	334	3820	-6
49	3820	0	0	373	3446	-1
50	3446	0	0	467	2974	-5
51	2974	2362	0	341	5039	45
52	5039	0	0	518	4515	-6
53	4515	0	0	247	4265	-3
54	4265	0	0	322	3938	-6
55	3938	3046	0	342	6720	78
56	6720	0	0	179	6535	-6
57	6535	0	0	286	6248	-2
58	6248	0	0	357	5887	-4
59	5887	0	0	556	5329	-3
60	5329	0	0	211	5118	0
61	5118	0	0	233	4877	-8
62	4878	0	0	140	4731	-7
63	4731	0	0	235	4498	2
64	4498	0	0	278	4218	-2
65	4218	0	0	336	3879	-4
66	3879	0	0	201	3676	-2
67	3676	0	0	253	3421	-2
68	3421	0	0	232	3183	-6
69	3183	0	0	308	2875	0
70	2875	3060	0	273	5721	59

71	5721	0	0	495	5220	-6
72	5220	0	0	313	4902	-5
73	4902	0	0	440	4461	-1
74	4461	0	0	388	4067	-6
75	4067	0	0	550	3512	-5
76	3512	0	0	743	2765	-5
77	2764	0	0	969	1794	-1
78	1793	3060	0	891	4004	42
79	4004	3359	0	1736	5695	68
80	5695	0	0	1072	4609	-14
81	4609	0	0	621	3979	-8
82	3979	0	0	365	3610	-4
83	3610	0	0	619	2983	-8
84	2983	0	0	354	2627	-2
85	2627	0	0	336	2292	0
86	2292	997	0	414	2856	-20
87	2856	0	0	128	2726	-1
88	2726	2729	0	127	5380	52
89	5381	0	0	294	5092	5
90	5092	0	0	217	4871	-4
91	4871	0	0	242	4629	0
92	4629	0	0	277	4348	-4
93	4348	0	0	198	4142	-8
94	4142	0	0	274	3865	-4

E.2. Data for the tank in Site D

Table E.3. Site D daily real time data

Day	Initial Temp. (°C)	Initial Level (mm)	Initial Volume (L)	Delivery (L)	Cor. (L)	Sales (L)	Final Temp. (°C)	Final Level (mm)	Final Volume (L)	Var (L)
1	24.78	1825.95	23210	0	0	2076	24.79	1664.77	20931	-202
2	24.79	1664.77	20931	0	0	2260	24.81	1507.60	18603	-67
3	24.81	1507.60	18603	0	0	2048	24.82	1369.39	16499	-56
4	24.82	1369.39	16499	0	0	2398	24.79	1210.19	14050	-51
5	24.79	1210.19	14050	0	0	1821	24.75	1089.12	12199	-30
6	24.75	1089.12	12199	0	0	1841	24.70	965.58	10341	-18
7	24.70	965.58	10341	0	0	2105	24.61	821.25	8229	-7
8	24.61	821.25	8229	20521	0	1909	21.64	2153.83	27256	416
9	21.64	2153.83	27256	0	0	2433	22.64	1936.10	24674	-149

10	22.64	1936.10	24674	0	0	1934	23.01	1785.66	22657	-84
11	23.01	1785.66	22657	0	0	2171	23.20	1628.74	20405	-81
12	23.20	1628.74	20405	0	0	1737	23.33	1508.70	18618	-50
13	23.33	1508.70	18618	0	0	1445	23.43	1410.98	17135	-39
14	23.43	1410.98	17135	0	0	2483	23.51	1245.95	14603	-49
15	23.51	1245.95	14603	0	0	2200	23.55	1100.08	12366	-37
16	23.55	1100.08	12366	0	0	2671	23.60	921.05	9678	-16
17	23.60	921.05	9678	0	0	2216	23.60	767.04	7460	-2
18	23.60	767.04	7460	0	0	2150	23.60	609.31	5329	19
19	23.60	609.31	5329	23230	0	1790	21.72	2163.29	27358	589
20	21.72	2163.29	27358	0	0	1313	22.29	2036.62	25927	-118
21	22.29	2036.62	25927	0	0	2274	22.53	1850.21	23539	-114
22	22.53	1850.21	23539	0	0	2311	22.67	1678.81	21135	-93
23	22.67	1678.81	21135	0	0	2234	22.74	1522.93	18830	-71
24	22.74	1522.93	18830	0	0	2632	22.80	1344.72	16117	-82
25	22.80	1344.72	16117	11784	0	2316	20.64	2037.48	25935	351
26	20.64	2037.48	25935	0	0	2041	21.45	1865.63	23747	-147
27	21.45	1865.63	23747	0	0	1694	21.72	1740.42	22017	-35
28	21.72	1740.42	22017	0	0	1898	21.87	1603.55	20038	-81
29	21.87	1603.55	20038	0	0	2029	21.98	1464.84	17952	-57
30	21.98	1464.84	17952	0	0	2409	22.05	1303.70	15488	-55
31	22.05	1303.70	15488	0	0	1988	22.07	1171.55	13460	-40
32	22.07	1171.55	13460	0	0	3101	22.11	964.64	10326	-33
33	22.11	964.64	10326	0	0	1667	22.11	850.15	8649	-10
34	22.11	850.15	8649	0	0	1206	22.07	765.04	7434	-9
35	22.07	765.04	7434	0	0	2284	22.08	596.79	5167	17
36	22.08	596.79	5167	22817	0	2253	16.66	2049.57	26079	348
37	16.66	2049.57	26079	0	0	1778	18.53	1901.85	24239	-62
38	18.53	1901.85	24239	0	0	2437	19.26	1718.02	21703	-99
39	19.26	1718.02	21703	0	0	2401	19.69	1549.01	19224	-78
40	19.69	1549.01	19224	0	0	1952	20.00	1416.47	17218	-54
41	20.00	1416.47	17218	0	0	1765	20.22	1298.85	15413	-41
42	20.22	1298.85	15413	0	0	2056	20.37	1162.41	13319	-37
43	20.37	1162.41	13319	0	0	2464	20.51	998.04	10821	-34
44	20.51	998.04	10821	0	0	2554	20.60	823.24	8259	-8
45	20.60	823.24	8259	0	0	2590	20.71	636.04	5681	12
46	20.71	636.04	5681	22376	0	2003	13.93	2078.20	26419	365
47	13.93	2078.20	26419	0	0	1968	16.35	1912.44	24372	-79
48	16.35	1912.44	24372	0	0	1333	17.28	1809.30	22986	-52
49	17.28	1809.30	22986	0	0	2171	17.84	1650.99	20730	-85
50	17.84	1650.99	20730	0	0	2285	18.26	1492.94	18380	-65
51	18.26	1492.94	18380	0	0	2501	18.58	1325.03	15818	-62

52	18.58	1325.03	15818	0	0	2389	18.81	1166.37	13380	-49
53	18.81	1166.37	13380	0	0	1998	19.01	1033.32	11355	-27
54	19.01	1033.32	11355	15894	0	1659	15.11	2036.77	25927	337
55	15.11	2036.77	25927	0	0	1355	16.49	1923.54	24515	-56
56	16.49	1923.54	24515	0	0	2520	17.13	1731.30	21889	-107
57	17.13	1731.30	21889	0	0	2201	17.55	1575.26	19614	-74
58	17.55	1575.26	19614	0	0	2429	17.89	1410.03	17120	-65
59	17.89	1410.03	17120	0	0	1967	18.16	1278.95	15110	-43
60	18.16	1278.95	15110	0	0	2735	18.40	1097.68	12328	-47
61	18.40	1097.68	12328	0	0	2208	18.61	949.35	10098	-21
62	18.61	949.35	10098	0	0	1465	18.76	848.76	8626	-8
63	18.76	848.76	8626	18375	0	1956	12.78	1984.80	25295	250
64	12.78	1984.80	25295	0	0	1795	15.04	1843.43	23448	-52
65	15.04	1843.43	23448	0	0	2338	15.94	1671.71	21033	-77
66	15.94	1671.71	21033	0	0	2166	16.56	1521.19	18808	-60
67	16.56	1521.19	18808	0	0	2422	17.00	1350.64	16211	-175
68	17.00	1350.64	16211	0	0	1827	17.35	1226.74	14304	-80
69	17.35	1226.74	14304	0	0	1198	17.61	1149.75	13126	21
70	17.61	1149.75	13126	0	0	2311	17.86	995.26	10780	-36
71	17.86	995.26	10780	0	0	2383	18.06	832.54	8391	-5
72	18.06	832.54	8391	0	0	2265	18.27	669.83	6124	-3
73	18.27	669.83	6124	20909	0	2001	13.46	1985.77	25310	278
74	13.46	1985.77	25310	0	0	3208	15.27	1737.58	21980	-123
75	15.27	1737.58	21980	0	0	1859	16.03	1605.07	20061	-60
76	16.03	1605.07	20061	0	0	1303	16.53	1515.19	18717	-41
77	16.53	1515.19	18717	0	0	1944	16.91	1383.91	16718	-55
78	16.91	1383.91	16718	0	0	2740	17.21	1201.97	13925	-54
79	17.21	1201.97	13925	0	0	1845	17.47	1079.47	12055	-25
80	17.47	1079.47	12055	0	0	1990	17.70	946.00	10049	-16
81	17.70	946.00	10049	18556	0	2642	14.82	2070.89	26332	369
82	14.82	2070.89	26332	0	0	1636	15.95	1930.52	24603	-94
83	15.95	1930.52	24603	0	0	1723	16.45	1796.52	22812	-68
84	16.45	1796.52	22812	0	0	2496	16.79	1615.21	20208	-108
85	16.79	1615.21	20208	0	0	2380	17.08	1451.61	17752	-76
86	17.08	1451.61	17752	0	0	2408	17.33	1291.45	15299	-45
87	17.33	1291.45	15299	12853	0	2634	14.64	2029.11	25836	319
88	14.64	2029.11	25836	0	0	2420	15.88	1832.64	23301	-116
89	15.88	1832.64	23301	0	0	2258	16.37	1666.24	20954	-88
90	16.37	1666.24	20954	0	0	1567	16.71	1556.28	19330	-57
91	16.71	1556.28	19330	0	0	2128	16.98	1411.31	17139	-64
92	16.98	1411.31	17139	0	0	2339	17.21	1255.08	14743	-57
93	17.21	1255.08	14743	0	0	2082	17.37	1116.83	12623	-37

94	17.37	1116.83	12623	0	0	2819	17.55	926.72	9765	-39
95	17.55	926.72	9765	0	0	2953	17.67	720.55	6809	-3
96	17.67	720.55	6809	20131	0	2206	13.03	1962.57	25011	277
97	13.03	1962.57	25011	0	0	1189	14.63	1868.76	23793	-30
98	14.63	1868.76	23793	0	0	2736	15.33	1666.18	20954	-103
99	15.33	1666.18	20954	0	0	3105	15.83	1452.51	17767	-82
100	15.83	1452.51	17767	0	0	2241	16.21	1303.06	15481	-45
101	16.21	1303.06	15481	0	0	1784	16.49	1184.88	13664	-33
102	16.49	1184.88	13664	0	0	2335	16.77	1029.82	11302	-26
103	16.77	1029.82	11302	16073	0	2211	15.46	2002.05	25515	350
104	15.46	2002.05	25515	0	0	1532	16.05	1876.53	23895	-88
105	16.05	1876.53	23895	0	0	2279	16.38	1705.34	21522	-94
106	16.38	1705.34	21522	0	0	2249	16.63	1547.23	19194	-78
107	16.63	1547.23	19194	0	0	2517	16.86	1377.31	16620	-57
108	16.86	1377.31	16620	0	0	2607	17.05	1203.86	13955	-57
109	17.05	1203.86	13955	0	0	2513	17.23	1036.64	11404	-38
110	17.23	1036.64	11404	17070	0	1994	14.76	2121.23	26908	427
111	14.76	2121.23	26908	0	0	1795	15.68	1960.77	24989	-124
112	15.68	1960.77	24989	0	0	2239	16.10	1784.75	22646	-103
113	16.10	1784.75	22646	0	0	2808	16.39	1583.63	19739	-99
114	16.39	1583.63	19739	0	0	1898	16.63	1453.68	17786	-55
115	16.63	1453.68	17786	0	0	2799	16.85	1266.88	14924	-63
116	16.85	1266.88	14924	13035	0	3038	15.49	1976.04	25185	264
117	15.49	1976.04	25185	0	0	2030	16.12	1814.79	23062	-94
118	16.12	1814.79	23062	0	0	1208	16.41	1724.77	21798	-56
119	16.41	1724.77	21798	0	0	3103	16.66	1507.75	18603	-91
120	16.66	1507.75	18603	0	0	2803	16.87	1319.96	15738	-63
121	16.87	1319.96	15738	0	0	1911	17.05	1193.14	13789	-38
122	17.05	1193.14	13789	0	0	2339	17.23	1037.99	11427	-23
123	17.23	1037.99	11427	15828	0	2314	15.50	1984.31	25291	351
124	15.50	1984.31	25291	0	0	2013	16.28	1823.78	23183	-95
125	16.28	1823.78	23183	0	0	1498	16.62	1712.67	21628	-57
126	16.62	1712.67	21628	0	0	3143	16.69	1493.67	18391	-93

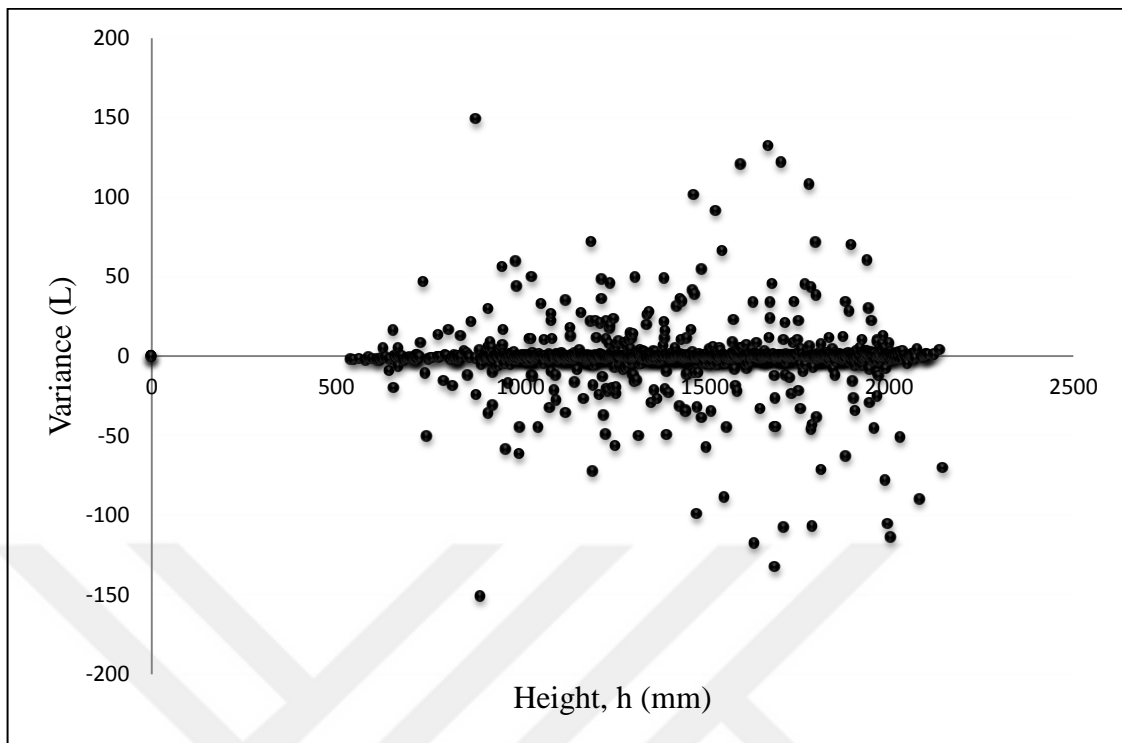


Figure E.1. Variance vs. fuel level with hourly real time data for Site D

Table E.4. Site D percentage reduction in variance

Day	Current Var (L)	Adjusted Var (L)	Absolute Current Var	Absolute Adjusted Var	Cumulative Abs. Current Var	Cumulative Abs. Adjusted Var
1	-202	-116.92	202	116.92	202	116.92
2	-67	0.88	67	0.88	269	117.80
3	-56	-1.90	56	1.90	325	119.70
4	-51	0.45	51	0.45	376	120.15
5	-30	-4.87	30	4.87	406	125.02
6	-18	-4.33	18	4.33	424	129.35
7	-7	-2.66	7	2.66	431	132.01
8	416	-110.35	416	110.35	847	242.36
9	-149	8.32	149	8.32	996	250.67
10	-84	1.77	84	1.77	1080	252.45
11	-81	2.62	81	2.62	1161	255.07
12	-50	3.06	50	3.06	1211	258.13
13	-39	0.27	39	0.27	1250	258.40
14	-49	4.17	49	4.17	1299	262.57
15	-37	-1.04	37	1.04	1336	263.61
16	-16	3.71	16	3.71	1352	267.32

17	-2	-6.60	2	6.60	1354	273.92
18	19	-12.57	19	12.57	1373	286.50
19	589	88.42	589	88.42	1962	374.91
20	-118	-19.35	118	19.35	2080	394.26
21	-114	6.86	114	6.86	2194	401.12
22	-93	-1.15	93	1.15	2287	402.27
23	-71	2.48	71	2.48	2358	404.75
24	-82	-12.10	82	12.10	2440	416.86
25	351	-3.38	351	3.38	2791	420.24
26	-147	-37.22	147	37.22	2938	457.46
27	-35	34.46	35	34.46	2973	491.92
28	-81	-18.31	81	18.31	3054	510.23
29	-57	8.92	57	8.92	3111	519.15
30	-55	1.76	55	1.76	3166	520.91
31	-40	-6.41	40	6.41	3206	527.32
32	-33	-0.60	33	0.60	3239	527.92
33	-10	-10.26	10	10.26	3249	538.18
34	-9	-10.76	9	10.76	3258	548.95
35	17	-15.63	17	15.63	3275	564.58
36	348	-57.49	348	57.49	3623	622.07
37	-62	23.73	62	23.73	3685	645.80
38	-99	10.93	99	10.93	3784	656.73
39	-78	5.26	78	5.26	3862	661.99
40	-54	0.97	54	0.97	3916	662.95
41	-41	2.23	41	2.23	3957	665.18
42	-37	-3.34	37	3.34	3994	668.52
43	-34	-3.63	34	3.63	4028	672.15
44	-8	-7.15	8	7.15	4036	679.31
45	12	-16.85	12	16.85	4048	696.16
46	365	-73.97	365	73.97	4413	770.13
47	-79	31.91	79	31.91	4492	802.04
48	-52	7.47	52	7.47	4544	809.52
49	-85	3.30	85	3.30	4629	812.82
50	-65	4.69	65	4.69	4694	817.51
51	-62	0.57	62	0.57	4756	818.08
52	-49	-4.57	49	4.57	4805	822.65
53	-27	-2.97	27	2.97	4832	825.63
54	337	-88.02	337	88.02	5169	913.65
55	-56	14.26	56	14.26	5225	927.90
56	-107	6.28	107	6.28	5332	934.18
57	-74	2.80	74	2.80	5406	936.98
58	-65	2.07	65	2.07	5471	939.06

59	-43	0.24	43	0.24	5514	939.30
60	-47	-0.06	47	0.06	5561	939.36
61	-21	-6.17	21	6.17	5582	945.53
62	-8	-6.19	8	6.19	5590	951.72
63	250	-152.33	250	152.33	5840	1104.05
64	-52	38.39	52	38.39	5892	1142.44
65	-77	14.36	77	14.36	5969	1156.81
66	-60	8.42	60	8.42	6029	1165.22
67	-175	-107.84	175	107.84	6204	1273.06
68	-80	-39.55	80	39.55	6284	1312.61
69	21	35.50	21	35.50	6305	1348.11
70	-36	-6.96	36	6.96	6341	1355.07
71	-5	-3.03	5	3.03	6346	1358.11
72	-3	-18.77	3	18.77	6349	1376.88
73	278	-112.06	278	112.06	6627	1488.94
74	-123	28.11	123	28.11	6750	1517.05
75	-60	3.23	60	3.23	6810	1520.28
76	-41	1.64	41	1.64	6851	1521.92
77	-55	0.21	55	0.21	6906	1522.13
78	-54	1.04	54	1.04	6960	1523.17
79	-25	-1.75	25	1.75	6985	1524.92
80	-16	0.12	16	0.12	7001	1525.04
81	369	-90.64	369	90.64	7370	1615.68
82	-94	3.03	94	3.03	7464	1618.71
83	-68	4.16	68	4.16	7532	1622.87
84	-108	-9.91	108	9.91	7640	1632.78
85	-76	-2.43	76	2.43	7716	1635.21
86	-45	11.93	45	11.93	7761	1647.14
87	319	-47.77	319	47.77	8080	1694.92
88	-116	9.45	116	9.45	8196	1704.37
89	-88	-1.82	88	1.82	8284	1706.19
90	-57	-3.09	57	3.09	8341	1709.27
91	-64	-5.37	64	5.37	8405	1714.64
92	-57	-6.93	57	6.93	8462	1721.57
93	-37	-4.68	37	4.68	8499	1726.25
94	-39	-17.09	39	17.09	8538	1743.34
95	-3	-4.41	3	4.41	8541	1747.74
96	277	-103.30	277	103.30	8818	1851.04
97	-30	23.80	30	23.80	8848	1874.84
98	-103	8.21	103	8.21	8951	1883.06
99	-82	14.38	82	14.38	9033	1897.44
100	-45	6.50	45	6.50	9078	1903.93

101	-33	0.50	33	0.50	9111	1904.43
102	-26	2.23	26	2.23	9137	1906.66
103	350	-60.58	350	60.58	9487	1967.24
104	-88	-1.02	88	1.02	9575	1968.25
105	-94	-2.07	94	2.07	9669	1970.32
106	-78	2.48	78	2.48	9747	1972.80
107	-57	7.31	57	7.31	9804	1980.11
108	-57	-4.70	57	4.70	9861	1984.81
109	-38	-4.44	38	4.44	9899	1989.25
110	427	-67.50	427	67.50	10326	2056.75
111	-124	-2.75	124	2.75	10450	2059.50
112	-103	-5.00	103	5.00	10553	2064.49
113	-99	6.52	99	6.52	10652	2071.01
114	-55	-1.16	55	1.16	10707	2072.18
115	-63	1.81	63	1.81	10770	2073.99
116	264	-72.51	264	72.51	11034	2146.49
117	-94	2.39	94	2.39	11128	2148.89
118	-56	-4.54	56	4.54	11184	2153.42
119	-91	12.42	91	12.42	11275	2165.84
120	-63	8.95	63	8.95	11338	2174.79
121	-38	-2.11	38	2.11	11376	2176.90
122	-23	3.67	23	3.67	11399	2180.57
123	351	-42.77	351	42.77	11750	2223.34
124	-95	5.64	95	5.64	11845	2228.98
125	-57	0.60	57	0.60	11902	2229.57
126	-93	12.38	93	12.38	11995	2241.95

E.3. Data for the tank in Site E

Table E.5. Site E daily real time data

Day	Initial Temp. (°C)	Initial Level (mm)	Initial Volume (L)	Delivery (L)	Correction (L)	Sales (L)	Final Temp. (°C)	Final Level (mm)	Final Volume (L)	Var (L)
1	21.71	1614.04	22176	0	0	1297	21.60	1523.26	20788	-91
2	21.60	1523.26	20788	0	0	797	21.54	1472.45	19993	2
3	21.54	1472.45	19993	0	0	972	21.48	1411.30	19023	2
4	21.48	1411.30	19023	0	0	947	21.39	1351.83	18068	-8
5	21.39	1351.83	18068	0	0	1331	21.33	1268.88	16722	-15
6	21.33	1268.88	16722	0	0	468	21.21	1239.63	16245	-9

7	21.21	1239.63	16245	5989	0	1353	20.32	1529.69	20888	7
8	20.32	1529.69	20888	0	0	1077	20.48	1461.55	19822	10
9	20.48	1461.55	19822	0	0	973	20.56	1400.64	18853	4
10	20.56	1400.64	18853	0	0	911	20.60	1343.63	17936	-6
11	20.60	1343.63	17936	8539	0	1472	19.32	1804.09	24902	-100
12	19.32	1804.09	24902	0	0	782	19.64	1750.45	24162	42
13	19.64	1750.45	24162	3598	0	292	19.56	1991.11	27241	-227
14	19.56	1991.11	27241	0	0	1010	19.70	1913.96	26328	97
15	19.70	1913.96	26328	0	0	1304	19.80	1819.49	25110	86
16	19.80	1819.49	25110	0	0	992	19.85	1750.45	24162	45
17	19.85	1750.45	24162	0	0	1251	19.90	1665.96	22948	37
18	19.90	1665.96	22948	0	0	575	19.88	1627.91	22384	11
19	19.88	1627.91	22384	0	0	830	19.86	1573.76	21566	11
20	19.86	1573.76	21566	0	0	504	19.80	1541.19	21066	4
21	19.80	1541.19	21066	0	0	1420	19.76	1450.94	19654	8
22	19.76	1450.94	19654	0	0	870	19.70	1396.22	18782	-2
23	19.70	1396.22	18782	6478	0	973	18.88	1752.21	24187	-101
24	18.88	1752.21	24187	4487	0	1507	18.60	1967.23	26967	-200
25	18.60	1967.23	26967	0	0	1056	18.75	1888.07	26004	93
26	18.75	1888.07	26004	0	0	943	18.81	1820.21	25119	59
27	18.81	1820.21	25119	0	0	331	18.83	1796.90	24805	16
28	18.83	1796.90	24805	0	0	1225	18.85	1712.75	23627	47
29	18.85	1712.75	23627	0	0	903	18.87	1652.25	22746	21
30	18.87	1652.25	22746	4491	0	1084	17.84	1885.46	25971	-181
31	17.84	1885.46	25971	0	0	1526	18.07	1776.90	24530	85
32	18.07	1776.90	24530	0	0	1046	18.14	1702.03	23473	-11
33	18.14	1702.03	23473	0	0	1085	18.19	1629.38	22406	18
34	18.19	1629.38	22406	6001	0	729	17.06	2001.41	27357	-321
35	17.06	2001.41	27357	0	0	1133	17.23	1914.28	26332	108
36	17.23	1914.28	26332	0	0	1276	17.32	1821.74	25140	85
37	17.32	1821.74	25140	0	0	1025	17.35	1750.39	24161	46
38	17.35	1750.39	24161	4512	0	1270	16.46	1984.15	27162	-242
39	16.46	1984.15	27162	0	0	737	16.65	1927.94	26499	74
40	16.65	1927.94	26499	0	0	912	16.74	1860.70	25653	67
41	16.74	1860.70	25653	0	0	349	16.76	1835.66	25325	21
42	16.76	1835.66	25325	0	0	879	16.77	1773.75	24487	41
43	16.77	1773.75	24487	0	0	985	16.77	1706.65	23540	37
44	16.77	1706.65	23540	0	0	767	16.79	1655.21	22789	17
45	16.79	1655.21	22789	0	0	1164	16.77	1578.98	21645	20
46	16.77	1578.98	21645	6031	0	990	15.30	1924.13	26453	-234
47	15.30	1924.13	26453	0	0	1011	15.59	1850.27	25517	76
48	15.59	1850.27	25517	0	0	363	15.70	1824.45	25176	22

49	15.70	1824.45	25176	0	0	1118	15.77	1746.46	24106	48
50	15.77	1746.46	24106	0	0	718	15.77	1697.70	23410	23
51	15.77	1697.70	23410	0	0	1106	15.82	1623.59	22319	15
52	15.82	1623.59	22319	0	0	1199	15.81	1543.54	21102	-18
53	15.81	1543.54	21102	0	0	1016	15.78	1478.62	20090	4
54	15.78	1478.62	20090	0	0	945	15.75	1418.69	19141	-4
55	15.75	1418.69	19141	0	0	300	15.68	1399.94	18842	1
56	15.68	1399.94	18842	0	0	1270	15.66	1320.27	17558	-14
57	15.66	1320.27	17558	4013	0	1230	14.47	1492.48	20308	-33
58	14.47	1492.48	20308	3017	0	1346	14.00	1598.28	21938	-41
59	14.00	1598.28	21938	0	0	783	14.32	1548.02	21171	16
60	14.32	1548.02	21171	0	0	1902	14.51	1427.54	19282	13
61	14.51	1427.54	19282	0	0	803	14.63	1377.20	18477	-3
62	14.63	1377.20	18477	0	0	159	14.62	1367.16	18315	-2
63	14.62	1367.16	18315	0	0	931	14.63	1309.00	17375	-9
64	14.63	1309.00	17375	0	0	1137	14.63	1238.05	16219	-19
65	14.63	1238.05	16219	0	0	636	14.62	1197.94	15563	-20
66	14.62	1197.94	15563	10068	0	928	12.47	1782.40	24606	-96
67	12.47	1782.40	24606	0	0	1110	12.96	1707.36	23550	53
68	12.96	1707.36	23550	0	0	196	13.18	1694.36	23362	9
69	13.18	1694.36	23362	0	0	236	13.30	1678.58	23133	7
70	13.30	1678.58	23133	0	0	469	13.42	1647.35	22673	10
71	13.42	1647.35	22673	0	0	449	13.45	1617.91	22234	9
72	13.45	1617.91	22234	0	0	683	13.47	1573.32	21559	8
73	13.47	1573.32	21559	0	0	1113	13.49	1501.87	20455	9
74	13.49	1501.87	20455	6562	0	940	11.91	1876.39	25855	-222
75	11.91	1876.39	25855	0	0	1168	12.20	1793.59	24760	72
76	12.20	1793.59	24760	0	0	328	12.34	1770.81	24446	15
77	12.34	1770.81	24446	0	0	925	12.44	1707.95	23558	37
78	12.44	1707.95	23558	0	0	925	12.55	1646.32	22658	24
79	12.55	1646.32	22658	0	0	836	12.61	1590.67	21823	1
80	12.61	1590.67	21823	0	0	1066	12.67	1522.02	20769	12
81	12.67	1522.02	20769	0	0	831	12.72	1469.18	19942	3
82	12.72	1469.18	19942	0	0	722	12.75	1423.67	19221	1
83	12.75	1423.67	19221	0	0	303	12.76	1404.70	18918	0
84	12.76	1404.70	18918	0	0	918	12.79	1347.12	17992	-8
85	12.79	1347.12	17992	0	0	960	12.81	1287.29	17022	-10
86	12.81	1287.29	17022	0	0	1209	12.85	1212.10	15794	-18
87	12.85	1212.10	15794	0	0	814	12.86	1161.21	14961	-19
88	12.86	1161.21	14961	13097	0	1207	9.55	1934.38	26577	-274
89	9.55	1934.38	26577	0	0	767	10.32	1878.48	25882	72
90	10.32	1878.48	25882	0	0	228	10.71	1862.50	25677	23

91	10.71	1862.50	25677	0	0	963	10.98	1794.31	24769	56
92	10.98	1794.31	24769	4018	0	1159	10.54	2003.22	27377	-251
93	10.54	2003.22	27377	0	0	845	10.81	1938.30	26625	92
94	10.81	1938.30	26625	0	0	1161	10.99	1852.79	25550	87
95	10.99	1852.79	25550	0	0	937	11.13	1786.70	24665	52
96	11.13	1786.70	24665	0	0	778	11.23	1733.48	23923	35
97	11.23	1733.48	23923	0	0	247	11.30	1716.78	23685	9
98	11.30	1716.78	23685	0	0	934	11.44	1654.52	22779	28
99	11.44	1654.52	22779	0	0	1035	11.55	1587.07	21768	24
100	11.55	1587.07	21768	0	0	1083	11.66	1517.68	20701	16
101	11.66	1517.68	20701	0	0	1051	11.78	1451.19	19658	8
102	11.78	1451.19	19658	6012	0	988	11.60	1777.81	24543	-139
103	11.60	1777.81	24543	0	0	869	11.72	1718.58	23711	37
104	11.72	1718.58	23711	0	0	350	11.80	1695.10	23373	12
105	11.80	1695.10	23373	0	0	859	11.91	1638.15	22537	23
106	11.91	1638.15	22537	0	0	1090	11.98	1567.19	21465	18
107	11.98	1567.19	21465	6403	0	782	10.74	1952.45	26794	-293
108	10.74	1952.45	26794	0	0	832	11.06	1890.68	26037	75
109	11.06	1890.68	26037	0	0	1272	11.24	1799.79	24844	79
110	11.24	1799.79	24844	0	0	1219	11.38	1716.24	23677	52
111	11.38	1716.24	23677	0	0	409	11.45	1688.83	23282	14
112	11.45	1688.83	23282	0	0	1183	11.57	1610.90	22129	30
113	11.57	1610.90	22129	0	0	992	11.64	1546.83	21153	16
114	11.64	1546.83	21153	0	0	1205	11.72	1470.13	19957	10
115	11.72	1470.13	19957	6477	0	748	11.84	1850.33	25518	-167
116	11.84	1850.33	25518	0	0	924	11.83	1785.23	24645	51
117	11.83	1785.23	24645	0	0	1393	11.89	1690.69	23309	57
118	11.89	1690.69	23309	0	0	468	11.97	1659.57	22854	13
119	11.97	1659.57	22854	7033	0	1336	11.41	2072.38	28107	-444
120	11.41	2072.38	28107	0	0	1111	11.66	1983.06	27150	154
121	11.66	1983.06	27150	0	0	1189	11.82	1893.55	26073	112
122	11.82	1893.55	26073	0	0	742	11.93	1839.91	25381	50
123	11.93	1839.91	25381	0	0	1217	12.05	1755.22	24229	65
124	12.05	1755.22	24229	0	0	1585	12.20	1648.44	22689	46
125	12.20	1648.44	22689	0	0	282	12.28	1630.48	22422	15
126	12.28	1630.48	22422	5022	0	1284	12.25	1886.85	25989	-172

Table E.6. Site E percentage reduction in variance

Day	Current Var (L)	Adjusted Var (L)	Absolute Current Var	Cumulative Abs. Current Var	Absolute Adjusted Var	Cumulative Abs. Adjusted Var
1	-19	-3.89	19	19	3.89	3.89
2	-20	-9.44	20	39	9.44	13.33
3	-18	-1.37	18	57	1.37	14.70
4	-19	-5.00	19	76	5.00	19.71
5	-9	-2.93	9	85	2.93	22.63
6	-15	-2.73	15	100	2.73	25.37
7	-10	-1.80	10	110	1.80	27.17
8	-9	-2.91	9	119	2.91	30.08
9	-14	-7.23	14	133	7.23	37.32
10	-6	-2.14	6	139	2.14	39.46
11	-8	-3.96	8	147	3.96	43.42
12	-8	-4.72	8	155	4.72	48.13
13	-2	-1.83	2	157	1.83	49.96
14	-3	-0.92	3	160	0.92	50.89
15	-2	-1.67	2	162	1.67	52.56
16	1	0.78	1	163	0.78	53.34
17	4	3.69	4	167	3.69	57.03
18	0	0.44	0	167	0.44	57.47
19	2	0.30	2	169	0.30	57.77
20	-4	-6.39	4	173	6.39	64.16
21	1	-0.74	1	174	0.74	64.90
22	13	2.12	13	187	2.12	67.02
23	8	-1.34	8	195	1.34	68.36
24	8	1.54	8	203	1.54	69.90
25	10	3.66	10	213	3.66	73.56
26	3	-1.39	3	216	1.39	74.95
27	10	-0.19	10	226	0.19	75.14
28	2	-3.08	2	228	3.08	78.22
29	4	-3.63	4	232	3.63	81.85
30	-33	-36.40	33	265	36.40	118.25
31	9	-2.98	9	274	2.98	121.23
32	16	2.79	16	290	2.79	124.02
33	12	-1.70	12	302	1.70	125.72
34	-91	-110.50	91	393	110.50	236.22
35	7	-7.15	7	400	7.15	243.37
36	4	-2.48	4	404	2.48	245.85

37	-18	-37.56	18	422	37.56	283.41
38	16	1.01	16	438	1.01	284.42
39	16	4.44	16	454	4.44	288.87
40	18	-0.58	18	472	0.58	289.45
41	8	-3.70	8	480	3.70	293.15
42	11	-2.71	11	491	2.71	295.87
43	20	-2.75	20	511	2.75	298.61
44	24	3.71	24	535	3.71	302.32
45	1	-15.49	1	536	15.49	317.81
46	-41	-21.71	41	577	21.71	339.52
47	30	2.19	30	607	2.19	341.71
48	9	0.41	9	616	0.41	342.12
49	15	-12.98	15	631	12.98	355.10
50	11	-2.18	11	642	2.18	357.28
51	18	-10.08	18	660	10.08	367.36
52	15	8.91	15	675	8.91	376.27
53	23	0.78	23	698	0.78	377.04
54	24	-0.36	24	722	0.36	377.40
55	10	-2.25	10	732	2.25	379.66
56	46	-3.43	46	778	3.43	383.09
57	21	-3.68	21	799	3.68	386.76
58	28	2.01	28	827	2.01	388.77
59	17	-4.36	17	844	4.36	393.13
60	13	0.36	13	857	0.36	393.50
61	37	-3.01	37	894	3.01	396.51
62	7	-0.18	7	901	0.18	396.69
63	14	1.19	14	915	1.19	397.88
64	57	6.61	57	972	6.61	404.48
65	9	2.46	9	981	2.46	406.94
66	12	1.23	12	993	1.23	408.17
67	23	-1.91	23	1016	1.91	410.08
68	-11	-51.40	11	1027	51.40	461.48
69	37	1.75	37	1064	1.75	463.23
70	53	12.63	53	1117	12.63	475.86
71	37	3.54	37	1154	3.54	479.40
72	47	-0.23	47	1201	0.23	479.63
73	52	4.22	52	1253	4.22	483.84
74	9	0.72	9	1262	0.72	484.56
75	37	3.99	37	1299	3.99	488.54
76	35	4.78	35	1334	4.78	493.32
77	48	-1.75	48	1382	1.75	495.07
78	46	0.84	46	1428	0.84	495.91

79	42	8.76	42	1470	8.76	504.67
80	45	0.46	45	1515	0.46	505.13
81	-101	-15.93	101	1616	15.93	521.06
82	65	8.25	65	1681	8.25	529.30
83	15	0.34	15	1696	0.34	529.65
84	41	-1.62	41	1737	1.62	531.26
85	85	3.61	85	1822	3.61	534.88
86	-139	-39.41	139	1961	39.41	574.29
87	-96	-27.24	96	2057	27.24	601.53
88	51	4.21	51	2108	4.21	605.74
89	52	4.19	52	2160	4.19	609.93
90	72	8.98	72	2232	8.98	618.91
91	56	4.98	56	2288	4.98	623.89
92	16	0.03	16	2304	0.03	623.92
93	79	7.04	79	2383	7.04	630.96
94	-100	12.16	100	2483	12.16	643.12
95	86	5.52	86	2569	5.52	648.63
96	59	3.16	59	2628	3.16	651.79
97	85	5.00	85	2713	5.00	656.79
98	22	1.94	22	2735	1.94	658.72
99	21	0.95	21	2756	0.95	659.67
100	50	4.49	50	2806	4.49	664.16
101	76	8.27	76	2882	8.27	672.43
102	-167	-18.02	167	3049	18.02	690.46
103	87	6.38	87	3136	6.38	696.83
104	67	3.22	67	3203	3.22	700.05
105	23	8.75	23	3226	8.75	708.80
106	-222	-52.85	222	3448	52.85	761.66
107	72	17.37	72	3520	17.37	779.02
108	-181	-39.74	181	3701	39.74	818.77
109	-172	-21.03	172	3873	21.03	839.79
110	93	9.91	93	3966	9.91	849.70
111	75	12.13	75	4041	12.13	861.83
112	112	15.23	112	4153	15.23	877.06
113	97	8.76	97	4250	8.76	885.81
114	108	6.91	108	4358	6.91	892.72
115	-234	-32.62	234	4592	32.62	925.34
116	74	9.32	74	4666	9.32	934.65
117	-274	-89.41	274	4940	89.41	1024.06
118	92	14.16	92	5032	14.16	1038.23
119	-293	-58.43	293	5325	58.43	1096.66
120	-200	-18.04	200	5525	18.04	1114.70

121	154	22.96	154	5679	22.96	1137.65
122	-242	-37.74	242	5921	37.74	1175.40
123	-227	-14.73	227	6148	14.73	1190.13
124	-321	-42.84	321	6469	42.84	1232.97
125	-251	-49.76	251	6720	49.76	1282.73
126	-444	-68.94	444	7164	68.94	1351.67

E.4. Data for the tank in Site B

Table E.7. Site B daily real time data

Day	Initial Temp. (°C)	Initial Level (mm)	Initial Volume (L)	Delivery (L)	Correction (L)	Sales (L)	Final Temp. (°C)	Final Level (mm)	Final Volume (L)	Var (L)
1	21.60	880.75	6779	5166	0	6311	21.25	710.72	5087	-547
2	21.25	710.72	5087	9984	0	8467	19.21	868.77	6658	54
3	19.21	868.77	6658	14759	13700	5139	21.26	443.83	2695	117
4	21.26	443.83	2695	0	-13700	5628	19.96	1278.37	10946	179
5	19.96	1278.37	10946	11507	700	5781	18.00	1778.37	16018	46
6	18.00	1778.37	16018	0	-700	6036	19.94	1265.24	10806	124
7	19.94	1265.24	10806	5264	0	7480	19.57	1081.62	8422	-168
8	19.57	1081.62	8422	0	0	3634	20.83	720.31	5182	394
9	20.83	720.31	5182	10717	0	3864	20.94	1414.71	12381	346
10	20.94	1414.71	12381	5537	0	3732	21.14	1581.56	14099	-87
11	21.14	1581.56	14099	0	0	6612	21.16	946.09	7449	-38
12	21.16	946.09	7449	8767	0	6259	19.94	1210.08	10223	266
13	19.94	1210.08	10223	0	0	5210	21.14	696.44	4951	-62
14	21.14	696.44	4951	7292	0	5941	18.99	833.10	6294	-7
15	18.99	833.10	6294	9149	0	7439	19.11	1006.00	8039	35
16	19.11	1006.00	8039	7248	0	4149	18.35	1305.72	11234	95
17	18.35	1305.72	11234	5429	0	6554	18.58	1253.94	10685	576
18	18.58	1253.94	10685	0	0	5423	19.82	723.34	5212	-51
19	19.82	723.34	5212	5879	0	7125	18.96	584.63	3910	-56
20	18.96	584.63	3910	12191	0	4946	17.80	1306.54	11242	87
21	17.80	1306.54	11242	0	0	7260	19.40	582.55	3891	-91
22	19.40	582.55	3891	7142	0	5595	17.04	749.29	5466	28
23	17.04	749.29	5466	9965	0	4518	17.88	1283.04	10995	83
24	17.88	1283.04	10995	0	0	4822	18.50	815.16	6113	-61
25	18.50	815.16	6113	10100	0	5181	18.11	1335.92	11552	520
26	18.11	1335.92	11552	0	0	6117	18.61	816.73	6132	697

27	18.61	816.73	6132	7245	0	5633	17.89	900.00	6972	-772
28	17.89	900.00	6972	8405	0	5806	17.70	1151.31	9338	-233
29	17.70	1151.31	9338	6984	0	4432	17.69	1393.00	12154	264
30	17.69	1393.00	12154	4298	0	6866	17.09	1304.57	11223	1636
31	17.09	1304.57	11223	5843	0	6029	17.48	1266.68	10821	-215
32	17.48	1266.68	10821	5991	0	5213	16.49	1340.44	11601	2
33	16.49	1340.44	11601	6782	0	5960	15.94	1419.83	12434	11
34	15.94	1419.83	12434	0	0	4239	16.89	1013.92	8077	-118
35	16.89	1013.92	8077	7361	350	6287	15.41	1109.05	8660	-141
36	15.41	1109.05	8660	13659	-350	7363	11.95	1700.94	15284	-22
37	11.95	1700.94	15284	0	0	4912	14.21	1221.63	10344	-28
38	14.21	1221.63	10344	12024	1700	4667	11.32	1776.03	15995	-6
39	11.32	1776.03	15995	0	-1700	6324	13.76	1320.46	11389	17
40	13.76	1320.46	11389	0	0	5532	14.86	782.76	5791	-66
41	14.86	782.76	5791	10297	0	4840	13.77	1308.11	11260	12
42	13.77	1308.11	11260	0	0	4807	15.05	840.58	6370	-83
43	15.05	840.58	6370	11933	0	5646	13.76	1443.18	12676	19
44	13.76	1443.18	12676	4915	0	4698	13.64	1470.49	12960	67
45	13.64	1470.49	12960	0	0	5237	14.70	967.70	7672	-50
46	14.70	967.70	7672	11557	0	5608	12.31	1519.71	13467	-154
47	12.31	1519.71	13467	0	0	4832	13.78	1067.95	8354	-281
48	13.78	1067.95	8354	7591	0	4484	13.33	1347.55	11673	212
49	13.33	1347.55	11673	0	0	5421	14.20	831.56	6279	27
50	14.20	831.56	6279	10196	0	6795	12.38	1186.05	9890	210
51	12.38	1186.05	9890	7871	0	5981	12.38	1322.84	11416	-365
52	12.38	1322.84	11416	5528	0	6072	12.56	1312.13	11302	430
53	12.56	1312.13	11302	7023	0	6517	12.21	1356.00	11760	-48
54	12.21	1356.00	11760	0	0	4731	13.25	896.18	6934	-95
55	13.25	896.18	6934	6643	0	4728	12.14	1082.34	8425	-424
56	12.14	1082.34	8425	10042	0	6260	11.43	1438.91	12631	423
57	11.43	1438.91	12631	0	0	5273	12.86	932.58	7309	-48
58	12.86	932.58	7309	11019	0	5463	11.66	1466.00	12911	45
59	11.66	1466.00	12911	0	0	5888	12.89	898.84	6961	-62
60	12.89	898.84	6961	7315	0	5703	11.79	1051.77	8270	-302
61	11.79	1051.77	8270	0	0	4543	13.00	586.38	3925	198
62	13.00	586.38	3925	8923	0	2702	10.08	1209.00	10208	62
63	10.08	1209.00	10208	10551	0	4814	9.37	1749.63	15746	-200
64	9.37	1749.63	15746	0	0	3453	10.34	1416.56	12400	107
65	10.34	1416.56	12400	12086	0	4331	9.93	1772.51	15961	-4193
66	9.93	1772.51	15961	4224	0	4507	10.96	1764.78	15889	212
67	10.96	1764.78	15889	0	0	4463	11.71	1377.09	11987	561
68	11.71	1377.09	11987	0	0	1459	12.28	1237.32	10511	-18

69	12.28	1237.32	10511	6501	3500	4218	12.51	1134.09	9061	-232
70	12.51	1134.09	9061	0	-3500	4368	10.10	1015.39	8085	-109
71	10.10	1015.39	8085	0	0	3159	11.48	697.28	4958	32
72	11.48	697.28	4958	17121	1500	4661	9.86	1768.98	15927	9
73	9.86	1768.98	15927	0	-1500	4737	10.17	1439.54	12638	-53
74	10.17	1439.54	12638	4989	0	6385	10.55	1306.18	11238	-4
75	10.55	1306.18	11238	10058	0	5768	9.00	1724.23	15503	-25
76	9.00	1724.23	15503	0	0	4484	10.59	1282.13	10984	-36
77	10.59	1282.13	10984	0	0	6448	11.39	640.65	4425	-112
78	11.39	640.65	4425	12028	0	4828	9.35	1351.54	11718	94
79	9.35	1351.54	11718	9531	4000	4073	10.50	1484.32	13104	-73
80	10.50	1484.32	13104	0	-4000	4430	9.96	1448.00	12721	48
81	9.96	1448.00	12721	0	0	4579	10.92	1007.66	8043	-100
82	10.92	1007.66	8043	9549	0	5338	10.04	1405.00	12279	24
83	10.04	1405.00	12279	0	0	4880	11.02	937.86	7362	-37
84	11.02	937.86	7362	13495	0	4504	8.88	1795.87	16185	-168
85	8.88	1795.87	16185	5846	0	5817	9.31	1767.00	15912	-302
86	9.31	1767.00	15912	0	0	8127	10.28	1004.96	8032	246
87	10.28	1004.96	8032	8692	0	6737	8.89	1218.95	10314	328
88	8.89	1218.95	10314	6294	0	6217	8.94	1198.00	10087	-304
89	8.94	1198.00	10087	6806	0	6724	8.73	1201.22	10129	-41
90	8.73	1201.22	10129	0	0	6109	10.05	585.83	3917	-102
91	10.05	585.83	3917	9509	0	8123	8.95	726.08	5238	-65
92	8.95	726.08	5238	13574	0	8642	9.06	1224.00	10367	197
93	9.06	1224.00	10367	0	0	8597	10.47	301.83	1597	-173
94	10.47	301.83	1597	10117	0	8127	11.25	548.19	3584	-3
95	11.25	548.19	3584	12008	0	6985	11.19	1060.95	8316	-292
96	11.19	1060.95	8316	0	0	6726	11.56	326.27	1783	193
97	11.56	326.27	1783	14665	0	4258	12.06	1444.13	12687	498
98	12.06	1444.13	12687	0	0	5791	12.32	886.00	6832	-64
99	12.32	886.00	6832	9326	0	4824	12.22	1320.23	11385	52
100	12.22	1320.23	11385	12005	4800	5098	12.11	1518.37	13456	-37
101	12.11	1518.37	13456	0	-4800	4823	11.75	1514.54	13414	-19
102	11.75	1514.54	13414	0	0	6066	12.28	930.58	7290	-58
103	12.28	930.58	7290	9610	0	6484	11.88	1330.00	11488	1071
104	11.88	1330.00	11488	0	0	4118	12.36	933.75	7320	-49
105	12.36	933.75	7320	8009	0	4355	12.10	1281.46	10977	2
106	12.10	1281.46	10977	0	0	5393	12.47	754.02	5511	-72
107	12.47	754.02	5511	10936	0	5652	10.75	1285.38	10939	144
108	10.75	1285.38	10939	0	0	7328	11.72	548.00	3584	-26
109	11.72	548.00	3584	11957	0	5690	9.19	1176.45	9315	-536
110	9.19	1176.45	9315	0	0	6601	9.55	1022.16	8119	5405

111	9.55	1022.16	8119	6279	0	6299	9.96	1046.18	8240	141
112	9.96	1046.18	8240	0	0	7102	11.38	247.45	1241	103
113	11.38	247.45	1241	19922	0	5602	10.06	1764.39	15515	-46
114	10.06	1764.39	15515	0	0	5624	10.85	1302.59	11200	1309
115	10.85	1302.59	11200	0	0	6580	11.29	653.14	4542	-78
116	11.29	653.14	4542	11015	0	4674	11.35	1280.08	10852	-31
117	11.35	1280.08	10852	0	0	6002	11.84	690.10	4890	41
118	11.84	690.10	4890	10992	0	3770	10.73	1402.43	12252	139
119	10.73	1402.43	12252	0	0	6779	11.51	742.96	5193	-280
120	11.51	742.96	5193	11409	0	6085	11.60	1319.71	11382	864
121	11.60	1319.71	11382	0	0	4916	12.17	844.63	6139	-326
122	12.17	844.63	6139	12340	0	5608	10.99	1465.73	12911	39
123	10.99	1465.73	12911	4206	0	6469	11.49	1294.86	11090	442
124	11.49	1294.86	11090	0	0	7409	12.01	538.87	3501	-180
125	12.01	538.87	3501	12136	0	6063	11.22	1159.72	9141	-433
126	11.22	1159.72	9141	0	0	8551	11.84	963.72	7631	7041

Table E.8. Site B percentage reduction in variance

Day	Var _chart (L)	Var _adjusted (L)	Abs_Var _chart	Cumulative_Abs _Var_chart	Abs_Var _adjusted	Cumulative_Abs _Var_adjusted
1	-46	13.22	46	46	13.22	13.22
2	-3	0.026	3	49	0.03	13.24
3	497	13.64	497	546	13.64	26.89
4	179	12.53	179	725	12.53	39.42
5	-433	6.82	433	1158	6.82	46.24
6	-536	7.36	536	1694	7.36	53.60
7	-291	6.21	291	1985	6.21	59.80
8	28	-0.26	28	2013	0.26	60.06
9	87	11.87	87	2100	11.87	71.93
10	-65	-0.12	65	2165	0.12	72.05
11	62	9.52	62	2227	9.52	81.57
12	93	12.36	93	2320	12.36	93.94
13	-31	12.29	31	2351	12.29	106.22
14	140	13.04	140	2491	13.04	119.26
15	-8	-0.17	8	2499	0.17	119.44
16	9	13.20	9	2508	13.20	132.63
17	54	-0.13	54	2562	0.13	132.76
18	346	13.34	346	2908	13.34	146.10
19	-56	0.10	56	2964	0.10	146.20
20	197	11.05	197	3161	11.05	157.25
21	865	12.09	865	4026	12.09	169.34

22	82	12.54	82	4108	12.54	181.88
23	144	12.52	144	4252	12.52	194.40
24	12	12.23	12	4264	12.23	206.63
25	520	12.41	520	4784	12.41	219.04
26	-772	0.00	772	5556	0.00	219.04
27	210	7.94	210	5766	7.94	226.99
28	35	-0.29	35	5801	0.29	227.27
29	19	13.65	19	5820	13.65	240.92
30	40	13.64	40	5860	13.64	254.57
31	117	-0.01	117	5977	0.01	254.58
32	-547	0.18	547	6524	0.18	254.76
33	51	12.11	51	6575	12.11	266.87
34	-424	7.18	424	6999	7.18	274.05
35	-303	5.56	303	7302	5.56	279.61
36	-233	6.83	233	7535	6.83	286.44
37	1072	12.40	1072	8607	12.40	298.84
38	46	13.91	46	8653	13.91	312.76
39	3	12.72	3	8656	12.72	325.48
40	-168	14.39	168	8824	14.39	339.87
41	266	10.22	266	9090	10.22	350.09
42	-154	14.28	154	9244	14.28	364.38
43	327	10.99	327	9571	10.99	375.37
44	96	12.33	96	9667	12.33	387.70
45	25	13.44	25	9692	13.44	401.14
46	-141	6.62	141	9833	6.62	407.76
47	32	-0.35	32	9865	0.35	408.12
48	141	3.46	141	10006	3.46	411.58
49	103	-4.76	103	10109	4.76	416.34
50	198	-5.28	198	10307	5.28	421.62
51	193	-6.23	193	10500	6.23	427.85
52	212	5.83	212	10712	5.83	433.68
53	394	-6.99	394	11106	6.99	440.67
54	424	6.58	424	11530	6.58	447.25
55	-22	5.77	22	11552	5.77	453.02
56	-108	-6.20	108	11660	6.20	459.22
57	264	6.35	264	11924	6.35	465.57
58	7041	-7.62	7041	18965	7.62	473.19
59	5405	-6.10	5405	24370	6.10	479.28
60	-364	4.13	364	24734	4.13	483.42
61	-40	0.26	40	24774	0.26	483.67
62	-103	-8.84	103	24877	8.84	492.51
63	-199	3.29	199	25076	3.29	495.81
64	-62	-9.62	62	25138	9.62	505.43
65	-304	-1.89	304	25442	1.89	507.31

66	-6	2.67	6	25448	2.67	509.98
67	-173	-11.06	173	25621	11.06	521.04
68	-233	-5.31	233	25854	5.31	526.35
69	-50	-12.51	50	25904	12.51	538.86
70	-168	-5.57	168	26072	5.57	544.42
71	2	-0.25	2	26074	0.25	544.67
72	46	1.10	46	26120	1.10	545.78
73	40	-12.31	40	26160	12.31	558.08
74	-73	-12.59	73	26233	12.59	570.67
75	-111	-12.25	111	26344	12.25	582.93
76	-60	-12.55	60	26404	12.55	595.48
77	-27	-12.33	27	26431	12.33	607.82
78	-180	-12.18	180	26611	12.18	620.00
79	-78	-11.88	78	26689	11.88	631.88
80	-216	0.57	216	26905	0.57	632.45
81	576	0.52	576	27481	0.52	632.97
82	-25	0.76	25	27506	0.76	633.73
83	-91	-11.87	91	27597	11.87	645.61
84	-83	-12.00	83	27680	12.00	657.60
85	-48	0.62	48	27728	0.62	658.22
86	-327	-12.00	327	28055	12.00	670.22
87	-36	1.42	36	28091	1.42	671.65
88	-66	-12.24	66	28157	12.24	683.89
89	430	-0.06	430	28587	0.06	683.96
90	-50	-12.44	50	28637	12.44	696.39
91	697	-12.40	697	29334	12.40	708.79
92	11	1.11	11	29345	1.11	709.90
93	27	-12.52	27	29372	12.52	722.42
94	-72	1.08	72	29444	1.08	723.49
95	-95	-12.73	95	29539	12.73	736.22
96	-17	-0.84	17	29556	0.84	737.06
97	1637	-1.01	1637	31193	1.01	738.07
98	-280	-13.28	280	31473	13.28	751.36
99	-37	-13.57	37	31510	13.57	764.92
100	-87	-0.49	87	31597	0.49	765.42
101	-4194	0.01	4194	35791	0.01	765.43
102	-118	-13.12	118	35909	13.12	778.55
103	-49	-13.90	49	35958	13.90	792.45
104	-4	-1.63	4	35962	1.63	794.08
105	67	-0.01	67	36029	0.01	794.09
106	-64	-13.75	64	36093	13.75	807.84
107	-99	-13.86	99	36192	13.86	821.70
108	442	-1.46	442	36634	1.46	823.16
109	-62	-13.78	62	36696	13.78	836.94

110	-51	-14.50	51	36747	14.50	851.44
111	47	0.04	47	36794	0.04	851.48
112	-58	-13.71	58	36852	13.71	865.20
113	-19	0.03	19	36871	0.03	865.23
114	-281	-6.77	281	37152	6.77	872.00
115	-38	-13.36	38	37190	13.36	885.35
116	-28	-1.88	28	37218	1.88	887.23
117	-35	-0.34	35	37253	0.34	887.57
118	107	0.46	107	37360	0.46	888.04
119	1309	-1.17	1309	38669	1.17	889.20
120	561	-0.40	561	39230	0.40	889.60
121	247	-13.67	247	39477	13.67	903.27
122	-52	0.30	52	39529	0.30	903.57
123	211	-0.20	211	39740	0.20	903.77
124	18	-1.51	18	39758	1.51	905.28
125	124	-0.99	124	39882	0.99	906.27

APPENDIX F: MATLAB CODES

```

function Vol=fuel_volume(R,H,r,L,M,alpha,beta,h_alpha_beta,fuel,T,T_ref,kappa,summary);

% Convert degree to radian
% alpha=degtorad(alpha);
% beta=degtorad(beta);
% Alternatively (for R2013a version);
alpha = alpha*pi/180; % convert degrees to radians
beta = beta*pi/180; % convert degrees to radians

% Convert h_alpha_beta to h_alpha
h_alpha= h_alpha_beta/sec(beta)+ 2*R*(sin(beta))^2;

% Calculate h_critical_positive
h_critical_positive= (L-M)*tan(alpha);

% Calculate h_critical_negative
h_critical_negative= M*tan(alpha);

level_type = 'N/A for capped tank';
cap_type = 'N/A for simple cylinder';

if (alpha==0)&(H==0); disp 'simple cylinder alpha = 0'; Vol=cylindrical_tank_volume(R,L,h_alpha);tank_type = 1; alpha_case = '=' 0'; end

if (alpha==0)&(H>0); disp 'caps cylinder alpha = 0'; Vol=horizontal_tank_volume(R,H,L,h_alpha); tank_type = 2; alpha_case = '=' 0';end

if (alpha>0)&(H==0)&(h_alpha_beta<=h_critical_positive); disp 'low level cylinder'; Vol=low_level_tilted_simple_cylinder_tank(alpha,M,h_alpha,R,L); tank_type = 1; level_type = 'Low level'; alpha_case = '> 0'; V0=nonmeasurable_volume_for_positive_alpha_without_dished(alpha,M,R); Vol=Vol+V0; end

if (alpha>0)&(H==0)&(h_alpha_beta>h_critical_positive); disp 'high level cylinder'; Vol=high_level_tilted_simple_cylinder_tank(alpha,M,h_alpha,R,L); tank_type = 1; level_type = 'High level'; alpha_case = '> 0'; V0=nonmeasurable_volume_for_positive_alpha_without_dished(alpha,M,R); Vol=Vol+V0; end

if (alpha>0)&(H>0)&(h_alpha_beta<=h_critical_positive); disp 'single cap volume'; Vol=single_cap_volume(alpha, M,H,h_alpha,r,R,L); tank_type = 2; cap_type = 'Single'; alpha_case = '> 0'; V0=nonmeasurable_volume_for_positive_alpha_case(alpha,M,H,r,R); Vol=Vol+V0; end

if (alpha>0)&(H>0)&(h_alpha_beta>h_critical_positive); disp 'double cap volume'; Vol=double_cap_volume(alpha, M,H,h_alpha,r,R,L); tank_type = 2; cap_type = 'Double'; alpha_case = '> 0'; V0=nonmeasurable_volume_for_positive_alpha_case(alpha,M,H,r,R); Vol=Vol+V0; end

if (alpha<0)&(H==0)&(h_alpha_beta<=(-h_critical_negative)); disp 'low level negative tilted cylinder'; Vol=low_level_negative_tilted_simple_cylinder_tank(alpha,M,h_alpha_beta,R,L); tank_type = 1; level_type = 'Low level'; alpha_case = '< 0'; V0=nonmeasurable_volume_for_negative_alpha_without_dished_head(alpha,L,M,R); Vol=Vol+V0; end

if (alpha<0)&(H==0)&(h_alpha_beta>(-h_critical_negative)); disp 'high level negative tilted cylinder'; Vol=high_level_negative_tilted_simple_cylinder_tank(alpha,M,h_alpha_beta,R,L); tank_type = 1; level_type = 'High level'; alpha_case = '< 0'; V0=nonmeasurable_volume_for_negative_alpha_case(alpha,L,M,R); Vol=Vol+V0; end

if (alpha<0)&(H>0)&(h_alpha_beta<=(-h_critical_negative)); disp 'one cap volume negative alpha'; Vol=one_cap_volume_negative_alpha(alpha, M,H,h_alpha_beta,r,R,L); tank_type = 2; cap_type = 'Single'; alpha_case = '< 0'; V0=nonmeasurable_volume_for_negative_alpha_case(alpha, M,L,H,r,R); Vol=Vol+V0; end

if (alpha<0)&(H>0)&(h_alpha_beta>(-h_critical_negative)); disp 'two caps volume negative alpha'; Vol=two_caps_volume_negative_alpha(alpha, M,H,h_alpha_beta,r,R,L); tank_type = 2; cap_type = 'Double'; alpha_case = '< 0'; V0=nonmeasurable_volume_for_negative_alpha_case(alpha, M,L,H,r,R); Vol=Vol+V0; end

% Temperature correction to calculate the correct volume
switch fuel
case 'Diesel'
display('diesel fuel')
dV = (T-T_ref)*kappa;

```

```

Vol = Vol-dV
case 'Gasoline'
display('gasoline fuel')
dV = (T-T_ref)*kappa;
Vol= Vol-dV
end

if summary==1
sprintf('SUMMARY \n \n Constant Values\n _____\n Radius of Tank\t\t\t:.2f \n Dished Head Radius\t\t:f \n Length
of Tank\t\t:f \n Vertical Tilt\t\t:f \n Horizontal Tilt\t\t:f \n Manhole Distance\t\t:f \n Measured Fuel Level\t:f \n Fuel
Type\t\t:s \n Temperature\t\t:f \n Reference Temperature\t:f \n alpha\t\t:t\t\t:s \n Tank type \t\t:t\t\t:s \n Level type\t\t:t\t\t:s
\n Filled caps\t\t:s',R, H, L, alpha, beta, M, h_alpha_beta, fuel, T, T_ref, alpha_case, tank_type, level_type,cap_type)
end

end

```

Figure F.1. Main algo of fuel volume

```

function V = cylindrical_tank_volume(R,L,h_alpha);
A = sqrt(((2*R)-h_alpha)*h_alpha);
B = h_alpha-R;
C = (R^2)*acos(1-(h_alpha/R));
V = L*(A*B+C); %(mm3)
V = V*10^-6; %(L)
end

```

Figure F.2. SCT volume

```

function V = horizontal_tank_volume(R,H,L,h_alpha);
A = sqrt(((2*R)-h_alpha)*h_alpha);
B = h_alpha-R;
C = (R^2)*acos(1-(h_alpha/R));
D = (pi*H*(3*R-h_alpha)*(h_alpha^2))/(3*R);
V = L*(A*B+C)+D; %(mm3)
V = V*10^-6; %(L)
end

```

Figure F.3. CTDH volume

```

function Vol=low_level_tilted_simple_cylinder_tank(alpha,M,h_alpha_beta,R,L);
% L1 calculation- junction point of the liquid level surface and the tank bottom
L1 =((h_alpha_beta*cot(alpha))+M);

% h3 calculation-maximum distance from oil surface to bottom of tank
h3=h_alpha_beta +(M*tan(alpha));

% Simple Cylindrical Body Volume Calculation

Vol=L1 *(sqrt(((2*R)-h3)*h3)*(h3-R)+((R^2)*acos(1-(h3/R)))); % in mm3
Vol = (Vol*10^-6)/2; %(L)

end

```

Figure F.4. Low level positive axial tilted SCT

```

function V0=nonmeasurable_volume_for_positive_alpha_without_dished(alpha,M,R);

% Calculate h0 (nonmeasurable fuel height)
h0 = M*tan(alpha);

% Simple Cylindrical Body Volume Calculation
V_h0_cyl = M .*(sqrt(((2.*R)-h0).*h0).*h0+(R.^2).*acos(1-(h0/R)))); % in mm3

```

```

V_h0_cyl = V_h0_cyl*10^-6; %(L)

% Nonmeasurable Volume for the positive alpha case
V0 = V_h0_cyl/2;

end

```

Figure F.5. Nonmeasurable fuel volume for positive axial tilted SCT

```

function Vol= high_level_simple_cylinder_tank(alpha,M,h_alpha_beta,R,L);

% h1 calculation - minimum distance from oil surface to bottom of tank
h1=h_alpha_beta-((L-M)*tan(alpha));

% h2 calculation-maximum distance from oil surface to bottom of tank
h2=h_alpha_beta + (M*tan(alpha));

% Simple Cylindrical Body Volume Calculation
V_h1_cyl=L*(sqrt(((2*R)-h1)*(h1-R)+((R^2)*acos(1-(h1/R)))); % in mm3
V_h1_cyl=V_h1_cyl*10^-6; %(L)

V_h2_cyl=L*(sqrt(((2*R)-h2)*(h2-R)+((R^2)*acos(1-(h2/R)))); % in mm3
V_h2_cyl=V_h2_cyl*10^-6; %(L)

% Total Volume for Oil on both End Caps
Vol =(V_h1_cyl + V_h2_cyl)/2;

end

```

Figure F.6. High level positive axial tilted SCT

```

function Vol=single_cap_volume(alpha,M,H,h_alpha,r,R,L);

% Calculate x1
x1=(h_alpha/tan(alpha))+M+H;

% Calculate x2 (ax2^2 + bx2 + c = 0)
c1 = -tan(alpha);
c2 = h_alpha+ M*tan(alpha)+ H*tan(alpha);
c3 = r;
c4 = c2-R;
a = 1+ c1^2;
b = -2*c3 + 2*c1*c4;
c =c4^2 + c3^2 - r^2;

p = [a b c];
x2_soln = roots(p);
x2 = x2_soln(x2_soln>=0);

if numel(x2)>1
    x2=min(x2);
end

% h3 calculation-maximum distance from oil surface to bottom of tank
h3=h_alpha -((x2-M-H)*tan(alpha));

% Simple Cylindrical Body Volume Calculation
V_h3_cyl=L*(sqrt(((2*R)-h3)*(h3-R)+((R^2)*acos(1-(h3/R)))); % in mm3
V_h3_cyl=V_h3_cyl*10^-6; %(L)

% Dished Head Volume Calculation (Curvature)
V_h3_curv= pi*H*(3*R-h3)*h3^2/(3*R); % in mm3
V_h3_curv=V_h3_curv*10^-6; %(L)

% Cylindrical Element Volume Calculation
V_h3_element=(L+H-x1)*((sqrt(((2*R)-h3)*(h3-R))+((R^2)*acos(1-(h3/R)))); % in mm3
V_h3_element=V_h3_element*10^-6; %(L)

% Total Volume for Oil on One End Cap

```

```

Vol = ((V_h3_cyl + V_h3_curv) - V_h3_element)/2;
end

```

Figure F.7. Fuel on one dished head for positive axial tilted CTDH

```

function V0=nonmeasurable_volume_for_positive_alpha_case(alpha,M,H,r,R);
% Calculate x2 (ax2^2 + bx2 + c = 0)

a = 1+ (tan(alpha)^2);
b = -2*r -(2*(M+H)*(tan(alpha)^2))+2*R*tan(alpha);
c = (((M+H)^2)*(tan(alpha)^2))-(2*R*(M+H)*tan(alpha))+ R^2;

p = [a b c];
x2_soln = roots(p);
x2 = x2_soln(x2_soln>=0)

if numel(x2)>1
    x2 = min(x2)
end

% y2 calculation
y2 = (M+H-x2)*tan(alpha);

% h calculation
h = y2;

% Simple Cylindrical Body Volume Calculation

V_h_cyl = M .*(sqrt(((2.*R)-h).*h).*(h-R)+((R.^2).*acos(1-(h/R)))); % in mm3
V_h_cyl = V_h_cyl*10^-6; %(L)

% Dished Head Volume Calculation (End Caps)
V_h_curv = pi.*H.*(3.*R-h).*h.^2/(3.*R); % in mm3
V_h_curv = V_h_curv*10^-6 ; %(L)

% Nonmeasurable Volume for the positive alpha case
V0 = (V_h_cyl +V_h_curv)/2;

end

```

Figure F.8. Nonmeasurable fuel volume for positive axial tilted CTDH

```

function Vol=double_cap_volume(alpha,M,H,h_alpha,r,R,L);
echo off

% Calculate x1 (ax1^2 + bx1 + c = 0)
c1 = -tan(alpha);
c2 = h_alpha+ M*tan(alpha)+ H*tan(alpha);
c3 = L+ 2*H-r;
c4 = c2-R;
a = 1+ c1^2;
b = -2*c3 + 2*c1*c4;
c =c4^2 + c3^2 - r^2;

p = [a b c];
x1_soln = roots(p);
x1 = x1_soln(x1_soln>=0);

%clear c1,c2,c3,c4,a,b,c,p,x1_soln;

if numel(x1)>1
    x1=max(x1);
end

% Calculate x2 (ax2^2 + bx2 + c = 0)
c1 = -tan(alpha);
c2 = h_alpha+ M*tan(alpha)+ H*tan(alpha);
c3 = r;
c4 = c2-R;
a = 1+ c1^2;
b = -2*c3 + 2*c1*c4;
c =c4^2 + c3^2 - r^2;

p = [a b c];
x2_soln = roots(p);
x2 = x2_soln(x2_soln>=0);

if numel(x2)>1
    x2=min(x2);
end

% h1 calculation - minimum distance from oil surface to bottom of tank
h1=h_alpha-((x1-M-H)*tan(alpha));

% h2 calculation-maximum distance from oil surface to bottom of tank
h2=h_alpha -((x2-M-H)*tan(alpha));

% Simple Cylindrical Body Volume Calculation
V_h1_cyl=L*(sqrt(((2*R)-h1)*h1)*(h1-R)+((R^2)*acos(1-(h1/R)))); % in mm3
V_h1_cyl=V_h1_cyl*10^-6; %(L)

% Dished Head Volume Calculation (Curvature)
V_h1_curv= pi*H*(3*R-h1)*h1^2/(3*R); % in mm3
V_h1_curv=V_h1_curv*10^-6; %(L)
V_h2_cyl=L*(sqrt(((2*R)-h2)*h2)*(h2-R)+((R^2)*acos(1-(h2/R)))); % in mm3
V_h2_cyl=V_h2_cyl*10^-6; %(L)

V_h2_curv= pi*H*(3*R-h2)*h2^2/(3*R); % in mm3
V_h2_curv=V_h2_curv*10^-6; %(L)

% Total Volume for Oil on both End Caps
Vol =(V_h1_cyl +V_h1_curv + V_h2_cyl + V_h2_curv)/2;

end

```

Figure F.9. Fuel on both dished head for positive axial tilted CTDH

```

function Vol=low_level_negative_tilted_simple_cylinder_tank(alpha,M,h_alpha_beta,R,L);

% A calculation- junction point of the liquid level surface and the tank bottom
A=-(M-(h_alpha_beta*cot(-alpha)))

% h1 calculation-maximum distance from oil surface to bottom of tank
h1=h_alpha_beta +((L-M)*tan(-alpha));

% Simple Cylindrical Body Volume Calculation
% V_cyl=L*((sqrt(((2*R)-h)*h)*(h-R)+(R^2)*acos(1-(h/R)))) % in mm3

Vol=(L-A)*(sqrt(((2*R)-h1)*(h1-R)+(R^2)*acos(1-(h1/R)))); % in mm3
Vol=Vol*10^-6; %(L)
Vol=Vol/2 % in liter

end

```

Figure F.10. Low level negative axial tilted SCT

```

function
V0=nonmeasurable_volume_for_negative_alpha_without_dished_head(alpha,L,M,R);

% Calculate h0 (nonmeasurable fuel height)
h0 = (L-M)*tan(-alpha);

% Simple Cylindrical Body Volume Calculation
V_h0_cyl = (L-M).*(sqrt(((2.*R)-h0).*h0).*(h0-R)+((R.^2).*acos(1-(h0/R)))); % in mm3
V_h0_cyl = V_h0_cyl*10^-6; %(L)

% Nonmeasurable Volume for the negative alpha case
V0 = V_h0_cyl/2;

end

```

Figure F.11. Nonmeasurable fuel volume for negative axial tilted SCT

```

function Vol= high_level_negative_tilted_simple_cylinder_tank(alpha,M,h_alpha_beta,R,L);

% h1 calculation - minimum distance from oil surface to bottom of tank
h1= h_alpha_beta -(M*tan(-alpha));

% h2 calculation-maximum distance from oil surface to bottom of tank
h2=h_alpha_beta +((L-M)*tan(-alpha));

% Simple Cylindrical Body Volume Calculation
V_h1_cyl=L*(sqrt(((2*R)-h1)*h1)*(h1-R)+(R^2)*acos(1-(h1/R)))); % in mm3
V_h1_cyl=V_h1_cyl*10^-6; %(L)

V_h2_cyl=L*(sqrt(((2*R)-h2)*h2)*(h2-R)+(R^2)*acos(1-(h2/R)))); % in mm3
V_h2_cyl=V_h2_cyl*10^-6; %(L)

% Total Volume
Vol = (V_h1_cyl + V_h2_cyl)/2;

end

```

Figure F.12. High level negative axial tilted SCT

```

function Vol=one_cap_volume_negative_alpha(alpha, M,H,h_alpha_beta,r,R,L);

% Calculate x2 (ax2^2 + bx2 + c = 0)
c1 = tan(-alpha);
c2 = h_alpha_beta - ((M+H)*tan(-alpha));
c3 = L+2*R-r;
c4 = c2-R;

```

```

a = 1+c1^2;
b = -2*c3 + 2*c1*c4;
c = c4^2 + c3^2 - r^2;

p = [a b c];
x2_soln = roots(p);
x2 = x2_soln(x2_soln>=0)

if numel(x2)>1
    x2=max(x2);
end

% x1 calculation
x1 = M+H-(h_alpha_beta/tan(-alpha));

% y2 calculation
y2 = h_alpha_beta+ ((x2-M-H)*tan(-alpha));

% h calculation
h = y2;

% Simple Cylindrical Body Volume Calculation
V_h_cyl=(L+H-x1)*(sqrt(((2*R)-h)*h)*(h-R)+((R^2)*acos(1-(h/R)))); % in mm3
V_h_cyl=V_h_cyl*10^-6; %(L)

% Dished Head Volume Calculation (Curvature)
V_h_curv= pi*H*(3*R-h)*h^2/(3*R); % in mm3
V_h_curv=V_h_curv*10^-6; %(L)

% Total Volume for Oil on One End Cap
Vol = (V_h_cyl + V_h_curv)/2;
end

```

Figure F.13. Fuel on one dished head for negative axial tilted CTDH

```

function V0=nonmeasurable_volume_for_negative_alpha_case(alpha, M,L,H,r,R);

% Calculate x2 (ax2^2 + bx2 + c = 0)
c1 = tan(-alpha);
c2 = -(M+H)*tan(-alpha);
c3 = L+ 2*H-r;
c4 = c2-R;
a = 1+c1^2;
b = -2*c3 + 2*c1*c4;
c = c4^2 + c3^2 - r^2;

p = [a b c];
x2_soln = roots(p);
x2 = x2_soln(x2_soln>=0)

if numel(x2)>1
    x2 = max(x2)
end

% y2 calculation
y2 = (x2-M-H)*tan(-alpha);

% h calculation
h = y2;

% Simple Cylindrical Body Volume Calculation
V_h_cyl = (L-M) .* (sqrt(((2.*R)-h).*h).* (h-R)+((R.^2).*acos(1-(h/R)))); % in mm3
V_h_cyl = V_h_cyl*10^-6; %(L)

% Dished Head Volume Calculation (End Caps)
V_h_curv = pi.*H.* (3.*R-h).*h.^2/(3.*R); % in mm3
V_h_curv = V_h_curv*10^-6 ; %(L)

% Nonmeasurable Volume for the negative alpha case
V0 = (V_h_cyl + V_h_curv)/2;
end

```

Figure F.14. Nonmeasurable fuel volume for negative axial tilted CTDH

```

function Vol=two_caps_volume_negative_alpha(alpha, M,H,h_alpha_beta,r,R,L);

% Calculate x1 (ax1^2 + bx1 + c = 0)
c1 = tan(-alpha);
c2 = h_alpha_beta - ((M+H)*tan(-alpha));
c3 = r;
c4 = c2-R;
a = 1+c1^2;
b = -2*c3 + 2*c1*c4;
c = c4^2 + c3^2 - r^2;

p = [a b c];
x1_soln = roots(p);
x1 = x1_soln(x1_soln>=0)

if numel(x1)>1
    x1=max(x1)
end

% y1 calculation
y1 = h_alpha_beta-((M+H-x1)*tan(-alpha));

% h1 calculation
h1 = y1

% Calculate x2 (ax2^2 + bx2 + c = 0)
c1 = tan(-alpha);
c2 = h_alpha_beta - ((M+H)*tan(-alpha));
c3 = L+2*R-r;
c4 = c2-R;
a = 1+c1^2;
b = -2*c3 + 2*c1*c4;
c = c4^2 + c3^2 - r^2;

p = [a b c];
x2_soln = roots(p);
x2 = x2_soln(x2_soln>=0)

if numel(x2)>1
    x2=max(x2)
end

% y2 calculation
y2 = h_alpha_beta+((x2-M-H)*tan(-alpha));

% h2 calculation
h2 = y2

% Simple Cylindrical Body Volume Calculation
V_h1_cyl=L*(sqrt(((2*R)-h1)^2*h1)*(h1-R)+((R^2)*acos(1-(h1/R)))); % in mm3
V_h1_cyl=V_h1_cyl*10^-6; %(L)

V_h2_cyl=L*(sqrt(((2*R)-h2)^2*h2)*(h2-R)+((R^2)*acos(1-(h2/R)))); % in mm3
V_h2_cyl=V_h2_cyl*10^-6; %(L)

% Dished Head Volume Calculation (Curvature)
V_h1_curv= pi*H*(3*R-h1)*h1^2/(3*R); % in mm3
V_h1_curv=V_h1_curv*10^-6; %(L)

V_h2_curv= pi*H*(3*R-h2)*h2^2/(3*R); % in mm3
V_h2_curv=V_h2_curv*10^-6; %(L)

% Total Volume for Oil on One End Cap
Vol = (V_h1_cyl+V_h1_curv+V_h2_cyl+V_h2_curv)/2;
end

```

Figure F.15. Fuel on both dished head for negative axial tilted CTDH

```
% Main Algo __ Daily Data __ T4 Site D
clc; clear;
% Parameters (Constants)
R=1245; %radius of tank (mm)
L=5990; %length of tank (mm)
M=840; %manhole distance (mm)
T_ref = 15; %Reference Temperature in Celcius
alpha=3.75; % vert tilt (degree)
beta=18.00; %horz tilt (degree)
x=0;

%Variables
%tank_type= 1; % Simple Cylinder
tank_type= 2; % Simple Cylinder with Caps
H=340; % dished head radius (mm)

% Calculate sphere (cap) radius
r=(R^2+H^2)/(2*H);

fuel = 'Diesel'; %fuel type
%fuel = 'Gasoline'; %fuel type
switch fuel
case 'Diesel'
display('diesel fuel')
kappa= 0.000792;
case 'Gasoline'
display('gasoline fuel')
kappa=0.001251;
end

% files to run
run ('level_ini_1.m');
run ('level_fin_1.m');
run ('Delta_vol_1.m');
run ('temperature_ini_1.m');
run ('temperature_fin_1.m');

% vectors
Vol_ini_ideal=zeros(numel(h_ini_1),1);
Vol_ini=zeros(numel(h_ini_1),1);
Vol_fin_ideal=zeros(numel(h_fin_1),1);
Vol_fin=zeros(numel(h_fin_1),1);
dV_temp=zeros(numel(h_fin_1),1);
dV_theo_ideal=zeros(numel(h_fin_1),1);
dV_theo=zeros(numel(h_fin_1),1);
Var_ideal=zeros(numel(h_ini_1),1);
Var=zeros(numel(h_ini_1),1);
Var_norm_ideal=zeros(numel(h_ini_1),1);
Var_norm=zeros(numel(h_ini_1),1);

for i= 1:numel(h_ini_1) % i: data count

    Vol_ini_ideal(i)=fuel_volume(1250,350,2407,6000,600,0,0,h_ini_1(i),fuel,temp_ini_1(i),15,kappa,0);
    Vol_ini (i)=fuel_volume(R,H,r,L,M,alpha,beta,h_ini_1(i),fuel,temp_ini_1(i),T_ref,kappa,0);

    Vol_fin_ideal (i)=fuel_volume(1250,350,2407,6000,600,0,0,h_fin_1(i),fuel,temp_fin_1(i),15,kappa,0);
    Vol_fin (i)=fuel_volume(R,H,r,L,M,alpha,beta,h_fin_1(i),fuel,temp_fin_1(i),T_ref,kappa,0);

    dV_theo_ideal(i)= Vol_fin_ideal(i)- Vol_ini_ideal(i);
    dV_theo(i)= Vol_fin(i)- Vol_ini(i);

    Var_ideal(i)= dV_theo_ideal(i)- dV_theo_ideal(i);
    Var(i)= dV_theo(i)+ dV_act_1(i);

    Var_norm_ideal(i)= (dV_theo_ideal(i)/(-dV_theo_ideal(i)))+1;
    Var_norm(i)=(dV_theo(i)/dV_act_1(i))+1;

end
plot (h_fin_1, Var, '*')
hold on
plot (h_fin_1, Var_ideal)
```

Figure F.16. Main algo for the tank in Site D variance calculation

```
%BEST PARAMETERS DETERMINATION _ Daily Data _ T4 in Site D

clc; clear;

% Parameters (Constants)
R=1250; %radius of tank (mm)
L=6000; %length of tank (mm)
M=600; %manhole distance (mm)
T_ref = 15; %Reference Temperature in Celcius
alpha=0.00; %vert tilt (degree)
beta=0.00; %horz tilt (degree)
x=0;

%Variables
%tank_type= 1; % Simple Cylinder
tank_type= 2; % Simple Cylinder with Caps
H=350; % dished head radius (mm)

% Calculate sphere (cap) radius
r=(R^2+H^2)/(2*H);

fuel = 'Diesel'; %fuel type
%fuel = 'Gasoline'; %fuel type
switch fuel
case 'Diesel'
display('diesel fuel')
kappa= 0.000792;
case 'Gasoline'
display('gasoline fuel')
kappa=0.001251;
end

% files to run
run ('level_ini_1.m');
run ('level_fin_1.m');
run ('Delta_vol_1.m');
run ('temperature_ini_1.m');
run ('temperature_fin_1.m');

% vectors
Vol_ini=zeros(numel(h_ini_1),1);
Vol_fin=zeros(numel(h_fin_1),1);
dV_temp=zeros(numel(h_fin_1),1)
dV_theo=zeros(numel(h_fin_1),1);
Var=zeros(numel(h_ini_1),1);

z=0;

%for R=(R-5):5:(R+5);
%for R=1245;
% for H = (H-10):10:(H+10);
% for H = 340;
% for L = (L-10):10:(L+10);
% for L = 5990;
% for M = (M-240):120:(M+240);
% for M = 840;
% for alpha = 0:0.25:4;
% for alpha = 3.75;
% for beta = 14:2:20;
% z=z+1;
% G=0;
% for i= 1:numel(h_ini_1) % i: data count

    Vol_ini (i)=fuel_volume(R,H,r,L,M,alpha,beta,h_ini_1(i),fuel,temp_ini_1(i),T_ref,kappa,0);
    Vol_fin (i)=fuel_volume(R,H,r,L,M,alpha,beta,h_fin_1(i),fuel,temp_fin_1(i),T_ref,kappa,0);
    dV_theo(i)= Vol_fin(i)- Vol_ini(i);
    Var(i)= dV_theo(i)+ dV_act_1(i);

%end

figure()
plot (h_fin_1, Var, '*')

title(['R=',num2str(R), 'H=',num2str(H), 'L=',num2str(L), 'M=',num2str(M), 'alpha=',num2str(alpha), 'beta=',num2str(beta)])
```

```

        G= sum(abs(Var));
        G_table(:,z) = [R H L M alpha beta G Var'];

    end
end
end
end
end
end
end
end

[min_G, I] = min(G_table(7,:));
format long
G_table(:,I)

```

Figure F.17. Determination of optimal parameters for the tank in Site D

```

% Check of best parameters with 2nd Group Data__ Daily Data_ T4 in Site D

clc; clear;

% Parameters (Constants)
R=1245;           %radius of tank (mm)
L=5990;           %length of tank (mm)
M=840;            %manhole distance (mm)
T_ref = 15;        %Reference Temperature in Celcius
alpha=3.75;        %vert tilt (degree)
beta=18.00;        %horz tilt (degree)
x=0;

%Variables
%tank_type= 1;   % Simple Cylinder
tank_type= 2;     % Simple Cylinder with Caps
H=340;            % dished head radius (mm)

% Calculate sphere (cap) radius
r=(R^2+H^2)/(2*H);

fuel = 'Diesel';  %fuel type
%fuel = 'Gasoline'; %fuel type
switch fuel
case 'Diesel'
display('diesel fuel')
kappa= 0.000792;
case 'Gasoline'
display('gasoline fuel')
kappa=0.001251;
end

% files to run
run ('level_ini_2.m');
run ('level_fin_2.m');
run ('Delta_vol_2.m');
run ('temperature_ini_2.m');
run ('temperature_fin_2.m');

% vectors
Vol_ini_ideal=zeros(numel(h_ini_2),1);
Vol_ini=zeros(numel(h_ini_2),1);
Vol_fin_ideal=zeros(numel(h_fin_2),1);
Vol_fin=zeros(numel(h_fin_2),1);
dV_temp=zeros(numel(h_fin_2),1);
dV_theo_ideal=zeros(numel(h_fin_2),1);
dV_theo=zeros(numel(h_fin_2),1);
Var_ideal=zeros(numel(h_ini_2),1);
Var=zeros(numel(h_ini_2),1);
Var_norm_ideal=zeros(numel(h_ini_2),1);
Var_norm=zeros(numel(h_ini_2),1);

for i= 1:numel(h_ini_2)  % i: data count

    Vol_ini_ideal (i)=fuel_volume(1250,350,2407,6000,600,0,0,h_ini_2(i),fuel,temp_ini_2(i),15,kappa,0);
    Vol_ini (i)=fuel_volume(R,H,r,L,M,alpha,beta,h_ini_2(i),fuel,temp_ini_2(i),T_ref,kappa,0);

```

```

Vol_fin_ideal(i)=fuel_volume(1250,350,2407,6000,600,0,0,h_fin_2(i),fuel,temp_fin_2(i),15,kappa,0);
Vol_fin(i)=fuel_volume(R,H,r,L,M,alpha,beta,h_fin_2(i),fuel,temp_fin_2(i),T_ref,kappa,0);

dV_theo_ideal(i)= Vol_fin_ideal(i)- Vol_ini_ideal(i);
dV_theo(i)= Vol_fin(i)- Vol_ini(i);

Var_ideal(i)= dV_theo_ideal(i)- dV_theo_ideal(i);
Var(i)= dV_theo(i)+ dV_act_2(i);

Var_norm_ideal(i)= (dV_theo_ideal(i)/(-dV_theo_ideal(i)))+1;
Var_norm(i)=(dV_theo(i)/dV_act_2(i))+1;

end

plot (h_fin_2, Var, '*')
hold on
plot (h_fin_2, Var_ideal)

```

Figure F.18. Check of optimal parameters for the tank in Site D

```

% Check of best parameters ____ Hourly Data_ T4 in Site D

clc; clear;

% Parameters (Constants)
R=1245; %radius of tank (mm)
L=5990; %length of tank (mm)
M=840; %manhole distance (mm)
T_ref = 15; %Reference Temperature in Celcius
alpha=3.75; %vert tilt (degree)
beta=18.00; %horz tilt (degree)
x=0;

% Variables
%tank_type= 1; % Simple Cylinder
tank_type= 2; % Simple Cylinder with Caps
H=340; % dished head radius (mm)

% Calculate sphere (cap) radius
r=(R^2+H^2)/(2*H);

fuel = 'Diesel'; %fuel type
%fuel = 'Gasoline'; %fuel type
switch fuel
case 'Diesel'
display('diesel fuel')
kappa= 0.000792;
case 'Gasoline'
display('gasoline fuel')
kappa=0.001251;
end

% files to run
run ('hmeasured_initial_O2.m');
run ('hmeasured_final_O2.m');
run ('Delta_volume_O2.m');
run ('temperature_initial_O2.m');
run ('temperature_final_O2.m');

% vectors
Vol_ini_ideal=zeros(numel(level_ini_O2),1);
Vol_ini=zeros(numel(level_ini_O2),1);
Vol_fin_ideal=zeros(numel(level_fin_O2),1);
Vol_fin=zeros(numel(level_fin_O2),1);
dV_temp=zeros(numel(level_fin_O2),1)
dV_theo_ideal=zeros(numel(level_fin_O2),1);
dV_theo=zeros(numel(level_fin_O2),1);
Var_ideal=zeros(numel(level_ini_O2),1);
Var=zeros(numel(level_ini_O2),1);
Var_norm_ideal=zeros(numel(level_ini_O2),1);

```

```

Var_norm=zeros(numel(level_ini_O2),1);

for i= 1:numel(level_ini_O2) % i: data count

Vol_ini_ideal(i)=fuel_volume(1250,350,2407,6000,600,0,0,level_ini_O2(i),fuel,temp_ini_O2(i),15,kappa,0);
Vol_ini(i)=fuel_volume(R,H,r,L,M,alpha,beta,level_ini_O2(i),fuel,temp_ini_O2(i),T_ref,kappa,0);

Vol_fin_ideal(i)=fuel_volume(1250,350,2407,6000,600,0,0,level_fin_O2(i),fuel,temp_fin_O2(i),15,kappa,0);
Vol_fin(i)=fuel_volume(R,H,r,L,M,alpha,beta,level_fin_O2(i),fuel,temp_fin_O2(i),T_ref,kappa,0);

dV_theo_ideal(i)= Vol_fin_ideal(i)- Vol_ini_ideal(i);
dV_theo(i)= Vol_fin(i)- Vol_ini(i);

Var_ideal(i)= dV_theo_ideal(i)- dV_theo_ideal(i);
Var(i)= dV_theo(i)+ dV_actual_O2(i);

Var_norm_ideal(i)=(dV_theo_ideal(i)/(-dV_theo_ideal(i)))+1;
Var_norm(i)=(dV_theo(i)/dV_actual_O2(i))+1;

end

plot (level_fin_O2, Var_norm)
hold on
plot (level_fin_O2, Var_norm_ideal)

```

Figure F.19. Check of optimal parameters with hourly data for the tank in Site D

```

% % Main Algo __ Daily Data __ T3 Site E

clc; clear;

% Parameters (Constants)
R=1220; %radius of tank (mm)
L=5990; %length of tank (mm)
M=600; %manhole distance (mm)
T_ref = 15; %Reference Temperature in Celcius
alpha=0.95; %vert tilt (degree)
beta=3.00; %horz tilt (degree)

% Variables
%tank_type= 1; %Simple Cylinder
tank_type= 2; %Simple Cylinder with Caps
H=400; %Dished head radius (mm)

% Calculate sphere (cap) radius
r=(R^2+H^2)/(2*H);

fuel = 'Diesel'; %fuel type
%fuel = 'Gasoline'; %fuel type
switch fuel
case 'Diesel'
display('diesel fuel')
kappa= 0.000792;
case 'Gasoline'
display('gasoline fuel')
kappa=0.001251;
end

% files to run
run ('level_in_Y1.m');
run ('level_fin_Y1.m');
run ('Delta_volume_Y1.m');
run ('temperature_in_Y1.m');
run ('temperature_fin_Y1.m');

% vectors
Vol_ini_ideal=zeros(numel(hin_Y1),1);
Vol_ini=zeros(numel(hin_Y1),1);
Vol_fin_ideal=zeros(numel(hfin_Y1),1);
Vol_fin=zeros(numel(hfin_Y1),1);
dV_temp=zeros(numel(hfin_Y1),1)
dV_theo_ideal=zeros(numel(hfin_Y1),1);

```

```

dV_theo=zeros(numel(hfin_Y1),1);
Var_ideal=zeros(numel(hin_Y1),1);
Var=zeros(numel(hin_Y1),1);
Var_norm_ideal=zeros(numel(hin_Y1),1);
Var_norm=zeros(numel(hin_Y1),1);

for i= 1:numel(hin_Y1) % i: data count

    Vol_ini_ideal(i)=fuel_volume(1240,400,2122,6000,700,0,0,hin_Y1(i),fuel,temp_in_Y1(i),15,kappa,0);
    Vol_ini(i)=fuel_volume(R,H,r,L,M,alpha,beta,hin_Y1(i),fuel,temp_in_Y1(i),T_ref,kappa,0);

    Vol_fin_ideal(i)=fuel_volume(1240,400,2122,6000,700,0,0,hfin_Y1(i),fuel,temp_fin_Y1(i),15,kappa,0);
    Vol_fin(i)=fuel_volume(R,H,r,L,M,alpha,beta,hfin_Y1(i),fuel,temp_fin_Y1(i),T_ref,kappa,0);

    dV_theo_ideal(i)= Vol_fin_ideal(i)- Vol_ini_ideal(i);
    dV_theo(i)= Vol_fin(i)- Vol_ini(i);

    Var_ideal(i)= dV_theo_ideal(i)- dV_theo_ideal(i);
    Var(i)= dV_theo(i)+ dV_act_Y1(i);

    Var_norm_ideal(i)= (dV_theo_ideal(i)/(-dV_theo_ideal(i)))+1;
    Var_norm(i)=(dV_theo(i)/dV_act_Y1(i))+1;

end

plot (hfin_Y1, Var, '*')
hold on
plot (hfin_Y1, Var_ideal)

```

Figure F.20. Main algo for the tank in Site E variance calculation

```

% %BEST PARAMETERS DETERMINATION _ Daily Data _ T3 in Site E

clc; clear;

% Parameters (Constants)
R=1240; %radius of tank (mm)
L=6000; %length of tank (mm)
M=700; %manhole distance (mm)
T_ref = 15; %Reference Temperature in Celcius
alpha=0.00; %vert tilt (degree)
beta=0.00; %horz tilt (degree)
x=0;

%Variables
%tank_type= 1; % Simple Cylinder
tank_type= 2; % Simple Cylinder with Caps
H=400; % dished head radius (mm)

% Calculate sphere (cap) radius
r=(R^2+H^2)/(2*H);

fuel = 'Diesel'; %fuel type
%fuel = 'Gasoline'; %fuel type
switch fuel
case 'Diesel'
display('diesel fuel')
kappa= 0.000792;
case 'Gasoline'
display('gasoline fuel')
kappa=0.001251;
end

% files to run
run ('level_in_Y1.m');
run ('level_fin_Y1.m');
run ('Delta_volume_Y1.m');
run ('temperature_in_Y1.m');
run ('temperature_fin_Y1.m');

% vectors
Vol_ini=zeros(numel(hin_Y1),1);

```

```

Vol_fin=zeros(numel(hfin_Y1),1);
dV_temp=zeros(numel(hfin_Y1),1)
dV_theo=zeros(numel(hfin_Y1),1);
Var=zeros(numel(hin_Y1),1);

z=0;

%for R=(R-24):2:(R+24);
for R=1220;
%   for H = (H-10):10:(H+10);
%      for H = 400;
%         for L = (L-10):10:(L+10);
%            for L = 5990;
%               for M = (M-100):100:(M+100);
%                  for M = 600;
%                     for alpha = 0:0.05:2;
%                        for alpha = 0.95;
%                           for beta = 2.50:0.5:4.50;
%                              z=z+1;
%                              G=0;
%                              for i= 1:numel(hin_Y1) % i: data count

                                 Vol_ini (i)=fuel_volume(R,H,r,L,M,alpha,beta,hin_Y1(i),fuel,temp_in_Y1(i),T_ref,kappa,0);
                                 Vol_fin (i)=fuel_volume(R,H,r,L,M,alpha,beta,hfin_Y1(i),fuel,temp_fin_Y1(i),T_ref,kappa,0);
                                 dV_theo(i)= Vol_fin(i)- Vol_ini(i);
                                 Var(i)= dV_theo(i)+ dV_act_Y1(i);

                           end

                           figure()
                           plot (hfin_Y1, Var, '*')
                           title(['R=' num2str(R), 'H=' num2str(H), 'L=' num2str(L), 'M=' num2str(M), 'alpha=' num2str(alpha), 'beta=' num2str(beta)])
                           G= sum(abs(Var));
                           G_table(:,z) = [R H L M alpha beta G Var'];
                           end
                           end
                           end
                           end
                           end
                           end
                           end
                           end

[min_G, I] = min(G_table(7,:))
format long
G_table(:,I)

```

Figure F.21. Determination of optimal parameters for the tank in Site E

```

% Check of best parameters with 2nd Group Data____ Daily Data_ T3 in Site E

clc; clear;

% Parameters (Constants)
R=1220; %radius of tank (mm)
L=5990; %length of tank (mm)
M=600; %manhole distance (mm)
T_ref = 15; %Reference Temperature in Celcius
alpha=0.95; %vert tilt (degree)
beta=3.00; %horz tilt (degree)

%Variables
%tank_type= 1; %Simple Cylinder
tank_type= 2; %Simple Cylinder with Caps
H=400; %Dished head radius (mm)

% Calculate sphere (cap) radius
r=(R^2+H^2)/(2*H);

fuel = 'Diesel'; %fuel type
%fuel = 'Gasoline'; %fuel type
switch fuel

```

```

case 'Diesel'
display('diesel fuel')
kappa= 0.000792;
case 'Gasoline'
display('gasoline fuel')
kappa=0.001251;
end

% files to run
run ('level_in_Y2.m');
run ('level_fin_Y2.m');
run ('Delta_volume_Y2.m');
run ('temperature_in_Y2.m');
run ('temperature_fin_Y2.m');

% vectors
Vol_ini_ideal=zeros(numel(hin_Y2),1);
Vol_ini=zeros(numel(hin_Y2),1);
Vol_fin_ideal=zeros(numel(hfin_Y2),1);
Vol_fin=zeros(numel(hfin_Y2),1);
dV_temp=zeros(numel(hfin_Y2),1)
dV_theo_ideal=zeros(numel(hfin_Y2),1);
dV_theo=zeros(numel(hfin_Y2),1);
Var_ideal=zeros(numel(hin_Y2),1);
Var=zeros(numel(hin_Y2),1);
Var_norm_ideal=zeros(numel(hin_Y2),1);
Var_norm=zeros(numel(hin_Y2),1);

for i= 1:numel(hin_Y2) % i: data count

    Vol_ini_ideal(i)=fuel_volume(1240,400,2122,6000,700,0.0,hin_Y2(i),fuel,temp_in_Y2(i),15,kappa,0);
    Vol_ini(i)=fuel_volume(R,H,r,L,M,alpha,beta,hin_Y2(i),fuel,temp_in_Y2(i),T_ref,kappa,0);

    Vol_fin_ideal(i)=fuel_volume(1240,400,2122,6000,700,0.0,hfin_Y2(i),fuel,temp_fin_Y2(i),15,kappa,0);
    Vol_fin(i)=fuel_volume(R,H,r,L,M,alpha,beta,hfin_Y2(i),fuel,temp_fin_Y2(i),T_ref,kappa,0);

    dV_theo_ideal(i)= Vol_fin_ideal(i)- Vol_ini_ideal(i);
    dV_theo(i)= Vol_fin(i)- Vol_ini(i);

    Var_ideal(i)= dV_theo_ideal(i)- dV_theo_ideal(i);
    Var(i)= dV_theo(i)+ dV_act_Y2(i);

    Var_norm_ideal(i)= (dV_theo_ideal(i)/(-dV_theo_ideal(i)))+1;
    Var_norm(i)=(dV_theo(i)/dV_act_Y2(i))+1;

end

plot (hfin_Y2, Var, '*')
hold on
plot (hfin_Y2, Var_ideal)

```

Figure F.22. Check of optimal parameters for the tank in Site E

```

clc;clear;

% (1)Level ini (2)Vol_in(3)Level fin (4)Vol_fin (5)Delivery (6)Invoiced_Del(7)Correction (8)Sales (9)Var_ATG (10)dV_actual
(11)Var
DATA =[

247.454 301.826 326.273 443.828 538.87 547.999 548.193 582.554 584.628 585.832 586.378 640.65 653.139 690.102 696.444
697.275 710.715 720.307 723.336 726.079 742.962 749.29 754.018 782.762 815.159 816.728 831.562 833.103 840.578 844.631
868.772 880.746 886.184 898.839 899.996 930.583 932.579 933.746 937.855 946.087 967.696 1004.96 1006 1007.66 1013.92
1015.39 1022.16 1046.18 1051.77 1060.95 1067.95 1081.62 1082.34 1109.05 1134.09 1151.31 1159.72 1176.45 1186.05 1198
1201.22 1209 1210.08 1218.95 1221.63 1224 1237.32 1253.94 1265.24 1266.68 1278.37 1280.08 1281.46 1282.13 1283.04
1285.38 1294.86 1302.59 1304.57 1305.72 1306.18 1306.54 1308.11 1312.13 1319.71 1320.23 1320.46 1322.84 1330 1335.92
1340.44 1347.55 1351.54 1356 1377.09 1393 1402.43 1405 1414.71 1416.56 1419.83 1438.91 1439.54 1443.18 1444.13 1448
1465.73 1466 1470.49 1484.32 1514.54 1518.37 1519.71 1581.56 1700.94 1724.23 1749.63 1764.39 1764.78 1767 1768.98
1772.51 1776.03 1778.37 1795.87
1241 1597 1783 2695 3501 3584 3584 3891 3910 3917 3925 4425 4542 4890 4951 4958 5087 5182
5212 5238 5193 5466 5511 5791 6113 6132 6279 6294 6370 6139 6658 6779 6832 6934 6961 6972
7290 7309 7320 7362 7449 7672 8032 8039 8043 8077 8085 8119 8240 8270 8316 8354 8422 8425
8660 9061 9338 9141 9315 9890 10087 10129 10208 10223 10314 10344 10367 10511 10685 10806 10821

```



```

var_norm = var./dV;
var = var_norm;

% Now form the [A] matrix according to method 2

A = eye(n); % Form an identity matrix of (n*n)
for i=1:(n-1);
    A(i,i+1) = -1;
end
A(n,1) = 1;

% Form [B] matrix
B = [var(1:(n-1)) ; sum( var( 1:(n-1) ) )];

% solve for [E]
E = inv(A)*B;

E_ini = E(1:(n-1)); % = E1, E2, ... , E(n-1)
E_fin = E(2:n); % = E2, E3, ... , En

var_E = E_ini - E_fin;

VAR1 = [hi(1:n-1) var var_E];

%% now we have dV values (i.e. Y-values) and the h values (i.e. X-values).
% So. we can make a function f(x) by curve fitting:

% Fit: 'correction'.
[xData, yData] = prepareCurveData( hi, E );

% Set up fittype and options.
ft = fittype('smoothing spline');
opts = fitoptions( ft );
opts.SmoothingParam = 0.0001; % This is smoothing factor. May be changed

% Fit model to data.
[err_vol, gof] = fit( xData, yData, ft, opts );

% Plot fit with data.
figure('Name', 'E_vol');
h1 = plot( err_vol, xData, yData );
legend( h1, 'E vs. h', 'E_{vol}' );
'Location', 'NorthEast' );
% Label axes
xlabel( 'hi' );
ylabel( 'E_{vol}' );
grid on

%% now we can evaluate the correction function at any h value. For ex: a = err_vol(110);
% Apply the formula var = E_ini - E_fin
E_ini = err_vol(hi);
E_fin = err_vol(hf);

var_err = E_ini - E_fin;
VAR2 = [hi(1:n-1) var_unnorm var_err(1:n-1)];

% a plot of variance(from data) and variance after volume correction
plot(VAR2(:,1), VAR2(:,2), VAR2(:,1), VAR2(:,3))
% a plot of chart volume and corrected volume
figure()
plot(hi, Vi, hi, Vi+E_ini)

```

Figure F.23. Variance minimization by non-uniform adjustment for the tank in Site B